Results on the Small Dispersion Limits of the Intermediate Long Wave and Benjamin-Ono Equations

by

Matthew Dominique Mitchell

A dissertation submitted in partial fulfillment
of the requirements for the degree of
Doctor of Philosophy
(Physics)
in the University of Michigan
2024

Doctoral Committee:

Professor Peter David Miller, Co-Chair
Professor Henriette Elvang, Co-Chair
Professor Dante Amidei
Professor Jinho Baik
Professor Zaher Hani

Matthew Dominique Mitchell
mattdmit@umich.edu
ORCID iD: 0000-0002-8451-6746

© Matthew Dominique Mitchell 2024

DEDICATION

For Gabbi. To the long road ahead.

ACKNOWLEDGEMENTS

> As Robert Plant says in *Stairway to Heaven*, "There's still time to change the road you're on."
>
> Peter Miller, during a lecture given at the University of Michigan's Random Matrix Theory Summer School (2022)

First, a thank you to the institutions that have helped me along the way: Rackham Graduate School for their generous travel grants, the physics department here at the University of Michigan for the extensive financial support that they have awarded me over the years, and the Graduate Employees' Organization for helping me to give back to a graduate student body that, time and time again, put themselves on the line for my benefit.

Second, I'd like to thank the mentors and colleagues that I've had throughout my graduate career. To Henriette Elvang, for going above and beyond in her role as my advisor and letting me find my own way when it was what I needed the most. To Peter Miller, who took me under his wing in my third year and introduced me to the wonderful world of solitons. To the members of the Integrable Systems and Random Matrix Theory group, especially Ahmad, Andrei, Joanne, and Chris, for both the personal and professional support they have lent me. To Tom Claeys for inviting me to give my first seminar talk, offering me some much needed feedback, and for financially supporting my trip. And to Dante Amidei, for helping me to become a better educator.

Third, a thanks to the friends that I've made while in graduate school and the adventures we've had together. To Ibrahim, for unending physics jokes and insightful conversations. To Haley, for always nourishing my inner child. To Liana, for tolerating my poor roommate habits and feeding my growing podcast diet. To David, for also tolerating my poor roommate habits and for keeping me sharp with physics questions. To Thomas, for teaching me about Wronskians and for not being upset when I plowed his Ford Taurus into a snow bank. To Joe and Christina, for improving my climbing skills and for always being willing to help with the pup. To Kevin and Mia, for reviving the board game addiction that I thought I kicked years ago. To Chami, for introducing me to King Gizzard and the Lizard Wizard and giving me the confidence to musically express myself. To Jen, for the years we spent together. And

to Miles, for always being there to cheer me up. For the many others I've met along the way, I thank you for making the inevitable pains of grad school just a little more bearable.

Lastly, but never least, to those who came before grad school. To my family: Mom, Dad, Ben, Natalie, Joan, Migi, Dave, Mike, Iliana, Gigi, and Sasha. Never a dull day when you're all around! To my friends: Ross, Michael, Benjy, Russel, Vanessa, Dani, Massimo, Elliot, Hannah, Adam, Daniel, Ryan, Will, Colby, and Alex. I'm incredibly grateful for you all having kept in touch.

TABLE OF CONTENTS

DEDICATION ii

ACKNOWLEDGEMENTS iii

LIST OF FIGURES vii

ABSTRACT x

CHAPTER

1 Introduction 1

1.1 The Inverse Scattering Transform 4
1.2 The Intermediate Long Wave Equation 9
1.3 The Benjamin-Ono Equation 20
1.4 The Small Dispersion Limit and Universality 21
1.4.1 Overview of Previous Results 25
1.5 Outline for the Dissertation 26
1.5.1 Past and Expected Publications 27

2 Intermediate Long Wave Direct Scattering Problem with Small Dispersion 28

2.1 A Formal WKB Analysis of the ILW Scattering Equation 29
2.1.1 Interpretation of the Formal Asymptotic Solutions 33
2.2 The Model Turning Point Equation 37
2.2.1 Solving the Model Turning Point Equation by Laplace Transform . 40
2.2.2 A Basis of Solutions to the Model Turning Point Equation 41
2.2.3 The Behavior of the Saddle Points 44
2.2.4 Basis Solution Asymptotics for Matching Across the Turning Point 45
2.3 WKB Matching Argument and the Formal Asymptotic Scattering Data . . . 80
2.4 The Modified Scattering Data 97

3 Intermediate Long Wave Equation Inverse Problem for Modified Scattering Data 100

3.1 Expanding the Determinant 100
3.2 From Discrete Minimizing Subset to Continuous Minimizing Distribution . . 106
3.3 The Distributional Limit of the Solution 109
3.4 Solving the Energy Minimization Problem 115
3.4.1 Solving the Variational Conditions 120

4 Universality in the Benjamin-Ono Small Dispersion Limit for Rational Initial Data 141

4.1 Steepest Descent Analysis of the Exponential Integrals 144
4.1.1 Choice of Contours for steepest descent analysis 148
4.1.2 Steepest Descent Approximation for Colliding Saddle Points 150
4.1.3 Steepest descent Approximation for Simple Saddle Points 155
4.2 Universal Behavior at the Soliton Edge 157
4.2.1 Interpretation of the Small Dispersion Formula 164
4.3 Universal Behavior at the Dispersive Edge 166
4.3.1 Interpretation of the Formula at the Dispersive Edge 175

5 Conclusion 178

BIBLIOGRAPHY 182

LIST OF FIGURES

FIGURE

1.1 Sketches from John Scott Russell's *Report on Waves* [50] depicting solitary waves generated in a wave tank and their dynamics. 3

1.2 A Figure from Zabusky and Kruskal's paper [56, Figure 1] showing the solitons emerging from the initial condition, rank-ordered by height. 4

1.3 A schematic example potential $-u$ which decays to zero at infinity, energy level E_n and normalizable wavefunction ψ_n. 6

1.4 A schematic example potential $-u$ which decays to zero at infinity, energy level E and scattering experiment expressed in terms of the wavefunction's asymptotic phases. 7

1.5 Comparison of the method of solving a linear PDE using the Fourier transform and the inverse scattering transform for the KdV equation. 8

1.6 Schematic for the two dimensional incompressible and irrotational fluid system from which the ILW equation is derived. The equilibrium position (dashed black) of the thin pycnocline (solid black) between the two fluid densities (yellow and blue) are depicted above. We require the density of the top fluid ρ_1 to be less than that of the lower fluid ρ_2 so the fluids are stably separated by gravity. The system is confined between two rigid and flat surfaces, a ceiling and floor. Labeled in the schematic, h and δ are the equilibrium depths of the fluids, a is the maximum amplitude of the disturbance of the pycnocline and λ is a characteristic wavelength of the disturbance. We characterize the nonlinearity governing the dynamics of the system by the parameter $\alpha = a/h$ as well as that for the linear dispersion by $\epsilon = h/\lambda$. The ILW equation obtains in the asymptotic limit where $h \to 0^+$, δ and ϵ/α fixed with ϵ and α individually bounded. Here, the top layer is depicted with vanishing depth h while the bottom layer has fixed depth δ, but the model is independent of which layer has the fixed depth δ and which has the vanishing depth h [31]. 9

1.7 Plots of $\tau(\delta k)$, the Fourier transform of the kernel of T_δ, over the domain $k \in [-4, 4]$ and for several identified values of δ. It can be seen that for small δ, the graph becomes more linear with a diminishing slope proportional to δ. For large δ, the graph approaches a sgn function. 10

1.8 The strip domain of analyticity of the wavefunction $\psi(z)$. Also shown are the definitions of the continuous boundary values $\psi^{\pm}(x)$ via limits from inside the strip. 11

1.9 The ILW scattering equation spectrum in the ζ plane. The blue contours are the visible portion of the quadratrix of Hippias, solid for the quadratrix and dashed for the other disconnected branches. The discrete spectrum shows up on the quadratrix and the continuous spectrum is labeled in solid yellow. 14
1.10 Fourier split-step simulation of the KdV equation in the small dispersion limit. The first row is at different times before and at critical while the second row shows the effect of decreasing ϵ at fixed time. 24

2.1 $z \mapsto W_n(z)$ demonstrated for three characteristic branches: $n = -2, -1$, and 0. The colored z-planes map into the same colored branch ranges indicated below. Additionally, the colored edges in the z-planes indicate the direction that the same colored range boundaries are approaches from each side of the branch cut. The edge of the same color as the plane are the ones that are included in that branch. The $n = 1$ maps like the $n = -1$ branch while all others are similar to the $n = -2$ branch. 35
2.2 An example potential $-u(x)$ and level $E(\zeta)$ (top) with schematics (bottom) of the behaviors of $W_n(-2\delta\zeta \mathrm{e}^{-2\delta(\zeta+u(x))})$ at some chosen points in the classically forbidden region (left), at the turning point (middle) and in the classically allowed region (right). The values for the extraneous solutions ($n \neq -1, 0$) are shown in red and those for the scattering solutions ($n = -1, 0$) are shown in green. 38
2.3 The landscape of $\mathrm{Im}\,[f(k)]$. Yellow shading corresponds to a positive value while blue shading corresponds to a negative value. Additionally, the fine black lines are some particular level contours. The basin and range structure can be clearly seen on the left of the image with the basins in blue and the ranges in yellow. We also see the beginnings of the Rockies (yellow) and the Grande valley (blue) in the first and fourth quadrants respectively. Some representative choices of basis contours C_ν as defined above are depicted in red with their labels. 43

3.1 $z \mapsto W(-z\mathrm{e}^{-z-y})$ demonstrated via three intermediate mappings for three characteristic branch regions. The colored regions and boundaries describe where the points in the top image are mapped to in the complex plane at each step. . . . 124

4.1 Example for $N = 5$ of some admissible contours $C_1, \ldots, C_5$ for the Benjamin-Ono solution with initial rational data. 143
4.2 A multivalued solution to Burgers' equation with initial condition corresponding to $N = 2$, $c_1 = 1/4 - \mathrm{i}3/4$, $c_2 = -1/10 - \mathrm{i}1/2$, $p_1 = -6 + \mathrm{i}$ and $p_2 = 5 + \mathrm{i}3/2$. . 146
4.3 Schematics of the local landscapes around the real saddle points near to (left column) and at (right column) the soliton (top row) and dispersive (bottom row) edges. The color and saturation indicate the value of $\mathrm{Im}\,[h(\diamond; x, t)]$ relative to that at the associated saddle point(s), blue is below and yellow is above. Schematics of the contours constructed by the procedure [6, Section 4] W_{y_0} and $W_{y_{1,2}}$ as well as the modified contours that we define C_0 and C_1 are also depicted in maroon and labeled. 150

4.4 An example soliton edge approximation formula for the same initial condition provided in Figure 4.2. On the left is the full formula plotted for $X \in [-10, 10]$, $\epsilon = 0.1$, $t = 1.5$, and $x_{\mathrm{s}}(t) \approx -1.180$. On the right is the same solution, but shifted by the Airy zeros and horizontally scaled by $\epsilon^{1/3}$ to focus on the first four soliton peaks. Also plotted for comparison (dashed) is a true BO soliton Lorenzian profile (4.99) with a constant background, amplitude, horizontal scaling, and horizontal shift that match those predicted by the approximation formula. . 166

4.5 An example dispersive edge approximation formula for the same initial condition provided in Figure 4.2. Plotted for $X \in [-10, 10]$, $\epsilon = 0.001$, $t = 1.5$, and $x_{\mathrm{d}}(t) \approx -2.547$. Also plotted is the Airy modulus amplitude profile (dashed). . 177

ABSTRACT

The small dispersion limits of both the intermediate long wave and Benjamin-Ono equations are analyzed, albeit, in dramatically different contexts. While there is little rigorous theory regarding the solutions and scattering data of the intermediate long wave equation's direct scattering problem for general positive, "single lobed" potentials in the semiclassical limit, a formal WKB approximation process is known. In this work, new details regarding matching formal solutions at the turning points and the asymptotic formula for the norming constants are presented. Taking the reflection coefficient to be zero, the rigorous inverse scattering problem is studied using the N-soliton formula as N tends to infinity. Interestingly, this problem reduces to studying the limit of the thermodynamical partition function of a system of N two dimensional Coulomb charges with temperature roughly proportional to $1/N^2$, the limit of which is shown to be dominated by the equilibrium charge density. The resulting solution of the intermediate long wave equation is shown to limit in a strong L^2 sense to the chosen initial condition at $t = 0$ and the associated inviscid Burgers' solution up until its own break time. For the Benjamin-Ono equation, the behavior at the edges of dispersive shock waves formed in the small dispersion limit with rational initial conditions are described. New approximate formulæ that are uniform in shrinking space-time regions around the two caustic curves which bound the dispersive shock wave are derived and are interpreted physically.

CHAPTER 1

Introduction

> I believe I shall best introduce this phænomenon by describing the circumstances of my own first acquaintance with it. I was observing the motion of a boat which was rapidly drawn along a narrow channel by a pair of horses, when the boat suddenly stopped–not so the mass of water in the channel which it had put in motion; it accumulated round the prow of the vessel in a state of violent agitation, then suddenly leaving it behind, rolled forward with great velocity, assuming the form of a large solitary elevation, a rounded, smooth and well-defined heap of water, which continued its course along the channel apparently without change of form or diminution of speed. I followed it on horseback, and overtook it still rolling on at a rate of some eight or nine miles an hour, preserving its original figure some thirty feet long and a foot to a foot and a half in height. Its height gradually diminished, and after a chase of one or two miles I lost it in the windings of the channel. [50, Section 1]

These are the words of John Scott Russell in his 1844 *Report on Waves* to the British Association for the Advancement of Science. This quotation is found near the beginning of many great introductions to integrable systems and soliton dynamics such as Newell's *Solitons in Mathematics and Physics* [47] as well as Drazin and Johnson's *Solitons: An Introduction* [18]. While I thought it important to keep the tradition, Russel's particularly detailed and enthralling description leaves an impression on the reader with what he dubs the "Wave of Translation." Later known as a "solitary wave," this takes the form of a localized heap of water above the equilibrium surface level that travels with more or less a constant speed and profile (see Figure 1.1). Russel conducted controlled experiments in wave tanks on the solitary waves, deriving the empirical law relating the speed and width of the wave to the acceleration of gravity and the height of the wave above the equilibrium surface level. It was not until several decades later that Bousinessq in 1872 [8] and Korteweg and de Vries

in 1895 [28] independently derived the mathematical form of the solitary wave

$$u(x,t) = 2\kappa^2 \operatorname{sech}^2\left(\kappa\left[x - x_0 - \frac{4}{3}\kappa^2 t\right]\right) \tag{1.1}$$

where $x, t \in \mathbb{R}$ are scaled space and time coordinates and $\kappa, x_0 \in \mathbb{R}$ are constants. Modulo the initial position of the solitary wave, these comprise a family of solutions whose height, width and speed are all determined by the value of $\kappa > 0$. From (1.1), we see that the taller solitons are thinner and have greater speed. Korteweg and de Vries were the first to write down an asymptotic equation governing the evolution of a fluid's surface under the assumptions that the wavelength of the disturbance is long compared to the depth of the fluid and the amplitude is not too large. The result is a shallow water, weakly nonlinear model that has since come to be known as the Korteweg-de Vries (KdV) equation

$$0 = u_t + 2uu_x + \frac{1}{3}u_{xxx}\,. \tag{1.2}$$

where u is the scaled height of the surface above the equilibrium level. In a general sense, the nonlinear term $2uu_x$ in (1.2) tends to steepen negative slopes in the solution (see the discussion of Invicid Burgers' equation (1.80) in Section 1.4 for more explanation), while the dispersive term u_{xxx}, so called because the linearized equation has a dispersion relation where waves of different wavelength travel at different speeds, would tend to spread a solution out. The solitary wave profiles appear to be a family of solutions where these two effects perfectly balance, and the solution propagates with a fixed shape.

While the soliton was first glimpsed by Russell in the mid 1800's, it would not be seen again until almost a hundred years later in Los Alamos National Lab. In 1953, Fermi, Pasta, Ulam and Tsingou (FPUT) were using the newly built MANIAC mainframe computer to conduct numerical simulations of a one-dimensional periodic lattice of coupled masses and springs [47]. The spring force they used was Hooke's law plus a small nonlinear term. The expectation was that, being close to linear, the normal modes of vibration in the lattice would be almost stationary states of the dynamics, but the small nonlinear term would result in diffusion of energy between modes. If the energy of the system began in only the lowest wave number mode, eventually one might expect an equilibrium to be reached in thermalization of the system, where energy was equally distributed over all modes. To their surprise, the system exhibited nearly perfect recurrence of the initial condition at almost periodic time intervals.

In 1965, Zabusky and Kruskal resolved this "problem" when they conducted one of the first numerical studies of the KdV equation [56]. They were able to show that the system

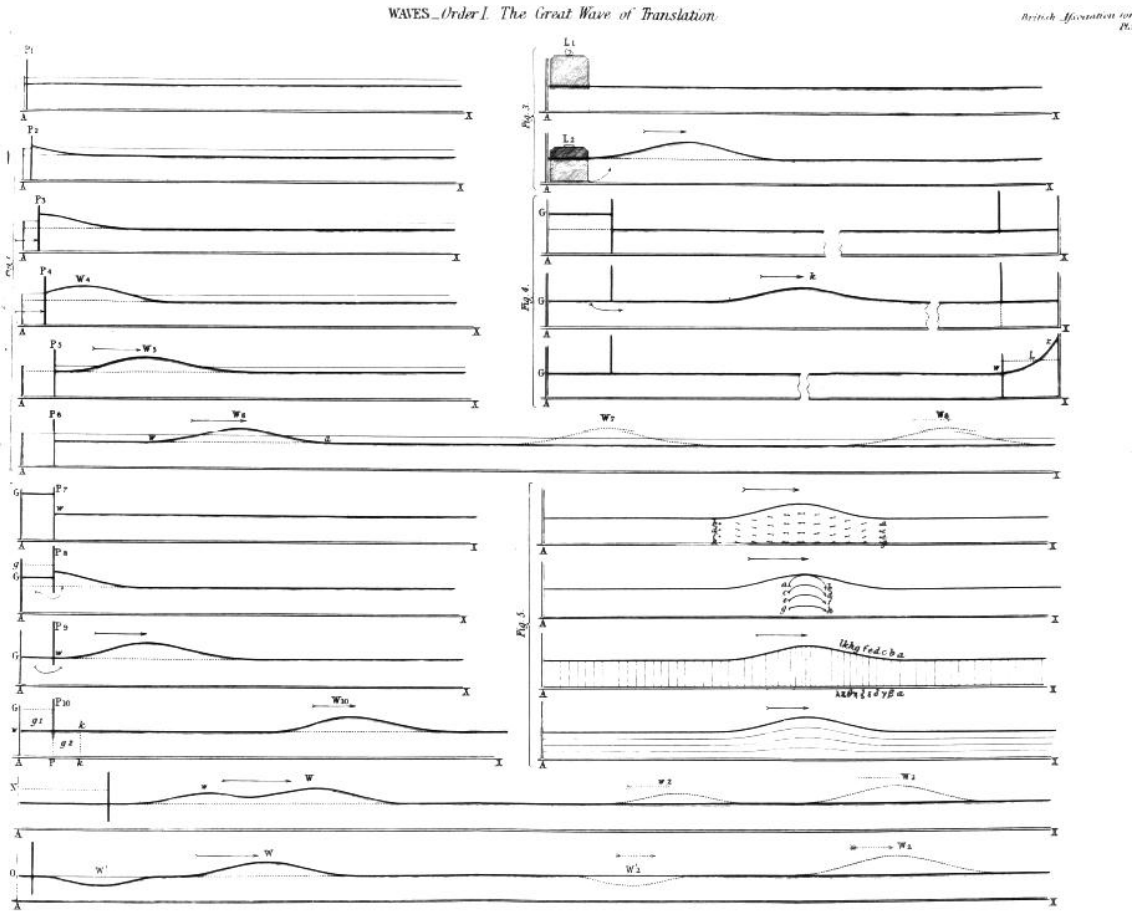


Figure 1.1: Sketches from John Scott Russell's *Report on Waves* [50] depicting solitary waves generated in a wave tank and their dynamics.

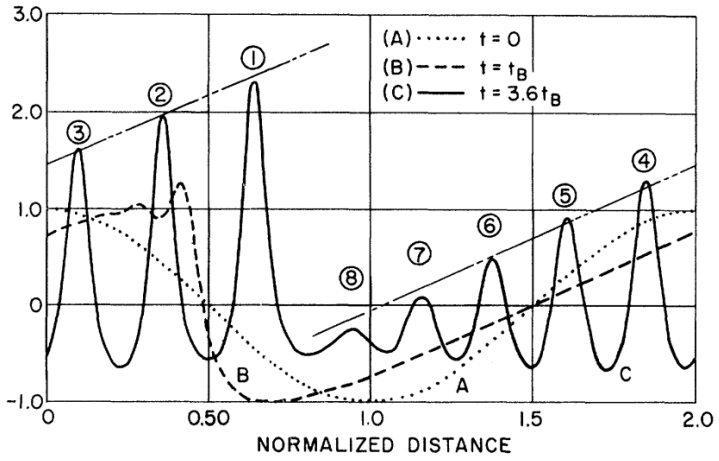


Figure 1.2: A Figure from Zabusky and Kruskal's paper [56, Figure 1] showing the solitons emerging from the initial condition, rank-ordered by height.

simulated by the FPUT team was a discretization of the KdV equation, and furthermore, the recurrence of the initial condition seemed to be be directly due to the solitary waves. Exhibiting a sort of "nonlinear superposition principle," they found that a broad initial condition could have several solitary waves of about linearly spaced κ somehow superimposing in a coherent manner so as to be undetected at first. After letting some time pass, the different speeds of the solitary waves would cause them to spatially separate, and thus the broad initial profile would break up into recognizable individual solitary waves (see Figure 1.2). The periodicity of the simulation meant that the fast solitary waves would outpace the slow ones and eventually catch back up to them, like fast and slow sprinters on a track. The faster solitary waves would then overtake slower ones, with only a constant shift in their linear trajectories to remember the brief interaction by. At roughly periodic time intervals, Zabusky and Kruskal saw an approximate recurrence of the initial condition when all of the solitary waves happened to end up on top of each other, just like they were in the beginning. Because the solitary waves appeared to be stable through these interactions, maintaining their individual identities in the form of their heights and widths, Zabusky and Kruskal dubbed them *solitons* drawing a parallel with subatomic particles (electrons, protons, muons, etc.) which behave similarly in low energy collisions.

1.1 The Inverse Scattering Transform

While superimposing solutions is a valid way of generating new solutions to a linear partial differential equation (PDE), the KdV equation is expressly nonlinear and so it seems quite

bizarre that we would be able to superimpose many solitary waves and form a valid new solution. The special underlying structure that makes this true for the KdV equation was first demonstrated by Gardner, Greene, Kruskal, and Miura in 1967 [22]. They showed that the KdV equation has an infinite hierarchy of conserved quantities, one of which is a Hamiltonian whose flow reproduces the KdV equation. They also showed that the Hamiltonian system is *integrable* in the sense that there is a "change of coordinates" which puts the system into action-angle variables. Amazingly, this is done using the spectral data of a specific quantum mechanical scattering problem. A concise formulation of this change of variables was developed a year later by Lax [33] involving two linear operators known as a *Lax pair*.

For the KdV equation, the Lax pair is the two operators $L, B : L^2(\mathbb{R}) \to L^2(\mathbb{R})$ given by:

$$L = -\frac{\partial^2}{\partial x^2} - u \quad \text{and} \quad B = -\frac{4}{3}\frac{\partial^3}{\partial x^3} - 2u\frac{\partial}{\partial x} - u_x \tag{1.3}$$

where $u : \mathbb{R}^2 \to \mathbb{R}$ and the KdV equation can be deduced as the compatibility condition, $L_t = [L,\ B]$, between the two linear problems,

$$L\psi = E\psi \quad \text{and} \quad B\psi = \psi_t\,, \tag{1.4}$$

for spectral parameter $E \in \mathbb{C}$ and wavefunction $\psi : \mathbb{R}^2 \to \mathbb{C}$. This means, there are simultaneous solutions to (1.4) if and only if $u(x,t)$ is a solution to the KdV equation. Note that the first equation in (1.4) is the eigenvalue problem for the Schrödinger operator and determines the energy eigenstates of a nonrelativistic quantum mechanical particle with total energy E and potential energy $-u(x)$, specifically in units where $\hbar^2/2m = 1$. For $u(x)$ which decays to zero as $x \to \pm\infty$, the *spectral data* of the Schrödinger operator consists of three pieces of information: *discrete eigenvalues*, an associated set of *norming constants* and the *reflection coefficient*. The discrete eigenvalues can only occur when the total energy of the particle is less than the potential at spatial infinity $E = -\kappa^2 < 0$ for $\kappa > 0$. Asymptotically as $x \to \pm\infty$, wavefunctions must exponentially grow or decay like $\mathrm{e}^{\pm\kappa x}$. The modulus squared of the wavefunction, by the Born rule, describes the probability density of finding the quantum particle in a region of space. Thus, for probability to be finite, the wavefunction must be normalizable, i.e. exhibit decay as $x \to \pm\infty$. In general, solutions which decay on one side at $x \to \pm\infty$ will exhibit a sum of exponential decay and growth on the other side. It turns out that it is only for discrete values, $E_n = -\kappa_n^2$ for $1 \le n \le N$, where a normalizable wavefunction ψ_n exists. These represent bound states for the particle, where it has ever smaller probability of being found further into the regions on either side where $E_n < -u$. For this eigenvalue, the associated norming constant C_n is defined using a normalized

eigenfunction ψ_n by

$$\psi_n(x) = \mathrm{e}^{-\kappa_n x}\left(1 + o\left(1\right)\right) \text{ as } x \to \infty \quad \text{and then} \quad C_n^{-1} = ||\psi_n||^2_{L^2(\mathbb{R})} \,. \tag{1.5}$$

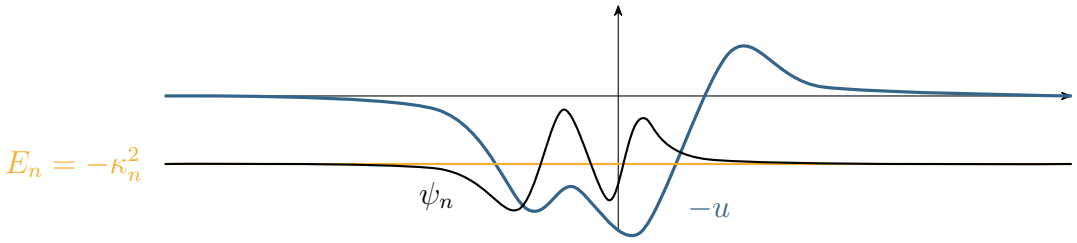


Figure 1.3: A schematic example potential $-u$ which decays to zero at infinity, energy level E_n and normalizable wavefunction ψ_n.

Conversely, when the energy of the quantum particle is greater than the potential at spatial infinity, $E = k^2 > 0$ for $k > 0$, then the particle is unbounded and we call this the continuous spectrum. Out where $x \to \pm\infty$, the wavefunction solutions look like pure exponential phases $\mathrm{e}^{\pm \mathrm{i}kx}$, with the interpretation that $\mathrm{e}^{\mathrm{i}kx}$ is the wavefunction of a free particle moving to the right, while $\mathrm{e}^{-\mathrm{i}kx}$ is the wavefunction of a free particle moving to the left. Since there are only two independent solutions to the second order linear operator, by fixing the coefficients of just two of the pure phases at infinity, we have a unique solution $\psi(x;k)$. If we select the coefficient of the particle moving to the right at $x \to -\infty$ to be one and the coefficient of the particle moving to the left at $x \to +\infty$ to be zero, then the solution represents a quantum scattering experiment: a particle coming in from $x \to -\infty$ and having some probability of reflection back to $x \to -\infty$ or transmission to $x \to +\infty$,

$$\begin{cases} \psi(x;k) = \mathrm{e}^{ikx} + r(k)\mathrm{e}^{-ikx} + o\left(1\right) & \text{as } x \to -\infty \\ \psi(x;k) = t(k)\mathrm{e}^{ikx} + o\left(1\right) & \text{as } x \to +\infty \end{cases}, \tag{1.6}$$

where $r : \mathbb{R}_+ \to \mathbb{C}$ is the reflection coefficient and $t : \mathbb{R}_+ \to \mathbb{C}$ is the transmission coefficient. It turns out that the transmission coefficient is redundant with the reflection coefficient, so we only include the latter in the spectral data.

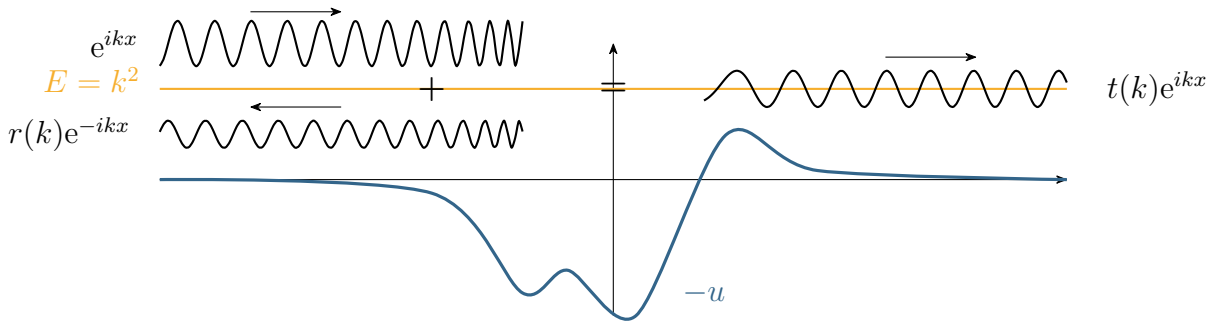


Figure 1.4: A schematic example potential $-u$ which decays to zero at infinity, energy level E and scattering experiment expressed in terms of the wavefunction's asymptotic phases.

Returning to the Lax pair, the second equation in (1.4) imposes a time dependence on the wavefunctions. The scattering data inherits time dependence through their definitions in terms of the wavefunction and can be shown to be

$$\begin{cases} \kappa_n(t) = \kappa_n(0) & \text{for } 1 \le n \le N \\ C_n(t) = C_n(0)e^{4\kappa_n^3 t/3} & \text{for } 1 \le n \le N \\ r(k,t) = r(k,0)e^{8ik^3 t/3} & \text{for all } k > 0 \end{cases} \tag{1.7}$$

for $t \in \mathbb{R}$. From the compatibility condition, for a solution of the KdV equation $u(x,t)$, the spectral data of L with potential $-u(x,t)$ evolves in time according to the simple multiplicative formula above. If we want to exploit this simple time dependence as a method of solving the KdV equation, we need only a method of reconstructing the potential in L from a set of spectral data. This can be done with the Gel'fand-Levitan-Marchenko (GLM) equation,

$$0 = K(x,y) + F(x,y) + \int_x^\infty K(x,z)F(z,y)\,\mathrm{d}z\,, \tag{1.8}$$

where F is constructed from the scattering data and the unknown to be solved for, K, encodes the potential. In more modern approaches, and for equations where one exists, a Riemann-Hilbert problem (RHP) is used to conduct potential reconstruction [17] in place of a GLM equation. RHPs tend to be more amenable to recovering rigorous results than a GLM equation, but for many equations, and specifically the ones we study in this work, a RHP does not exist or has yet to be properly formulated.

The process of extracting the spectral data from a potential is referred to as the *(forward or direct) scattering problem* and the process of reconstructing the potential from some scattering data is the *inverse scattering problem*. The forward and inverse scattering problems, together with the simple time dynamics of the scattering data, collectively form a process

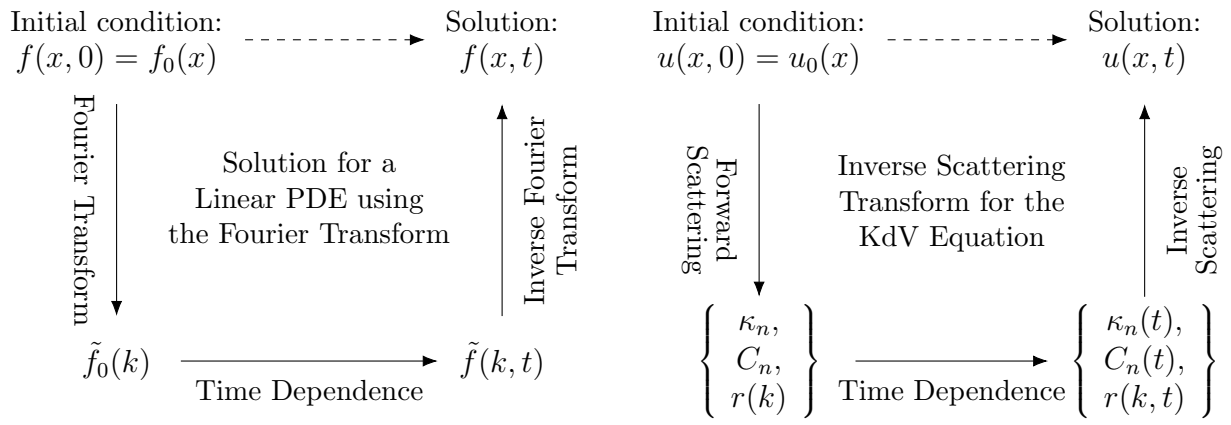


Figure 1.5: Comparison of the method of solving a linear PDE using the Fourier transform and the inverse scattering transform for the KdV equation.

that solves the KdV equation and is refereed to as an *inverse scattering transform* (IST). It can be thought of as a nonlinear analog of the Fourier transform method of solving a linear PDE [1] as the commuting diagrams in Figure 1.5 demonstrate.

The direct scattering problem functions as the coordinate transformation to the action-angle variables, i.e. the spectral data. We see there are conserved quantities, κ_n for $1 \leq n \leq N$ and $|r(k,t)|$ for all $k \in \mathbb{R}$ (essentially, the actions), and quantities that are linear in time, $\ln(C_n(t))$ for $1 \leq n \leq N$ and $\arg(r(k,t))$ for all $k \in \mathbb{R}$ (essentially, the angles). By studying the IST for the KdV equation, one discovers that each eigenvalue of the scattering equation κ_n corresponds directly to a soliton in the KdV solution. Moreover, each soliton, once well separated from any others, has a characteristic hyperbolic secant-squared profile with the soliton's height proportional to κ_n^2, its width proportional to $1/\kappa_n$ and its velocity proportional to κ_n^2, just like is seen in the one-soliton solution (1.1). The reflection coefficient corresponds generally to a dispersive wave that travels to the left, opposite of the solitons.

Since the discovery of the inverse scattering transform for the KdV equation, many physically relevant equations have been shown to have Lax pairs and integrable structure [39], methods for constructing new integrable PDE and their Lax pairs were devised [1] and new techniques for rigorous analysis of the inverse scattering problems have been introduced [17]. Today, the mathematics of integrable systems touches many other areas of analysis such as the study of orthogonal polynomials [2] and integrable probability [38, 29].

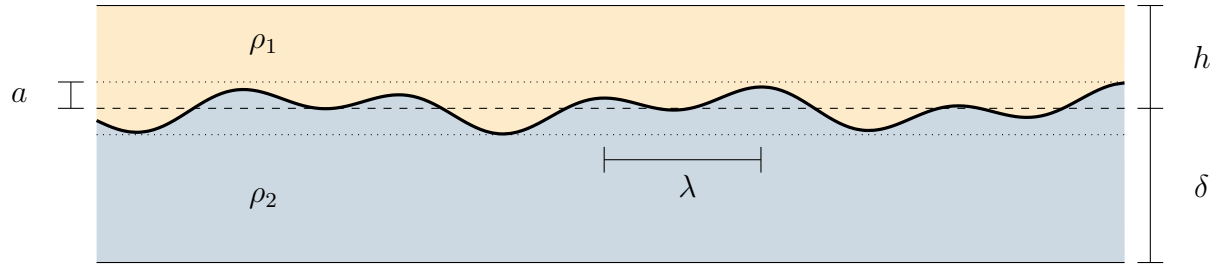


Figure 1.6: Schematic for the two dimensional incompressible and irrotational fluid system from which the ILW equation is derived. The equilibrium position (dashed black) of the thin pycnocline (solid black) between the two fluid densities (yellow and blue) are depicted above. We require the density of the top fluid ρ_1 to be less than that of the lower fluid ρ_2 so the fluids are stably separated by gravity. The system is confined between two rigid and flat surfaces, a ceiling and floor. Labeled in the schematic, h and δ are the equilibrium depths of the fluids, a is the maximum amplitude of the disturbance of the pycnocline and λ is a characteristic wavelength of the disturbance. We characterize the nonlinearity governing the dynamics of the system by the parameter $\alpha = a/h$ as well as that for the linear dispersion by $\epsilon = h/\lambda$. The ILW equation obtains in the asymptotic limit where $h \to 0^+$, δ and ϵ/α fixed with ϵ and α individually bounded. Here, the top layer is depicted with vanishing depth h while the bottom layer has fixed depth δ, but the model is independent of which layer has the fixed depth δ and which has the vanishing depth h [31].

1.2 The Intermediate Long Wave Equation

First introduced in 1977, the intermediate long wave (ILW) equation describes the long-wavelength, weakly nonlinear perturbations for a thin pycnocline boundary layer between two density striated fluids in two dimensions [24, 31, 12, 52]

$$0 = u_t + 2uu_x + T_\delta[u_{xx}] \tag{1.9}$$

where T_δ is the singular convolution operator

$$T_\delta[f](x) := \frac{1}{2\delta}\,\text{P.V.}\int_{\mathbb{R}}\left[\coth\left(\frac{\pi}{2\delta}(y-x)\right) - \operatorname{sgn}(y-x)\right] f(y)\,\mathrm{d}y\,. \tag{1.10}$$

Note that the principal value in (1.10) is with regard to the simple pole present in the kernel at $y = x$. For more specifics regarding the fluid system, see Figure 1.6.

The two extremes of the parameter $0 < \delta < \infty$ present interesting limits in the ILW equation; the behaviour T_δ in these limits is easiest to analyze in the Fourier domain due to the convolution:

$$\widehat{T_\delta[f]}(k) = -\mathrm{i}\,\tau(\delta k)\hat{f}(k) \tag{1.11}$$

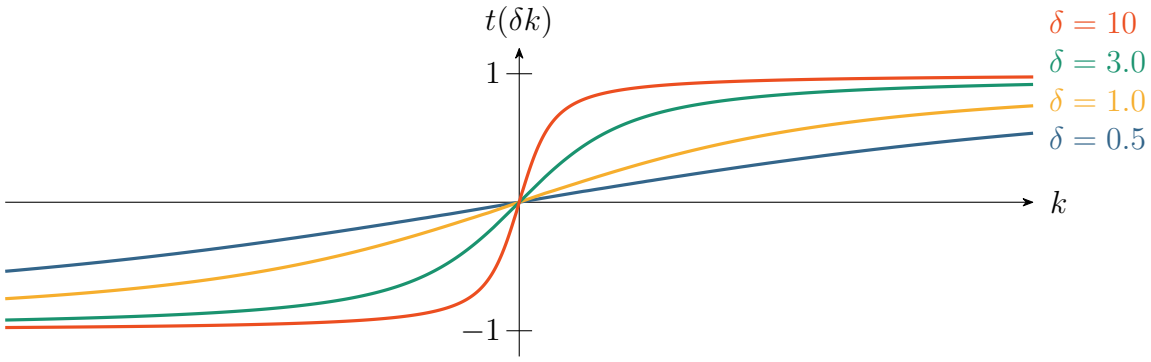


Figure 1.7: Plots of $\tau(\delta k)$, the Fourier transform of the kernel of T_δ, over the domain $k \in [-4, 4]$ and for several identified values of δ. It can be seen that for small δ, the graph becomes more linear with a diminishing slope proportional to δ. For large δ, the graph approaches a sgn function.

where

$$\tau(k) := \begin{cases} 0 & k = 0 \\ \coth(k) - \dfrac{1}{k} & k \neq 0 \end{cases}, \tag{1.12}$$

i.e. the removable singularity in τ is plugged. The behavior of $t(\delta k)$ in the two limits is depicted in Figure 1.7. As $\delta \to 0^+$, the profile of τ stretches horizontally and we can approximate using the Laurent series of hyperbolic-cotangent at zero,

$$\tau(\delta k) = \frac{\delta}{3} k + O\left(\delta^3\right), \tag{1.13}$$

uniformly on compact subsets of $k \in \mathbb{R}$. By taking an inverse Fourier transform, we see that formally the ILW equation (1.9) becomes a δ-scaled version of the KdV equation: $T_\delta[u_{xx}] = \frac{\delta}{3} u_{xxx} + O(\delta^3)$. Scaling the value of u by δ and time by $1/\delta$ as we take the limit $\delta \to 0^+$, the factor of δ on the linear dispersive term can be removed to yield the form (1.2). As $\delta \to +\infty$, the profile of τ shrinks horizontally, approaching

$$\tau(\delta k) = \operatorname{sgn}(k) + O\left(\frac{1}{\delta R}\right) \tag{1.14}$$

uniformly on $k \in \mathbb{R} \setminus [-R, R]$ with any $R > 0$. Again, by taking an inverse Fourier transform, formally $T_\delta[u_{xx}] \to H[u_{xx}]$ where H is the Hilbert transform. This is the linear dispersive term of the Benjamin-Ono (BO) equation (1.71) discussed in the Section 1.3 below. In these formal senses, the ILW equation is an interpolation between the KdV and BO equations.

The IST of the ILW equation was first laid out in 1982 by Kodama, Ablowitz and Satsuma

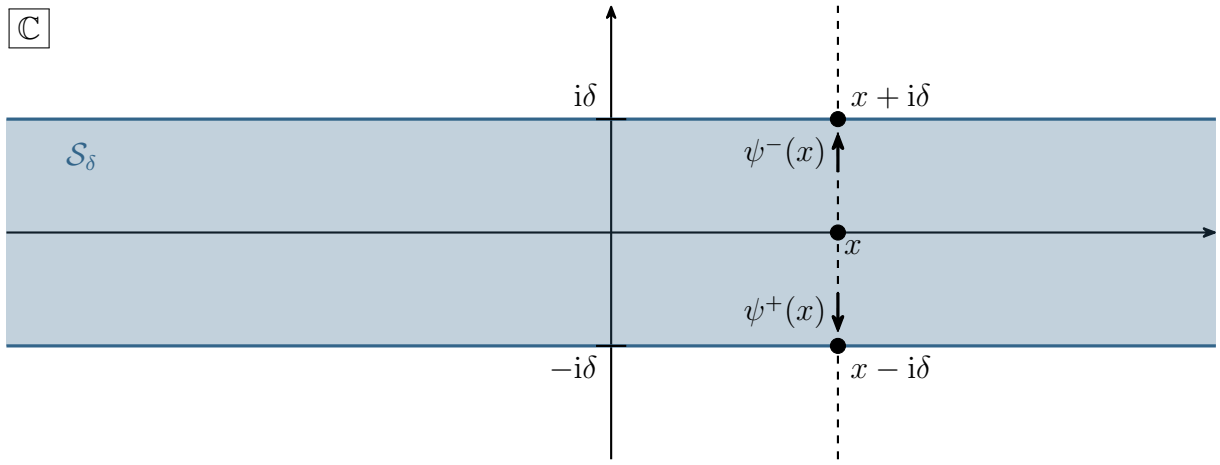


Figure 1.8: The strip domain of analyticity of the wavefunction $\psi(z)$. Also shown are the definitions of the continuous boundary values $\psi^{\pm}(x)$ via limits from inside the strip.

[27]. They gave the scattering equation as

$$-\mathrm{i}\psi_x^+(x) + (u(x) - \lambda(k))\psi^+(x) = \mu(k)\psi^-(x)\,. \tag{1.15}$$

with wavefunction $\psi : \mathcal{S}_\delta \to \mathbb{C}$ analytic on the interior of the closed complex strip denoted by

$$\mathcal{S}_\delta = \{\ z \in \mathbb{C} \mid\ -\delta \leq \mathrm{Im}\,[z] \leq \delta\ \}\,. \tag{1.16}$$

The notation $\psi^{\pm}$ in (1.15) represents the continuous boundary values of the function at the bottom and top edges of the strip:

$$\psi^{\pm}(x) := \lim_{y \to \mp\delta^{\pm}} \psi(x + iy)\,. \tag{1.17}$$

Additionally, k as the spectral parameter showing up in the equation through the functions λ and μ, which are

$$\lambda(k) := -k\coth(2\delta k) \quad \text{and} \quad \mu(k) := k\,\mathrm{csch}(2\delta k)\,. \tag{1.18}$$

The spectrum for potential u which decays to zero sufficiently fast as $x \to \pm\infty$ is reported in [27] to be continuous for real k and discrete for imaginary $k = \mathrm{i}\kappa$ with $0 < \kappa < \pi/2\delta$. The authors give a minimal justification that this indeed constitutes the spectrum, relying on the the condition of a particular Neumann series converging, which they show to be true when several norms of the potential and δ are small enough. To the knowledge of the author of this dissertation, the only other rigorous analysis of the ILW scattering equation is done

in Klipfel's dissertation [26] which sharpens the analysis in [27] and shows that the direct scattering map is well-defined for a space of small-norm potentials.

As discussed in Section 1.1, we substitute $u(x) = 0$ identically into (1.15) in order to probe the expected behavior of the wavefunction as $x \to \pm\infty$. The resulting equation can be solved exactly by an exponential ansatz: $\psi(z) = \mathrm{e}^{\mathrm{i}\sigma z}$ where

$$-\sigma - \lambda(k) = \mu(k)\mathrm{e}^{-2\delta\sigma}\,. \tag{1.19}$$

There are countably infinitely many solutions for σ to (1.19), but only two of them are identified in [27] as important by analogue with the Schrödinger operator: $\sigma = \pm k$. The rest appear to be considered extraneous by the authors. Then, for $k > 0$, these two exponential solutions are bounded and oscillatory, like the continuous spectrum of the Schrödinger operator, while for $k = \mathrm{i}\kappa$ and $\kappa > 0$, these solutions are real and exponential. Note that $\lambda(k)$ and $\mu(k)$ blow up for $k = \mathrm{i}n\pi/2\delta$ with $n \in \mathbb{Z}$, thus [27] only includes the imaginary portion around zero up to the first blow up, $\kappa \in (0, \pi/2\delta)$, in the discrete spectrum. They also define the normalization constant C_n associated to an eigenvalue κ_n by using the normalizable wavefunction ψ_n

$$\psi_n(x) = \mathrm{e}^{-\kappa_n x}\left(1 + o\left(1\right)\right) \text{ as } x \to \infty \quad \text{and then} \quad C_n^{-1} = ||\psi_n||^2_{L^2(\mathbb{R})}\,. \tag{1.20}$$

Finally, they also define a reflection coefficient in a manner analogous to that for the Schrödinger operator. As we will not be needing the reflection coefficient in this work, we direct the reader to [27] for the exact formulation. These three constituent quantities, the eigenvalues, norming constants and reflection coefficient, make up the formal ILW scattering data.

A more useful reformulation of the ILW scattering equation, which also appears in [27], requires the substitution

$$\psi(z) = \mathrm{e}^{\mathrm{i}kz}\phi(z) \tag{1.21}$$

which, plugging into (1.15) yields, after some rearranging

$$-\mathrm{i}\phi^+_x(x) - u(x)\phi^+(x) = \zeta(k)\left(\phi^+(x) - \phi^-(x)\right) \tag{1.22}$$

where $\zeta(k)$ is given by

$$\zeta(k) := k - \lambda(k) = \mu(k)\mathrm{e}^{2\delta k} = \frac{k}{1 - \mathrm{e}^{-4\delta k}}\,. \tag{1.23}$$

It turns out that in some senses, ζ is a preferred spectral parameter over k. If we use the

definitions above of the discrete and continuous spectrums for k, we can see that, in the ζ complex plane, the continuous spectrum lies on the positive, real axis while the discrete spectrum lies on the central connected component of a δ-scaled version of the quadratrix of Hippias [5] with parameterization given by

$$\zeta(\mathrm{i}\kappa) = \kappa\cot(2\delta\kappa) + \mathrm{i}\kappa = \kappa\csc(2\delta\kappa)\mathrm{e}^{\mathrm{i}2\delta\kappa}\,. \tag{1.24}$$

The quadratrix of Hippias is the curve in the complex plane where the argument is equal to the imaginary part. It consists of an infinite vertical stack of continuous components, one for each branch of the argument function. The central connected component, henceforth just the quadratrix, is the one that corresponds to the principal argument. The quadratrix crosses the real axis at the value 1 and is depicted in Figure 1.9. To be accurate, the true quadratrix is parameterized by $2\delta\zeta(\mathrm{i}\kappa)$ for $-\pi/2\delta < \kappa < \pi/2\delta$, but since a value of δ is always implied in an ILW context, we will use the term quadratrix to refer to both the true quadratrix and the $1/2\delta$-scaled version,

$$\mathcal{Q}_\delta := \left\{\ \zeta(\mathrm{i}\kappa)\ \middle|\ -\frac{\pi}{2\delta} < \kappa < \frac{\pi}{2\delta}\ \right\}, \tag{1.25}$$

in which the discrete ζ-spectrum lies. It will be clear from context which we are referring to. We will also need to distinguish the portion with positive imaginary part $\mathcal{Q}_{\delta+}$ from the portion with negative imaginary part $\mathcal{Q}_{\delta-}$ so that $\mathcal{Q}_\delta = \mathcal{Q}_{\delta-} \cup \{1/2\delta\} \cup \mathcal{Q}_{\delta+}$. Lastly, we also define an interval notation for arcs along the quadratrix, i.e. for $\eta, \xi \in \mathcal{Q}_\delta$ such that $\mathrm{Im}\,[\eta] < \mathrm{Im}\,[\xi]$,

$$(\eta, \xi)_{\mathcal{Q}_\delta} = \{\ \zeta(\mathrm{i}\kappa) \mid \mathrm{Im}\,[\eta] < \kappa < \mathrm{Im}\,[\xi]\ \}\ , \tag{1.26}$$

and with the usual square bracket interchanges made to denote inclusion of the endpoints in the arc.

Kodama, Ablowitz and Satsuma continue in [27], formally dictating the inverse scattering problem via a GLM equation governing the reconstruction of the potential to the ILW scattering equation. For the case of a zero reflection coefficient and $N \in \mathbb{N}$ distinct eigenvalues $\{\zeta_n\}_{n=1}^N \subset \mathcal{Q}_{\delta+}$ with their associated norming constants $\{C_n\}_{n=1}^N \subset \mathbb{R}_+$, the GLM equation can be solved explicitly; the solution they write as the N-soliton formula,

$$u_N^{\mathrm{ILW}}(x,t) = -\mathrm{i}\partial_x \ln\det\left(\frac{\mathrm{I}_N + \Delta_N(x+\mathrm{i}\delta, t)}{\mathrm{I}_N + \Delta_N(x-\mathrm{i}\delta, t)}\right)\ , \tag{1.27}$$

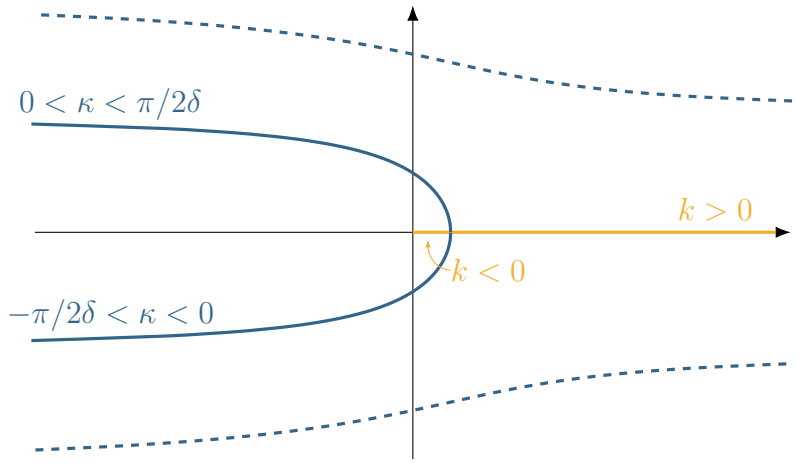


Figure 1.9: The ILW scattering equation spectrum in the ζ plane. The blue contours are the visible portion of the quadratrix of Hippias, solid for the quadratrix and dashed for the other disconnected branches. The discrete spectrum shows up on the quadratrix and the continuous spectrum is labeled in solid yellow.

where Δ_N is an $N \times N$ matrix defined element-wise for $z \in \mathbb{C}$ and $t \in \mathbb{R}$ by

$$[\Delta_N(z,t)]_{n\,\ell} = C_n C_\ell \, \mathrm{i} \frac{\exp\left(-\mathrm{Im}\left[\zeta_n + \zeta_\ell\right] z - \mathrm{Im}\left[\left(\zeta_n - \frac{1}{2\delta}\right)^2 + \left(\zeta_\ell - \frac{1}{2\delta}\right)^2\right] t\right)}{\zeta_\ell - \zeta_n^*}, \quad (1.28)$$

where $1 \leq n, \ell \leq N$. The definition of $\Delta_N(z,t)$ (1.28) differs from that reported in [27] by a matrix similarity transformation. Because of the determinants in (1.27), the two matrix definitions yield identical ILW solutions. A small note on the notation: the matrix "division" in (1.27) is shorthand for the multiplication by the inverse and, due to the determinant operation, the ordering of this matrix multiplication is irrelevant, hence the notation. Finally, it will be a useful fact that the $\Delta_N(z,t)$ matrix (1.28) has a particular factorization

$$\Delta_N(z,t) = D_N(z,t)\; C_N \; D_N(z,t)\,, \quad (1.29)$$

where the $N \times N$ matrix $D_N(z,t)$ is diagonal and carries all of the z and t dependence,

$$[D_N(z,t)]_{n\,n} = C_n^{1/2} \exp\left(-\mathrm{Im}\left[\zeta_n\right] z - \mathrm{Im}\left[\left(\zeta_n - \frac{1}{2\delta}\right)^2\right] t\right) \quad (1.30)$$

for all $1 \leq n \leq N$, and C_N is an $N \times N$ Cauchy matrix,

$$[C_N]_{n\,\ell} = \frac{\mathrm{i}}{\zeta_\ell - \zeta_n^*} \quad (1.31)$$

for all $1 \leq n, \ell \leq N$.

Now while this N-soliton formula was derived by Kodama, Ablowitz and Satsuma from a formal GLM equation [27], Matsuno has shown that it is indeed an exact solution of the ILW equation [42, Chapter 5]. However, just looking at the N-soliton formula (1.27), the reader may not be convinced that the logarithmic-derivative is nonsingular where it needs to be evaluated. We can show this by providing a nonzero lower bound to the absolute value $|\det(\mathrm{I}_N + \Delta_N(z,t))|$ for all $z \in \mathcal{S}_\delta$ and $t \in \mathbb{R}$. This bound that will also be important to our evaluation of the N-soliton formula in Chapter 3.

Lemma 1.2.1. *Let $N \in \mathbb{N}$, $\{\zeta_n\}_{n=1}^N \subset \mathcal{Q}_{\delta+}$ be a distinct set of eigenvalues, and $\{C_n\}_{n=1}^N \subset \mathbb{R}_+$ a set of norming constants. Then, for all $t \in \mathbb{R}$ and $z \in \mathcal{S}_\delta$ with*

$$h := \frac{\pi}{2 \max\limits_{1 \leq n \leq N} \mathrm{Im}\left[\zeta_n\right]}, \tag{1.32}$$

the principal argument of any eigenvalue λ of $\Delta_N(z,t)$ is bounded by

$$0 \leq -\operatorname{sgn}(\mathrm{Im}\left[z\right]) \arg(\lambda) \leq \frac{\pi}{h} \left|\mathrm{Im}\left[z\right]\right|. \tag{1.33}$$

From this, it follows that $\det\left(\mathrm{I}_N + \Delta_N(z,t)\right)$ is bounded below in magnitude by

$$0 < \left[d\left(\frac{\pi \left|\mathrm{Im}\left[z\right]\right|}{h}\right)\right]^N \leq \left|\det\left(\mathrm{I}_N + \Delta_N(z,t)\right)\right|, \tag{1.34}$$

where

$$d(\theta) := \begin{cases} 1 & 0 \leq \theta \leq \frac{\pi}{2} \\ \sin\theta & \frac{\pi}{2} < \theta \leq \pi \end{cases}. \tag{1.35}$$

Additionally, the argument of $\det\left(\mathrm{I}_N + \Delta_N(z,t)\right)$ has the bounds

$$0 \leq -\operatorname{sgn}(\mathrm{Im}\left[z\right]) \arg\Big(\det\left(\mathrm{I}_N + \Delta_N(z,t)\right)\Big) \leq N\frac{\pi}{h}\left|\mathrm{Im}\left[z\right]\right|, \tag{1.36}$$

where the argument here is defined to be zero when $z \in \mathbb{R}$ and continuous for the rest of $z \in \mathcal{S}_\delta$.

Proof. Assume the hypothesis and let $x, t \in \mathbb{R}$ while $-\delta \leq y \leq \delta$. We begin by using the

factorization (1.29) to peel off the matrix multiplicative contributions dependent on y,

$$\Delta_N(x+\mathrm{i}y,t) = D_N(x+\mathrm{i}y,t)\ C_N\ D_N(x+\mathrm{i}y,t) \tag{1.37}$$

$$= \exp(-\mathrm{i}Ky)\ D_N(x,t)\ C_N\ D_N(x,t)\ \exp(-\mathrm{i}Ky) \tag{1.38}$$

$$= \exp(-\mathrm{i}Ky)\ \Delta_N(x,t)\ \exp(-\mathrm{i}Ky)\ , \tag{1.39}$$

where K is the $N\times N$ diagonal matrix carrying the $\mathrm{Im}\,[\zeta]$ values, $K_{nn} := \mathrm{Im}\,[\zeta_n]$ for all $1\le n\le N$. Let λ be an eigenvalue of $\Delta_N(x+\mathrm{i}y,t)$, then it follows by matrix similarity that it is also an eigenvalue of the matrix

$$A := \exp(-\mathrm{i}Ky)\ \Delta_N(x+\mathrm{i}y,t)\ \exp(\mathrm{i}Ky) = \exp(-\mathrm{i}2Ky)\ \Delta_N(x,t)\,. \tag{1.40}$$

It is clear that the exponential matrix on the right of (1.40) is unitary. Now we want to show $\Delta_N(x,t)$ is positive-definite. This is easily seen by taking the determinants of the principal minors $\det \mathrm{Minor}_S(\Delta_N(x,t))$, where $S\subset\mathbb{Z}_N$ is the index set of a chosen matrix minor. Since the left and right matrices in the decomposition (1.29) are diagonal, it follows that this decomposition is also valid for any principal minor,

$$\mathrm{Minor}_S(\Delta_N(x,t)) = \mathrm{Minor}_S(D_N(x,t))\ \mathrm{Minor}_S(C_N)\ \mathrm{Minor}_S(D_N(x,t))\ . \tag{1.41}$$

The determinant of $\mathrm{Minor}_S(D_N(x,t))$, being diagonal, is easy to compute. For the Cauchy matrix, $\mathrm{Minor}_S(C_N)$, the determinant is also known:

$$\det\mathrm{Minor}_S(C_N) = \frac{\displaystyle\prod_{n<\ell\in S}(-\mathrm{i}\zeta_\ell+\mathrm{i}\zeta_n)(-\mathrm{i}\zeta_n^*+\mathrm{i}\zeta_\ell^*)}{\displaystyle\prod_{n,\ell\in S}(-\mathrm{i}\zeta_n+\mathrm{i}\zeta_\ell^*)} = \prod_{n\in S}\frac{1}{2\kappa_n}\prod_{n<\ell\in S}\frac{|\zeta_\ell-\zeta_n|^2}{|\zeta_\ell-\zeta_n^*|^2}\,. \tag{1.42}$$

Together, we have the determinant of any principal minor $\det \mathrm{Minor}_S\left(\Delta_N(x,t)\right)$ as

$$\begin{aligned}
\det \mathrm{Minor}_S\left(\Delta_N(x,t)\right) &= \det\left(\mathrm{Minor}_S\left(D_N(z,t)\right)\right)^2 \ \det\left(\mathrm{Minor}_S\left(C_N\right)\right) && (1.43)\\
&= \left(\prod_{n\in S} C_n \exp\left(-2\mathrm{Im}\left[\zeta_n\right] z - 2\mathrm{Im}\left[\left(\zeta_n - \frac{1}{2\delta}\right)^2\right] t\right)\right) \\
&\qquad \times \left(\prod_{n\in S} \frac{1}{2\kappa_n} \prod_{n<\ell\in S} \frac{\left|\zeta_\ell - \zeta_n\right|^2}{\left|\zeta_\ell - \zeta_n^*\right|^2}\right) && (1.44)\\
&= \exp\left(-2\sum_{n\in S}\left(\mathrm{Im}\left[\zeta_n\right] z + \mathrm{Im}\left[\left(\zeta_n - \frac{1}{2\delta}\right)^2\right] t\right)\right) \\
&\qquad \times \prod_{n\in S} \frac{C_n^2}{2\kappa_n} \prod_{n<\ell\in S} \frac{\left|\zeta_\ell - \zeta_n\right|^2}{\left|\zeta_\ell - \zeta_n^*\right|^2}\,. && (1.45)
\end{aligned}$$

The determinants of every $\mathrm{Minor}_S\left(\Delta_N(x,t)\right)$, as calculated in (1.45), are manifestly positive since $x, t \in \mathbb{R}$. Applying Sylvester's criterion, we have demonstrated $\Delta_N(x,t)$ is positive definite. Now, for each distinct eigenvalue λ, we have at least one eigenvector $v \in \mathbb{C}^N$ of the similar matrix A. Consider the calculation:

$$\begin{aligned}
|\lambda|\ ||v|| &= ||\lambda\ v|| && (1.46)\\
&= ||A\ v|| && (1.47)\\
&= ||\exp\left(-\mathrm{i}2Ky\right)\ \Delta_N(x,t)\ v|| && (1.48)\\
&= ||\Delta_N(x,t)\ v||\ . && (1.49)
\end{aligned}$$

Since $||v|| \neq 0$, due to the definition of an eigenvector, and $||\Delta_N(x,t)\ v|| \neq 0$ due to positive-definiteness, we have

$$|\lambda| = \frac{||\Delta_N(x,t)\ v||}{||v||} > 0\,. \tag{1.50}$$

This means, all of the eigenvalues of $\Delta_N(x+\mathrm{i}y,t)$ are nonzero, that is, the arguments are well-defined. For simplicity, let $u = \Delta_N(x,t)\,v$ and consider

$$\begin{aligned}
\lambda\, u^\dagger v &= u^\dagger\ (\lambda\, v) && (1.51)\\
&= u^\dagger\, A\, v && (1.52)\\
&= u^\dagger\ \exp\left(\mathrm{i}2Ky\right)\ \Delta_N(x,t)\ v && (1.53)\\
&= u^\dagger\ \exp\left(\mathrm{i}2Ky\right)\ u\,. && (1.54)
\end{aligned}$$

We first note that, again, since $\Delta_N(x,t)$ is positive definite,

$$u^\dagger v = v^\dagger \ \Delta_N(x,t) \ v > 0\,. \tag{1.55}$$

Thus, the principal argument of λ must coincide with the principal argument of the right side of (1.54). We divide by the nonzero and real $||u||^2$ and then can simplify this using the diagonal form of K and the components of u, $u_n \in \mathbb{C}$ for $1 \le n \le N$,

$$\arg(\lambda) = \arg\left(\frac{\lambda\ u^\dagger v}{||u||^2}\right) = \arg\left(\frac{u^\dagger\ \exp\left(-\mathrm{i}2Ky\right)\ u}{||u||^2}\right) = \arg\left(\sum_{n=1}^{N} \mathrm{e}^{-\mathrm{i}2\mathrm{Im}[\zeta_n]y}\frac{|u_n|^2}{||u||^2}\right)\,. \tag{1.56}$$

We note from the conjugate symmetry of the phases across $y = 0$, we have

$$\arg(\lambda) = \left\{ \begin{array}{cc} -\arg\left(\sum_{n=1}^{N} \mathrm{e}^{\mathrm{i}2\mathrm{Im}[\zeta_n]|y|}\frac{|u_n|^2}{||u||^2}\right) & \text{if } y > 0 \\ 0 & \text{if } y = 0 \\ \arg\left(\sum_{n=1}^{N} \mathrm{e}^{\mathrm{i}2\mathrm{Im}[\zeta_n]|y|}\frac{|u_n|^2}{||u||^2}\right) & \text{if } y < 0 \end{array} \right\} = -\,\mathrm{sgn}(y)\arg\left(\sum_{n=1}^{N} \mathrm{e}^{\mathrm{i}2\mathrm{Im}[\zeta_n]|y|}\frac{|u_n|^2}{||u||^2}\right)\,. \tag{1.57}$$

From the definition of h, for all $1 \le n \le N$,

$$0 \le 2\mathrm{Im}\left[\zeta_n\right]|y| \le 2\left(\max_{j\in\mathbb{Z}_N}\mathrm{Im}\left[\zeta_j\right]\right)|y| = \frac{\pi}{h}|y|\,. \tag{1.58}$$

Since $\{\zeta_n\}_{n=1}^N \subset \mathcal{Q}_{\delta+}$, we have

$$h = \frac{\pi}{2\max\limits_{1\le n\le N}\mathrm{Im}\left[\zeta_n\right]} > \frac{\pi}{2(\pi/2\delta)} = \delta\,. \tag{1.59}$$

This confines all of the phases to the sector

$$0 \le 2\mathrm{Im}\left[\zeta_n\right]|y| \le \frac{\pi}{h}|y| < \pi\,. \tag{1.60}$$

Since the sum in (1.57) is a weighted average of phases, due to the fact that

$$\frac{|u_n|^2}{||u||^2} \ge 0 \quad \text{for all} \quad 1 \le n \le N \quad \text{and} \quad \sum_{n=1}^{N}\frac{|u_n|^2}{||u||^2} = 1\,, \tag{1.61}$$

by convexity of sectors with angle less than π, it follows that the weighted average of the

phases is also contained in the sector and therefore shares the principal argument bounds

$$0 \leq \arg\left(\sum_{n=1}^{N} \mathrm{e}^{\mathrm{i}2\mathrm{Im}[\zeta_n]|y|} \frac{|u_n|^2}{||u||^2}\right) \leq \frac{\pi}{h}|y| < \pi\,. \tag{1.62}$$

Relating this to the principal argument of λ by (1.57), and accounting for the factor of $-\operatorname{sgn}(y)$ there, we have arrived at the bound (1.33).

Now we wish to bound below $\det\left(\mathrm{I}_N + \Delta_N(x+\mathrm{i}y,t)\right)$ in magnitude. Noting that this is the characteristic polynomial of the matrix evaluated at one, we can let $\{\lambda_n\}_{n=1}^N$ be the set of eigenvalues (not necessarily distinct, duplicates accounting for algebraic multiplicity of the root) and we have

$$|\det(\mathrm{I}_N + \Delta(x+\mathrm{i}y,t)| = \prod_{n=1}^{N} |1+\lambda_n|\,. \tag{1.63}$$

For each factor above, we can bound them below by using the principal argument bound (1.33). For each $1 \leq n \leq N$,

$$|1+\lambda_n|^2 = \left|1 + |\lambda_n| \mathrm{e}^{\mathrm{i}\arg(\lambda_n)}\right|^2 \tag{1.64}$$

$$= 1 + 2|\lambda_n|\cos\left(|\arg(\lambda_n)|\right) + |\lambda_n|^2. \tag{1.65}$$

Subject to the constraints $0 \leq |\arg(\lambda_n)| \leq \pi|y|/h < \pi$, the expression is always minimized for fixed $|\lambda_n| \geq 0$ at the right end:

$$|1+\lambda_n|^2 \geq 1 + 2|\lambda_n|\cos\left(\frac{\pi|y|}{h}\right) + |\lambda_n|^2 \tag{1.66}$$

$$= \left(|\lambda_n| + \cos\left(\frac{\pi|y|}{h}\right)\right)^2 + \sin^2\left(\frac{\pi|y|}{h}\right)\,. \tag{1.67}$$

If $|y| < h/2$, then $\cos(\pi|y|/h) > 0$ and the quadratic is strictly increasing for $|\lambda_n| \geq 0$, thus the minimum is obtained at $|\lambda_n| = 0$, which has the value one. If $h/2 \leq |y| \leq h$, then $\cos(\pi|y|/h) \leq 0$ and the quadratic has its minimum at $|\lambda_n| = -\cos(\pi|y|/h)$, which has the value $\sin^2(\pi|y|/h)$. These are the only two cases that need to be considered since by assumptions and (1.59) $|y| \leq \delta < h$. Putting these cases together and taking the positive square-root, we have from the definition (1.35)

$$|1+\lambda_n| \geq d\left(\frac{\pi|y|}{h}\right)\,. \tag{1.68}$$

Using this bound for each factor in (1.63), we get the desired right inequality in (1.34).

The left inequality in (1.34) follows from the fact that $d(\theta) > 0$ for all $0 \leq \theta < \pi$ and $\pi|y|/h \leq \pi\delta/h < \pi$ by (1.59).

Lastly, because of the left inequality in (1.34), the argument of $\det(\mathrm{I}_N + \Delta_N(\diamond, t))$ can be defined to be continuous throughout the strip $\mathcal{S}_\delta$. Moreover, since $\Delta_N(x,t)$ is positive definite, $\det(\mathrm{I}_N + \Delta_N(x,t)) > 0$, and so the argument can be taken to be zero on the real line. Because the eigenvalues λ_n must be continuous and positive on the real line, we can compute the argument of the determinant according to

$$\arg\left(\det\left(\mathrm{I}_N + \Delta_N(x+\mathrm{i}y,t)\right)\right) = \sum_{n=1}^{N} \arg(1+\lambda_n)\,. \tag{1.69}$$

From a simple geometric argument involving the phase bounds of λ_n (1.33), we can demonstrate that

$$0 \leq -\operatorname{sgn}(y)\arg(1+\lambda_n) \leq -\operatorname{sgn}(y)\arg(\lambda_n) \leq \frac{\pi}{h}|y|\,, \tag{1.70}$$

which, with (1.69), gives the bound (1.36). □

To convince the reader that indeed the N-soliton formula is well-defined, we note that, since $\det(\mathrm{I}_N + \Delta_N(z,t))$ is clearly analytic on $z \in \mathcal{S}_\delta$ for all $t \in \mathbb{R}$. Then, on any open set in z where the determinant is nonzero, $\log\det(\mathrm{I}_N + \Delta_N(z,t))$ is also analytic. If we take the open set to be the interior of the strip $\mathcal{S}_h$ with h as in (1.32), then the bound (1.34) demonstrates exactly that the determinant $\det(\mathrm{I}_N + \Delta_N(z,t))$ is nonzero here. , and so $\log\det(\mathrm{I}_N + \Delta_N(z,t))$ is analytic for all $z \in \mathcal{S}_\delta$. The N-soliton formula (1.27) is well-defined for all $x, t \in \mathbb{R}$ and can be computed as the difference between the derivatives of this analytic function at the boundaries of $\mathcal{S}_\delta$.

1.3 The Benjamin-Ono Equation

First introduced in 1967, the Benjamin-Ono (BO) equation describes the long-wavelength, weakly nonlinear perturbations for a thin pycnocline boundary layer against a rigid flat surface with an infinite total depth of the fluid system [4],

$$0 = u_t + 2uu_x + H\left[u_{xx}\right]\,, \tag{1.71}$$

where H is the Hilbert transform

$$H[f](x) := \frac{1}{\pi}\mathrm{P.V.}\int_{\mathbb{R}} \frac{f(y)}{y-x}\,\mathrm{d}y\,. \tag{1.72}$$

Benjamin showed that (1.71) admitted a family of solitons which have Lorentzian profiles [4],

$$u(x,t) = \frac{2\lambda}{\lambda^2 \left(x - \lambda t + x_0\right)^2 + 1}, \tag{1.73}$$

with $\lambda > 0$ a parameter and $x_0 \in \mathbb{R}$ the initial position. A little later, in 1975, Ono made a connection with the integrable structure of this equation and derived several conserved quantities [49]. Today, it is known to be integrable by Lax pair [52].

The Benjamin-Ono inverse scattering transform has been analyzed in some simple cases [55, 43, 44], but, like ILW, has yet to be put on rigorous foundations. For a full explanation of the Benjamin-Ono IST, we direct the reader to [52]. In this work, we need not introduce the IST to the uninitiated reader because recently an explicit formula for solving the Benjamin-Ono equation has been discovered by Gérard [23]. In essence, this solution formula bypasses the inverse scattering transform for the Benjamin-Ono equation. Considering again the analogue between the IST and solving a linear PDE by Fourier transform (see Figure 1.5), this new result is comparable to solving the heat equation by convolving the initial condition with a Gaussian kernel. The formula reads as follows: for $u \in C(H^2_r(\mathbb{R}), \mathbb{R})$, where $H^2_r(\mathbb{R})$ is the Sobolev space of real valued functions with two derivatives in L^2, and $u(0) = u_0$, then $u(t) = \Pi u(t) + (\Pi u(t))^*$, with Π denoting the orthogonal projection of L^2 onto L^2_+, the space of L^2 functions with Fourier transforms supported on the positive half-line, and

$$\Pi u(z,t) = \frac{1}{2\mathrm{i}\pi} I_+[(G + 2tL_{u_0} - z\mathrm{Id})^{-1}\Pi u_0] \tag{1.74}$$

for all $z \in \mathbb{C}^+$. I_+ denotes the limit of the Fourier transform at zero from the right, G is the $L^2_+(\mathbb{R})$ adjoint of the operator of the multiplication by the independent variable, and L_{u_0} is the semi-bounded selfadjoint operator defined by $L_{u_0} f = -\mathrm{i}\partial_x f + \Pi(u_0 f)$.

Remarkably, the application of this formula to real rational initial data is tractable [7], reducing to analyzing a linear ordinary differential equation and a finite linear system. We write this solution and analyze the behavior in a particular regime in Chapter 4.

1.4 The Small Dispersion Limit and Universality

In the KdV, ILW and BO equations, we introduce the small dispersion limit by conducting a spacetime scaling,

$$\begin{cases} x \to x/\epsilon \\ t \to t/\epsilon \end{cases}, \tag{1.75}$$

where $\epsilon > 0$ and is thought of as a small parameter. Under this change of variables, the equations (1.2), (1.9) and (1.71) each take on their small dispersion forms

$$0 = u_t + 2uu_x + \frac{\epsilon^2}{3}u_{xxx}\,, \tag{1.76}$$

$$0 = u_t + 2uu_x + \epsilon T_{\delta\epsilon}[u_{xx}]\,, \tag{1.77}$$

$$0 = u_t + 2uu_x + \epsilon H[u_{xx}]\,, \tag{1.78}$$

respectively. The meaning of "small dispersion" is now clear: the small parameter ϵ shows up in front of (and in the cases of the ILW equation (1.77), inside) the dispersive terms. The *small dispersion limit* then refers to studying the solution $u(x,t;\epsilon)$ to the Cauchy problem for an initial condition independent of ϵ

$$u(x,0;\epsilon) = u_0(x) \tag{1.79}$$

as $\epsilon \to 0^+$, at any time $t > 0$.

If, in a first attempt to make progress, we set $\epsilon = 0$ in (1.76), (1.77) and (1.78), we recover the same nonlinear equation, known as invicid Burgers' equation [3, 10]

$$0 = u^{\mathrm{B}}_t + 2u^{\mathrm{B}}u^{\mathrm{B}}_x\,. \tag{1.80}$$

The superscript B here is just to distinguish the solutions to invicid Burgers' equation from those of the KdV, ILW and Benjamin-Ono equations. The Cauchy problem of invicid Burgers' equation is classical and is solved by the method of characteristics, where trajectories (also "characteristics") are introduced in spacetime $x = y(t)$ in order to form a coupled system of ordinary differential equations (ODE) determining both the trajectories and the value of the solution along them $u^{\mathrm{B}}(y(t),t)$. For invicid Burgers', the resulting ODE yields trajectories with constant speed on which the value of the solution does not change:

$$y(t) = y_0 + 2u_0(y_0)t, \tag{1.81}$$

$$u^{\mathrm{B}}(t) := u^{\mathrm{B}}\big(y(t),t\big) = u_0(y_0)\,, \tag{1.82}$$

for any $y_0 \in \mathbb{R}$. Interpreted graphically, the levels of the solution travel at constant speeds which are exactly twice the value of the level. If we wish to know the solution at the spacetime point (x,t), we simply need to solve the implicit equation

$$x = y + 2u_0(y)t \tag{1.83}$$

for y to determine the origin point of a characteristic which has traveled to the point (x,t). However, this may fail to have a unique solution if multiple characteristics happen to travel through the point (x,t). For invicid Burgers' equation, this always happens when u_0 has a section where it decreases, since the difference in speeds between a higher and lower levels is always positive. If u_0 is differentiable, it can be shown that the maximum time when the solution described by the characteristics is single valued everywhere is

$$t_{\mathrm{c}} := \frac{1}{\max\limits_{x\in\mathbb{R}} \big\{ -2u_0'(x) \big\}} > 0\,. \tag{1.84}$$

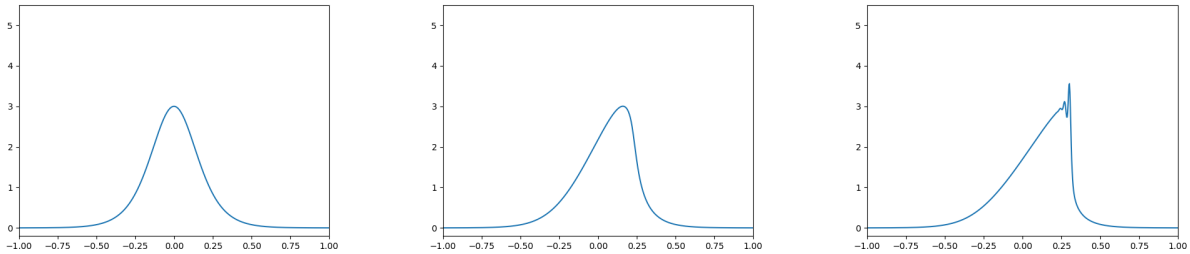
At this *break time*, a *gradient catastrophe* occurs: the slope becomes infinite at a point. After this time, the solution as described by the characteristics "folds over" generating a multivalued "solution," i.e. the individual branches of the multivalued function are still solutions of invicid Burgers' equation on their spacetime regions of definition, but a single-valued global solution ceases to exist.

Since for $\epsilon > 0$, (1.76), (1.77) and (1.78) are all integrable, we expect the solutions to be well-defined for all time, so the small, but nonzero, dispersive term must regulate the gradient catastrophe. We can gain some intuition by looking at some simple numerical simulations of the KdV equation: Figure 1.10. We see that for small ϵ and before break time (Figures 1.10a and 1.10b), the numerical solution exhibits the shearing behavior of invicid Burgers' equation, as all the positive levels travel to the right and the higher ones travel faster than the lower ones. At just about the invicid Burgers' break time $t = t_{\mathrm{c}}$ (Figure 1.10c), we see the emergence of a localized, highly oscillatory feature. Beyond break time (Figure 1.10f), the solution exhibits a *dispersive shock wave*, an extended region of space where the solution rapidly oscillates.

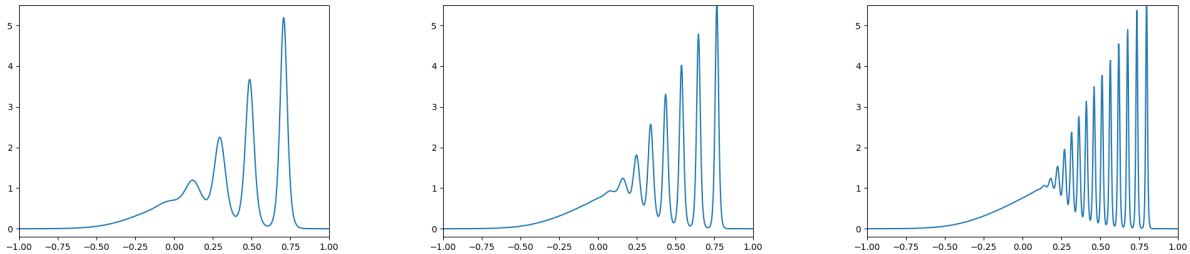
It appears that as ϵ is decreased, the wavelength of the dispersive shock wave decreases too (Figures 1.10d, 1.10e, and 1.10f). This can be understood if we look at how the small dispersion scaling (1.75) impacts the inverse scattering transform through the Lax pair (1.3)

$$L_\epsilon = -\epsilon^2 \frac{\partial^2}{\partial x^2} - u \quad \text{and} \quad B_\epsilon = -\epsilon^3 \frac{4}{3}\frac{\partial^3}{\partial x^3} - 2\epsilon u \frac{\partial}{\partial x} - \epsilon u_x\,. \tag{1.85}$$

Again, L_ϵ can be recognized as the Schrödinger operator but now with $\hbar^2/2m = \epsilon^2$. This means, the small dispersion limit of the KdV has as its scattering equation the semi-classical limit of the time-independent Schrödinger equation. As is well known from a Wentzel–Kramers–Brillouin (WKB) analysis, for potential $-u < 0$ the number of eigenvalues of the Schrödinger operator increases like $1/\epsilon$, the asymptotic description of which is known as the *Weyl law*. The soliton profiles (1.1), after the small dispersion scaling (1.75),



(a) $\epsilon = 0.01$, $t = 0.00$ (b) $\epsilon = 0.01$, $t = 0.04$ (c) $\epsilon = 0.01$, $t = 0.07$



(d) $\epsilon = 0.04$, $t = 0.26$ (e) $\epsilon = 0.02$, $t = 0.26$ (f) $\epsilon = 0.01$, $t = 0.26$

Figure 1.10: Fourier split-step simulation of the KdV equation in the small dispersion limit. The first row is at different times before and at critical while the second row shows the effect of decreasing ϵ at fixed time.

have a width proportional to ϵ. Thus, for $\epsilon > 0$, the solution in Figure 1.10 can be thought of as an ensemble of a large number of solitons, coherently superimposed and which reproduce invicid Burgers' equation at first, and then after some solitons eventually become separated, generate a dispersive shock wave formed of rank-ordered solitons.

1.4.1 Overview of Previous Results

In 1983, Lax and Levermore analyzed in extensive detail the asymptotic solution of the small dispersion limit for the KdV equation with a positive "single lobe" (sufficiently smooth, single maximum, and decays to zero at infinity) initial condition u_0 [34, 35, 36]. Their investigation led to the description of the KdV solution via a two-dimensional electrostatic optimization problem dependent on x and t as parameters. They were able to show that the small dispersion limit for $0 \leq t < t_c$ approaches invicid Burgers' solution in an L^2 sense. For $t \geq t_c$, they were able to give a formula which the solution approaches in a weak-L^2 sense, essentially describing the spatial average of the dispersive shock wave without resolving the rapid oscillations themselves. Additionally, they confirmed the validity of Whitham's averaged equations [54], a general scheme for describing modulated wave trains in a broad class of PDE.

In 1990, Venakides [53] went beyond the Lax-Levermore theory to formally construct the strong asymptotics of the rapidly oscillating soliton train after the wave breaking by considering the next-to-leading order correction in ϵ. Considering step-like initial conditions u_0, i.e. those that limit to a positive level as $x \to -\infty$ and zero as $x \to +\infty$, his solution was given in terms of a multiperiodic theta function for a Riemann surface that had been studied ten years earlier in the context of KdV modulated wave trains by Flaschka, Forest and McLaughlin [21]. Soon after, Deift, Venakides and Zhou [16] made these results more rigorous, this time for negative single lobe initial conditions, using the Riemann-Hilbert formulation of the KdV inverse scattering problem and Deift and Zhou's new nonlinear steepest descent method for Riemann-Hilbert problems [17]. The problem of rigorous asymptotics for positive single lobe initial conditions, like Lax and Levermore considered and which has a large number of discrete eigenvalues in the semi-classical limit, remains open today.

The work on the small dispersion limit of the BO equation has differed significantly from Lax and Levermore's analysis for the KdV equation. Due to its particular character, a WKB analysis is not tractable for the semi-classical limit of the BO scattering equation. Despite this difficulty, in 1981 an ingenious solution was proposed by Matsuno to calculate the Weyl law using physical justification and the infinitely many conserved quantities of the BO equation [41]. In the small dispersion limit, the resulting identities lead to a moment

problem for the density of the eigenvalues in terms of integrals of powers of the initial condition. Inverting the relationship, Matsuno arrived at a BO Weyl law. More recently, Xu completed the story for the weak small dispersion limit for BO in his 2010 thesis [45, 55]. For a positive single lobe initial condition, Xu showed that, for a particular ansatz of the BO scattering data, indeed the weak solution was governed by invicid Burgers' equation before break time and was given by an alternating sum of the Burgers' branches after break time. Matsuno's Weyl law and Xu's ansatz were later rigorously justified for the case of rational bell-shaped initial data in [43, 44].

Compared to the KdV and BO equations, relatively little work has been done on the small dispersion limit of the ILW equation. In 1994, Miloh and Minzoni conducted a WKB-style formal analysis on the semi-classical limit of the ILW scattering equation with a negative single lobe potential [46]. Their analysis provides a Weyl law for the ILW scattering equation.

In addition to these results, there are several conjectures about universal behaviour of the small dispersion limits of these equations. Specifically, these all take the form of considering the solution for a broad class of initial conditions in an ϵ-shrinking spacetime region around the point of invicid Burgers' gradient catastrophe. The solution is then expected to take a particular functional form at leading order and next-to-leading order in ϵ which only depends on the particular initial condition through a small number of parameters [19, 40]. The fact that the functional forms and the powers of relevant factors of ϵ only depend on the equation, be it KdV, ILW or BO, not on any particular initial condition, this expected behavior is often referred to as *universality*. Up until now, only for KdV has the conjecture been verified rigorously for negative single lobe and analytic initial conditions [15]. In addition to universal behavior at the gradient catastrophe, universal behaviors have also been described at the leading [14] and trailing [13] edges of a dispersive shock wave spacetime region.

1.5 Outline for the Dissertation

In this dissertation, we articulate new results in the small dispersion limit of the ILW and BO equations with positive single lobe and rational initial conditions respectively.

In Chapter 2, we augment Miloh and Minzoni's [46] argument for the WKB analysis of the semi-classical ILW scattering equation using an alternative but equivalent formulation and with additional justification. In Section 2.2, we provide a rigorous analysis of the model turning point equation used to match solutions in the WKB scheme. This is done uniformly for the infinite basis of solutions and, to this authors' knowledge, will be one of only two rigorous analyzes in the literature of exact solutions to the ILW scatting equation. In Section 2.1, we reproduce the ILW Weyl law (2.349) that Miloh and Minzoni present and

also provide a new asymptotic formula for the ILW norming constants (Proposition 2.3.2). This culminates in Section 2.4, where we define a formal set of scattering data (Definition 2.4.1) for the small dispersion limit.

In Chapter 3, we analyze the small dispersion limit of the ILW inverse scattering problem using a constructed series of N-soliton solutions (1.27). The limit is expressed through an equilibrium problem for a particular electrostatic system. The chapter culminates with Theorem 3.4.6, where we show that the small dispersion limit is approximated by the solution to invicid Burgers' equation up to break time in an L^2 sense. This material follows closely Lax and Levermore's analysis for the small dispersion limit of the KdV equation [34, 35]. When possible, we use their results and prove additional theorems for the case of the ILW small dispersion limit when required.

In Chapter 4, we use Gérards formula [23] in the small dispersion limit and applied to rational initial conditions [7, 6] to establish new formulas, (4.98) and (4.155), which the solution converges uniformly to and describe universal behavior near the leading and trailing edges of the dispersive shock wave. These results are the BO analogues of previous results for the KdV equation [13, 14]. The first describes solitons emerging from the dispersive shock wave whose asymptotic spacing is determined by the zeros of the Airy function with an $\epsilon^{2/3}$ scaling. The second describes a linear dispersive wave with fast oscillations emerging from a slowly varying background with spatially growing amplitude proportional to $\epsilon^{1/6}$ and which has the functional form of the inverse modulus of a particular solution to Airy's equation.

1.5.1 Past and Expected Publications

We would like to point out, for clarity, that the author of this dissertation at the time of submission has one publication [20] with Elvang (University of Michigan) in theoretical high-energy physics. After changing emphases, the author worked on the material presented in this dissertation. The first two chapters together are expected to be published as joint work between the author and Miller (University of Michigan) in the coming year. The last chapter is the author's contribution to joint work with Blackstone (University of Michigan), Miller, Gassot (Institut de Recherche mathématique de Rennes) and Gérard (Université Paris-Saclay) and is expected to be available as a pre-print in the next month. This publication will also contain additional information about universal behaviour at the invicid Burgers' gradient catastrophe point and will comment on the conjecture laid out in [40].

CHAPTER 2

Intermediate Long Wave Direct Scattering Problem with Small Dispersion

> Whoever has examined, even cursorily, the map of Western America must have noticed the following arrangement of the mountain masses: The great belt of cordilleras coming up through Mexico and crossing into United States territory is depicted as being composed of many short, abrupt ranges or ridges, looking upon the map like an army of caterpillars; crawling northward.
>
> Clarence Dutton, *Mount Taylor and the Zuñi Plateau* (1886)

In a 1993 paper [46], Miloh and Minzoni were the first to analyze the asymptotics of the eigenvalues of the ILW scattering equation (1.15) for negative, single maximum, slowly varying (semi-classical) potentials. They used a WKB-style approach to determine formal asymptotics of the solutions to the scattering equation. From these solutions, they derived an integral condition which determines the approximate number and values of the discrete eigenvalues as a function of the semi-classical parameter, a so called Weyl law for the ILW scattering equation. In this chapter, we present their arguments with several key modifications:

1. their analysis reveals an infinite number of asymptotic solutions of which they throw away all but two, whereas we categorize these solutions into those that can form normalizable wavefunctions (scattering) and those that cannot (extraneous),

2. they expand the wavefunction along the lower boundary of the strip and neglect information about the solution interior to in the strip or on the upper boundary, whereas we expand the wavefunction around the center of the strip, correctly account for the ϵ-sized imaginary component of the strip, and give an expansion formally valid for the whole strip,

3. their asymptotic wavefunctions are given in terms of implicit solutions to transcendental equations, whereas we write our solutions in terms of classical functions,

4. and lastly, they only identify and make use of one solution to model turning point equation, whereas we provide a uniform analysis of the infinitely many solutions and demonstrate via a matching argument that only the one identified by Miloh and Minzoni participates in the construction of normalizable wavefunctions.

Additionally, we also provide a formal asymptotic formula for the norming constants associated to the eigenvalues in the ILW scattering data, an entirely new result.

While the scattering data that we extract from the formal arguments presented here are not rigorously derived, we point out that in Chapter 3 we prove rigorously that with this scattering data as input, the ILW inverse scattering problem returns an approximation of the original initial condition used to derive the scattering data. This provides strong evidence that this formal procedure returns the correct leading order asymptotics for the scattering data.

2.1 A Formal WKB Analysis of the ILW Scattering Equation

Under the small dispersion change of variables, the ILW scattering equation becomes

$$\mathrm{i}\epsilon\phi_x^+(x) + u(x)\phi^+(x) = \zeta\left(\phi^-(x) - \phi^+(x)\right) \tag{2.1}$$

where $\phi : \mathcal{S}_{\delta\epsilon} \to \mathbb{C}$ is a function analytic on the interior of the strip and for $x \in \mathbb{R}$, $\phi^{\pm}(x)$ are the continuous boundary values at $z = x \mp \mathrm{i}\delta\epsilon$, respectively. The $\pm$ on ϕ is meant to indicate the direction in the imaginary coordinate that the boundary is approach from inside the strip, i.e. $+$ indicates we approach from above, hence the sign flip for the $\mathrm{Im}\,[z]$ coordinate. See Figure 1.8 for more information. Additionally, we take the potential in the scattering equation u to be continuous, positive, single-lobed with decay to zero as $z \to \pm\infty$ and fixed for all $\epsilon > 0$.

Let us first make a substitution

$$\phi(z) = \Phi(z)\exp\left(\mathrm{i}\frac{\zeta}{\epsilon}z\right) \tag{2.2}$$

to put (2.1) into what we will call "canonical form"

$$\mathrm{i}\epsilon\Phi_x^+(x) + u(x)\Phi^+(x) = \zeta \mathrm{e}^{-2\delta\zeta}\Phi^-(x)\,. \tag{2.3}$$

We wish to learn something about the solutions to (2.3) as we take the semi-classical limit $\epsilon \to 0^+$. Miloh and Minzoni based their approximation method on the WKB approximation for the semi-classical limit of the time-independent Schrödinger equation. If we suppose that $\Phi(z)$ does not vanish in the strip, we can make the exponential substitution

$$\Phi(z) = \exp\left(S(z)\right) \tag{2.4}$$

and, moving all the exponentials to one side, we obtain the new form of the scattering equation

$$\mathrm{i}\epsilon S_x^+ + u = \zeta \exp\left(-2\delta\zeta + S^- - S^+\right)\,. \tag{2.5}$$

If we begin looking for a dominant balance between the two terms on the left, this suggests a formal expansion in integer powers of ϵ with leading coefficient $1/\epsilon$,

$$S(z) = -\frac{\mathrm{i}}{\epsilon}\theta(z) + \alpha(z) + \mathrm{i}\epsilon\beta(z) + O\left(\epsilon^2\right)\,. \tag{2.6}$$

Note though, that because the vertical width of the strip $\mathcal{S}_{\delta\epsilon}$ is shrinking as $\epsilon \to 0^+$, the real and imaginary parts of $z = x + \mathrm{i}y$ technically contribute at different orders to this series, i.e. since $-\delta\epsilon \le y \le \delta\epsilon$, y is itself $O(\epsilon)$. If the functions are assumed analytic in the expansion, then we should Taylor expand them away from the center of the strip to be able to accurately order every term in the series;

$$S(z) = -\frac{\mathrm{i}}{\epsilon}\theta(x) + \left(\alpha(x) + \frac{y}{\epsilon}\theta_x(x)\right) + \mathrm{i}\epsilon\left(\beta(x) + \frac{y}{\epsilon}\alpha_x(x) + \frac{y^2}{\epsilon^2}\theta_{xx}(x)\right) + O\left(\epsilon^2\right)\,. \tag{2.7}$$

Plugging this expansion into (2.5), we note that this expansion also brings the right side into the balance, verifying that this is indeed a dominant balance for this equation,

$$\begin{aligned}\theta_x + u + \mathrm{i}\epsilon\alpha_x - \mathrm{i}\delta\epsilon\theta_{xx} + O\left(\epsilon^2\right) &= \zeta\exp\left(-2\delta\zeta + 2\delta\theta_x + \mathrm{i}2\delta\epsilon\alpha_x + O\left(\epsilon^2\right)\right) &(2.8)\\ &= \zeta\mathrm{e}^{-2\delta(\zeta-\theta_x)}\left(1 + \mathrm{i}2\delta\epsilon\alpha_x + O\left(\epsilon^2\right)\right)\,. &(2.9)\end{aligned}$$

Equating order-by-order in ϵ, we have the relations determining the formal functions θ and

α,

$$\theta_x + u = \zeta \mathrm{e}^{-2\delta(\zeta-\theta_x)}\,, \tag{2.10}$$

$$\alpha_x - \delta\theta_{xx} = 2\delta\zeta \mathrm{e}^{-2\delta(\zeta-\theta_x)}\alpha_x\,. \tag{2.11}$$

We will define a function for $\eta, \zeta \in \mathbb{C}$ by

$$G(\eta, \zeta) := -\eta + \zeta \mathrm{e}^{-2\delta(\zeta-\eta)}\,, \tag{2.12}$$

then the relationship (2.10) determines θ_x by the equation

$$G(\theta_x(x); \zeta) = u(x) \tag{2.13}$$

for $x \in \mathbb{R}$. It is clear that this relationship is transcendental with infinitely many solutions due to the exponential function in G. However, with some simple manipulations, we can solve this equation using the Lambert W-function [48, Section 4.13], also known as the product-logarithm, which is the multivalued inverse of the function $z \mapsto z\mathrm{e}^z$. We will let $U \in \mathbb{R}$ stand for the output of G to conduct our manipulations in order to construct the inverse function of G.

$$U = G(\eta; \zeta) = -\eta + \zeta \mathrm{e}^{-2\delta(\zeta-\eta)} \tag{2.14}$$

$$\implies 2\delta(U+\eta) = 2\delta\zeta \mathrm{e}^{-2\delta(\zeta+U-U-\eta)} \tag{2.15}$$

$$\implies -2\delta(U+\eta)\mathrm{e}^{-2\delta(U+\eta)} = -2\delta\zeta \mathrm{e}^{-2\delta(\zeta+U)} \tag{2.16}$$

$$\implies -2\delta(U+\eta) = W_n(-2\delta\zeta \mathrm{e}^{-2\delta(\zeta+U)}) \tag{2.17}$$

$$\implies \eta = -U - \frac{1}{2\delta} W_n\left(-2\delta\zeta \mathrm{e}^{-2\delta(\zeta+U)}\right) \tag{2.18}$$

where $n \in \mathbb{Z}$ denotes which of the standard branches of the Lambert W-function we use. From this we define the branched inverse function for G on its first variable (i.e. considering ζ as a constant parameter), for $U \in \mathbb{R}$,

$$G_n^{-1}(U; \zeta) := -U - \frac{1}{2\delta} W_n(-2\delta\zeta \mathrm{e}^{-2\delta(\zeta+U)})\,. \tag{2.19}$$

This means for each $n \in \mathbb{Z}$, there is a leading-order phase which is given by

$$\theta_x(x) = G_n^{-1}(u(x); \zeta)\,. \tag{2.20}$$

Once we have a solution for θ_x, now we look at the next-to-leading-order amplitude, deter-

mined by (2.11), and rearrange to get for $x \in \mathbb{R}$,

$$\alpha_x(x) = \frac{\delta\ \theta_{xx}(x)}{1 - 2\delta\zeta \mathrm{e}^{-2\delta(\zeta - \theta_x(x))}} = \partial_x \int^{\theta_x(x)} \frac{\delta\, \mathrm{d}\eta}{1 - 2\delta\zeta \mathrm{e}^{-2\delta(\zeta-\eta)}}\,. \tag{2.21}$$

This integral can be evaluated with a change of variables $u = 2\delta\zeta \mathrm{e}^{-2\delta(\zeta-\eta)}$ and then a partial-fraction decomposition. Using the implicit definition of θ_x (2.13) as well as its explicit definition (2.20) we simplify the result:

$$\begin{aligned}
\int^{\theta_x(x)} \frac{\delta\, \mathrm{d}\eta}{1 - 2\delta\zeta \mathrm{e}^{-2\delta(\zeta-\eta)}} &= \frac{1}{2} \log\left(\frac{2\delta\zeta \mathrm{e}^{-2\delta(\zeta - \theta_x(x))}}{1 - 2\delta\zeta \mathrm{e}^{-2\delta(\zeta-\theta_x(x))}} \right) + C && (2.22)\\
&= \frac{1}{2} \log\left(\frac{2\delta\,(\theta_x(x) + u(x))}{1 - 2\delta\,(\theta_x(x) + u(x))} \right) + C && (2.23)\\
&= \frac{1}{2} \log\left(\frac{-W_n\left(-2\delta\zeta \mathrm{e}^{-2\delta(\zeta - u(x))}\right)}{1 + W_n\left(-2\delta\zeta \mathrm{e}^{-2\delta(\zeta-u(x))}\right)} \right) + C && (2.24)
\end{aligned}$$

where $C \in \mathbb{C}$ is an integration constant. The presence of the logarithm in (2.24) and the exponential in (2.4) motivates the definition of the amplitude functions for $n \in \mathbb{Z}$, $U \in \mathbb{R}$ and $\zeta \in \mathbb{C}$

$$A_n(U;\zeta) := \left(\frac{-W_n\left(-2\delta\zeta \mathrm{e}^{-2\delta(\zeta+U)}\right)}{1 + W_n\left(-2\delta\zeta \mathrm{e}^{-2\delta(\zeta+U)}\right)} \right)^{1/2} \tag{2.25}$$

where we take the principal square-root for $U > 0$ near zero and then use the continuous branch from then on. Should we run into a zero or singularity for $U \in \mathbb{R}$ inside of the square-root, we can always arbitrarily choose to extend the function around this by taking the branch that is continuous for U with a small positive imaginary part. Then, choosing a branch $n \in \mathbb{Z}$ of the Lambert W-function and taking the integration constant to be zero (a freedom we have because the scattering equation is linear), we have from (2.24) $\mathrm{e}^{\alpha(x)} = A_n(u(x);\zeta)$. Integrating θ_x from (2.20) in x, and assembling the remaining terms in (2.7) to constant order in ϵ, we can define the formal expansions for the solutions to the scattering equation for each $n \in \mathbb{Z}$, any spectral parameter value $\zeta \in \mathbb{C}$ and any initial point $x_0 \in \mathbb{R}$

$$\Phi_n(z;\zeta,x_0) := A_n\big(u(x);\zeta\big) \exp\left(-\frac{\mathrm{i}}{\epsilon} \int_{x_0}^{x} G_n^{-1}(u(x');\zeta)\, \mathrm{d}x' + \frac{y}{\epsilon} G_n^{-1}(u(x);\zeta) \right) \big(1 + O\left(\epsilon\right)\big)\,. \tag{2.26}$$

2.1.1 Interpretation of the Formal Asymptotic Solutions

We note that this formal asymptotic solution (2.26) shares many characteristics with the solution generated from WKB analysis of the time-independent Schrödinger equation. The fast instantaneous phase coefficient θ_x and the slowly varying amplitude $A = \mathrm{e}^{\alpha}$ are both locally determined as functions of the potential. There also appear to be quite a few differences, like the fact that there are infinitely many formal asymptotic solutions. We also note that this limit appears to be singular, in the sense that we lose all information about the function's analyticity inside the strip: if u is not analytic, $G_n^{-1}(u(x);\zeta)$, its integral, or $A_n\big(u(x);\zeta\big)$ are not either. Of course, this was to be expected as the strip's vertical width shrinks to zero, and to keep terms well-aligned in our formal ϵ-series, we had to break the analyticity at the outset.

2.1.1.1 Explanation of the Standard Branches of the Lambert W-function

To understand the behavior of the solutions, we give a brief overview of the standard branch definitions of the Lambert W-function. As mentioned before, the Lambert W-function is the infinite-branch inverse of the complex analytic function $w \mapsto w\mathrm{e}^w$, where each branch range in the w-plane is a maximal domain of univalence of this inverse mapping. The standard branch definitions have as the boundaries of their ranges the curves defined by $w\mathrm{e}^w < 0$, excluding the line segment from $w = -1$ to $w = 0$. One of the connected curves of these branch range boundaries is exactly the unit-scaled negative quadratrix. There are an infinite number of branches due to the exponential in the mapping $w \mapsto w\mathrm{e}^w$, falling into three qualitative categories:

1. $n \neq \pm 1, 0$. These branches all have one branch point at $z = 0$ and the cuts are taken along the negative real axis. The value along the cuts are taken to be continuous with the values above the cut. For $n > 0$, $W_n(z)$ for z just above the cut limit to a smooth curve from $z = +\infty + \mathrm{i}(2n+3)\pi$ to $z = -\infty + \mathrm{i}(2n+1)\pi$. From below, they limit to another smooth curve from $z = +\infty + \mathrm{i}(2n+1)\pi$ to $z = -\infty + \mathrm{i}2n\pi$. In this sense, these branch ranges behave very similar to the branch ranges of the logarithm, but right sides of the ranges have been sheared vertically by π. For $n < 0$, the right sides are sheared downwards by π.

2. $n = \pm 1$. These branches have two branch points, one at $z = 0$ which is logarithmic in nature, and one at $z = -\mathrm{e}^{-1}$ which has a square-root behavior. Again, the values along the branch cut are taken to be continuous with those just above. $W_1(z)$ for z just above the cut map to a smooth curve from $z = +\infty + \mathrm{i}3\pi$ to $z = -\infty + \mathrm{i}2\pi$. For

just below the cut, the behavior is different and depends on which side of the branch point $z = -e^{-1}$ we evaluate on: for $\mathrm{Re}\,[z] < -e^{-1}$, this approaches the lower half of the negative quadratrix, and if $-e^{-1} < \mathrm{Re}\,[z] < 0$, then this approaches the half line $(-\infty, -1)$. $W_{-1}(z)$ is similar but the behavior is flipped between the directions approaching the cut and its the upper half of the negative quadratrix.

3. $n = 0$. This branch has only one branch point at $z = -e^{-1}$ of a square-root nature, the cut extends out along the negative real axis. This branch maps the entire plane minus the cut to the interior of the negative quadratrix in a one-to-one manner. $W_0(z)$ for z just above the cut approach the upper half of the negative quadratrix while those below map to the lower half.

For a graphical representation of the Lambert W-function, see Figure 2.1.

2.1.1.2 Identifying Extraneous and Scattering Solutions

We group the formal asymptotic solutions into two well-distinguished groups:

- *Extraneous solutions* are the solution $\Phi_n(x; \zeta, x_0)$ for any $n \in \mathbb{Z}$ such that $n \neq -1, 0$. We note that for all $\zeta \in \mathbb{C}/\{0\}$, they are continuous for all $x \in \mathbb{R}$. This is because the argument of Lambert W terms in the constituent parts is always $-2\delta\zeta e^{-2\delta(\zeta+u(x))}$. Thus, the portion $-2\delta\zeta e^{-2\delta\zeta}$ is always nonzero. The multiplying term $0 < e^{-2\delta u(x)} < 1$ for all $x \in \mathbb{R}$, so changing $x \in \mathbb{R}$ just amounts to moving the argument of the Lambert W-function along a single ray, with a minimum and maximum possible distance from the origin since $u(x)$ is bounded. Therefore, all Lambert W terms in (2.26) are continuous and bounded. The only issue could arise is the denominator of $A_n(x, \zeta, x_0)$, which is
$$1 + W_n(-2\delta\zeta e^{-2\delta(\zeta+u(x))})\,. \tag{2.27}$$
Only the branch ranges $n = -1$ and 0 contain the point -1. It turns out that the $n = +1$ branch does border on this point too, this is the point where the three branch ranges for $n = \pm 1, 0$ meet, but -1 is not actually in the $n = +1$ branch range. This is because this lies along the lower boundary of the $n = +1$ branch range, and this boundary is not contained in the range. Thus, the formal asymptotic solutions in this case are always continuous.

- *Scattering solutions*, in contrast, correspond to solutions with $n = -1, 0$. As discussed above, the amplitude term has the potential to blow up for these branches. The pre-image of the value -1 on these branches is exactly the square-root branch point

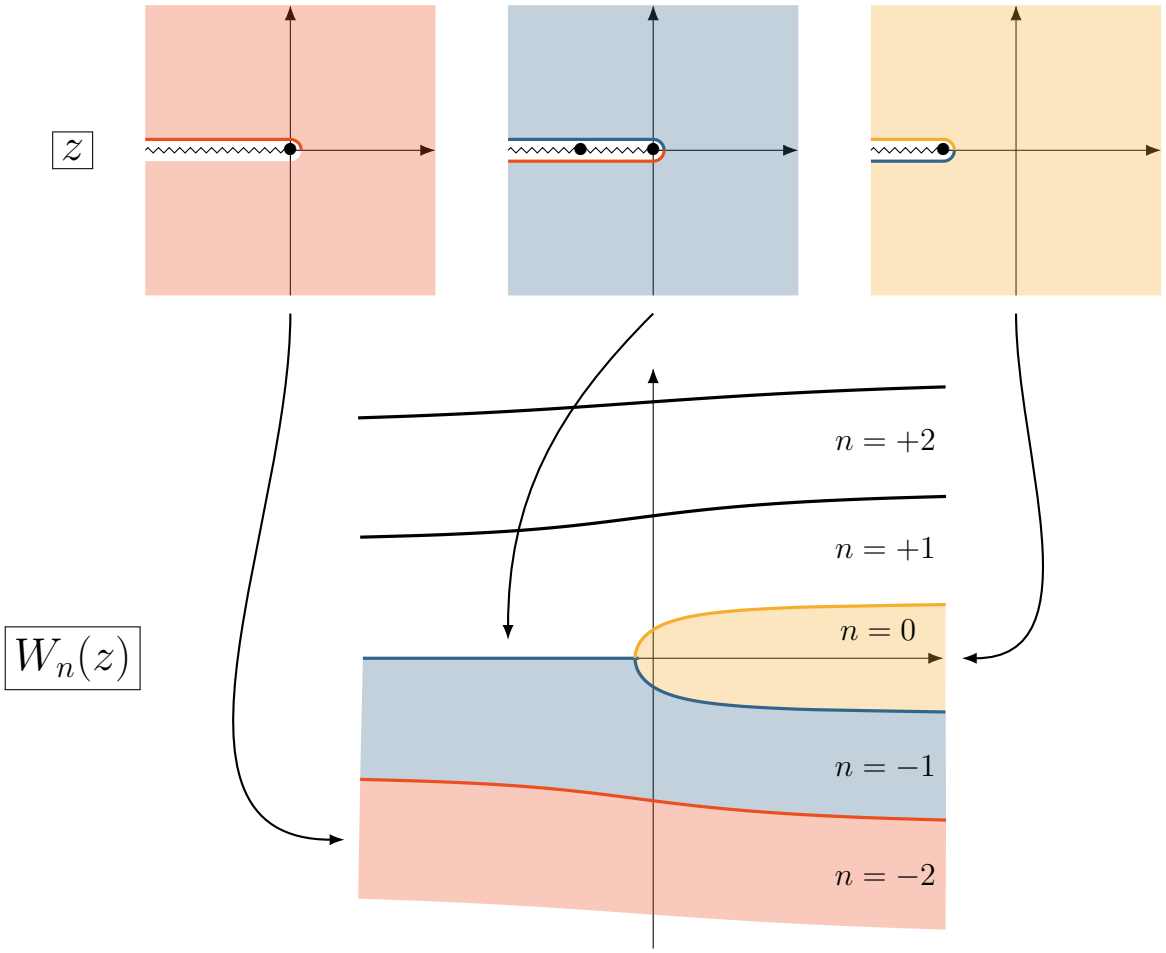


Figure 2.1: $z \mapsto W_n(z)$ demonstrated for three characteristic branches: $n = -2, -1$, and 0. The colored z-planes map into the same colored branch ranges indicated below. Additionally, the colored edges in the z-planes indicate the direction that the same colored range boundaries are approaches from each side of the branch cut. The edge of the same color as the plane are the ones that are included in that branch. The $n = 1$ maps like the $n = -1$ branch while all others are similar to the $n = -2$ branch.

$z = -\mathrm{e}^{-1}$. So the amplitude becomes undefined at any $x_0 \in \mathbb{R}$ which satisfies

$$-2\delta\zeta \mathrm{e}^{-2\delta(\zeta+u(x_0))} = -\mathrm{e}^{-1}\,. \tag{2.28}$$

Since $u(x) > 0$, this can happen for $-2\delta\zeta\mathrm{e}^{-2\delta\zeta} < -\mathrm{e}^{-1}$. Miraculously, the left of this inequality is exactly the inverse of the Lambert W-function applied to $-2\delta\zeta$. That means if $-2\delta\zeta$ is in the image of the half line $(-\infty, -\mathrm{e}^{-1})$ under any of the Lambert W branches, then there is the potential for a blow up, essentially contingent on if $u(x)$ gets large enough. From our explanation of the Lambert W branches above, we see that this image contains a subset of every branch range boundary, but the one that interests us most is the unit negative quadratrix, the upper half of which is the image of $(-\infty, -\mathrm{e}^{-1})$ under W_0 and the lower half of which is under W_{-1}. Thus, if $\zeta \in \mathcal{Q}_\delta$, and we take a principal logarithm of (2.28), then if we have for some $x_0 \in \mathbb{R}$

$$u(x_0) = E(\zeta) := -\zeta + \frac{1}{2\delta}\left(1 + \log(2\delta\zeta)\right)\,, \tag{2.29}$$

the amplitude term blows up and we refer to the point x_0 as a *turning point*. When $u(x) < E(\zeta)$,

$$-2\delta\zeta \mathrm{e}^{-2\delta(\zeta+u(x))} < -\mathrm{e}^{-1}\,, \tag{2.30}$$

and so the Lambert W expressions are on the quadratrix, specifically

$$-\frac{1}{2\delta}W_{-1}(-2\delta\zeta\mathrm{e}^{-2\delta(\zeta+u(x))}) \in \left(\frac{1}{2\delta}, \zeta\right)_{\mathcal{Q}_\delta}\,, \tag{2.31}$$

$$-\frac{1}{2\delta}W_{0}(-2\delta\zeta\mathrm{e}^{-2\delta(\zeta+u(x))}) \in \left(\zeta^*, \frac{1}{2\delta}\right)_{\mathcal{Q}_\delta}\,, \tag{2.32}$$

where we are using the quadratrix interval notation (1.26). Roughly, this means the formal asymptotic solutions have an exponentially growing or decaying magnitude due to the nonzero imaginary parts. When $u(x) > E(\zeta)$,

$$-2\delta\zeta \mathrm{e}^{-2\delta(\zeta+u(x))} > -\mathrm{e}^{-1}\,, \tag{2.33}$$

and so the Lambert W expressions are real, specifically

$$-\frac{1}{2\delta}W_{-1}(-2\delta\zeta\mathrm{e}^{-2\delta(\zeta+u(x))}) \in \left(\frac{1}{2\delta}, +\infty\right)\,, \tag{2.34}$$

$$-\frac{1}{2\delta}W_{0}(-2\delta\zeta\mathrm{e}^{-2\delta(\zeta+u(x))}) \in \left(0, \frac{1}{2\delta}\right)\,. \tag{2.35}$$

Roughly, this means that the formal asymptotic solutions do not have any exponential behavior, just oscillatory. From this we see that, not only do the solutions blow up at a turning point, but if $u(x) - E(\zeta)$ changes sign across the turning point, then the behavior of the scattering solutions changes dramatically as well.

The term "turning point" comes from the WKB analysis of the time-independent Schrödinger equation, where the analogue of this condition is where the classical potential energy of a particle is equal to the total energy of the particle. Classically, the particle then must be momentarily at rest here as it turns around in its motion. This also gives rise to the nomenclature in quantum mechanics of the *classically allowed* and *classically forbidden* regions. The reason that the modifier "classically" remains in these terms is because solutions to the Schrödinger equation, the norm-squared of which describes the probability density of a quantum particle's location by the Born rule, does not go to zero at the turning points. Instead, it exhibits a roughly exponential decay in the classically forbidden region. So what is classically forbidden is not necessarily quantum forbidden. We will commandeer this nomenclature for the ILW scattering equation, where classically allowed refers to where $u(x) > E(\zeta)$ and classically forbidden refers to where $u(x) < E(\zeta)$.

A similar blow up of the amplitude occurs in the WKB analysis of the Schödinger operator, and the interpretation is that the dominant balance which we considered in (2.5) is only appropriate for $u(x)$ away from the level $E(\zeta)$. In the neighborhood of their equality, some terms in the scattering equation that were previously leading order, cancel, and a new dominant balance is formed.

2.2 The Model Turning Point Equation

We derive the model equation for a transition across a turning point by fixing $\zeta \in \mathcal{Q}_\delta$ and considering a shrinking interval in $x \in [a(\epsilon), b(\epsilon)] \subset \mathbb{R}$ where there is one and only one point $x_0 \in [a(\epsilon), b(\epsilon)]$ such that (2.28), or equivalently (2.29), is satisfied. Then, by substituting

$$\Phi(z) = \Psi(z) \exp\left(\mathrm{i}\frac{u(x_0)}{\epsilon} z\right) \tag{2.36}$$

into the canonical scattering equation, we have after clearing exponential factors

$$\mathrm{i}\epsilon\Psi^+_x + (u(x) - u(x_0))\Psi^+ = \zeta \mathrm{e}^{-2\delta(\zeta + u(x_0))}\Psi^- = \frac{\mathrm{e}^{-1}}{2\delta}\Psi^- \,. \tag{2.37}$$

If the rate at which the interval shrinks around the turning point is chosen appropriately, we expect that we may expand $u(x) - u(x_0) = u'(x_0)\ (x - x_0) + O\left((x - x_0)^2\right)$ and, as long as

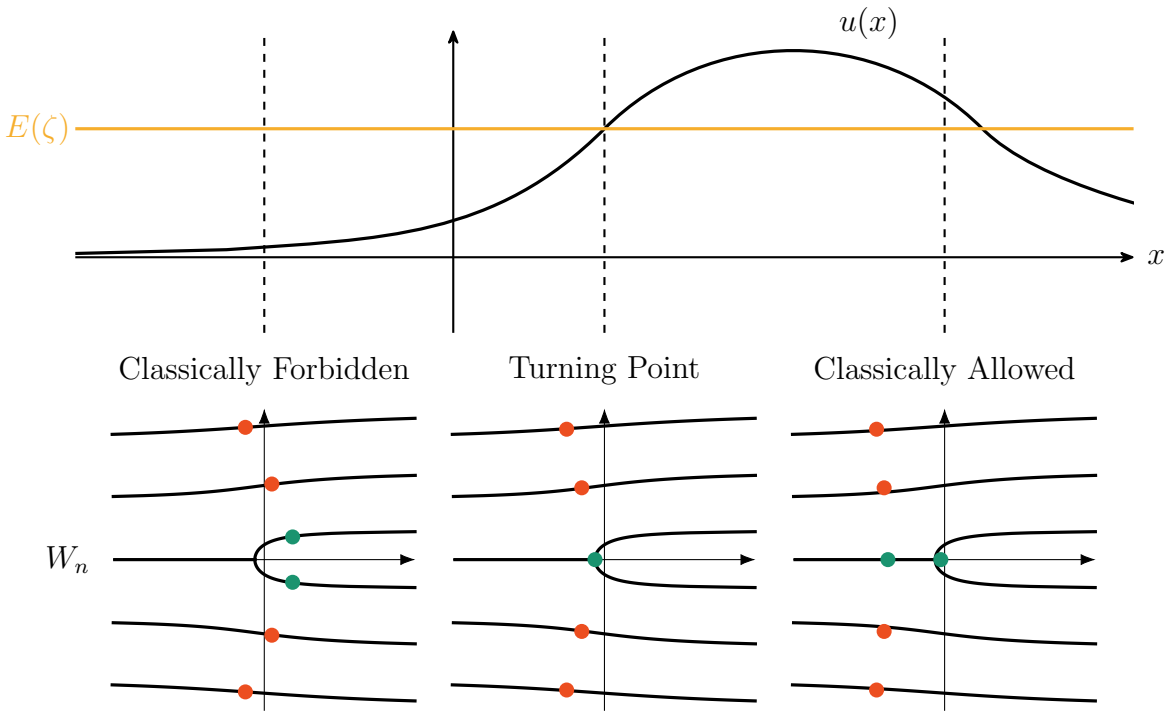


Figure 2.2: An example potential $-u(x)$ and level $E(\zeta)$ (top) with schematics (bottom) of the behaviors of $W_n(-2\delta\zeta \mathrm{e}^{-2\delta(\zeta+u(x))})$ at some chosen points in the classically forbidden region (left), at the turning point (middle) and in the classically allowed region (right). The values for the extraneous solutions ($n \neq -1, 0$) are shown in red and those for the scattering solutions ($n = -1, 0$) are shown in green.

we require $u'(x_0) \neq 0$, then we may neglect the sub-leading terms in the Taylor expansion. Thus, we now have

$$\mathrm{i}\epsilon\Psi_x^+ + u'(x_0)\ (x - x_0)\Psi^+ = \frac{\mathrm{e}^{-1}}{2\delta}\Psi^- \,. \tag{2.38}$$

Considering the turning point analysis for the Schrödinger equation as a guide, we may now want to remove dependence of the equation on $u'(x_0), \epsilon$, and x_0 via a shift and re-scaling. For this, let $\psi(Z) := \Psi(z)$ where $Z := a(z - x_0)$ for some yet undetermined $a \in \mathbb{R}$ and $a \neq 0$. Then the equation becomes for $X = \mathrm{Re}\,[Z]$,

$$\mathrm{i}\epsilon a\ \psi_X^+ + \frac{u'(x_0)}{a} X\psi^+ = \frac{\mathrm{e}^{-1}}{2\delta}\psi^- \,. \tag{2.39}$$

Additionally, due to the scaling ψ is analytic on the strip $\mathcal{S}_{\delta\epsilon a}$. It is now apparent that ϵ can not be removed entirely from the equation: trying to equate any two terms, in an attempt to factor out an overall scale, will always leave the third term ϵ-dependent. This simply indicates that the solutions to the scattering equation depend nontrivially on the small dispersion parameter ϵ. Instead, we use this scaling to reduce the number of parameters in the equation from two, $u'(x_0)$ and δ, to one. First, we will consider $u'(x_0) > 0$, then define a and the new height parameter $h > 0$ by

$$a = \frac{1}{2\delta} \quad \text{and} \quad h = (2\delta)^2 u'(x_0)\,. \tag{2.40}$$

Then, after multiplying through by 2δ and bringing all of the terms to the same side, we have the model equation for the behavior near a turning point as

$$0 = \mathrm{i}\epsilon\psi_X^+ + hX\psi^+ - \mathrm{e}^{-1}\psi^- \tag{2.41}$$

where ψ is analytic on the strip $\mathcal{S}_{\epsilon/2}$.

We have yet to consider $u'(x) < 0$. This is because, the sign of $u'(x_0)$ also plays a nontrivial role. If we leave the sign and just scale by the magnitude, the middle term retains the sign. If we instead try to scale by a negative number, the orientation of the strip will flip, flipping too the evaluation of the boundary values. Both of these operations yield different equations to analyze, and so are not ideal. However, if we combine negation with a conjugation, we can correct the flipped boundary values. We return to before our scaling (2.39), and instead we make the substitution $\psi(Z) := \Psi(-z^*)^*$ where $Z := (z - x_0)/2\delta$. Then

$$\psi^\pm(X) = \psi\left(X \mp \mathrm{i}\frac{\epsilon}{2}\right) = \Psi(-2\delta X \mp \mathrm{i}\delta)^* = \Psi^\pm(-2\delta X)^* \,. \tag{2.42}$$

Taking the conjugate of (2.39) and using these boundary value identities and evaluating at $x = -2\delta X + x_0$, we have

$$0 = -\mathrm{i}\epsilon\Psi_x^+(-2\delta X)^* - 2\delta u'(x_0)\, X\, \Psi^+(-2\delta X)^* - \frac{\mathrm{e}^{-1}}{2\delta}\Psi^-(-2\delta X)^* \tag{2.43}$$

$$= \mathrm{i}\frac{\epsilon}{2\delta}\psi_X^+(X) - 2\delta u'(x_0)\, X\, \psi^+(X) - \frac{\mathrm{e}^{-1}}{2\delta}\psi^-(X)\,. \tag{2.44}$$

After multiplying through by 2δ and defining

$$h = -(2\delta)^2 u'(x_0) \tag{2.45}$$

we have the same form as (2.41). Since both negation and conjugation leave the strip $\mathcal{S}_{\delta\epsilon}$ invariant, conjugating both the argument and value of an analytic function yields another analytic function, and taking into account the scaling 2δ on the input, we conclude that ψ is analytic in the strip $\mathcal{S}_{\epsilon/2}$. Thus, we can handle the analysis at both turning points in a uniform manner.

2.2.1 Solving the Model Turning Point Equation by Laplace Transform

We solve this equation just like we would solve Airy's equation: suppose there is an analytic function $\hat{\psi} : \mathbb{C} \to \mathbb{C}$ such that a solution to the above equation could be formulated as

$$\psi(Z) = \int_C \hat{\psi}(k)\mathrm{e}^{\mathrm{i}kZ/\epsilon}\mathrm{d}k \tag{2.46}$$

where, of course, C is a contour on which the integral above converges rapidly enough for any $Z \in \mathcal{S}_{\epsilon/2}$. We also want rapid convergence so that we may differentiate under the integral,

$$\psi_X^+(X) = \int_C \hat{\psi}(k)\partial_X \mathrm{e}^{\mathrm{i}k(X/\epsilon - \mathrm{i}/2)}\mathrm{d}k = \int_C \mathrm{i}\frac{k}{\epsilon}\,\hat{\psi}(k)\mathrm{e}^{\mathrm{i}k(X/\epsilon-\mathrm{i}/2)}\mathrm{d}k\,; \tag{2.47}$$

that we may integrate-by-parts with zero boundary term,

$$X\psi^+(X) = \int_C \hat{\psi}(k)\left(\mathrm{i}\frac{\epsilon}{2}\mathrm{e}^{\mathrm{i}k(X/\epsilon-\mathrm{i}/2)} - \mathrm{i}\epsilon\partial_k \mathrm{e}^{\mathrm{i}k(X/\epsilon-\mathrm{i}/2)}\right)\mathrm{d}k \tag{2.48}$$

$$= \int_C \mathrm{i}\epsilon\left(\frac{1}{2}\hat{\psi}(k) + \hat{\psi}'(k)\right)\mathrm{e}^{\mathrm{i}k(X/\epsilon-\mathrm{i}/2)}\mathrm{d}k; \tag{2.49}$$

and that evaluating at both the upper and lower boundaries are simultaneously well defined

$$\psi^-(X) = \int_C \hat{\psi}(k) \mathrm{e}^{\mathrm{i}k(X/\epsilon + \mathrm{i}/2)} \, \mathrm{d}k = \int_C \hat{\psi}(k) \, \mathrm{e}^{-k} \, \mathrm{e}^{\mathrm{i}k(X/\epsilon - \mathrm{i}/2)} \, \mathrm{d}k \, . \tag{2.50}$$

Plugging this form into the model turning point equation (2.41),

$$0 = \int_C \left(-k\hat{\psi}(k) + \mathrm{i}h^2\epsilon \left(\frac{1}{2}\hat{\psi}(k) + \hat{\psi}'(k) \right) - \mathrm{e}^{-k-1}\hat{\psi}(k) \right) \mathrm{e}^{\mathrm{i}k(X/\epsilon - \mathrm{i}/2)} \, \mathrm{d}k \, , \tag{2.51}$$

and simply requiring the integrand be zero identically, we get a first-order differential equation for $\hat{\psi}$. This has the solution

$$\hat{\psi}(k) = A \exp\left(-\frac{\mathrm{i}}{h\epsilon} \left[\frac{k^2}{2} - \mathrm{e}^{-k-1} \right] - \frac{k}{2} \right) \tag{2.52}$$

for any $A \in \mathbb{C}$ independent of the variables Z and k. This gives our solution as

$$\psi(Z) = A \int_C \exp\left(-\frac{\mathrm{i}}{h\epsilon} \left[\frac{k^2}{2} - \mathrm{e}^{-k-1} \right] + \mathrm{i}k \left(\frac{Z}{\epsilon} + \frac{\mathrm{i}}{2} \right) \right) \, \mathrm{d}k \, . \tag{2.53}$$

For large k and fixed $Z \in \mathbb{C}$, the real part of the exponent is dominated by the behavior of the imaginary part of the function

$$f(k) = \frac{k^2}{2} - \mathrm{e}^{-k-1} \, . \tag{2.54}$$

For $\mathrm{Re}\,[k] < 0$, the exponential term dominates $\mathrm{Im}\,[f]$ and so we see there is an infinite alternating series of "valleys" and "mountains" spreading out in the imaginary direction. For $\mathrm{Re}\,[k] > 0$, the quadratic term dominates, and we get just one valley and one mountain in the lower and upper half-planes respectively. To the author, this landscape bears a striking resemblance to the southwest region of the United States, and in honor of the geography of where the author grew up, we will refer to the alternating mountains and valleys as the *basin and range*, the mountain in the first quadrant as *the Rockies*, and the valley in the fourth quadrant as *the Grande valley*. These features are easily seen in the landscape of Figure 2.3.

2.2.2 A Basis of Solutions to the Model Turning Point Equation

From a cursory glance at the imaginary part of f,

$$\mathrm{Im}\,[f(k)] = \mathrm{Im}\,[k]\,\mathrm{Re}\,[k] + \mathrm{e}^{-\mathrm{Re}[k]-1} \sin(\mathrm{Im}\,[k]) \, , \tag{2.55}$$

we see that basins lie around the lines $\mathrm{Im}\,[k] = \pi\nu$ where $\nu \in 2\mathbb{Z} - 1/2$, a so-called lower-half-integer. The mountains occur in between, around the lines $\mathrm{Im}\,[k] = \pi\nu$ where $\nu \in 2\mathbb{Z} + 1/2$, a so-called upper-half-integer. Additionally, the Rockies lie around the argument $\pi/4$ and the fourth quadrant contains the Grande valley around the argument $-\pi/4$.

By taking a piece-wise smooth contour C which extends out to infinity at its beginning and end in one of the basins or the Grande valley, the exponential for all $Z \in \mathbb{C}$ goes rapidly to zero at its endpoints. This guarantees that we satisfy the requirements listed above and have generated a solution to the model turning point scattering equation.

Its clear that there are infinitely many homotopy classes of solution contours, and towards constructing a basis of solutions, we define the basis of contours C_ν for $\nu \in 2\mathbb{Z} - 1/2$ be any piece-wise smooth, nonself-intersecting contour such that

$$C_\nu : \quad \text{begins at} \quad k = -\infty + \mathrm{i}\pi\nu \quad \text{and ends at} \quad k = -\infty + \mathrm{i}\pi\,(\nu + 2)\ . \tag{2.56}$$

These are contours which connect pairs of nearest-neighbor basins. Additionally, we define $C_{-\infty}$ to be any smooth, nonself-intersecting contour such that

$$C_{-\infty} : \quad \text{begins at} \quad k = -\infty - \mathrm{i}\frac{\pi}{2} \quad \text{and ends at} \quad k = \infty\ \mathrm{e}^{-\mathrm{i}\pi/4}\,. \tag{2.57}$$

The collection of these contours forms a basis of contours. This is because any contour which connects any basin to any other is Cauchy-equivalent to a series of nearest neighbor contours between the initial and final basin. Additionally, any contour connecting a basin to the Grande valley can be made from a series of nearest-neighbor contours and $C_{-\infty}$.

With these contours, we introduce the associated fundamental solutions:

$$\psi_\nu(Z;\epsilon,h) := \int_{C_\nu} \exp\left(-\frac{\mathrm{i}}{h\epsilon}f(k) + \mathrm{i}k\left(\frac{Z}{\epsilon} + \frac{\mathrm{i}}{2}\right)\right)\mathrm{d}k \quad \text{for all } \nu \in \{-\infty\} \cup \left(2\mathbb{Z} - \frac{1}{2}\right)\ . \tag{2.58}$$

By Cauchy's theorem, we may choose the actual contours C_ν to be any piece-wise smooth contour we wish so long as they eventually enter and remain inside the dictated basin or the Grande valley as the contour travels off to infinity. Later, we will pick particular contours and parametrizations that will be amenable to a steepest descent analysis. For this purpose, it is important that we understand the behavior of any saddle points of f.

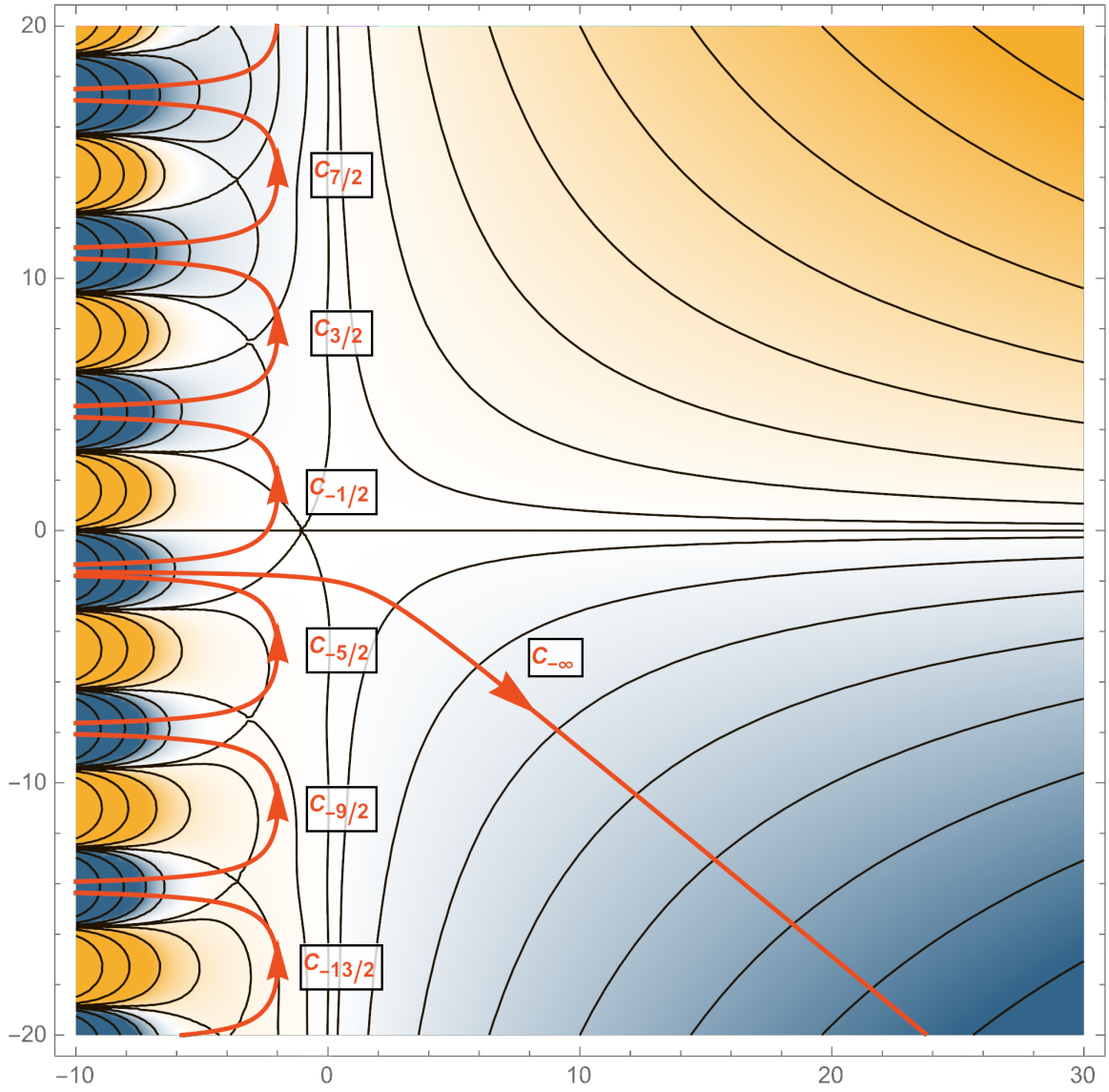


Figure 2.3: The landscape of $\mathrm{Im}\,[f(k)]$. Yellow shading corresponds to a positive value while blue shading corresponds to a negative value. Additionally, the fine black lines are some particular level contours. The basin and range structure can be clearly seen on the left of the image with the basins in blue and the ranges in yellow. We also see the beginnings of the Rockies (yellow) and the Grande valley (blue) in the first and fourth quadrants respectively. Some representative choices of basis contours C_ν as defined above are depicted in red with their labels.

2.2.3 The Behavior of the Saddle Points

Consider $Z = X + \mathrm{i}\epsilon(\tilde{Y} - 1/2) \in \mathcal{S}_{\epsilon/2}$ with $\tilde{Y} \in [0,1]$, then the contribution of $\tilde{Y}$ to the exponent in the integrand of (2.58) is next-too-leading-order in ϵ,

$$\exp\left(-\frac{\mathrm{i}}{h\epsilon}f(k) + \mathrm{i}k\left(\frac{Z}{\epsilon} + \frac{\mathrm{i}}{2}\right)\right) = \exp\left(-\frac{\mathrm{i}}{h\epsilon}f(k;\tilde{X}) - k\tilde{Y}\right) \tag{2.59}$$

where we've introduced

$$f(k;\tilde{X}) := f(k) - k\tilde{X} = \frac{k^2}{2} - \mathrm{e}^{-k-1} - k\tilde{X} \quad \text{and} \quad \tilde{X} = hX \tag{2.60}$$

to simplify notation. This means the saddle points that we are interested in are defined by

$$0 = \partial_k f(k;\tilde{X}) = k + \mathrm{e}^{-k-1} - \tilde{X}\,, \tag{2.61}$$

and they can be expressed in terms of the Lambert W-function

$$k_n(\tilde{X}) = \tilde{X} + W_n(-\mathrm{e}^{-\tilde{X}-1}) \quad \text{for all} \quad n \in \mathbb{Z}\,. \tag{2.62}$$

There are three qualitatively distinct configurations of these saddle points as $X \in \mathbb{R}$ is allowed to vary:

1. For $\tilde{X} < 0$ large, we see from the asymptotics of the Lambert-W function [48, Equation 4.13.1_1],

$$k_n(\tilde{X}) = \tilde{X} + \big(-\tilde{X} - 1 - \log\big|\tilde{X}+1\big| + \mathrm{i}(2n+1)\pi + o(1)\big) \tag{2.63}$$

$$= -\big(\log\big|\tilde{X}+1\big| + 1\big) + \mathrm{i}(2n+1)\pi + o(1)\,. \tag{2.64}$$

   That is, they are about evenly spaced in the imaginary direction and with real part going like a negative log of $|\tilde{X}|$. The saddle points $k_n(\tilde{X})$ for $n \in \mathbb{Z}$ are all simple.

2. As $\tilde{X}$ increases towards zero, the saddle points below the real-line move upwards and the saddle points above the real-line move down. All of the saddle points maintain their distance from each other except for $k_0(\tilde{X})$ and $k_{-1}(\tilde{X})$, which coincide at $\tilde{X} = 0$. As $\tilde{X}$ increases past zero, the saddle points $k_0(\tilde{X})$ and $k_{-1}(\tilde{X})$ move apart again but now on the real line, in the character of a fold coalescing of saddle points.

3. For $\tilde{X} > 0$ large, we note the asymptotics of the Lambert-W function are distinct

between the 0-branch and the others.

$$k_0(\tilde{X}) = \tilde{X} + O\left(\mathrm{e}^{-\tilde{X}-1}\right) \tag{2.65}$$

while

$$k_n(\tilde{X}) = \tilde{X} + \left(-\tilde{X} - 1 - \log\left|\tilde{X}+1\right| + \mathrm{i}2n_+\pi + o(1)\right) \quad \text{for all} \quad n \neq 0 \tag{2.66}$$

$$= -\left(\log\left|\tilde{X}+1\right| + 1\right) + \mathrm{i}2n_+\pi + o(1)\,. \tag{2.67}$$

with $n_+ = n$ if $n > 0$ and $n_+ = n+1$ if $n < 0$. So there is again a vertical tower of about evenly spaced saddle points in the imaginary direction and with real part going like a negative $\log|\tilde{X}|$. However, this tower of saddle points is now centered on the real line instead of symmetric about it and there is one saddle point which has split off and is at about $\tilde{X}$ on the real-line. Once again, the saddle points $k_n(\tilde{X})$ for $n \in \mathbb{Z}$ are all simple.

2.2.4 Basis Solution Asymptotics for Matching Across the Turning Point

Looking back at the process of deriving the model turning point equation, we formally neglected the higher order terms $O\left((x-x_0)^2\right)$ from the Taylor expansion of the potential in (2.38). We realize that this can only be reasonable if we are working in a shrinking x window around a turning point. By the transformation $\tilde{X} = h(x-x_0)/2\delta$, this would be a shrinking window around $\tilde{X} = 0$, exactly where the $\mathrm{Im}\,[f]$ landscape has two colliding saddle points. In order to determine the rate at which the window needs to shrink, we expand the exponent around the meeting point, $k = -1$:

$$f(k;\tilde{X}) = \tilde{X} - \frac{1}{2} - \tilde{X}\,(k+1) + (k+1)^3 + O\left((k+1)^4\right)\,. \tag{2.68}$$

The idea is to find a rescaling of $\tilde{X}$ and k so we have a leading-order dominant balance in our exponent. The constant term we can disregard since we can factor out an overall constant from the exponential and bring the multiplicative factor outside of the integral. Thus, we search for a balance between the linear and cubic terms. Additionally, to pick the scale to resolve the features of the small ϵ limit of the transition equation, we should want the overall exponent to be independent of ϵ after the scaling. These two requirements fix the scalings to $\tilde{X} = O\left(\epsilon^{2/3}\right)$ and $k = O\left(\epsilon^{1/3}\right)$. From the cubic nature of the problem, we are assured that the resolved profile will be a linear combination of Airy functions, just like the transition

equation for the Schrödinger equation, and as already stated by Miloh and Minzoni [46]. Of course, we are interested in using the asymptotics of the functions to tie them together with the outer approximations. This means we should choose an $\tilde{X}$ scaling that is larger than $\epsilon^{2/3}$, but still shrinks as $\epsilon \to 0$. For simplicity, we take

$$\tilde{X} = \epsilon^{\alpha} h\chi \tag{2.69}$$

with $0 < \alpha < 2/3$ and consider χ in a compact interval that includes zero, i.e. there is an $M_\chi > 0$ such that $|h\chi| < M_\chi$ on this compact interval. Lastly, in order to formally justify that the other basis functions do not play a role in matching, we compute their asymptotics in the same scaling limits. Towards this end, we will need to make a choice of the particular basis contours we wish to use to rigorously compute the asymptotics of the basis solutions $\psi_n u$.

2.2.4.1 Chosen Basis of Contours and Bounding Contributions Away from Saddle Points

The basis contours chosen will be have constituent portions that are divided into two groups, those portions that are "away from," and those that are "close to" the associated saddle points. The precise definition will be whether the portion of the contour in question falls outside or inside, respectively, some disks which enclose the saddle points. The parametrizations of the basis contours are given below. There are five cases that have to be considered separately due to the geometry of the landscape, these are given below in cases ordered by $\nu \in \{-\infty\} \cup (2\mathbb{Z} - 1/2)$

1. $\nu = -\infty$. We define $C_{-\infty} = C_{-\infty}^{(a)} \cup C_{-\infty}^{(b)} \cup C_{-\infty}^{(c)}$ with

$$C_{-\infty}^{(a)}: \quad k_{-\infty}^{(a)}(s) = s - 1 - \mathrm{i}\frac{\pi}{2}, \quad s \in \left(-\infty,\ -\frac{\pi}{2}\right], \tag{2.70}$$

$$C_{-\infty}^{(b)}: \quad k_{-\infty}^{(b)}(s) = (1+\mathrm{i})s - 1, \quad s \in \left[-\frac{\pi}{2},\ 0\right], \tag{2.71}$$

$$C_{-\infty}^{(c)}: \quad k_{-\infty}^{(c)}(s) = (1-\mathrm{i})s - 1, \quad s \in [0,\ \infty)\ . \tag{2.72}$$

   $C_{-\infty}$ passes through the center of the colliding saddle points at the end of $C_{-\infty}^{(b)}$ and beginning of $C_{-\infty}^{(c)}$. We factor out the multiplicative contribution to $\psi_{-\infty}$ from the collided saddle points and rearrange some terms in the exponent, and split the contributions

between those contour arcs that are near and far from the saddle points.

$$\psi_{-\infty}(Z;h,\epsilon) = \mathrm{e}^{-\mathrm{i}f\left(-1;\tilde{X}\right)/h\epsilon+\tilde{Y}} \times \int_{C_{-\infty}} \exp\left(-\frac{\mathrm{i}}{h\epsilon}\left[f(k;\tilde{X}) - f(-1;\tilde{X})\right] - (k+1)\tilde{Y}\right)\mathrm{d}k \tag{2.73}$$

$$= E_0(\tilde{X},\tilde{Y}) \times \int_{C_{-\infty}} \exp\left(-\frac{\mathrm{i}}{h\epsilon}\left[\frac{k^2}{2} - \mathrm{e}^{-k-1} - (k+1)\,\tilde{X} + \frac{1}{2}\right] - (k+1)\tilde{Y}\right)\mathrm{d}k \tag{2.74}$$

$$= E_0(\tilde{X},\tilde{Y})\Big[I_0\left(C_{-\infty}^{(a)}\right) + I_0\left(C_{-\infty}^{(b)} \cap \mathcal{D}_0(R_2)\right) + I_0\left(C_{-\infty}^{(b)}/\mathcal{D}_0(R_2)\right) + I_0\left(C_{-\infty}^{(c)} \cap \mathcal{D}_0(R_2)\right) + I_0\left(C_{-\infty}^{(c)}/\mathcal{D}_0(R_2)\right)\Big] \tag{2.75}$$

where

$$E_0(\tilde{X},\tilde{Y}) := \mathrm{e}^{-\mathrm{i}f\left(-1;\tilde{X}\right)/\epsilon+\tilde{Y}} = \mathrm{e}^{-\mathrm{i}(\tilde{X}-1/2)/h\epsilon+\tilde{Y}}\,, \tag{2.76}$$

$$I_0(C) := \int_C \exp\left(-\frac{\mathrm{i}}{h\epsilon}\left[\frac{k^2}{2} - \mathrm{e}^{-k-1} - (k+1)\,\tilde{X} + \frac{1}{2}\right] - (k+1)\tilde{Y}\right)\mathrm{d}k, \tag{2.77}$$

and

$$\mathcal{D}_0(R) := \{\; z \in \mathbb{C} \mid |z+1| \le R \;\}\,. \tag{2.78}$$

For now, all we require is that $0 < R_2 < \pi/2h$ so that the contour $C_{-\infty}^{(a)}$ lies entirely outside of $\mathcal{D}_0(R_2)$. In just a bit, we will chose the appropriate R_2 for each ϵ in order to bound the integrals over contour arcs that are away from the saddle points and demonstrate that they contribute very little as $\epsilon \to 0$.

Beginning with $I_0\left(C_{-\infty}^{(a)}\right)$, we use our parameterization and conduct some moderate bounding.

$$\left|I_0\left(C_{-\infty}^{(a)}\right)\right| = \left|\int_{-\infty}^{-\pi/2} \exp\Big(-\frac{\mathrm{i}}{h\epsilon}\left[\frac{1}{2}\left(s-1-\mathrm{i}\frac{\pi}{2}\right)^2 - \mathrm{e}^{-s+\mathrm{i}\pi/2} - \left(s-\mathrm{i}\frac{\pi}{2}\right)\tilde{X} + \frac{1}{2}\right] - \left[s-\mathrm{i}\frac{\pi}{2}\right]\tilde{Y}\Big)\,\mathrm{d}s\right| \tag{2.79}$$

$$\le \int_{-\infty}^{-\pi/2} \exp\left(\frac{1}{h\epsilon}\left[-\frac{\pi}{2}(s-1) - \mathrm{e}^{-s} + \frac{\pi}{2}\tilde{X}\right] - s\tilde{Y}\right)\mathrm{d}s \tag{2.80}$$

$$\le \int_{-\infty}^{-\pi/2} \exp\left(\frac{1}{h\epsilon}\left[\frac{\pi}{2}(\tilde{X}-s+1) - \mathrm{e}^{-s}\right] - s\right)\mathrm{d}s\,. \tag{2.81}$$

The leading-order function in the exponent is clearly concave-down and has one critical

point for $s \in \mathbb{R}$ at $s_c = -\ln(\pi/2)$. From properties of the natural logarithm, we have that $\ln(\pi/2) < \pi/2$, and thus $-\pi/2 < s_c$ so this function is monotone increasing on the integration range. This is useful because concave-down functions are always bounded above by any tangent line. We use this to bound above our function by the tangent line at the maximum on the integration range, $s = -\pi/2$

$$\frac{\pi}{2}(\tilde{X} - s + 1) - \mathrm{e}^{-s} \leq \frac{\pi}{2}\left(\tilde{X} + \frac{\pi}{2} + 1\right) - \mathrm{e}^{\pi/2} + \left(\mathrm{e}^{\pi/2} - \frac{\pi}{2}\right)\left(s + \frac{\pi}{2}\right) \tag{2.82}$$

for $s \leq -\pi/2$. Defining the positive constants $B^{(a)}_{-\infty} = \mathrm{e}^{\pi/2} - \pi/2$ and $\lambda^{(a)}_{-\infty} = \mathrm{e}^{\pi/2} - \pi/2\,(1 + \pi/2)$ (positive by numerical evaluation) this gives an upper bound for our integrand that we can explicitly integrate.

$$\left|I_0\left(C^{(a)}_{-\infty}\right)\right| \leq \exp\left(\frac{\pi\tilde{X}/2 - \lambda^{(a)}_{-\infty}}{h\epsilon}\right)\int_{-\infty}^{-\pi/2} \exp\left(\frac{B^{(a)}_{-\infty}}{h\epsilon}\left[s + \frac{\pi}{2}\right] - s\right)\,\mathrm{d}s \tag{2.83}$$

$$= \exp\left(\frac{\pi X/2 - \lambda^{(a)}_{-\infty}}{h\epsilon} + \frac{\pi}{2}\right)\frac{h\epsilon}{B^{(a)}_{-\infty} - h\epsilon} \tag{2.84}$$

$$\leq \exp\left(\frac{\pi\tilde{X}/2 - \lambda^{(a)}_{-\infty}}{h\epsilon} + \frac{\pi}{2}\right)\frac{2h\epsilon}{B^{(a)}_{-\infty}} \tag{2.85}$$

where we required in the last step that $\epsilon < B^{(a)}_{-\infty}/2h$. Lastly, if we also make sure that $|\tilde{X}| < \lambda^{(a)}_{-\infty}/\pi$, which is satisfied for all $\epsilon < (\lambda^{(a)}_{-\infty}/\pi M_\chi)^{1/\alpha}$ from the ϵ-scaling (2.69), then we have the final $\tilde{X}$-independent bound

$$\left|I_0\left(C^{(a)}_{-\infty}\right)\right| < \exp\left(\frac{\pi}{2} - \frac{\lambda^{(a)}_{-\infty}}{2h\epsilon}\right)\frac{2h\epsilon}{B^{(a)}_{-\infty}} \tag{2.86}$$

which is beyond all orders in ϵ.

Next, we look at $I_0\left(C^{(b)}_{-\infty}/\mathcal{D}_0(R_2)\right)$. The idea is to keep the colliding saddle points always interior to the disk, and then bound the integral on the contour outside of the disk like the one above. If we look at the definition of the saddle points (2.61), we conclude that $|\mathrm{e}^{-k-1} - 1 - (-k-1)| = |\tilde{X}|$, where k is the position of a saddle point. Then from a simple lower bound on the exponential minus its first two Taylor series

terms gives

$$|\tilde{X}| = |\mathrm{e}^{-k-1} - 1 - (-k-1)| \tag{2.87}$$

$$> \frac{1}{4}|k+1|^2 \tag{2.88}$$

$$\implies |k+1| \leq \frac{\sqrt{|\tilde{X}|}}{2} \leq \epsilon^{7/12}\frac{\sqrt{M_\chi}}{2} \tag{2.89}$$

when $|k+1| < 1$, so once ϵ is small enough that the saddle points are inside the disk of radius 1 around -1, then they are interior to the smaller, ϵ-shrinking disk with radius $\epsilon^{7/12}\sqrt{M_\chi}/2$. To add extra space between the saddle points and boundary, we will set the radius of $\mathcal{D}_0(R_2)$ to be $R_2 = \epsilon^{\beta/2}\sqrt{M_\chi}/2$ where $0 < \beta < \alpha < 2/3$. Now we can begin bounding the integral $I_0\left(C^{(b)}_{-\infty}/\mathcal{D}_0(R_2)\right)$ noting that the boundary of the disk is at $s = -R_2/\sqrt{2}$:

$$\begin{aligned}
&\left|I_0\left(C^{(b)}_{-\infty}/\mathcal{D}_0(R_2)\right)\right| \\
&\quad= \left|\int_{-\pi/2}^{-R_2/\sqrt{2}} \exp\left(-\frac{\mathrm{i}}{h\epsilon}\left[\frac{1}{2}\big((1+\mathrm{i})s-1\big)^2 - \mathrm{e}^{-(1+\mathrm{i})s} - (1+\mathrm{i})s\tilde{X} + \frac{1}{2}\right]\right.\right. \\
&\qquad\qquad \left.\left. - (1+\mathrm{i})s\tilde{Y}\right)(1+\mathrm{i})\,\mathrm{d}s\right| \qquad (2.90)\\
&\quad\leq \int_{-\pi/2}^{-R_2/\sqrt{2}} \exp\left(\frac{1}{h\epsilon}\left[s\,(s-1) + \mathrm{e}^{-s}\sin(s) - sX\right] - s\tilde{Y}\right)\sqrt{2}\,\mathrm{d}s \qquad (2.91)\\
&\quad\leq \mathrm{e}^{\pi/2}\sqrt{2}\int_{-\pi/2}^{-R_2/\sqrt{2}} \exp\left(\frac{1}{h\epsilon}\left[s^2 - (\tilde{X}+1)s + \mathrm{e}^{-s}\sin(s)\right]\right)\,\mathrm{d}s\,. \qquad (2.92)
\end{aligned}$$

When $\tilde{X} = 0$, the quadratic polynomial in the exponent cancels exactly the first three terms of the Taylor series of the expo-sinusoidal term at $s = 0$. This is, of course, a direct consequence of the fact that the saddle points merge at the parameterization value of $s = 0$ when $\tilde{X} = 0$ to become a second order saddle point. From some simple numerical bounding, we have for $-\pi/2 \leq s \leq 0$

$$s^2 - s + \mathrm{e}^{-s}\sin(s) \leq \frac{s^3}{6}\,. \tag{2.93}$$

Using this bound, along with the fact that the bounding cubic is concave-down and

that $-\tilde{X}s \leq -\epsilon^\alpha M_\chi s$ on the integration range, we get the tangent line upper bound

$$s^2 - (\tilde{X}+1)s + \mathrm{e}^{-s}\sin(s) \leq -\tilde{X}s + \frac{s^3}{6} \leq -\epsilon^\alpha M_\chi s + \frac{s^3}{6} \tag{2.94}$$

$$\leq \frac{R_2}{\sqrt{2}}\left(\epsilon^\alpha M_\chi - \frac{R_2^2}{12}\right) + \left(-\epsilon^\alpha M_\chi + \frac{R_2^2}{4}\right)\left(s + \frac{R_2}{\sqrt{2}}\right) \tag{2.95}$$

$$= \epsilon^{3\beta/2}\frac{M_\chi^{3/2}}{4\sqrt{2}}\left(\epsilon^{\alpha-\beta} - \frac{1}{48}\right) + \epsilon^\beta M_\chi\left(-\epsilon^{\alpha-\beta} + \frac{1}{16}\right)\left(s + \frac{R_2}{\sqrt{2}}\right) \tag{2.96}$$

$$\leq -\epsilon^{3\beta/2}\frac{M_\chi^{3/2}}{384\sqrt{2}} + \epsilon^\beta\frac{5M_\chi}{96}\left(s + \frac{R_2}{\sqrt{2}}\right) \tag{2.97}$$

where we have required $\epsilon < (1/96)^{1/(\alpha-\beta)}$. Now, we use this to bound our integral, and noticing that extending the lower bound to $-\infty$ only increases the result, we get

$$\left|I_0\left(C_{-\infty}^{(b)}/\mathcal{D}_0(R_2)\right)\right|$$

$$\leq \mathrm{e}^{\pi/2}\sqrt{2}\int_{-\infty}^{-R_2/\sqrt{2}} \exp\left(\frac{1}{h\epsilon}\left[-\epsilon^{3\beta/2}\frac{M_\chi^{3/2}}{384\sqrt{2}} + \epsilon^\beta\frac{5M_\chi}{96}\left(s + \frac{R_2}{\sqrt{2}}\right)\right]\right)\mathrm{d}s \tag{2.98}$$

$$= \epsilon^{1-\beta}\frac{96\sqrt{2}h}{5M_\chi}\exp\left(\frac{\pi}{2} - \frac{1}{h\epsilon^{1-3\beta/2}}\frac{M_\chi^{3/2}}{384\sqrt{2}}\right) \tag{2.99}$$

which, since $1 - 3\beta/2 > 0$ and $1 - \beta > 1/3$, goes to zero beyond all orders.

Lastly, we conduct a very similar bounding argument for $I_0\left(C_{-\infty}^{(c)}/\mathcal{D}_0(R_2)\right)$. In this case, the edge of the disk is the lower integration bound $s = R_2/\sqrt{2}$.

$$\left|I_0\left(C_{-\infty}^{(c)}/\mathcal{D}_0(R_2)\right)\right|$$

$$= \left|\int_{R_2/\sqrt{2}}^{\infty} \exp\left(-\frac{\mathrm{i}}{h\epsilon}\left[\frac{1}{2}\left((1-\mathrm{i})s - 1\right)^2 - \mathrm{e}^{-(1-\mathrm{i})s} - (1-\mathrm{i})s\tilde{X} + \frac{1}{2}\right]\right.\right.$$

$$\left.\left. - (1-\mathrm{i})s\tilde{Y}\right)(1-\mathrm{i})\,\mathrm{d}s\right| \tag{2.100}$$

$$\leq \int_{R_2/\sqrt{2}}^{\infty}\exp\left(\frac{1}{h\epsilon}\left[-s(s-1) - \mathrm{e}^{-s}\sin(s) + s\tilde{X}\right] - s\tilde{Y}\right)\sqrt{2}\,\mathrm{d}s \tag{2.101}$$

$$\leq \sqrt{2}\int_{R_2/\sqrt{2}}^{\infty}\exp\left(\frac{1}{h\epsilon}\left[-s^2 + (\tilde{X}+1)s + \mathrm{e}^{-s}\sin(s)\right]\right)\mathrm{d}s\,. \tag{2.102}$$

Again, as expected, the polynomial terms in the exponent with $\tilde{X} = 0$ cancel the behavior of the expo-sinusoid at $s = 0$. Looking quickly at the second derivative of the

exponent function, we can bound numerically by

$$-2 + 2\mathrm{e}^{-s}\sin(s) \leq \begin{cases} -s & \text{if } 0 < s < 1 \\ -1 & \text{if } s > 1 \end{cases} . \tag{2.103}$$

Integrating this up twice and taking the first derivative and value to be zero at $s = 0$, we get the bound

$$-s^2 + s + \mathrm{e}^{-s}\sin(s) \leq \begin{cases} -\dfrac{s^3}{6} & \text{if } 0 < s < 1 \\ -\dfrac{s^2}{2} - \dfrac{s}{2} + \dfrac{5}{6} & \text{if } s > 1 \end{cases} . \tag{2.104}$$

Since the piece-wise function is concave-down on both sections of its domain, and the derivative matches at the connection point $s = 1$, the whole function is concave-down. We simply then need to have ϵ small enough so that $R_2/\sqrt{2} < 1$ and then we can bound by the tangent line on the domain $0 \leq s \leq 1$. Under the change of variables $s \to -s$, the tangent lines and domain are the same as the integral we just evaluated, thus the same final bounds can be performed and the answer works out the same:

$$\left| I_0\left(C^{(c)}_{-\infty}/\mathcal{D}_0(R_2)\right)\right| \leq \epsilon^{1-\beta}\frac{96\sqrt{2}h}{5M_\chi}\exp\left(\frac{\pi}{2} - \frac{1}{h\epsilon^{1-3\beta/2}}\frac{M_\chi^{3/2}}{384\sqrt{2}}\right) . \tag{2.105}$$

So this is too is beyond all orders in ϵ. This finishes off the justification that the contributions from the contours sections that are far from the saddle points rapidly go to zero, leaving just the contributions from contour sections near by the saddle points that need to be evaluated.

2. $\nu \in 2\mathbb{Z}-1/2$ with $\nu \leq -9/2$. Define $C_\nu(\tilde{X}, b) = C^{(a)}_\nu(\tilde{X}, b) \cup C^{(b)}_\nu(\tilde{X}, b) \cup \left(-C^{(a)}_{\nu+2}(\tilde{X}, b)\right)$ (the minus sign indicates the reversal of the contour orientation) for all $\tilde{X}, b \in \mathbb{R}$ and associate to each $\nu \leq -5/2$ the integer $n = (\nu - 3/2)/2$,

$$C^{(a)}_\nu(\tilde{X}, b): \quad k^{(a)}_\nu(s; \tilde{X}, b) = s - \mathrm{i}\mathrm{Im}\left[k_n(\tilde{X})\right], \quad s \in (-\infty,\ b] \tag{2.106}$$

$$C^{(b)}_\nu(\tilde{X}, b): \quad k^{(b)}_\nu(s; \tilde{X}, b) = b + \mathrm{i}s, \quad s \in \left[\mathrm{Im}\left[k_n(\tilde{X})\right],\ \mathrm{Im}\left[k_{\nu+1}(\tilde{X})\right]\right]. \tag{2.107}$$

First off, we note that the imaginary parts of these contours as they extend out to $\mathrm{Re}\,[k] = -\infty$ are not the same as the ones listed in the definition of the C_ν contours (2.56). However, the contours given above can always be deformed to those described in the original definition with no change in the value of the integral. This is because from

properties of the Lambert W function, $\pi(\nu-1/2) < \mathrm{Im}\left[k_n(\tilde{X})\right] < \pi(\nu+1/2)$ and $\pi(\nu+3/2) < \mathrm{Im}\left[k_{n+1}(\tilde{X})\right] < \pi(\nu+5/2)$ for all $\tilde{X} \in \mathbb{R}$. This means that the two horizontal components lie in the same basins as those in the contour definitions' beginning and ending, $\mathrm{Im}\,[k] = \pi\nu$ and $\mathrm{Im}\,[k] = \pi(\nu+2)$ respectively. Deforming the contour to have the correct imaginary part can be done for each $\tilde{X} \in \mathbb{R}$ by adding small vertical arcs to jump between the two different imaginary parts at some real value, say $a \in \mathbb{R}$. Then, as we take $a \to -\infty$, since the vertical segments are each entirely contained in one basin, the value on these vertical sections goes to zero super-exponentially. The last thing to check is that the integrals on the $\tilde{X}$-dependent contours are always convergent, which will be done automatically in this case as we bound contour contributions below. Lastly, we remark that each contour integral is independent of $b \in \mathbb{R}$ by Cauchy's theorem. We then split the integral defining ψ_ν by

$$\begin{aligned}\psi_\nu(Z;\epsilon,h) &= \mathrm{e}^{-\mathrm{i}f\left(k_n(\tilde{X});\tilde{X}\right)/h\epsilon - k_n(\tilde{X})\tilde{Y}} \\ &\qquad \times \int_{C_\nu(\tilde{X},b)} \exp\left(-\frac{\mathrm{i}}{h\epsilon}\left[f(k;\tilde{X}) - f\left(k_n(\tilde{X});\tilde{X}\right)\right] - [k-k_n(\tilde{X})]\tilde{Y}\right)\mathrm{d}k \qquad (2.108)\\ &= E_n(\tilde{X},\tilde{Y})\Big[I_n\left(C_\nu^{(a)}(\tilde{X},b)\cap\mathcal{D}_n(R_1)\right) + I_n\left(C_\nu^{(a)}(\tilde{X},b)/\mathcal{D}_n(R_1)\right) \\ &\qquad\qquad + I_n\left(C_\nu^{(b)}(\tilde{X},b)\right)\Big] \\ &\quad - E_{n+1}(\tilde{X},\tilde{Y})\Big[I_{n+1}\left(C_{\nu+2}^{(a)}(\tilde{X},b)\cap\mathcal{D}_{n+1}(R_1)\right) \\ &\qquad\qquad + I_{n+1}\left(C_{\nu+2}^{(a)}(\tilde{X},b)/\mathcal{D}_{n+1}(R_1)\right)\Big] \qquad (2.109)\end{aligned}$$

where for $m \in \mathbb{Z}$ but $m \neq -1, 0$, we define the integrals

$$I_m(C) := \int_C \exp\left(-\frac{\mathrm{i}}{h\epsilon}\left[f(k;\tilde{X}) - f(k_m(\tilde{X});\tilde{X})\right] - [k-k_m(\tilde{X})]\tilde{Y}\right)\mathrm{d}k\,, \qquad (2.110)$$

the exponential factors

$$E_m(\tilde{X},\tilde{Y}) := \mathrm{e}^{-\mathrm{i}f(k_m(\tilde{X});\tilde{X})/h\epsilon - k_m(\tilde{X})\tilde{Y}}\,, \qquad (2.111)$$

and the $\tilde{X}$-dependent disks centered on the saddle points for all $\tilde{X} \in \mathbb{R}$

$$\mathcal{D}_m(R) := \{\ z \in \mathbb{C} \mid |z - k_m(\tilde{X})| \leq R\ \}\,. \qquad (2.112)$$

Note that we suppress the $\tilde{X}$-dependence of the centers of these disks for notational brevity, and that this should not be confused with the fact that the center of the disk $\mathcal{D}_0(R_2)$ is $\tilde{X}$-independent.

First, let us consider $I_n\left(C_\nu^{(b)}(\tilde{X},b)\right)$ for any $b\in\mathbb{R}$. We simplify the exponent function

$$f(k;\tilde{X})-f(k_n(\tilde{X});\tilde{X})=\frac{k^2}{2}-\mathrm{e}^{-k-1}-k\tilde{X}-\frac{k_n(\tilde{X})^2}{2}+\mathrm{e}^{-k_n(\tilde{X})-1}+k_n(\tilde{X})\tilde{X} \tag{2.113}$$

$$=\frac{(k-\tilde{X})^2}{2}-\frac{(k_n(\tilde{X})-\tilde{X})^2}{2}-\mathrm{e}^{-k-1}+\tilde{X}-k_n(\tilde{X}) \tag{2.114}$$

where in the last step, we have used the relationship that defines the saddle points to replace $\mathrm{e}^{-k_n(\tilde{X})-1}=\tilde{X}-k_n(\tilde{X})$. Now we consider the bound

$$\begin{aligned}&\left|I_n\left(C_\nu^{(b)}(\tilde{X},b)\right)\right|\\&=\left|\int_{\mathrm{Im}\left[k_n(\tilde{X})\right]}^{\mathrm{Im}\left[k_{n+1}(\tilde{X})\right]}\exp\left(-\frac{\mathrm{i}}{h\epsilon}\left[\frac{(b+\mathrm{i}s-\tilde{X})^2}{2}-\frac{(k_n(\tilde{X})-\tilde{X})^2}{2}-\mathrm{e}^{-2h(b+\mathrm{i}s)-1}\right.\right.\right.\\&\qquad\left.\left.\left.+\tilde{X}-k_n(\tilde{X})\right]-[b+\mathrm{i}s-k_n(\tilde{X})]\tilde{Y}\right)\mathrm{d}s\right| \qquad (2.115)\\&\leq\int_{\mathrm{Im}\left[k_n(\tilde{X})\right]}^{\mathrm{Im}\left[k_{n+1}(\tilde{X})\right]}\exp\left(\frac{1}{h\epsilon}\left[s(b-\tilde{X})-\mathrm{Im}\left[k_n(\tilde{X})\right]\left(\mathrm{Re}\left[k_n(\tilde{X})\right]-\tilde{X}\right)\right.\right.\\&\qquad\left.\left.+\mathrm{e}^{-b-1}\sin(s)-\mathrm{Im}\left[k_n(\tilde{X})\right]\right]-\left(b-\mathrm{Re}\left[k_n(\tilde{X})\right]\right)\tilde{Y}\right)\mathrm{d}s \qquad (2.116)\\&\leq\int_{\mathrm{Im}\left[k_n(\tilde{X})\right]}^{\mathrm{Im}\left[k_{n+1}(\tilde{X})\right]}\exp\left(\frac{1}{h\epsilon}\left[s(b-\tilde{X})-\mathrm{Im}\left[k_n(\tilde{X})\right]\left(\mathrm{Re}\left[k_n(\tilde{X})\right]-\tilde{X}+1\right)\right.\right.\\&\qquad\left.\left.+\mathrm{e}^{-b-1}\right]\right)\mathrm{d}s \qquad (2.117)\end{aligned}$$

where all we did was use the fact that sine is less than or equal to one in order to bound the exponent above by a linear function and we have assumed without loss of generality that $b>\mathrm{Re}\left[k_n(\tilde{X})\right]$ so $-\left(b-\mathrm{Re}\left[k_n(\tilde{X})\right]\right)\tilde{Y}\leq 0$ for $0\leq\tilde{Y}\leq 1$. This is

then directly integrable for any $b > \tilde{X} \in \mathbb{R}$ as well,

$$\begin{aligned}
&\left|I_n\left(C_\nu^{(b)}(\tilde{X},b)\right)\right| \\
&\quad\leq \exp\left(\frac{1}{h\epsilon}\left[-\mathrm{Im}\left[k_n(\tilde{X})\right]\left(\mathrm{Re}\left[k_n(\tilde{X})\right]-\tilde{X}+1\right)+\mathrm{e}^{-b-1}\right]\right) \\
&\qquad\times h\epsilon\frac{\mathrm{e}^{(b-\tilde{X})\mathrm{Im}\left[k_{n+1}(\tilde{X})\right]/h\epsilon}-\mathrm{e}^{(b-\tilde{X})\mathrm{Im}\left[k_n(\tilde{X})\right]/h\epsilon}}{b-\tilde{X}} \qquad (2.118)\\
&\quad= \exp\left(\frac{1}{h\epsilon}\left[(b-\tilde{X})\mathrm{Im}\left[k_{n+1}(\tilde{X})\right]-\mathrm{Im}\left[k_n(\tilde{X})\right]\left(\mathrm{Re}\left[k_n(\tilde{X})\right]-\tilde{X}+1\right)\right.\right. \\
&\qquad\left.\left.+\mathrm{e}^{-b-1}\right]\right)h\epsilon\frac{1-\mathrm{e}^{-(b-\tilde{X})\left(\mathrm{Im}\left[k_{n+1}(\tilde{X})\right]-\mathrm{Im}\left[k_n(\tilde{X})\right]\right)/h\epsilon}}{b-\tilde{X}}\,. \qquad (2.119)
\end{aligned}$$

Moreover, we have the universal bounds $\mathrm{Im}\left[k_n(\tilde{X})\right] < -\pi$ and $\mathrm{Im}\left[k_{n+1}(\tilde{X})\right] - \mathrm{Im}\left[k_n(\tilde{X})\right] > \pi$ for all $n \leq 2$. We can also bound $\mathrm{Re}\left[k_n(\tilde{X})\right]$ by noting that

$$\begin{aligned}
\tilde{X}-k_n(\tilde{X}) &= \mathrm{e}^{-k_n(\tilde{X})-1}\,, &(2.120)\\
\implies |\tilde{X}-k_n(\tilde{X})| &= \mathrm{e}^{-\mathrm{Re}\left[k_n(\tilde{X})\right]-1}\,, &(2.121)\\
\implies \mathrm{Re}\left[k_n(\tilde{X})\right]+1 &= -\ln\left|\tilde{X}-k_n(\tilde{X})\right|\,. &(2.122)
\end{aligned}$$

Then, since $\mathrm{Im}\left[k_n(\tilde{X})\right] < \pi(\nu+1/2)/2$, we have

$$\left|\tilde{X}-k_n(\tilde{X})\right| \geq \left|\mathrm{Im}\left[\tilde{X}-k_n(\tilde{X})\right]\right| \geq -\pi(\nu+1/2) \geq 2\pi \qquad (2.123)$$

for all $\nu \leq -5/2$. This gives us the uniform bound

$$\mathrm{Re}\left[k_n(\tilde{X})\right]+1 \leq -\ln(2\pi)\,. \qquad (2.124)$$

Lastly, if we require $\left|\tilde{X}\right| \leq \ln(2\pi)/2$, which will always be the case for small enough ϵ, then

$$\mathrm{Re}\left[k_n(\tilde{X})\right]-\tilde{X}+1 \leq \frac{1}{2}\ln(2\pi)-\ln(2\pi) = -\frac{1}{2}\ln(2\pi) < 0\,. \qquad (2.125)$$

These final bounds lets us write a uniform in ν upper bound to this integral

$$\begin{aligned}
\left|I_n\left(C_\nu^{(b)}(\tilde{X},b)\right)\right| \leq \frac{h\epsilon}{b-\tilde{X}}&\exp\left(\frac{1}{h\epsilon}\left[-\pi(b-\tilde{X})-\frac{\pi}{2}\ln(2\pi)+\mathrm{e}^{-b-1}\right]\right) \\
&\times\left(1-\mathrm{e}^{-\pi(b-\tilde{X})/h\epsilon}\right)\,. \qquad (2.126)
\end{aligned}$$

which is easily seen to go to zero as $b \to +\infty$ with ϵ and $\tilde{X}$ held fixed. This means as the contours are extend to real-part infinity, the vertical component can be eliminated and the horizontal contour components are the only ones that contribute, of course, so long as they remain integrable as $b \to +\infty$.

We will now consider the $I_n\left(C_\nu^{(b)}(\tilde{X}, b)/\mathcal{D}_n(R_1)\right)$ where R_1 will be determined by our analysis, and we will require that $b > \mathrm{Re}\left[k_n(\tilde{X})\right] + R_1$. But first, we do one small rework of the function that appears in the exponential

$$f(k;\tilde{X}) - f(k_n(\tilde{X});\tilde{X}) = \frac{(k-\tilde{X})^2}{2} - \frac{(k_n(\tilde{X})-\tilde{X})^2}{2} - \mathrm{e}^{-k-1} + \mathrm{e}^{-k_n(\tilde{X})-1} \tag{2.127}$$

$$= \frac{(k-\tilde{X})^2}{2} - \frac{(k_n(\tilde{X})-\tilde{X})^2}{2} + \mathrm{e}^{-k_n(\tilde{X})-1}\left(1 - \mathrm{e}^{-k+k_n(\tilde{X})}\right) \tag{2.128}$$

$$= \frac{(k-\tilde{X})^2}{2} - \frac{(k_n(\tilde{X})-\tilde{X})^2}{2} + (\tilde{X} - k_n(\tilde{X}))\left(1 - \mathrm{e}^{-k+k_n(\tilde{X})}\right) \tag{2.129}$$

where we just used the relationship $\mathrm{e}^{-k_n(\tilde{X})-1} = \tilde{X} - k_n(\tilde{X})$ twice and factored out an exponential term in between. Now plugging in the parametrization $k_\nu^{(a)}(s;\tilde{X},b)$ and taking the real-part of the exponent to get a bound on the norm, as has been done in all of the preceding parts, we get

$$\mathrm{Re}\left[-\frac{\mathrm{i}}{h\epsilon}\left[f(k;\tilde{X}) - f(k_n(\tilde{X});\tilde{X})\right] - [k - k_n(\tilde{X})]\tilde{Y}\right]$$

$$= \frac{1}{h\epsilon}\mathrm{Im}\left[\frac{\left(s + \mathrm{iIm}\left[k_n(\tilde{X})\right] - \tilde{X}\right)^2}{2} - \frac{(k_n(\tilde{X})-\tilde{X})^2}{2}\right.$$

$$\left. + (\tilde{X} - k_n(\tilde{X}))\left(1 - \mathrm{e}^{-s+\mathrm{Re}\left[k_n(\tilde{X})\right]}\right)\right] - \left(s - \mathrm{Re}\left[k_n(\tilde{X})\right]\right)\tilde{Y} \tag{2.130}$$

$$= \frac{\mathrm{Im}\left[k_n(\tilde{X})\right]}{h\epsilon}\left[\left(s - \mathrm{Re}\left[k_n(\tilde{X})\right]\right) - 1 + \mathrm{e}^{-s+\mathrm{Re}\left[k_n(\tilde{X})\right]}\right] - \left(s - \mathrm{Re}\left[k_n(\tilde{X})\right]\right)\tilde{Y}\,. \tag{2.131}$$

Very fortuitously, we can do the $\tilde{X}$ and n-dependent change of variables $s' = s - \mathrm{Re}\left[k_n(\tilde{X})\right]$, which brings every integral into the same form. Additionally, it is apparent now that as $b \to +\infty$, this upper bound remains finite since the above expression is exponentially close to linear in s with negative slope as $s \to +\infty$. Thus, we can upper bound for all b by taking $b \to +\infty$. Moreover, we can get a completely uniform in $\tilde{X}$

and n upper bound by using $\mathrm{Im}\left[k_n(\tilde{X})\right] < -\pi$

$$\left|I_n\left(C_\nu^{(a)}(\tilde{X},+\infty)/\mathcal{D}_n(R_1)\right)\right| \leq \int_{-\infty}^{-R_1} \exp\left(-\frac{\pi}{h\epsilon}\left[s'-1+\mathrm{e}^{-s'}\right]-s'\tilde{Y}\right)\mathrm{d}s' + \int_{R_1}^{+\infty} \exp\left(-\frac{\pi}{h\epsilon}\left[s'-1+\mathrm{e}^{-s'}\right]-s'\tilde{Y}\right)\mathrm{d}s'\,. \tag{2.132}$$

From a derivative bounding argument like those in the first case, it is easy to show that

$$s'-1+\mathrm{e}^{-s'} \leq \begin{cases} \dfrac{(s')^2}{4} & s' \leq 1 \\ \dfrac{s'}{2}-\dfrac{1}{2} & s' > 1 \end{cases}\,. \tag{2.133}$$

We then do the standard tangent-line bounds for $R_1 \leq 1$, which is only integrable if $\tilde{Y} < \pi R_1/2h\epsilon$, to get

$$\left|I_n\left(C_\nu^{(a)}(\tilde{X},+\infty)/\mathcal{D}_n(R_1)\right)\right| \leq \int_{R_1}^{+\infty} \exp\left(-\frac{\pi}{2h\epsilon}\left[\frac{R_1^2}{2}+R_1\left(s'-R_1\right)\right]-\tilde{Y}s'\right)\mathrm{d}s' + \int_{-\infty}^{-R_1} \exp\left(-\frac{\pi}{2h\epsilon}\left[\frac{R_1^2}{2}-R_1\left(s'+R_1\right)\right]-\tilde{Y}s'\right)\mathrm{d}s' \tag{2.134}$$

$$\leq \exp\left(-\frac{\pi R_1^2}{4h\epsilon}-R_1\tilde{Y}\right)\frac{2h\epsilon}{\pi R_1+2h\tilde{Y}\epsilon} + \exp\left(-\frac{\pi R_1^2}{4h\epsilon}+R_1\tilde{Y}\right)\frac{2h\epsilon}{\pi R_1-2h\tilde{Y}\epsilon}\,. \tag{2.135}$$

So if we take $R_1 = \epsilon^\gamma$ where $0 < \gamma < 1/2$ and use $0 \leq \tilde{Y} \leq 1$ then,

$$\left|I_n\left(C_\nu^{(a)}(\tilde{X},+\infty)/\mathcal{D}_n(R_1)\right)\right| \leq \exp\left(-\frac{\pi}{4h\epsilon^{1-2\gamma}}\right)\frac{2h\epsilon^{1-\gamma}}{\pi} + \exp\left(-\frac{\pi}{4h\epsilon^{1-2\gamma}}+\epsilon^\gamma\right)\frac{2h\epsilon^{1-\gamma}}{\pi-2h\epsilon^{1-\gamma}}\,. \tag{2.136}$$

and this goes to zero beyond all orders in ϵ. This means all that is left to evaluate of this contour are the sections in the ϵ-shrinking disks around the two saddle points $k_n(\tilde{X})$ and $k_{n+1}(\tilde{X})$, which will be done in the next subsection.

3. $\nu = -5/2$. This case looks similar to the last, but instead of the upper contour that returns to real-part $-\infty$ being a horizontal line, we go through the coalescing saddle point disk $\mathcal{D}_0(R_2)$ using some of the contours that were defined for the $\nu = -\infty$ case.

Specifically,

$$C_{-5/2} = C^{(a)}_{-5/2}\left(\tilde{X}, b_{-5/2}(\tilde{X})\right) \cup \left(-C^{(c)}_{-\infty} \cap \mathcal{D}_0\left(-\sqrt{2}\mathrm{Im}\left[k_{-2}(\tilde{X})\right]\right)\right) \cup \left(-C^{(b)}_{-\infty}\right) \cup \left(-C^{(a)}_{-\infty}\right). \tag{2.137}$$

where $b_{-5/2}(\tilde{X}) = -1 - \mathrm{Im}\left[k_{-2}(\tilde{X})\right]$. Note that this case can be handled entirely by using contours or sections of contours defined in the previous two cases. The choices of evaluation at $b_{-5/2}(\tilde{X})$ on the first contour segment and the intersection with the disk $\mathcal{D}_0\left(-\sqrt{2}\mathrm{Im}\left[k_{-2}(\tilde{X})\right]\right)$ on the second is so that the two contours have their endpoints meet at the point $k = -1 - (1-\mathrm{i})\mathrm{Im}\left[k_{-2}(\tilde{X})\right]$. Thus, working like in the previous case:

$$\begin{aligned}\psi_{-5/2}(Z;\epsilon,h) = E_{-2}(\tilde{X},\tilde{Y})\Big[&I_{-2}\left(C^{(a)}_{-5/2}(\tilde{X}, b_{-5/2}(\tilde{X})) \cap \mathcal{D}_{-2}(R_1)\right) \\ &+ I_{-2}\left(C^{(a)}_{-5/2}(\tilde{X}, b_{-5/2}(\tilde{X}))/\mathcal{D}_{-2}(R_1)\right)\Big] \\ + E_0(\tilde{X},\tilde{Y})\Big[&I_0\left(C^{(c)}_{-\infty} \cap \mathcal{D}_0(R_2)\right) \\ &+ I_0\left(C^{(c)}_{-\infty} \cap \mathcal{D}_0\left(R_{5/2}(\tilde{X})\right)/\mathcal{D}_0(R_2)\right) \\ &- I_0\left(C^{(b)}_{-\infty} \cap \mathcal{D}_0(R_2)\right) - I_0\left(C^{(b)}_{-\infty}/\mathcal{D}_0(R_2)\right) \\ &- I_0\left(C^{(a)}_{-\infty}\right)\Big]\end{aligned} \tag{2.138}$$

where we define $R_{5/2}(\tilde{X}) = \sqrt{2}\left|\mathrm{Im}\left[k_{-2}(\tilde{X})\right]\right|$ and we have required that ϵ is small enough so that $R_1 < 2\sqrt{2}\pi < R_{5/2}(\tilde{X})$. We have already bounded $I_0\left(C^{(b)}_{-\infty}/\mathcal{D}_0(R_2)\right)$ and $I_0\left(C^{(a)}_{-\infty}\right)$ in case 1. Noting that $C^{(c)}_{-\infty} \cap \mathcal{D}_0\left(R_{5/2}(\tilde{X})\right)/\mathcal{D}_0(R_2)$ is a section of the contour $C^{(c)}_{-\infty}/\mathcal{D}_0(R_2)$, after moving the absolute value into the integral, we can

increase the integration bound, which can only make the integral bigger.

$$\begin{aligned}
&\left|I_0\left(C^{(c)}_{-\infty}\cap\mathcal{D}_0\left(-\sqrt{2}\mathrm{Im}\left[k_{-2}(\tilde{X})\right]\right)/\mathcal{D}_0(R_2)\right)\right| \\
&\quad=\left|\int_{R_2/\sqrt{2}}^{-\mathrm{Im}\left[k_{-2}(\tilde{X})\right]}\exp\left(-\frac{\mathrm{i}}{h\epsilon}\left[\frac{1}{2}\left((1-\mathrm{i})s-1\right)^2-\mathrm{e}^{-(1-\mathrm{i})s}-(1-\mathrm{i})s\tilde{X}+\frac{1}{2}\right]\right.\right. \\
&\qquad\qquad\left.\left.-(1-\mathrm{i})s\tilde{Y}\right)(1-\mathrm{i})\,\mathrm{d}s\right| \qquad (2.139)\\
&\quad\leq\int_{R_2/\sqrt{2}}^{-\mathrm{Im}\left[k_{-2}(\tilde{X})\right]}\exp\left(\frac{1}{h\epsilon}\left[-s(s-1)-\mathrm{e}^{-s}\sin(s)+s\tilde{X}\right]-s\tilde{Y}\right)\sqrt{2}\,\mathrm{d}s \qquad (2.140)\\
&\quad\leq\int_{R_2/\sqrt{2}}^{\infty}\exp\left(\frac{1}{h\epsilon}\left[-s(s-1)-\mathrm{e}^{-s}\sin(s)+s\tilde{X}\right]-s\tilde{Y}\right)\sqrt{2}\,\mathrm{d}s\,. \qquad (2.141)
\end{aligned}$$

Then this is the same integral we bounded in case 1. With an identical procedure, we can bound $\left|I_{-2}\left(C^{(a)}_{-5/2}(\tilde{X},b_{-5/2}(\tilde{X}))/\mathcal{D}_{-2}(R_1)\right)\right|$ with the bound for $\left|I_{-2}\left(C^{(a)}_{\nu}(\tilde{X},+\infty)/\mathcal{D}_n(R_1)\right)\right|$ in (2.136) from case 2! That finishes this case.

4. $\nu=-1/2$. Here, the contour just goes through the colliding saddle points but in a different way from $\nu=-\infty$. Define $C_{-1/2}=C^{(a)}_{-\infty}\cup C^{(b)}_{-\infty}\cup C^{(a)}_{-1/2}\cup\left(-C^{(b)}_{-1/2}\right)$ with

$$C^{(a)}_{-1/2}:\quad k^{(a)}_{-1/2}(s)=-1+\mathrm{i}s,\quad s\in\left[0,\ \frac{3\pi}{2}\right], \qquad (2.142)$$

$$C^{(b)}_{-1/2}:\quad k^{(b)}_{-1/2}(s)=s-1+\mathrm{i}\frac{3\pi}{2},\quad s\in(-\infty,\ 0]\,. \qquad (2.143)$$

Expanding the contributions we have

$$\begin{aligned}
\psi_{-1/2}(Z;h)=E_0(\tilde{X},\tilde{Y})\Big[&I_0\left(C^{(a)}_{-\infty}\right)+I_0\left(C^{(b)}_{-\infty}\cap\mathcal{D}_0(R_2)\right)+I_0\left(C^{(a)}_{-\infty}/\mathcal{D}_0(R_2)\right)\\
&+I_0\left(C^{(a)}_{-1/2}\cap\mathcal{D}_0(R_2)\right)+I_0\left(C^{(a)}_{-1/2}/\mathcal{D}_0(R_2)\right)-I_0\left(C^{(b)}_{-1/2}\right)\Big].
\end{aligned} \qquad (2.144)$$

Again, we already have bounds on $I_0\left(C^{(a)}_{-\infty}(\tilde{X})\right)$ and $I_0\left(C^{(b)}_{-\infty}/\mathcal{D}_0(R_2)\right)$ from case 1.

Let us focus on $I_0\left(C^{(a)}_{-1/2}/\mathcal{D}_0(R_2)\right)$.

$$\left|I_0\left(C^{(a)}_{-1/2}/\mathcal{D}_0(R_2)\right)\right| = \left|\int_{R_2}^{3\pi/2} \exp\left(-\frac{\mathrm{i}}{h\epsilon}\left[\frac{1}{2}(1-\mathrm{i}s)^2 - \mathrm{e}^{-\mathrm{i}s} - \mathrm{i}s\tilde{X} + \frac{1}{2}\right] - \mathrm{i}s\tilde{Y}\right)\,\mathrm{d}s\right| \tag{2.145}$$

$$\leq \int_{R_2}^{3\pi/2} \exp\left(\frac{1}{h\epsilon}\left[-(1+\tilde{X})s + \sin(s)\right]\right)\,\mathrm{d}s\,. \tag{2.146}$$

From the numerical bound

$$-1+\cos(s) \leq \begin{cases} -\dfrac{s^2}{\pi^2} & \text{if } 0 \leq s \leq \pi \\ -1 & \text{if } \pi < s \leq \dfrac{3\pi}{2} \end{cases}, \tag{2.147}$$

we integrate from $s=0$ to get

$$-s+\sin(s) \leq \begin{cases} -\dfrac{s^3}{3\pi^2} & \text{if } 0 \leq s \leq \pi \\ \dfrac{2\pi}{3} - s & \text{if } \pi < s \leq \dfrac{3\pi}{2} \end{cases}. \tag{2.148}$$

This means we can use this to over-bound and again use the tangent line at the point $s = R_2$.

$$-(1+\tilde{X})s + \sin(s) \leq -\frac{R_2^3}{3\pi^2} - \tilde{X}R_2 - \left(\frac{R_2^2}{\pi^2} - \tilde{X}\right)(s-R_2) \tag{2.149}$$

$$\leq -\epsilon^{\beta/2}\frac{\sqrt{M_\chi}}{2}\left(\epsilon^\beta\frac{M_\chi}{12\pi^2} - \epsilon^\alpha M_\chi\right) - \left(\epsilon^\beta\frac{M_\chi}{4\pi^2} - \epsilon^\alpha M_\chi\right)(s-R_2) \tag{2.150}$$

$$\leq -\epsilon^{3\beta/2}\frac{M_\chi^{3/2}}{48\pi^2} - \epsilon^\beta M_\chi\frac{11}{48\pi^2}(s-R_2) \tag{2.151}$$

where we've taken $\epsilon < (1/24\pi^2)^{1/(\alpha-\beta)}$. Now we plug this in and integrate explicitly, extending the upper bound to infinity making the bound only larger,

$$\left|I_0\left(C^{(a)}_{-1/2}/\mathcal{D}_0(R_2)\right)\right| \leq \int_{R_2}^{\infty} \exp\left(-\frac{M_\chi^{3/2}}{48\pi^2 h\epsilon^{1-3\beta/2}} - \frac{11M_\chi}{48\pi^2 h\epsilon^{1-\beta}}(s-R_2)\right)\,\mathrm{d}s \tag{2.152}$$

$$\leq \frac{48\pi^2 h\epsilon^{1-\beta}}{11M_\chi}\exp\left(-\frac{M_\chi^{3/2}}{48\pi^2 h\epsilon^{1-3\beta/2}}\right). \tag{2.153}$$

This shows that the contribution is beyond all orders in ϵ.

Lastly, we look at $I_0\left(C^{(b)}_{-1/2}\right)$.

$$\left|I_0\left(C^{(b)}_{-1/2}\right)\right| = \left|\int_{-\infty}^{0} \exp\left(-\frac{\mathrm{i}}{h\epsilon}\left[\frac{1}{2}\left(s-1+\mathrm{i}\frac{3\pi}{2}\right)^2 - \mathrm{e}^{-s-\mathrm{i}3\pi/2} - \left(s+\mathrm{i}\frac{3\pi}{2}\right)\tilde{X} + \frac{1}{2}\right] - \left[s+\mathrm{i}\frac{3\pi}{2}\right]\tilde{Y}\right)\mathrm{d}s\right| \quad (2.154)$$

$$\leq \int_{-\infty}^{0} \exp\left(\frac{1}{h\epsilon}\left[\frac{3\pi}{2}(s-1-\tilde{X}) - \mathrm{e}^{-s}\right] - s\right)\mathrm{d}s\,. \quad (2.155)$$

Using $-\mathrm{e}^{-s} \leq -1$ on the integration domain and requiring $|X| \leq 1$ gives

$$\frac{3\pi}{2}(s-1-\tilde{X}) - \mathrm{e}^{-s} \leq \frac{3\pi}{2}s - 1\,. \quad (2.156)$$

Then, as long as $\epsilon < 2h/3\pi$, then we can integrate this upper bound explicitly to get the beyond all orders in ϵ bound

$$\left|I_0\left(C^{(b)}_{-1/2}\right)\right| \leq \frac{2h\epsilon}{3\pi - 2h\epsilon}\exp\left(-\frac{1}{h\epsilon}\right)\,. \quad (2.157)$$

5. $\nu \geq 3/2$ where $\nu \in 2\mathbb{Z} - 1/2$. Here, again we use an $\tilde{X}$-dependent contour, $C_\nu(\tilde{X}) = C^{(a)}_\nu(\tilde{X}) \cup C^{(b)}_\nu(\tilde{X}) \cup \left(-C^{(c)}_\nu(\tilde{X})\right)$ with the segments defined according to:

$$C^{(a)}_\nu(\tilde{X}): \quad k^{(a)}_\nu(s) = s + \mathrm{i}\pi\nu, \quad s \in \left(-\infty,\ \mathrm{Re}\left[k_n(\tilde{X})\right]\right], \quad (2.158)$$

$$C^{(b)}_\nu(\tilde{X}): \quad k^{(b)}_\nu(s;\tilde{X}) = \mathrm{Re}\left[k_n(\tilde{X})\right] + \mathrm{i}s, \quad s \in [\pi\nu,\ \pi(\nu+2)]\,, \quad (2.159)$$

$$C^{(c)}_\nu(\tilde{X}): \quad k^{(c)}_\nu(s) = s + \mathrm{i}\pi(\nu+2), \quad s \in \left(-\infty,\ \mathrm{Re}\left[k_n(\tilde{X})\right]\right], \quad (2.160)$$

where $n = (\nu+1/2)/2 \geq 1$. We are assured that the saddle points are always on the segment $C^{(b)}(\tilde{X})$ since, from properties of the Lambert-W function, $\pi(\nu+1/2) < \mathrm{Im}\left[k_n(\tilde{X})\right] < \pi(\nu+3/2)$ for all $\tilde{X} \in \mathbb{R}$. It can also be shown that the saddle points only get closer to the center of this interval, $\pi(\nu+1)$, as ν grows. This is because, from the saddle point definition equation (2.61), the real and imaginary parts must obey

$$0 = \mathrm{Re}\,[k] - \tilde{X} + \mathrm{e}^{-\mathrm{Re}[k]-1}\cos(\mathrm{Im}\,[k])\,, \quad (2.161)$$

$$0 = \mathrm{Im}\,[k] - \mathrm{e}^{-\mathrm{Re}[k)]-1}\sin(\mathrm{Im}\,[k])\,. \quad (2.162)$$

For $\mathrm{Im}\,[k] > 0$, we can solve for the real part in terms of imaginary part using the

second equation and then plug this into the first to get a condition that determines imaginary part of the saddle points:

$$0 = \ln\left(\mathrm{Im}\,[k]\csc(\mathrm{Im}\,[k])\right) + 1 + \tilde{X} - \mathrm{Im}\,[k]\cot(\mathrm{Im}\,[k])\,. \tag{2.163}$$

For $m \in \mathbb{Z}$ and $m \geq 1$, there is exactly one solution in the domain $2\pi m < \tilde{Y} < \pi(2m+1)$ which corresponds to $\mathrm{Im}\,[k_m(X)]$. As m gets larger, the final term dominates and the solutions approach $\pi(2m+1/2)$. This can be seen by shifting so that $u_m = \mathrm{Im}\,[k] - \pi(2m+1/2)$ and dividing through by $\pi(2m+1/2)$ to get

$$0 = \frac{\ln(u_m + \pi(2m+1/2))}{\pi(2m+1/2)} + \frac{\ln\left(\sec(u_m)\right) + 1 + \tilde{X} - u_m\tan(u_m)}{\pi(2m+1/2)} - \tan(u_m)\,. \tag{2.164}$$

For $|u_m| \leq \pi/6$ and $m \geq 1$, the first two terms clearly go to zero point-wise monotonically. If we require $|\tilde{X}| \leq 1$ we can show that for $m = 1$ the first two terms together are less that $1/\sqrt{3}$ in magnitude. Since for $|u_m| < \pi/6$, $|\tan(u_m)| \leq 1/\sqrt{3}$ on this interval, it must be that the solutions u_m are always on this interval for all $m \geq 1$. Thus,

$$\left|\mathrm{Im}\left[k_n(\tilde{X})\right] - \pi(\nu+1)\right| < \pi/6 \tag{2.165}$$

and so for small enough ϵ, uniform for all $\nu \geq 3/2$, $\mathcal{D}_n(R_1)$ is always away from the endpoints of $C^{(b)}(\tilde{X})$ and thus, only intersects it. Now we expand the contributions:

$$\begin{aligned}\psi_\nu(Z;\epsilon,h) = E_n(\tilde{X},\tilde{Y})\Big[&I_n\left(C_\nu^{(a)}(\tilde{X})\right) + I_n\left(C_\nu^{(b)}(\tilde{X}) \cap \mathcal{D}_n(R_1)\right) \\ &+ I_n\left(C_\nu^{(b)}(\tilde{X})/\mathcal{D}_n(R_1)\right) - I_n\left(C_\nu^{(c)}(\tilde{X})\right)\Big]\,.\end{aligned} \tag{2.166}$$

We will begin with the contour segment that contains the saddle point, using the

previously worked out form of the exponent (2.114),

$$\begin{aligned}
&\mathrm{Im}\left[f(k;\tilde{X}) - f(k_n(\tilde{X});\tilde{X})\right] \\
&\quad= \Bigg[\left(\mathrm{Re}\left[k_n(\tilde{X})\right] - \tilde{X}\right)s - \left(\mathrm{Re}\left[k_n(\tilde{X})\right] - \tilde{X}\right)\mathrm{Im}\left[k_n(\tilde{X})\right] + \mathrm{e}^{-\mathrm{Re}\left[k_n(\tilde{X})\right]-1}\sin(s) \\
&\qquad - \mathrm{e}^{-\mathrm{Re}\left[k_n(\tilde{X})\right]-1}\sin\left(\mathrm{Im}\left[k_n(\tilde{X})\right]\right)\Bigg] \qquad (2.167) \\
&\quad= \Bigg[\left(\mathrm{Re}\left[k_n(\tilde{X})\right] - \tilde{X}\right)\left(s - \mathrm{Im}\left[k_n(\tilde{X})\right]\right) \\
&\qquad + \left|k_n(\tilde{X}) - \tilde{X}\right|\left(\sin(s) - \sin\left(\mathrm{Im}\left[k_n(\tilde{X})\right]\right)\right)\Bigg] \qquad (2.168) \\
&\quad= \left|k_n(\tilde{X}) - \tilde{X}\right|\Bigg[\sin(s) - \sin\left(\mathrm{Im}\left[k_n(\tilde{X})\right]\right) \\
&\qquad\qquad - \cos\left(\mathrm{Im}\left[k_n(\tilde{X})\right]\right)\left(s - \mathrm{Im}\left[k_n(\tilde{X})\right]\right)\Bigg] \qquad (2.169)
\end{aligned}$$

where we've used that $\mathrm{e}^{-\mathrm{Re}\left[k_n(\tilde{X})\right]-1} = \left|k_n(\tilde{X}) - \tilde{X}\right|$ as well as that $\mathrm{Re}\left[k_n(\tilde{X})\right] - \tilde{X} = \left|k_n(\tilde{X}) - \tilde{X}\right|\cos\left(\mathrm{Im}\left[k_n(\tilde{X})\right]\right)$. We see that, exactly as expected, the second two terms cancel the first two of the Taylor polynomial of the sine as the point $s = \mathrm{Im}\left[k_n(X)\right]$. From numerical bounds, we have that

$$\sin(s) - \sin(s_0) - \cos(s_0)\big(s - s_0\big) \leq -\frac{(s-s_0)^2}{4\pi^2} \qquad (2.170)$$

for all $|s - \pi(2m + 1/2)| \leq \pi$ so long as $|s_0 - \pi(2m + 1/2)| \leq \pi/6$ and for any $m \in \mathbb{Z}$. Plugging in $s_0 = \mathrm{Im}\left[k_n\right](\tilde{X})$, these bounds are satisfied on the integration range and from the bound we verified earlier on $\mathrm{Im}\left[k_n\right](\tilde{X})$. Thus, the analysis from here continues as in case 2, and we've verified that $I_n\left(C_\nu^{(b)}(\tilde{X})\right)$ is beyond all orders in ϵ.

Finally, we have the two half-lines $C_\nu^{(a)}(\tilde{X})$ and $C_\nu^{(c)}(\tilde{X})$. These can be bounded with a similar process to the one used for $C_{-1/2}^{(b)}$. We begin with $C_\nu^{(a)}(\tilde{X})$ using the same form

of the exponent as above:

$$\begin{aligned}
&\mathrm{Im}\left[f(k;\tilde{X}) - f(k_n(\tilde{X});\tilde{X})\right] \\
&\quad= \Bigg[\left(s-\tilde{X}\right)\pi\nu - \left(\mathrm{Re}\left[k_n(\tilde{X})\right]-\tilde{X}\right)\mathrm{Im}\left[k_n(\tilde{X})\right] - \mathrm{e}^{-s-1} \\
&\qquad - \mathrm{e}^{-\mathrm{Re}\left[k_n(\tilde{X})\right]-1}\sin\left(\mathrm{Im}\left[k_n(\tilde{X})\right]\right)\Bigg] \qquad (2.171) \\
&\quad= \Bigg[\pi\nu\left(s-\mathrm{Re}\left[k_n(\tilde{X})\right]\right) + \left(\mathrm{Re}\left[k_n(\tilde{X})\right]-\tilde{X}\right)\left(\pi\nu - \mathrm{Im}\left[k_n(\tilde{X})\right]\right) \\
&\qquad + \left|k_n(\tilde{X})-\tilde{X}\right|\left(\mathrm{e}^{-(s-\mathrm{Re}\left[k_n(\tilde{X})\right])} - \sin\left(\mathrm{Im}\left[k_n(\tilde{X})\right]\right)\right)\Bigg] \qquad (2.172) \\
&\quad= \pi\nu\left(s-\mathrm{Re}\left[k_n(\tilde{X})\right]\right) \\
&\qquad + \frac{\left|k_n(\tilde{X})-\tilde{X}\right|}{h\epsilon}\Bigg[-\mathrm{e}^{-(s-\mathrm{Re}\left[k_n(\tilde{X})\right])} - \sin\left(\mathrm{Im}\left[k_n(\tilde{X})\right]\right) \\
&\qquad\qquad - \cos\left(\mathrm{Im}\left[k_n(\tilde{X})\right]\right)\left(\pi\nu - \mathrm{Im}\left[k_n(\tilde{X})\right]\right)\Bigg]. \qquad (2.173)
\end{aligned}$$

We note $-\mathrm{e}^{-(s-\mathrm{Re}\left[k_n(\tilde{X})\right])} \leq -1$ on the integration domain. Upon replacing this upper bound, we realize this entire second term is exactly (2.169) evaluated at the lower integration bound. Since we have the bound (2.170), we have that

$$\begin{aligned}
&-1-\sin\left(\mathrm{Im}\left[k_n(\tilde{X})\right]\right) - \cos\left(\mathrm{Im}\left[k_n(\tilde{X})\right]\right)\left(\pi\nu - \mathrm{Im}\left[k_n(\tilde{X})\right]\right) \\
&\qquad\qquad \leq -\frac{\left(\pi\nu - \mathrm{Im}\left[k_n(\tilde{X})\right]\right)^2}{4\pi^2}. \qquad (2.174)
\end{aligned}$$

Using the bound (2.165) again, we have

$$-\frac{\left(\pi\nu - \mathrm{Im}\left[k_n(\tilde{X})\right]\right)^2}{4\pi^2} \leq -\frac{4}{9}. \qquad (2.175)$$

Now, bringing this together with the universal bound (2.123) and the fact that $\nu \geq 3/2$,

we can integrate explicitly a universal bound

$$\left|I_n\left(C_\nu^{(a)}(\tilde{X})\right)\right| \leq \int_{-\infty}^{\mathrm{Re}\left[k_n(\tilde{X})\right]} \exp\left(\frac{3\pi}{2h\epsilon}\left(s - \mathrm{Re}\left[k_n(\tilde{X})\right]\right) - \frac{8\pi}{9h\epsilon} - \left(s - \mathrm{Re}\left[k_n(\tilde{X})\right]\right)\tilde{Y}\right) \mathrm{d}s \quad (2.176)$$

$$= \exp\left(-\frac{8\pi}{9h\epsilon}\right)\frac{2h\epsilon}{3\pi - 2h\epsilon\tilde{Y}} \quad (2.177)$$

which for small enough ϵ goes to zero beyond all orders. $\left|I_n\left(C_\nu^{(c)}(\tilde{X})\right)\right|$ can be bounded in the exact same manner. We leave this as an exercise for the reader.

2.2.4.2 Analysing the Contributions From Contour Segments Near the Saddle Points

We have reduced the evaluation of each contour integral to only contributions from contours that are interior to some ϵ-shrinking disks around specific saddle points plus some errors that are beyond all orders in ϵ. The process of analyzing contour integrals near simple and coalescing saddle points is a classical result of asymptotic analysis. We will apply the method of steepest decent to the simple saddle points as well as Chester, Friedman and Ursell's extension of the method of steepest descent [11] to the colliding saddle points. This will entail constructing an analytic change of variables to put our integrals into a canonical form and some more error bounding. We do this in two cases:

1. *Simple saddle points.* For any $\nu \in 2\mathbb{Z} - 1/2$ and $\nu \neq -1/2$, some terms that remain to be evaluated in the sums of integrals which determine $\psi_\nu(Z;\epsilon,h)$, (2.109), (2.138), and (2.166), are those that come from one or two separated simple saddle points. In all of these cases, the function in the integrand's exponential takes a uniform form. Consider the formula (2.129) and we will expand the quadratic parts and introduce some new term to recollect.

$$\begin{aligned} f(k;\tilde{X}) - f(k_n(\tilde{X});\tilde{X}) &= \frac{k^2 - 2k\tilde{X} + \tilde{X}^2}{2} - \frac{k_n(\tilde{X})^2 - 2k_n(\tilde{X})\tilde{X} + \tilde{X}^2}{2} \\ &\quad + \left(\tilde{X} - k_n(\tilde{X})\right)\left(1 - \mathrm{e}^{-2h(k-k_n(\tilde{X}))}\right) \quad (2.178) \\ &= \frac{(k-k_n(\tilde{X}))^2}{2} + \frac{\tilde{X} - k_n(\tilde{X})}{2h}\left(1 - 2h\big(k - k_n(\tilde{X})\big) - \mathrm{e}^{-2h(k-k_n(\tilde{X}))}\right) \quad (2.179) \end{aligned}$$

This means that with a simple shift in the complex integration variable, $p = (k - k_n(\tilde{X}))$, all of these integrals can be expressed uniformly. Define for $0 < \epsilon$ and $\Lambda \in \mathbb{C}$

$$\mathcal{I}_1(\epsilon, \tilde{Y}, \Lambda) := \int_{C(\epsilon,\Lambda)} \exp\left(-\frac{\mathrm{i}}{h\epsilon}\left[\frac{p^2}{2} - \Lambda\left(\mathrm{e}^{-p} - 1 + p\right)\right] - \tilde{Y}p\right) \mathrm{d}p \tag{2.180}$$

where $C(\epsilon, \Lambda)$ is the contour on the real line traced from right to left and inside the closed disk $\mathcal{D}(\epsilon^{\gamma/2})$ with

$$\mathcal{D}(R) := \{\ z \in \mathbb{C} \mid |z| \leq R\ \} \tag{2.181}$$

for $\mathrm{Im}\,[\Lambda] < 0$, and is the contour on the imaginary line traced bottom to top and inside $\mathcal{D}(\epsilon^{\gamma/2})$ for $\mathrm{Im}\,[\Lambda] > 0$. With this new, simplified notation, for ϵ, $|\tilde{X}|$ small enough, all of the contour integrals near the simple saddle points can be written with this form:

$$\mathcal{I}_1\left(\epsilon; \tilde{Y}, \tilde{X} - k_n(\tilde{X})\right) = \begin{cases} I_n\left(C^{(a)}_{2n+3/2}(\tilde{X}, +\infty) \cap \mathcal{D}_n(R_1)\right) & \text{if } n \leq -2 \\ I_n\left(C^{(b)}_{2n-1/2}(\tilde{X}) \cap \mathcal{D}_n(R_1)\right) & \text{if } n \geq 1 \end{cases} . \tag{2.182}$$

Furthermore, from the bounds (2.123) and (2.165), and the fact that the saddle points are Schwartz symmetric, the values $\tilde{X} - k_n(\tilde{X}) = \mathrm{e}^{-k_n(\tilde{X})-1}$ for all $n \neq -1, 0$ and $|\tilde{X}| \leq$ are in either of the two infinite annular sectors

$$\Sigma_\pm := \left\{\ z \in \mathbb{C}\ \middle|\ \left|\arg[z] \mp \frac{\pi}{2}\right| < \frac{\pi}{6} \text{ and } |z| > 2\pi\ \right\} \tag{2.183}$$

We will often restrict Λ to one or the union of these sets in the following analysis.

Clearly, the leading-order function in the exponential of (2.180) is analytic and vanishes quadratically at the origin. We wish to change variables in order to bring this exponent function into the canonical quadratic form. To do this, we define

$$F(p; \Lambda) := 2\frac{\mathrm{e}^{-p} - 1 + p}{p^2} - \frac{1}{\Lambda} = 1 + 2\left(\sum_{n=1}^{\infty} \frac{(-p)^n}{(n+2)!}\right) - \frac{1}{\Lambda} \tag{2.184}$$

which is analytic for all $\Lambda \in \Sigma_+ \cup \Sigma_-$. Since $1/2 + 1/2\pi < 1$, we can find a $K_1 > 0$ such that for all $p \in \mathcal{D}(K_1)$,

$$\left|2\frac{\mathrm{e}^{-p} - 1 + p}{p^2}\right| \geq \frac{1}{2} + \frac{1}{2\pi}\,. \tag{2.185}$$

Then, we have by an application of the triangle identities

$$\frac{1}{2} \leq \left| \left| 2\frac{\mathrm{e}^{-p} - 1 + p}{p^2} \right| - \frac{1}{|\Lambda|} \right| \leq |F(p;\Lambda)| \leq \left| 2\frac{\mathrm{e}^{-p} - 1 + p}{p^2} \right| + \frac{1}{|\Lambda|} \leq \frac{1}{2} + \frac{1}{\pi} \,. \tag{2.186}$$

Thus, we are assured that $F(p;\Lambda)$ has no zero on $\mathcal{D}(K_1)$. From here, we define

$$\Omega(p;\Lambda) := p\mathrm{e}^{\mathrm{i}(\arg[\Lambda]/2 - \pi/4)} \left(F(p;\Lambda)\right)^{1/2} \tag{2.187}$$

where we take the principal branch of the square-root at $p = 0$. Since $F(\diamond;\Lambda)$ has no zeros in $\mathcal{D}(K_1)$ for any $\Lambda \in \Sigma_+ \cup \Sigma_-$, we can extend the square-root analytically to all of $\mathcal{D}(K_1)$. Considering the p-derivative of the mapping,

$$\Omega_p(p;\Lambda) = \mathrm{e}^{\mathrm{i}(\arg[\Lambda]/2 + \pi/4)} \frac{F(p;\Lambda) + pF_p(p;\Lambda)}{\left(F(p;\Lambda)\right)^{1/2}} \,. \tag{2.188}$$

Since the first term in the numerator is nonzero while the second term is zero at $p = 0$, we can conduct another triangle inequality bounding to revise our $K_1 > 0$ so that $|\Omega_p(p;\Lambda)|$ is bounded away from zero. Furthermore, from the definition of $F(p;\Lambda)$ (2.184), it is easy to see that $F_p(p;\Lambda)$ is independent of lambda. Since we have the Λ-independent bound on $F(p;\Lambda)$ (2.186), we can bound $|\Omega_p(p;\Lambda)|$ away from zero uniformly for all $\Lambda \in \Sigma_+ \cup \Sigma_-$. This guarantees that the complex analytic map $\Omega_p(p;\Lambda)$ is always invertable. Squaring this mapping we see that we've converted the exponential function to a pure quadratic:

$$\Omega(p;\Lambda)^2 = \mathrm{i}\mathrm{e}^{\mathrm{i}\arg[\Lambda]} p^2 F(p;\Lambda) = -\frac{2\mathrm{i}}{|\Lambda|} \left(\frac{p^2}{2} - \Lambda \left(\mathrm{e}^{-p} - 1 + p \right) \right) \,. \tag{2.189}$$

And thus, after completing the change of variables $\omega = \Omega(\tilde{Y};\Lambda)$ in our uniform integral expression, we have

$$\mathcal{I}_1(\epsilon, \tilde{Y}, \Lambda) = \int_{\Omega_n(C_n(\epsilon,\Lambda);\Lambda)} \exp\left(-\frac{|\Lambda|}{2h\epsilon}\omega^2 - \tilde{Y}\,\Omega^{-1}(\omega;\Lambda) \right) \partial_\omega \Omega^{-1}(\omega;\Lambda)\,\mathrm{d}\omega \,. \tag{2.190}$$

We will collect the lower-order terms in the integral into one function

$$g(\omega;\tilde{Y},\Lambda) := \exp\left(-\tilde{Y}\,\Omega^{-1}(\omega;\Lambda) \right) \Omega_\omega^{-1}(\omega;\Lambda) \,. \tag{2.191}$$

Because $g(\diamond; \tilde{Y}, \Lambda)$ is analytic, from Taylor's theorem we can write it as

$$g(\omega; \tilde{Y}, \Lambda) = g(0; \tilde{Y}, \Lambda) + g_\omega(0; \tilde{Y}, \Lambda)\omega + \int_0^\omega g_{\omega\omega}(\omega; \tilde{Y}, \Lambda)\omega \, \mathrm{d}\omega \,. \tag{2.192}$$

The second derivative $g_{\omega\omega}(\omega; \tilde{Y}, \Lambda)$ can be computed in a straight forward way as

$$g_{\omega\omega}(\omega; \tilde{Y}, \Lambda) = \exp\left(-\tilde{Y}\,\Omega^{-1}\right)\left(\tilde{Y}^2\left(\Omega_\omega^{-1}\right)^3 + 3\tilde{Y}\Omega_\omega^{-1}\Omega_{\omega\omega}^{-1} + \Omega_{\omega\omega\omega}^{-1}\right) \tag{2.193}$$

where we've omitted for brevity the evaluations of the functions on the right at $(\omega; \tilde{Y}, \Lambda)$. If we work at $p = \Omega^{-1}(\omega; \Lambda)$, then we can rewrite all of the derivatives as

$$\Omega_\omega^{-1}(\omega; \Lambda) = \frac{1}{\Omega_p} \,, \tag{2.194}$$

$$\Omega_{\omega\omega}^{-1}(\omega; \Lambda) = \partial_\omega \frac{1}{\Omega_p} = \frac{1}{\Omega_p}\partial_p \frac{1}{\Omega_p} = -\frac{\Omega_{pp}}{(\Omega_p)^3} \,, \tag{2.195}$$

$$\Omega_{\omega\omega\omega}^{-1}(\omega; \Lambda) = -\partial_\omega \frac{\Omega_{pp}}{(\Omega_p)^3} = -\frac{1}{\Omega_p}\partial_p \frac{\Omega_{pp}}{(\Omega_p)^3} = \frac{3(\Omega_{pp})^2(\Omega_p)^2 - \Omega_{ppp}(\Omega_p)^3}{(\Omega_p)^7} \,, \tag{2.196}$$

where now all of the functions on the right are evaluated at $(p; \Lambda)$. Lastly, the derivatives of Ω can be written in terms of F as

$$\Omega_p(p; \Lambda) = \mathrm{e}^{\mathrm{i}(\arg[\Lambda]/2 + \pi/4)}\left(F^{1/2} + \frac{p}{2}\frac{F_p}{F^{1/2}}\right) \,, \tag{2.197}$$

$$\Omega_{pp}(p; \Lambda) = \mathrm{e}^{\mathrm{i}(\arg[\Lambda]/2 + \pi/4)}\left(\frac{F_p}{F^{1/2}} + \frac{p}{4}\frac{2F_{pp}F - F_p^2}{F^{3/2}}\right) \,, \tag{2.198}$$

$$\Omega_{ppp}(p; \Lambda) = \mathrm{e}^{\mathrm{i}(\arg[\Lambda]/2 + \pi/4)}\left(\frac{3}{4}\frac{2F_{pp}F - F_p^2}{F^{3/2}} + \frac{p}{8}\frac{3F_p^3 - 6F_pF_{pp} + 4F_{ppp}}{F^{5/2}}\right) \,, \tag{2.199}$$

and again all of the functions on the right are evaluated at $(p; \Lambda)$. We recall that $|F(p; \Lambda)|$ is bounded above and below by (2.186). We've already seen that $F_p(p; \Lambda)$ and the subsequent derivatives are independent of Λ. Since $\mathcal{D}(K_1)$ is compact, $|F_p(p; \Lambda)|$, $|F_{pp}(p; \Lambda)|$ and $|F_{ppp}(p; \Lambda)|$ are all bounded above. Additionally, we recall that $|\Omega_p(p; \Lambda)|$ is bounded away from zero on $\mathcal{D}(K_1)$ by construction and in a Λ-independent way. Rolling these bounds through the formulas (2.197), (2.198), (2.199), then through the formulas (2.194), (2.195) and (2.196), and finally through (2.193) with the bounds $\Omega^{-1}(\omega; \Lambda) \leq K_1$ and $0 \leq \tilde{Y} \leq 1$, we get a final, $\tilde{Y}$ and Λ-independent bound $|g_{\omega\omega}(\omega; \tilde{Y}, \Lambda)| \leq M_{g,2}$ for all $\omega \in \Omega(\mathcal{D}(K_1); \Lambda)$. Defining the remainder term, the

difference between $g(\omega;\tilde{Y},\Lambda)$ and its first two Taylor terms,

$$R_{g,2}(\omega;\tilde{Y},\Lambda) = g(\omega;\tilde{Y},\Lambda) - g(0;\tilde{Y},\Lambda) - g_\omega(0;\tilde{Y},\Lambda)\omega\,, \tag{2.200}$$

we have the bound

$$|R_{g,2}(\omega;\tilde{Y},\Lambda)| = \left|\int_0^\omega g_{\omega\omega}(\omega;\tilde{Y},\Lambda)\omega\,\mathrm{d}\omega\right| \leq M_{g,2}|\omega|^2\,. \tag{2.201}$$

Now, note that under the mapping, the integration contour $C(\epsilon^{\gamma/2})$ maps to some new contour $\Omega(C(\epsilon^{\gamma/2},\Lambda);\Lambda)$, where the endpoints are, for $\Lambda\in\Sigma_-$,

$$\omega_\pm = \Omega(\pm\epsilon^{\gamma/2};\Lambda) = \pm\epsilon^{\gamma/2}\mathrm{e}^{\mathrm{i}(\arg[\Lambda]/2+\pi/4)}\left(1-\frac{1}{\Lambda}+O\left(\epsilon^\gamma\right)\right)^{1/2} \tag{2.202}$$

$$= \pm\mathrm{e}^{\mathrm{i}(\arg[\Lambda]/2+\pi/4)}\left(1-\frac{1}{\Lambda}\right)^{1/2}\epsilon^{\gamma/2}+O\left(\epsilon^\gamma\right) \tag{2.203}$$

where the constants in the $O\left(\epsilon^\gamma\right)$ terms are universal for $\Lambda\in\Sigma_-$. For $\Lambda\in\Sigma_-$, we also have $-\pi/6\leq\arg[\Lambda]/2+\pi/4\leq\pi/6$. From a little geometry, $0\leq\arg[(1-1/\Lambda)^{1/2}]\leq\sin^{-1}(1/2\pi)<3\pi/48$ for all $\Lambda\in\Sigma_-$. Now for $\Lambda\in\Sigma_+$,

$$\omega_\pm = \Omega(\pm\mathrm{i}\epsilon^{\gamma/2};\Lambda) = \pm\mathrm{i}\epsilon^{\gamma/2}\mathrm{e}^{\mathrm{i}(\arg[\Lambda]/2+\pi/4)}\left(1-\frac{1}{\Lambda}+O\left(\epsilon^\gamma\right)\right)^{1/2} \tag{2.204}$$

$$= \mp\mathrm{e}^{\mathrm{i}(\arg[\Lambda]/2-\pi/4)}\left(1-\frac{1}{\Lambda}\right)^{1/2}\epsilon^{\gamma/2}+O\left(\epsilon^\gamma\right) \tag{2.205}$$

where, again, the constants in the $O\left(\epsilon^\gamma\right)$ terms are universal for $\Lambda\in\Sigma_+$. Here, $-\pi/6\leq\arg[\Lambda]/2-\pi/4\leq\pi/6$. From the same geometry, but inverted vertically, $3\pi/48<\sin^{-1}(1/2\pi)\leq\arg[(1-1/\Lambda)^{1/2}]\leq 0$ for all $\Lambda\in\Sigma_+$. The endpoints are again under the level of the saddle point in the exponent. This means we can then deform the contour $\Omega(C(\epsilon^{\gamma/2},\Lambda);\Lambda)$ to one that travels along the real line from left to right for $\Lambda\in\Sigma_+$ and left to right for $\Lambda\in\Sigma_-$, and then moves vertically to the endpoints, call it $\tilde{C}(\Lambda)$. We consider the bound on the difference between the original integral with

$g(\omega; \tilde{Y}, \lambda)$ and its Taylor terms:

$$\left| \int_{\tilde{C}(\Lambda)} \exp\left(-\frac{|\Lambda|}{2h\epsilon}\omega^2\right) R_{g,2}(\omega; \tilde{Y}; \Lambda)\, \mathrm{d}\omega \right|$$

$$\leq \int_{\tilde{C}(\Lambda)} \exp\left(-\frac{|\Lambda|}{2h\epsilon}\mathrm{Re}\left[\omega^2\right]\right) |R_{g,2}(\omega; \tilde{Y}; \Lambda)|\, |\mathrm{d}\omega| \quad (2.206)$$

$$\leq \int_{\tilde{C}(\Lambda)} \exp\left(-\frac{\pi}{h\epsilon}\mathrm{Re}\left[\omega^2\right]\right) M_{g,2}|\omega|^2\, |\mathrm{d}\omega|\,. \quad (2.207)$$

Since there is a maximum extent to these contours for all $\Lambda \in \Sigma_+ \cup \Sigma_-$, the vertical components can be bounded uniformly in Λ and shown to be beyond all orders. We can extend the real line segment of $\tilde{C}(\Lambda)$ to the full real line, and integrate for a Λ-independent bound that is $O\left(\epsilon^{3/2}\right)$.

Finally, with similar bounding techniques that we employed for the contour portions far from the saddle points, we may increase the contours to infinity adding an error beyond all orders so long as it stays below the level and extends out to the real part $-\infty$ and $+\infty$ directions for rapid convergence. The contour then can be deformed by Cauchy's theorem to lie just along the real axis, and the final step is simply to evaluate the resulting Gaussian integral:

$$\mathcal{I}_1(\epsilon, \tilde{Y}, \Lambda) = \sigma(\Lambda) \int_{-\infty}^{+\infty} \exp\left(-\frac{|\Lambda|}{2h\epsilon}\omega^2\right) \left(g(0; \tilde{Y}, \Lambda) + g_\omega(0; \tilde{Y}, \Lambda)\omega\right) \mathrm{d}\omega + O\left(\epsilon^{3/2}\right) \quad (2.208)$$

$$= \sigma(\Lambda)\sqrt{\frac{2\pi h\epsilon}{|\Lambda|}} g(0; \tilde{Y}, \Lambda) + O\left(\epsilon^{3/2}\right) \quad (2.209)$$

$$= \sigma(\Lambda)\sqrt{\frac{2\pi h\epsilon}{|\Lambda|}} \mathrm{e}^{-\mathrm{i}(\arg[\Lambda]/2+\pi/4)} \left(1 - \frac{1}{\Lambda}\right)^{-1/2} + O\left(\epsilon^{3/2}\right) \quad (2.210)$$

$$= \sigma(\Lambda) \left(\frac{2\pi h\epsilon}{\Lambda - 1}\right)^{1/2} \mathrm{e}^{-\mathrm{i}\pi/4} + O\left(\epsilon^{3/2}\right) \quad (2.211)$$

where $\sigma(\Lambda) = -1$ for $\Lambda \in \Sigma_+$ and $\sigma(\Lambda) = +1$ for $\Lambda \in \Sigma_-$ and all of the complex square-roots are evaluated on the principal branch.

2. *Coalescing saddle points.* For $\nu = -\infty, -5/2$, and $-1/2$, the expansion of $\psi_\nu(Z; \epsilon, h)$ contains integrals over contours that pass near to the colliding saddle points at $k = -1$. We will first perform the change of variables $k = p - 1$ that will center the colliding

saddle points in the exponent

$$f(p-1;\tilde{X}) - f(-1;\tilde{X}) = \frac{(p-1)^2}{2} - \mathrm{e}^{-p} - p\tilde{X} + \frac{1}{2} \tag{2.212}$$

$$= \frac{p^2}{2} - (\tilde{X}+1)p + 1 - \mathrm{e}^{-p}\,. \tag{2.213}$$

With this, we define the universal integral form that were interested in this case as

$$\mathcal{I}_2(\epsilon,\tilde{Y},C) := \int_{C\cap\mathcal{D}(R_2)} \exp\Big(-\frac{\mathrm{i}}{h\epsilon}\left[\frac{p^2}{2} - (\tilde{X}+1)p + 1 - \mathrm{e}^{-p}\right] - p\tilde{Y}\Big)\,\mathrm{d}p\,. \tag{2.214}$$

Then the integrals that we need to compute can be written as

$$\mathcal{I}_2\left(\epsilon;\tilde{Y},C_{\wedge}\right) = -I_0\left(C^{(b)}_{-\infty}\cap\mathcal{D}_0(R_2)\right) - I_0\left(C^{(c)}_{-\infty}\cap\mathcal{D}_0(R_2)\right) \tag{2.215}$$

$$= -I_0\left(C^{(b)}_{-\infty}\cap\mathcal{D}_0(R_2)\right) - I_0\left(C^{(c)}_{-\infty}\cap\mathcal{D}_0\left(R_{5/2}(\tilde{X})\right)/\mathcal{D}_0(R_2)\right)\,, \tag{2.216}$$

$$\mathcal{I}_2\left(\epsilon;\tilde{Y},C_{\rfloor}\right) = -I_0\left(C^{(b)}_{-\infty}\cap\mathcal{D}_0(R_2)\right) - I_0\left(C^{(a)}_{-1/2}\cap\mathcal{D}_0(R_2)\right)\,. \tag{2.217}$$

where $C_{\wedge}$ is the contour made of the two rays with arguments $-3\pi/4$ and $-\pi/4$ traced from left to right and $C_{\rfloor}$ is the contour made of the two rays with arguments $\pi/2$ and $-3\pi/4$ traced from top to bottom. We tediously explained every step in the previous case because we needed to be sure that every bound on every error term could be done in a uniform way for the infinitely many integrals to be carried out. Since there are only two integrals in this case, we use Chester, Friedman and Ursell's [11] extension of the method of steepest descent to two colliding saddle points out of the box, assured that the number of constants in error bounds generated is finite.

Continuing, we put the exponential into a canonical form, just like the case above. Since there are two colliding saddle points, the canonical form is a cubic with varying coefficients,

$$p^2 - 2(\tilde{X}+1)p + 2 - 2\mathrm{e}^{-p} = \frac{\omega^3}{3} - a(\tilde{X})\omega + b(\tilde{X})\,. \tag{2.218}$$

We can generate an analytic map $\omega = \Omega(p;\tilde{X})$ interior to $\mathcal{D}(K_2)$ for some $K_2 > 0$ by requiring that the left side function's value at the saddle points, so long as they remain in $\mathcal{D}(K_2)$, are equal to the value of the right side function's values at its saddle points. The saddle points in question on the left are at $p_{-1,0} = \tilde{X} + 1 + W_{-1,0}(-\mathrm{e}^{-\tilde{X}-1})$ while those on the right are at $\omega_{\pm} = \pm\left(a(X)\right)^{1/2}$ taking the principal square-root. We can evaluate and simplify the values at the saddle points explicitly with properties of the

Lambert W-function,

$$\begin{aligned}
&p_{-1,0}^2 - 2(\tilde{X}+1)p_{-1,0} + 2 - 2\mathrm{e}^{-p_{-1,0}} \\
&\quad = \frac{\left(\tilde{X}+1+W_{-1,0}(-\mathrm{e}^{-\tilde{X}-1})\right)^2}{2} - 2(\tilde{X}+1)\left(\tilde{X}+1+W_{-1,0}(-\mathrm{e}^{-\tilde{X}-1})\right) \\
&\qquad + 2 - 2\mathrm{e}^{-\tilde{X}-1-W_{-1,0}(-\mathrm{e}^{-\tilde{X}-1})} \qquad (2.219)\\
&\quad = \tilde{X}^2 + 1 + \left(W_{-1,0}(-\mathrm{e}^{-\tilde{X}-1})\right)^2 + 2\tilde{X} + 2W_{-1,0}(-\mathrm{e}^{-\tilde{X}-1}) + 2\tilde{X}W_{-1,0}(-\mathrm{e}^{-\tilde{X}-1}) \\
&\qquad - 2(\tilde{X}+1)\left(\tilde{X}+1+W_{-1,0}(-\mathrm{e}^{-\tilde{X}-1})\right) + 2 + 2W_{-1,0}(-\mathrm{e}^{-\tilde{X}-1}) \qquad (2.220)\\
&\quad = -\tilde{X}^2 - 2\tilde{X} + \left(W_{-1,0}(-\mathrm{e}^{-\tilde{X}-1}) + 1\right)^2, \qquad (2.221)
\end{aligned}$$

and then compute the values of the cubic at the saddle points,

$$\begin{aligned}
\frac{\omega_\pm^3}{3} + a(\tilde{X})\omega_\pm + b(\tilde{X}) &= \pm\frac{\left(a(\tilde{X})\right)^{3/2}}{3} \mp \left(a(\tilde{X})\right)^{3/2} + b(\tilde{X}) \qquad (2.222)\\
&= \mp\frac{2}{3}\left(a(\tilde{X})\right)^{3/2} + b(\tilde{X}). \qquad (2.223)
\end{aligned}$$

Picking two pairs of saddle points to equate on either side of the mapping gives the relations

$$\begin{aligned}
-\tilde{X}^2 - 2\tilde{X} + \left(W_{-1}(-\mathrm{e}^{-\tilde{X}-1}) + 1\right)^2 &= \frac{2}{3}\left(a(\tilde{X})\right)^{3/2} + b(\tilde{X}), \qquad (2.224)\\
-\tilde{X}^2 - 2\tilde{X} + \left(W_0(-\mathrm{e}^{-\tilde{X}-1}) + 1\right)^2 &= -\frac{2}{3}\left(a(\tilde{X})\right)^{3/2} + b(\tilde{X})\,. \qquad (2.225)
\end{aligned}$$

By adding and subtracting the two formulas, we can solve for a and b explicitly in terms of $\tilde{X}$.

$$\begin{aligned}
\left(a(\tilde{X})\right)^{3/2} &= \frac{3}{4}\left[\left(W_{-1}(-\mathrm{e}^{-\tilde{X}-1}) + 1\right)^2 - \left(W_0(-\mathrm{e}^{-\tilde{X}-1}) + 1\right)^2\right], \qquad (2.226)\\
b(\tilde{X}) &= -\tilde{X}^2 - 2\tilde{X} + \frac{\left(W_{-1}(-\mathrm{e}^{-\tilde{X}-1}) + 1\right)^2 + \left(W_0(-\mathrm{e}^{-\tilde{X}-1}) + 1\right)^2}{2}\,. \qquad (2.227)
\end{aligned}$$

Fortuitously, there is a known series expansion in half-powers for the Lambert W expressions above [48, Equation 4.13.6]. We can split the expansion into -1 plus the sum of an even-numerator (integer power) $\mathcal{E}(\tilde{X})$ and odd-numerator (half-integer

power) $\mathcal{O}(\tilde{X})$ series, resulting in

$$W_{-1}(-\mathrm{e}^{-\tilde{X}-1}) = -1 - \mathcal{O}(\tilde{X}) + \mathcal{E}(\tilde{X})\,, \tag{2.228}$$

$$W_0(-\mathrm{e}^{-\tilde{X}-1}) = -1 + \mathcal{O}(\tilde{X}) + \mathcal{E}(\tilde{X})\,, \tag{2.229}$$

where the series expansions are with the principal square-root,

$$\mathcal{O}(\tilde{X}) = \left(2\tilde{X}\right)^{1/2}\left(1 + \frac{1}{18}\tilde{X} + O\left(\tilde{X}^2\right)\right)\,, \tag{2.230}$$

$$\mathcal{E}(\tilde{X}) = -\frac{2}{3}\tilde{X} + O\left(\tilde{X}^2\right)\,. \tag{2.231}$$

These let us write the a and b explicitly in terms of these series and get the first few terms in the expansion:

$$\left(a(\tilde{X})\right)^{3/2} = \frac{3}{4}\left[\left(-\mathcal{O}(\tilde{X}) + \mathcal{E}(\tilde{X})\right)^2 - \left(\mathcal{O}(\tilde{X}) + \mathcal{E}(\tilde{X})\right)^2\right] \tag{2.232}$$

$$= -3\mathcal{O}(\tilde{X})\mathcal{E}(\tilde{X}) \tag{2.233}$$

$$= (2\tilde{X})^{3/2}\left(1 + O\left(\tilde{X}\right)\right)\,. \tag{2.234}$$

From the branch definitions we employed, we see the solution is analytic at $\tilde{X} = 0$ and has the series expansion

$$a(\tilde{X}) = 2\tilde{X} + O\left(\tilde{X}^2\right)\,. \tag{2.235}$$

Now, for b,

$$b(\tilde{X}) = -\tilde{X}^2 - 2\tilde{X} + \frac{\left(\mathcal{O}(\tilde{X}) + \mathcal{E}(\tilde{X})\right)^2 + \left(-\mathcal{O}(\tilde{X}) + \mathcal{E}(\tilde{X})\right)^2}{2} \tag{2.236}$$

$$= -\tilde{X}^2 - 2\tilde{X} + \left(\mathcal{O}(\tilde{X})\right)^2 + \left(\mathcal{E}(\tilde{X})\right)^2 \tag{2.237}$$

$$= -\tilde{X}^2 - 2\tilde{X} + 2\tilde{X} + \frac{2}{9}\tilde{X}^2 + \frac{4}{9}\tilde{X}^2 + O\left(\tilde{X}^3\right) \tag{2.238}$$

$$= -\frac{\tilde{X}^2}{3} + O\left(\tilde{X}^3\right)\,. \tag{2.239}$$

Now we use our constructed change of variables $\omega = \Omega(p;\tilde{X})$ in our integral and

factoring out the constant,

$$\mathcal{I}_2(\epsilon,\tilde{Y},C)=\exp\left(-\frac{\mathrm{i}}{2h\epsilon}b(\tilde{X})\right)\int_{\Omega(C\cap\mathcal{D}(R_2);\tilde{X})}\exp\left(-\frac{\mathrm{i}}{2h\epsilon}\left[\frac{\omega^3}{3}-a(\tilde{X})\omega\right]\right)g(\omega;\tilde{X},\tilde{Y})\,\mathrm{d}\omega \tag{2.240}$$

where $g(\omega;\tilde{X},\tilde{Y})$ is a function analytic on the first variable

$$g(\omega;\tilde{X},\tilde{Y}):=\exp\left(-\tilde{Y}\Omega^{-1}(\omega;\tilde{X})\right)\Omega_\omega^{-1}(\omega;\tilde{X})\,. \tag{2.241}$$

Now, we need to know the orientation of the contours that are mapped to under Ω, i.e. $\Omega(C_\wedge;\tilde{X})$ and $\Omega(C_\curlyvee;\tilde{X})$. In both cases, the endpoints take the form $p_\pm=R_2\mathrm{e}^{\mathrm{i}\phi_\pm}$. Plug this into the original exponent and set it equal to the new exponent at the new contour endpoints $\omega_\pm$,

$$\frac{\omega_\pm^3}{3}-a(\tilde{X})\omega_\pm+b(\tilde{X})=\left(R_2\mathrm{e}^{\mathrm{i}\phi_\pm}\right)^2-2(\tilde{X}+1)R_2\mathrm{e}^{\mathrm{i}\phi_\pm}+2-2\mathrm{e}^{-R_2\mathrm{e}^{\mathrm{i}\phi_\pm}}\,. \tag{2.242}$$

Expanding for small ϵ, we can make a dominant balance argument to discover the leading order behavior of the endpoints of the new contour,

$$\frac{\omega_\pm^3}{3}-\left(2h\epsilon^\alpha\chi+O\left(\epsilon^{2\alpha}\right)\right)\omega_\pm+O\left(\epsilon^{2\alpha}\right)=\epsilon^{3\beta/2}\frac{M_\chi^3}{6}\mathrm{e}^{3\mathrm{i}\phi_\pm}-\epsilon^{\alpha+\beta/2}h\chi M_\chi\mathrm{e}^{\mathrm{i}\phi_\pm}+O\left(\epsilon^{2\beta}\right)\,. \tag{2.243}$$

The balance between the cubic and linear terms on each side yields $\omega_\pm=\epsilon^{\beta/2}M_\chi\mathrm{e}^{\mathrm{i}\phi_\pm}/2+O\left(\epsilon^\beta\right)$. This mainly shows that the argument of the endpoints does not change to leading order under the mapping. With this knowledge, we can now introduce a final change of variables to put the exponent in the form of the Airy function integral and rotate the contour to be beginning around the argument $-\pi/3$ and ending around the argument $\pi/3$, we do this by letting $\eta=\mathrm{i}\mathrm{e}^{\mathrm{i}2\pi n/3}\omega/(2h\epsilon)^{1/3}$ for some $n=0,1$, or 2:

$$-\frac{\mathrm{i}}{2h\epsilon}\left[\frac{\omega^3}{3}-a(\tilde{X})\omega\right]=\frac{\eta^3}{3}+\frac{\mathrm{e}^{-\mathrm{i}2\pi n/3}}{(2h\epsilon)^{2/3}}a(\tilde{X})\eta\,. \tag{2.244}$$

Continuing with the standard argument [11], we get the uniform approximation

$$\begin{aligned}\mathcal{I}_2(\epsilon,\tilde{Y},C) = 2\pi(2h\epsilon)^{1/3}\exp\left(-\frac{\mathrm{i}}{2h\epsilon}b(\tilde{X})-\mathrm{i}\frac{2\pi}{3}n\right)\\ \times\left[\mathrm{Ai}\left(-\frac{\mathrm{e}^{-\mathrm{i}2\pi n/3}}{(2h\epsilon)^{2/3}}a(\tilde{X})\right)\left(g\left(0;\tilde{X},\tilde{Y}\right)+O\left(\epsilon^{2/3}\right)\right)\right.\\ \left.+\,\mathrm{Ai}'\left(-\frac{\mathrm{e}^{-\mathrm{i}2\pi n/3}}{(2h\epsilon)^{2/3}}a(\tilde{X})\right)O\left(\epsilon^{1/3}\right)\right].\end{aligned} \tag{2.245}$$

Note that, in general, the error term bounds should depend on the additional parameter $\tilde{Y}$. However, since the function $g(\omega;\tilde{X},\tilde{Y})$ and its derivatives are continuous in this parameter, we can make the error bounds uniform for all $0\leq\tilde{Y}\leq 1$.

Now using the expansion of $a(\tilde{X})$ and $b(\tilde{X})$ for small $\tilde{X}=\epsilon^{\beta/2}\chi$, we can expand the arguments of Ai and Ai$'$ in powers of ϵ as well,

$$-\frac{\mathrm{e}^{-\mathrm{i}2\pi n/3}}{(2h\epsilon)^{2/3}}a(\tilde{X}) = -\frac{2^{1/3}\mathrm{e}^{-\mathrm{i}2\pi n/3}}{(h\epsilon)^{2/3}}\tilde{X}+O\left(\tilde{X}^2\right) = -\frac{(2h)^{1/3}\mathrm{e}^{-\mathrm{i}2\pi n/3}}{\epsilon^{2/3-\alpha}}\left(\chi+O\left(\epsilon^{\alpha}\right)\right), \tag{2.246}$$

$$-\frac{\mathrm{i}}{2h\epsilon}b(\tilde{X}) = -\frac{\mathrm{i}}{2h\epsilon}O\left(\tilde{X}^2\right) = O\left(\epsilon^{2\alpha-1}\right). \tag{2.247}$$

If we amend the lower bound of of α to $1/2<\alpha<2/3$, then the error terms above go to zero. Moreover, since the map $\Omega(p;\tilde{X})$ is analytic in $\tilde{X}$, we can expand $g(0;\tilde{X},\tilde{Y})$ and, by constructing the map explicitly at $\tilde{X}=0$, we can compute $\Omega_\omega(0;0)=1$, to get

$$g(0;\tilde{X},\tilde{Y}) = g(0;0,\tilde{Y})+O\left(\tilde{X}\right) \tag{2.248}$$

$$= 1+O\left(\epsilon^{\alpha}\right) \tag{2.249}$$

where the error term can again be made uniform for $0\leq\tilde{Y}\leq 1$. The final uniform asymptotics are then given as

$$\begin{aligned}\mathcal{I}_2(\epsilon,\tilde{Y},C) = 2\pi(2h\epsilon)^{1/3}\mathrm{e}^{-\mathrm{i}2\pi n/3}\left[\mathrm{Ai}\left(-\frac{(2h)^{1/3}\mathrm{e}^{-\mathrm{i}2\pi n/3}}{\epsilon^{2/3-\alpha}}\left(\chi+O\left(\epsilon^{\alpha}\right)\right)\right)\left(1+O\left(\epsilon^{\alpha}\right)\right)\right.\\ \left.+\,\mathrm{Ai}'\left(-\frac{(2h)^{1/3}\mathrm{e}^{-\mathrm{i}2\pi n/3}}{\epsilon^{2/3-\alpha}}\left(\chi+O\left(\epsilon^{\alpha}\right)\right)\right)O\left(\epsilon^{1/3}\right)\right].\end{aligned} \tag{2.250}$$

For $C_\wedge$, we take $n=0$, so that the new contour beginning point has argument $-\pi/4$

and ending point has argument $\pi/4$. Since $|\pm\pi/4 \mp \pi/3| = \pi/12 \leq \pi/6$, after extending the contour to infinity in the approximation procedure, this contour satisfies the conditions of an Airy function integration contour. For $C_\jmath$, we take $n = 1$, so the new contour will have a starting point with argument $-\pi/3$ and an ending point at the argument $5\pi/12$. Since $|5\pi/12 - \pi/3| = \pi/12 < \pi/6$, this too will be an Airy function integration contour after extending it to infinity.

2.2.4.3 Assembling the Asymptotics of the Fundamental Basis Solutions

We now have all of the constituent parts to assemble the asymptotics of each of the fundamental basis solutions. Recall the change of variables employed is $Z = \epsilon^\alpha \chi + \mathrm{i}\epsilon(\tilde{Y} - 1/2)$ with $1/2 < \alpha < 2/3$. We enumerate these using the following cases:

1. $\nu = -\infty$. Combining the integral expansion of $\psi_{-\infty}$ (2.75) with the beyond all orders contributions from the contour segments far from the saddle points (2.86), (2.99) and (2.105) and the contributions of the segments that travel near the colliding saddle points (2.215) and (2.250), we have the approximation

$$\begin{aligned}\psi_{-\infty}(Z;\epsilon,h) = -2\pi(2h\epsilon)^{1/3}\exp\left(\frac{\mathrm{i}}{2h\epsilon} - \frac{\mathrm{i}}{\epsilon^{1-\alpha}}\chi + \tilde{Y}\right) \\ \times\left[\mathrm{Ai}\left(-\frac{(2h)^{1/3}}{\epsilon^{2/3-\alpha}}\big(\chi + O\left(\epsilon^\alpha\right)\big)\right)\left(1 + O\left(\epsilon^\alpha\right)\right)\right. \\ \left. + \mathrm{Ai}'\left(-\frac{(2h)^{1/3}}{\epsilon^{2/3-\alpha}}\big(\chi + O\left(\epsilon^\alpha\right)\big)\right) O\left(\epsilon^{1/3}\right)\right]. \qquad (2.251)\end{aligned}$$

For matching, we will need the asymptotics for χ strictly positive and strictly negative. If we let χ to be on a negative compact interval away from zero, then we can use the familiar Ai and Ai$'$ expansions [48, Section 9.7(ii)] to get

$$\begin{aligned}\mathrm{Ai}\left(-\frac{(2h)^{1/3}}{\epsilon^{2/3-\alpha}}\left(\chi + O\left(\epsilon^\alpha\right)\right)\right) = \frac{\epsilon^{1/6-\alpha/4}}{2\pi^{1/2}(2h)^{1/12}(-\chi)^{1/4}}\exp\left(-\frac{h^{1/2}}{3\epsilon^{1-3\alpha/2}}(-2\chi)^{3/2}\right) \\ \times\left(1 + O\left(\epsilon^{1-3\alpha/2}\right)\right), \qquad (2.252)\\ \mathrm{Ai}'\left(-\frac{(2h)^{1/3}}{\epsilon^{2/3-\alpha}}\left(\chi + O\left(\epsilon^\alpha\right)\right)\right) = -\frac{(2h)^{1/12}(-\chi)^{1/4}}{2\pi^{1/2}\epsilon^{1/6-\alpha/4}}\exp\left(-\frac{h^{1/2}}{3\epsilon^{1-3\alpha/2}}(-2\chi)^{3/2}\right) \\ \times\left(1 + O\left(\epsilon^{1-3\alpha/2}\right)\right). \qquad (2.253)\end{aligned}$$

On the Ai$'$ term, the additional factor $O\left(\epsilon^{1/3}\right)$ makes the overall epsilon power $7/24 < 1/6 + \alpha/4 < 1/3$, which means the Ai$'$ term goes to zero, so we have the simplified

asymptotics for $\chi < 0$

$$\psi_{-\infty}(Z;\epsilon,h) = -\frac{\pi^{1/2}(2h)^{1/4}\epsilon^{1/2-\alpha/4}}{(-\chi)^{1/4}} \exp\left(\frac{\mathrm{i}}{2h\epsilon} - \frac{h^{1/2}}{3\epsilon^{1-3\alpha/2}}(-2\chi)^{3/2} - \frac{\mathrm{i}}{\epsilon^{1-\alpha}}\chi + \tilde{Y}\right) \times \left(1 + O\left(\epsilon^{1-3\alpha/2}\right)\right). \tag{2.254}$$

Now we take χ to be on a positive compact interval away from zero, then we can use the other familiar Ai and Ai$'$ expansions to get

$$\mathrm{Ai}\left(-\frac{(2h)^{1/3}}{\epsilon^{2/3-\alpha}}\left(\chi + O\left(\epsilon^{\alpha}\right)\right)\right) = \frac{\epsilon^{1/6-\alpha/4}}{\pi^{1/2}(2h)^{1/12}(\chi)^{1/4}} \times \left(\cos\left(-\frac{h^{1/2}}{3\epsilon^{1-3\alpha/2}}(2\chi)^{3/2} - \frac{\pi}{4}\right) + O\left(\epsilon^{1-3\alpha/2}\right)\right), \tag{2.255}$$

$$\mathrm{Ai}'\left(-\frac{(2h)^{1/3}}{\epsilon^{2/3-\alpha}}\left(\chi + O\left(\epsilon^{\alpha}\right)\right)\right) = \frac{(2h)^{1/12}(\chi)^{1/4}}{\pi^{1/2}\epsilon^{1/6-\alpha/4}} \times \left(\sin\left(-\frac{h^{1/2}}{3\epsilon^{1-3\alpha/2}}(2\chi)^{3/2} - \frac{\pi}{4}\right) + O\left(\epsilon^{1-3\alpha/2}\right)\right). \tag{2.256}$$

Again, the Ai$'$ term is bounded above and tends to zero in this case, so we have the leading order asymptotics for $\chi > 0$

$$\psi_{-\infty}(Z;\epsilon,h) = -\frac{2\pi^{1/2}(2h)^{1/4}\epsilon^{1/2-\alpha/4}}{(\chi)^{1/4}} \exp\left(\frac{\mathrm{i}}{2h\epsilon} - \frac{\mathrm{i}}{\epsilon^{1-\alpha}}\chi + \tilde{Y}\right) \times \left(\cos\left(-\frac{h^{1/2}}{3\epsilon^{1-3\alpha/2}}(2\chi)^{3/2} - \frac{\pi}{4}\right) + O\left(\epsilon^{1-3\alpha/2}\right)\right). \tag{2.257}$$

Additionally, since Ai$'$ is bounded around the origin, these asymptotics demonstrate that the Ai$'$ term can be bounded in the error term for all $|\chi| \leq M_\chi/h$,

$$\psi_{-\infty}(Z;\epsilon,h) = -2\pi(2h\epsilon)^{1/3} \exp\left(\frac{\mathrm{i}}{2h\epsilon} - \frac{\mathrm{i}}{\epsilon^{1-\alpha}}\chi + \tilde{Y}\right) \times \left[\mathrm{Ai}\left(-\frac{(2h)^{1/3}}{\epsilon^{2/3-\alpha}}\big(\chi + O\left(\epsilon^{\alpha}\right)\big)\right) + O\left(\epsilon^{1-3\alpha/2}\right)\right]. \tag{2.258}$$

2. $\nu \in 2\mathbb{Z} - 1/2$ with $\nu \leq -9/2$. Let the integer $n = (\nu - 3/2)/2 \leq -3$ Combining the integral expansion of $\psi_{-\nu}$ (2.109) with the beyond all orders contributions from the contour segments far from the saddle points (2.136), (2.126) and the contributions of

the segments that travel near the simple saddle points (2.182) and (2.211), we have the approximation

$$\psi_\nu(Z;\epsilon,h) = E_n(\tilde{X},\tilde{Y})\left[\left(\frac{2\pi h\epsilon}{\tilde{X}-k_n(\tilde{X})-1}\right)^{1/2}\mathrm{e}^{-\mathrm{i}\pi/4}+O\left(\epsilon^{3/2}\right)\right] - E_{n+1}(\tilde{X},\tilde{Y})\left[\left(\frac{2\pi h\epsilon}{\tilde{X}-k_{n+1}(\tilde{X})-1}\right)^{1/2}\mathrm{e}^{-\mathrm{i}\pi/4}+O\left(\epsilon^{3/2}\right)\right]. \quad (2.259)$$

We will simplify the leading exponential terms defined in (2.111) for $m \in \mathbb{Z}$

$$E_m(\tilde{X},\tilde{Y}) = \exp\left(-\frac{\mathrm{i}}{h\epsilon}\left[\frac{k_m(\tilde{X})^2}{2}-\mathrm{e}^{-k_m(\tilde{X})-1}-\tilde{X}k_m(\tilde{X})\right]-k_m(\tilde{X})\tilde{Y}\right) \quad (2.260)$$

$$= \exp\left(\frac{\mathrm{i}}{2h\epsilon}\left[\tilde{X}^2+1-\left(k_m(\tilde{X})+1-\tilde{X}\right)^2\right]-k_m(\tilde{X})\tilde{Y}\right). \quad (2.261)$$

We note that from a Taylor series expansion,

$$k_m(\tilde{X})+1-\tilde{X} = 1+W_m(-\mathrm{e}^{-\tilde{X}-1}) \quad (2.262)$$

$$= 1+W_m(-\mathrm{e}^{-1})-\frac{W_m(-\mathrm{e}^{-1})}{1+W_m(-\mathrm{e}^{-1})}\tilde{X}+O\left(\tilde{X}^2\right) \quad (2.263)$$

where the constant bound in the error term can be shown to be uniform for $m \neq -1, 0$. Thus, the leading order we can expand in powers of epsilon

$$E_m(\tilde{X},\tilde{Y}) = \exp\left(\frac{\mathrm{i}}{2h\epsilon}\left[1-(1+W_m)^2+2h\epsilon^\alpha W_m\chi+O\left(\epsilon^{2\alpha}\right)\right]-\left[W_m+O\left(\epsilon^\alpha\right)\right]\tilde{Y}\right) \quad (2.264)$$

$$= \exp\left(\mathrm{i}\frac{1-(1+W_m)^2}{2h\epsilon}+\mathrm{i}\frac{W_m}{\epsilon^{1-\alpha}}\chi-W_m\tilde{Y}\right)\left(1+O\left(\epsilon^\alpha\right)\right) \quad (2.265)$$

where, from now on for brevity, we take $W_m = W_m(-\mathrm{e}^{-1})$. If we look at the ratio,

$$\left|\frac{E_{m+1}(\tilde{X},\tilde{Y})}{E_m(\tilde{X},\tilde{Y})}\right| = \exp\left(-\mathrm{i}\frac{(1+W_{m+1})^2-(1+W_m)^2}{2h\epsilon}+\mathrm{i}(W_{m+1}-W_m)\left(\frac{\chi}{\epsilon^{1-\alpha}}+\mathrm{i}\tilde{Y}\right)\right) \times\left(1+O\left(\epsilon^\alpha\right)\right), \quad (2.266)$$

we conclude that it tends to zero beyond all orders. This is because, from properties of the Lambert-W function, $\mathrm{Im}\left[(1+W_m)^2\right]$ is strictly decreasing as m increases. Moreover, the difference between subsequent imaginary parts is strictly increasing, thus the

leading order term above has a uniform negative upper bound. Since $|\mathrm{Im}\left[W_{m+1} - W_m\right]|$ and $|\chi|$ are also bounded uniformly, there is a uniform small enough ϵ such that the exponent tends to $-\infty$ with $O\left(1/\epsilon\right)$ for all $m \leq -3$. This shows that we may absorb the $m+1$ term in (2.259) into the error on the m term to get the simplified approximation,

$$\psi_\nu(Z;\epsilon,h) = \left(\frac{2\pi h\epsilon}{1+W_n}\right)^{1/2} \exp\left(\mathrm{i}\frac{1-(1+W_n)^2}{2h\epsilon} + \mathrm{i}\frac{W_n}{\epsilon^{1-\alpha}}\chi - W_n\tilde{Y} + \mathrm{i}\frac{\pi}{4}\right) \times \left[1 + O\left(\epsilon^\alpha\right)\right]. \tag{2.267}$$

3. $\nu = -5/2$. Combining the integral expansion of $\psi_{-5/2}$ (2.138) with the beyond all orders contributions from the contour segments far from the saddle points (2.86), (2.99), (2.105) and (2.136), and the contributions of the segments that travel near the simple saddle points (2.216) and (2.250), we have, along with the simplifications made in the previous two cases, the approximation

$$\begin{aligned}\psi_{-5/2}(Z;\epsilon,h) = \exp&\left(\mathrm{i}\frac{1-(1+W_{-2})^2}{2h\epsilon} + \mathrm{i}\frac{W_{-2}}{\epsilon^{1-\alpha}}\chi - W_{-2}\tilde{Y} + \mathrm{i}\frac{\pi}{4}\right) \\ &\times \left[\left(\frac{2\pi h\epsilon}{1+W_{-2}}\right)^{1/2} + O\left(\epsilon^{\alpha+1/2}\right)\right] \\ &+ 2\pi(2h\epsilon)^{1/3}\exp\left(\frac{\mathrm{i}}{2h\epsilon} - \frac{\mathrm{i}}{\epsilon^{1-\alpha}}\chi + \tilde{Y}\right) \\ &\times \left[\mathrm{Ai}\left(-\frac{(2h)^{1/3}}{\epsilon^{2/3-\alpha}}\left(\chi + O\left(\epsilon^\alpha\right)\right)\right) + O\left(\epsilon^{1-3\alpha/2}\right)\right]. \end{aligned} \tag{2.268}$$

If we factor out the first exponential from the entire approximation, the Ai term is multiplied by the exponential term

$$\begin{aligned}&\exp\left(\frac{\mathrm{i}}{2h\epsilon} - \frac{\mathrm{i}}{\epsilon^{1-\alpha}}\chi + \tilde{Y} - \mathrm{i}\frac{1-(1+W_{-2})^2}{2h\epsilon} - \mathrm{i}\frac{W_{-2}}{\epsilon^{1-\alpha}}\chi + W_{-2}\tilde{Y} - \mathrm{i}\frac{\pi}{4}\right) \\ &\qquad = \exp\left(\mathrm{i}\frac{(1+W_{-2})^2}{2h\epsilon} - \mathrm{i}(1+W_{-2})\left(\frac{\chi}{\epsilon^{1-\alpha}} + \mathrm{i}\tilde{Y}\right) - \mathrm{i}\frac{\pi}{4}\right)\end{aligned} \tag{2.269}$$

$\mathrm{Im}\left[(1+W_{-2})^2\right] > 0$, and since the rest of the exponent is bounded at $O\left(1/\epsilon^{1-\alpha}\right)$, this exponential goes to zero beyond all orders. Thus, after noting the Ai function is

uniformly bounded, we have the simplified approximation

$$\psi_{5/2}(Z;\epsilon,h) = \left(\frac{2\pi h\epsilon}{1+W_{-2}}\right)^{1/2} \exp\left(\mathrm{i}\frac{1-(1+W_{-2})^2}{2h\epsilon} + \mathrm{i}\frac{W_{-2}}{\epsilon^{1-\alpha}}\chi - W_{-2}\tilde{Y} + \mathrm{i}\frac{\pi}{4}\right) \times \left[1 + O\left(\epsilon^{\alpha}\right)\right] . \tag{2.270}$$

4. $\nu = -1/2$. Combining the integral expansion of $\psi_{-5/2}$ (2.144) with the beyond all orders contributions from the contour segments far from the saddle points (2.86), (2.99), (2.153), and (2.157), and the contributions of the segments that travel near the simple saddle points (2.217) and (2.250), we have, the approximation

$$\begin{aligned}\psi_{-1/2}(Z;\epsilon,h) = -2\pi(2h\epsilon)^{1/3}\exp\left(\frac{\mathrm{i}}{2h\epsilon} - \frac{\mathrm{i}}{\epsilon^{1-\alpha}}\chi + \tilde{Y}\right) \\ \times \left[\mathrm{Ai}\left(\frac{(2h)^{1/3}\mathrm{e}^{\mathrm{i}\pi/3}}{\epsilon^{2/3-\alpha}}\big(\chi + O\left(\epsilon^{\alpha}\right)\big)\right)\left(1 + O\left(\epsilon^{\alpha}\right)\right)\right. \\ \left. + \mathrm{Ai}'\left(\frac{(2h)^{1/3}\mathrm{e}^{\mathrm{i}\pi/3}}{\epsilon^{2/3-\alpha}}\big(\chi + O\left(\epsilon^{\alpha}\right)\big)\right) O\left(\epsilon^{1/3}\right)\right] .\end{aligned} \tag{2.271}$$

If we consider χ on the union of two intervals, one positive and one negative, then we can employ the Ai and Ai$'$ asymptotics,

$$\begin{aligned}&\mathrm{Ai}\left(-\frac{(2h)^{1/3}\mathrm{e}^{-\mathrm{i}2\pi/3}}{\epsilon^{2/3-\alpha}}\left(\chi + O\left(\epsilon^{\alpha}\right)\right)\right) \\ &\quad = \frac{\epsilon^{1/6-\alpha/4}}{2\pi^{1/2}(2h)^{1/12}(\mathrm{e}^{\mathrm{i}\pi/3}\chi)^{1/4}}\exp\left(-\frac{h^{1/2}}{3\epsilon^{1-3\alpha/2}}(2\mathrm{e}^{\mathrm{i}\pi/3}\chi)^{3/2}\right)\left(1 + O\left(\epsilon^{1-3\alpha/2}\right)\right) ,\end{aligned} \tag{2.272}$$

$$\begin{aligned}&\mathrm{Ai}'\left(-\frac{(2h)^{1/3}\mathrm{e}^{-\mathrm{i}2\pi/3}}{\epsilon^{2/3-\alpha}}\left(\chi + O\left(\epsilon^{\alpha}\right)\right)\right) \\ &\quad = -\frac{(2h)^{1/12}(\mathrm{e}^{\mathrm{i}\pi/3}\chi)^{1/4}}{2\pi^{1/2}\epsilon^{1/6-\alpha/4}}\exp\left(-\frac{h^{1/2}}{3\epsilon^{1-3\alpha/2}}(2\mathrm{e}^{\mathrm{i}\pi/3}\chi)^{3/2}\right)\left(1 + O\left(\epsilon^{1-3\alpha/2}\right)\right) .\end{aligned} \tag{2.273}$$

Again, like in the first case, we see that the Ai$'$ contribution is sub-leading after factoring out the common exponential, and so we can write the matching asymptotics

as

$$\psi_{-1/2}(Z;\epsilon,h) = -\frac{\pi^{1/2}(2h)^{1/4}\epsilon^{1/2-\alpha/4}}{(\mathrm{e}^{\mathrm{i}\pi/3}\chi)^{1/4}} \exp\left(\frac{\mathrm{i}}{2h\epsilon} - \frac{h^{1/2}}{3\epsilon^{1-3\alpha/2}}(2\mathrm{e}^{\mathrm{i}\pi/3}\chi)^{3/2} - \frac{\mathrm{i}}{\epsilon^{1-\alpha}}\chi + \tilde{Y}\right) \times \left(1 + O\left(\epsilon^{1-3\alpha/2}\right)\right) . \tag{2.274}$$

Since the ratio of Ai to Ai$'$ along the line with argument $\pi/3$ is bounded near zero, these asymptotics shows that the Ai$'$ term is sub-leading overall and we have the simplified asymptotics including $\chi = 0$,

$$\psi_{-1/2}(Z;\epsilon,h) = -2\pi(2h\epsilon)^{1/3} \exp\left(\frac{\mathrm{i}}{2h\epsilon} - \frac{\mathrm{i}}{\epsilon^{1-\alpha}}\chi + \tilde{Y}\right) \times \left[\mathrm{Ai}\left(\frac{(2h)^{1/3}\mathrm{e}^{\mathrm{i}\pi/3}}{\epsilon^{2/3-\alpha}}\big(\chi + O\left(\epsilon^{\alpha}\right)\big)\right) + O\left(\epsilon^{1-3\alpha/2}\right)\right] . \tag{2.275}$$

5. $\nu \in 2\mathbb{Z} - 1/2$ with $\nu \geq 3/2$. Let the integer $n = (\nu + 1/2)/2 \geq 1$. Combining the integral expansion of $\psi_{-\nu}$ (2.166) with the beyond all orders contributions from the contour segments far from the saddle points and the contributions of the segments that travel near the simple saddle points (2.182) and (2.211), along with the simplification of this formula established in case 2, we have the approximation

$$\psi_{\nu}(Z;\epsilon,h) = \left(\frac{2\pi h\epsilon}{1+W_n}\right)^{1/2} \exp\left(\mathrm{i}\frac{1-(1+W_n)^2}{2h\epsilon} + \mathrm{i}\frac{W_n}{\epsilon^{1-\alpha}}\chi - W_n\tilde{Y} - \mathrm{i}\frac{3\pi}{4}\right) \times \left[1 + O\left(\epsilon^{\alpha}\right)\right] . \tag{2.276}$$

2.3 WKB Matching Argument and the Formal Asymptotic Scattering Data

Our goal in this section is to heuristically justify the construction of normalizable eigenfunctions ψ of the ILW scattering equation (2.3) by matching the formal asymptotic solutions (2.26) across turning points by way of the rigorously proven asymptotics of our basis of solutions to the model turning point equation (2.41).

We begin with a $\mathcal{C}^2$ positive, single lobed potential $u : \mathbb{R} \to \mathbb{R}_+$ where the first derivative is nonvanishing except at the maximum $u_{\max}$ which is attained at $x_{\max} \in \mathbb{R}$. We also require that for all $x \in \mathbb{R}$, $u_0(x) \leq C\langle x\rangle^2$ for some $C > 0$. This implies the existence of two inverse functions of u, one that applies for x to the left of $x_{\max}$, $u_-^{-1} : [0, u_{\max}] \to (-\infty, x_{\max}]$, and one for the x to the right of $x_{\max}$, $u_+^{-1} : [0, u_{\max}] \to [x_{\max}, \infty)$. For $\zeta \in \mathcal{Q}_\delta$, the turning points

occur when the argument of the Lambert W-functions in the formal asymptotic solutions equals $-\mathrm{e}^{-1}$.

$$-2\delta\zeta \mathrm{e}^{-2\delta(\zeta-u_0(x))} = -\mathrm{e}^{-1} \tag{2.277}$$

$$\implies \zeta = -\frac{1}{2\delta} W_{-1}(-\mathrm{e}^{-1-2\delta u_0(x)}) \tag{2.278}$$

where we chose the -1 branch so that $\zeta \in \mathcal{Q}_{\delta+}$. Since u_0 covers the range $(0, u_{\max}]$, the infimum and supremum (by imaginary part) of all $\zeta \in \mathcal{Q}_{\delta+}$ that have turning points are $1/2\delta$ and

$$\zeta_{\max} := -\frac{1}{2\delta} W_{-1}\left(-\mathrm{e}^{-1-2\delta u_{\max}}\right) \tag{2.279}$$

respectively. We remind the reader that we denote intervals along the quadratrix with the usual interval notation for $\mathbb{R}$ but with the subscript $\mathcal{Q}$, see (1.26). For all $\zeta \in (1/2\delta, \zeta_{\max})_{\mathcal{Q}_\delta}$, there are two turning points $x_\pm(\zeta)$ defined by (2.277) which can be solved for explicitly with the use of the inverse functions of u_0.

$$x_\pm(\zeta) = u_\pm^{-1}\left(\zeta - \frac{1}{2\delta} - \frac{1}{2\delta}\log(2\delta\zeta)\right) \tag{2.280}$$

For a particular level $\zeta \in (1/2\delta, \zeta_{\max})_{\mathcal{Q}_\delta}$, split $\mathbb{R}$ into three regions, the "left classically forbidden" region $\mathcal{R}_{f-} = \big(-\infty, x_-(\zeta)\big)$, the "classically allowed" region $\mathcal{R}_a = \big(x_-(\zeta), x_+(\zeta)\big)$ and the "right classically forbidden" region $\mathcal{R}_{f+} = \big(x_+(\zeta), +\infty\big)$, where the naming convention comes from the quantum mechanical interpretation of the time independent Schrödinger equation. In each of these three regions, we consider an infinite linear combination of asymptotic solutions (2.26).

$$\Phi_{f-}(z) = \sum_{n\in\mathbb{Z}} F_n^- \Phi_n(z;\zeta,x_-) \text{ for } x \in \mathcal{R}_{f-}, \tag{2.281}$$

$$\Phi_a(z) = \sum_{n\in\mathbb{Z}} A_n^- \Phi_n(z;\zeta,x_-) = \sum_{n\in\mathbb{Z}} A_n^+ \Phi_n(z;\zeta,x_+) \text{ for } x \in \mathcal{R}_a, \tag{2.282}$$

$$\Phi_{f+}(z) = \sum_{n\in\mathbb{Z}} F_n^+ \Phi_n(z;\zeta,x_+) \text{ for } x \in \mathcal{R}_{f+}\,, \tag{2.283}$$

with $\{F_n^\pm, A_n^\pm\}_{n\in Z} \subset \mathbb{C}$ are some possibly ϵ-dependent but definitely z-independent constants. Additionally, we wrote the same expansion in the classically allowed region two different ways, one integrating in from the left turning point and one from the right turning

point. We can be assured that these are the same if we require that for all $n \in \mathbb{Z}$ and $x \in \mathcal{R}_a$,

$$A_n^- \Phi_n(z;\zeta,x_-) = A_n^+ \Phi_n(z;\zeta,x_+), \tag{2.284}$$

$$\implies A_n^- \exp\left(\frac{\mathrm{i}}{\epsilon}\int_{x_-}^{x} G_n^{-1}(u(x');\zeta)\,\mathrm{d}x'\right) = A_n^+ \exp\left(\frac{\mathrm{i}}{\epsilon}\int_{x_+}^{x} G_n^{-1}(u(x');\zeta)\,\mathrm{d}x'\right), \tag{2.285}$$

$$\implies \frac{A_n^+}{A_n^-} = \exp\left(\frac{\mathrm{i}}{\epsilon}\int_{x_-}^{x_+} G_n^{-1}(u(x');\zeta)\,\mathrm{d}x'\right) \tag{2.286}$$

which can be required as this is an z-independent constant.

We also introduce the transition regions around the turning points

$$\mathcal{R}_{t-} = \big(x_-(\zeta) - \epsilon^\alpha 2\delta M_\chi^-,\ x_-(\zeta) + \epsilon^\alpha 2\delta M_\chi^-\big) \tag{2.287}$$

$$\mathcal{R}_{t+} = \big(x_+(\zeta) - \epsilon^\alpha 2\delta M_\chi^+,\ x_+(\zeta) + \epsilon^\alpha 2\delta M_\chi^-\big) \tag{2.288}$$

for some $M_\chi^\pm > 0$ and $1/2 < \alpha < 2/3$. We write $x \in \mathcal{R}_{t\pm}$ as $x = x_\pm(\zeta) \mp \epsilon^\alpha 2\delta\chi_\pm$ where $|\chi_\pm| \le M_\chi^\pm$. Then we write the asymptotic solution in the transition regions as

$$\Phi_{t-}(z) = \exp\left(\mathrm{i}\frac{u(x_-)}{\epsilon}z\right)\left(T_{-\infty}^-\psi_{-\infty}(Z_-;\epsilon,h_-) + \sum_{\nu\in 2\mathbb{Z}-1/2} T_\nu^-\psi_\nu(Z_-;\epsilon,h_-)\right) \text{ for } x \in \mathcal{R}_{t-} \tag{2.289}$$

$$\Phi_{t+}(z) = \exp\left(\mathrm{i}\frac{u(x_+)}{\epsilon}z\right)\left(T_{-\infty}^+\psi_{-\infty}^*(-Z_+^*;\epsilon,h_+) + \sum_{\nu\in 2\mathbb{Z}-1/2} T_\nu^+\psi_\nu^*(-Z_+^*;\epsilon,h_+)\right) \text{for } x \in \mathcal{R}_{t+} \tag{2.290}$$

where $T_{-\infty}^\pm \in \mathbb{C}$ and $\{T^\pm\}_{\nu\in 2\mathbb{Z}-1/2} \subset \mathbb{C}$ are, again, some z-independent constants, $Z_\pm = \big(x - x_\pm(\zeta)\big)/2\delta = \mp\epsilon^\alpha\chi_\mp$ and finally $h_\pm = \mp 2\delta u_0'\big(x_\pm(\zeta)\big)$. With these coordinate definitions, positive $\chi_\pm$ is always in the classically allowed region while negative $\chi_\pm$ is always in one of the classically forbidden regions.

We begin by considering solutions in the left classically forbidden region. Here, $2\delta u_0(x) < 2\delta\zeta - 1 - \log(2\delta\zeta)$, so all of the values

$$G_n^{-1}(u_0(x);\zeta) = -u_0(x) - \frac{1}{2\delta}W_n(-2\delta\zeta \mathrm{e}^{-2\delta(\zeta+u_0(x))})$$

have nonzero imaginary parts. Moreover, as $x \to -\infty$, $G_n^{-1}(u_0(x);\zeta) \to G_n^{-1}(0;\zeta)$. For $n = -1$ this returns $G_{-1}^{-1}(0;\zeta) = \zeta$, and for $n = 0$, $G_0^{-1}(0;\zeta) = \zeta^*$. In the other cases of n, we have for $n \le -2$, $\mathrm{Im}\,[G_n(0;\zeta)] > \mathrm{Im}\,[\zeta]$ and for $n \ge 1$, $\mathrm{Im}\,[G_n(0;\zeta)] < -\mathrm{Im}\,[\zeta]$. This means

the integral in the exponent of the solutions $\Phi_n(x;\zeta,x_-(\zeta))$,

$$-\frac{\mathrm{i}}{\epsilon}\int_{x_-(\zeta)}^{x} G_n^{-1}(u(x');\zeta)\,\mathrm{d}x',$$

has a real part that increases without bound as $x \to -\infty$ if $n \geq -1$. This means the magnitude of $\Phi_n(x;\zeta,x_-(\zeta))$ will increase without bound, and the overall $\Phi^{(f-)}(x)$ will not be normalizable. Thus, we immediately conclude that all $F_n^- = 0$ for $n \geq 0$. Conversely, if $n \leq -1$ in the above integral, the real part will decrease without bound and there will be no problem integrating the norm-squared of the solution out to $x \to -\infty$, subject to convergent coefficients. Now we wish to match with the solution expansion in the transition region around the turning point $x_-(\zeta)$. We will expand the constituent parts of the asymptotic solutions (2.26) with the change of variables $x = x_-(\zeta) + \epsilon^\alpha 2\delta\chi_-$, $y = 2\delta\epsilon(\tilde{Y} - 1/2)$. Because of the different behavior for the solutions at a turning point, we will have to handle these expansions in two cases:

1. $n \in \mathbb{Z}$ but $n \neq -1, 0$. Then $G_n^{-1}(u_0(x);\zeta)$ is differentiable at the turning point:

$$\int_{x_-}^{x} G_n^{-1}(u_0(x');\zeta)\,\mathrm{d}x' = G_n^{-1}(u_0(x_-);\zeta)\ \epsilon^\alpha 2\delta\chi_- + O\left(\epsilon^{2\alpha}\right) \tag{2.291}$$

$$= -\left(2\delta u_0(x_-) + W_n(-\mathrm{e}^{-1})\right)\epsilon^\alpha\chi_- + O\left(\epsilon^{2\alpha}\right)\ . \tag{2.292}$$

   So the asymptotic solution (2.26) has the expansion

$$\Phi_n(z;\zeta) = \exp\left(\mathrm{i}\left(2\delta u_0(x_-) + W_n(-\mathrm{e}^{-1})\right)\left(\frac{\chi_-}{\epsilon^{1-\alpha}} + \mathrm{i}\tilde{Y} - \frac{\mathrm{i}}{2}\right)\right)$$
$$\times\left[\left(\frac{-2\delta W_n(-\mathrm{e}^{-1})}{1+W_n(-\mathrm{e}^{-1})}\right)^{1/2} + O\left(\epsilon^{2\alpha-1}\right)\right]. \tag{2.293}$$

   Because these solutions are regular across the turning point, this expansion is valid in the entire transition region $\mathcal{R}_{t-}$.

2. $n = -1, 0$. The difficulty in this case is handling the fact that $W_n(-2\delta\zeta\mathrm{e}^{-2\delta(\zeta+u_0(x))})$ is not differentiable at the turning point, it behaves like a square-root here. Thus, we will have different asymptotics depending on which side of the transition region we're expanding on. First, let us look at the case for $\chi_- < 0$. Expanding the argument of

the Lambert W-function,

$$\begin{aligned}-2\delta\zeta\exp\left(-2\delta\left[\zeta+u_0(x)\right]\right) &= -2\delta\zeta\exp\left(-2\delta\left[\zeta+u_0(x_-)+u_0'(x_-)2\delta\epsilon^\alpha\chi_-+O\left(\epsilon^{2\alpha}\right)\right]\right)\\ &= -\exp\left(-1-h_-\epsilon^\alpha\chi_-+O\left(\epsilon^{2\alpha}\right)\right)\,. \end{aligned} \tag{2.294}$$

We can now again make use of the series (2.229). Noticing that the leading order term is a principal square-root, we can pull out a negative sign to make the argument positive at the cost of a factor of i,

$$W_{-1}\left(-\mathrm{e}^{-1-h_-\epsilon^\alpha\chi_-+O\left(\epsilon^{2\alpha}\right)}\right) = -1-\mathrm{i}(2h_-)^{1/2}\epsilon^{\alpha/2}\left(-\chi_-\right)^{1/2}+O\left(\epsilon^\alpha\right)\,, \tag{2.295}$$

$$W_0\left(-\mathrm{e}^{-1-h_-\epsilon^\alpha\chi_-+O\left(\epsilon^{2\alpha}\right)}\right) = -1+\mathrm{i}(2h_-)^{1/2}\epsilon^{\alpha/2}\left(-\chi_-\right)^{1/2}+O\left(\epsilon^\alpha\right)\,. \tag{2.296}$$

From this, the expansions of the amplitude terms are

$$\left(\frac{-2\delta W_{-1}(-2\delta\zeta\mathrm{e}^{-2\delta(\zeta+u_0(x))})}{1+W_{-1}(-2\delta\zeta\mathrm{e}^{-2\delta(\zeta+u_0(x))})}\right)^{1/2} = \frac{(2\delta)^{1/2}\mathrm{e}^{\mathrm{i}\pi/4}}{(2h_-)^{1/4}\epsilon^{\alpha/4}\left(-\chi_-\right)^{1/4}}+O\left(\epsilon^{\alpha/4}\right), \tag{2.297}$$

$$\left(\frac{-2\delta W_{0}(-2\delta\zeta\mathrm{e}^{-2\delta(\zeta+u_0(x))})}{1+W_{0}(-2\delta\zeta\mathrm{e}^{-2\delta(\zeta+u_0(x))})}\right)^{1/2} = \frac{(2\delta)^{1/2}\mathrm{e}^{-\mathrm{i}\pi/4}}{(2h_-)^{1/4}\epsilon^{\alpha/4}\left(-\chi_-\right)^{1/4}}+O\left(\epsilon^{\alpha/4}\right)\,. \tag{2.298}$$

Additionally, the integral terms then has the expansions

$$\int_{x_-}^{x} G_{-1}^{-1}(u_0(x');\zeta)\,\mathrm{d}x' = -\left(2\delta u_0(x_-)+1\right)\epsilon^\alpha\chi_- - \mathrm{i}\frac{h_-^{1/2}\epsilon^{3\alpha/2}}{3}(-2\chi_-)^{3/2}+O\left(\epsilon^{2\alpha}\right)\,, \tag{2.299}$$

$$\int_{x_-}^{x} G_{0}^{-1}(u_0(x');\zeta)\,\mathrm{d}x' = -\left(2\delta u_0(x_-)+1\right)\epsilon^\alpha\chi_- + \mathrm{i}\frac{h_-^{1/2}\epsilon^{3\alpha/2}}{3}(-2\chi_-)^{3/2}+O\left(\epsilon^{2\alpha}\right)\,. \tag{2.300}$$

Plugging these into the formula for the asymptotic solution (2.26), we get

$$\Phi_{-1}(z;\zeta) = \exp\left(\mathrm{i}\left(2\delta u_0(x_-)+1\right)\left(\frac{\chi_-}{\epsilon^{1-\alpha}}+\mathrm{i}\tilde{Y}-\frac{\mathrm{i}}{2}\right)-\frac{h_-^{1/2}}{3\epsilon^{1-3\alpha/2}}(-2\chi_-)^{3/2}\right) \times \frac{(2\delta)^{1/2}\mathrm{e}^{\mathrm{i}\pi/4}}{(2h_-)^{1/4}\epsilon^{\alpha/4}\left(-\chi_-\right)^{1/4}}\left[1+O\left(\epsilon^{2\alpha-1}\right)\right], \tag{2.301}$$

$$\Phi_{0}(z;\zeta) = \exp\left(\mathrm{i}\left(2\delta u_0(x_-)+1\right)\left(\frac{\chi_-}{\epsilon^{1-\alpha}}+\mathrm{i}\tilde{Y}-\frac{\mathrm{i}}{2}\right)+\frac{h_-^{1/2}}{3\epsilon^{1-3\alpha/2}}(-2\chi_-)^{3/2}\right) \times \frac{(2\delta)^{1/2}\mathrm{e}^{-\mathrm{i}\pi/4}}{(2h_-)^{1/4}\epsilon^{\alpha/4}\left(-\chi_-\right)^{1/4}}\left[1+O\left(\epsilon^{2\alpha-1}\right)\right]. \tag{2.302}$$

Now we consider $\chi_- > 0$, then we do not need to pull a negative sign out of the principle square-root and there are no additional factors of i in the series expansions (2.295) and (2.296). Following this through the algebra, the effect is

$$\Phi_{-1}(z;\zeta) = \exp\left(\mathrm{i}\left(2\delta u_0(x_-)+1\right)\left(\frac{\chi_-}{\epsilon^{1-\alpha}}+\mathrm{i}\tilde{Y}-\frac{\mathrm{i}}{2}\right)+\mathrm{i}\frac{h_-^{1/2}}{3\epsilon^{1-3\alpha/2}}(2\chi_-)^{3/2}\right) \times \frac{\mathrm{i}(2\delta)^{1/2}}{(2h_-)^{1/4}\epsilon^{\alpha/4}\left(\chi_-\right)^{1/4}}\left[1+O\left(\epsilon^{2\alpha-1}\right)\right], \tag{2.303}$$

$$\Phi_{0}(z;\zeta) = \exp\left(\mathrm{i}\left(2\delta u_0(x_-)+1\right)\left(\frac{\chi_-}{\epsilon^{1-\alpha}}+\mathrm{i}\tilde{Y}-\frac{\mathrm{i}}{2}\right)-\mathrm{i}\frac{h_-^{1/2}}{3\epsilon^{1-3\alpha/2}}(2\chi_-)^{3/2}\right) \times \frac{(2\delta)^{1/2}}{(2h_-)^{1/4}\epsilon^{\alpha/4}\left(\chi_-\right)^{1/4}}\left[1+O\left(\epsilon^{2\alpha-1}\right)\right]. \tag{2.304}$$

Now we are finally ready to start matching in the left transition region. To cancel any ϵ-dependent but z-independent constants in the expansions on either side, we introduce the

new constants $\{f_n^-, a_n^-\}_{n\in\mathbb{Z}} \subset \mathbb{C}$ and $\{\tau_n^-\}_{n\in\mathbb{Z}} \subset \mathbb{C}$ such that

$$F_n^- = f_n^- \left(\frac{-2\delta W_n}{1+W_n}\right)^{-1/2} \exp\left(-\frac{2\delta u_0(x_-)+W_n}{2}\right) \text{ for } n \neq -1, 0\,, \tag{2.305}$$

$$F_{-1}^- = f_{-1}^- \frac{(2h_-)^{1/4}\epsilon^{\alpha/4}\mathrm{e}^{-\mathrm{i}\pi/4}}{(2\delta)^{1/2}} \exp\left(-\frac{2\delta u_0(x_-)+1}{2}\right), \tag{2.306}$$

$$F_0^- = f_0^- \frac{(2h_-)^{1/4}\epsilon^{\alpha/4}\mathrm{e}^{\mathrm{i}\pi/4}}{(2\delta)^{1/2}} \exp\left(-\frac{2\delta u_0(x_-)+1}{2}\right), \tag{2.307}$$

$$T_{-\infty}^- = \tau_{-1}^- \frac{-1}{\pi^{1/2}(2h)^{1/4}\epsilon^{1/2-\alpha/4}} \exp\left(-\frac{\mathrm{i}}{2h\epsilon}\right), \tag{2.308}$$

$$T_{2n+3/2}^- = \tau_n^- \left(\frac{2\pi h\epsilon}{1+W_n}\right)^{-1/2} \exp\left(-\mathrm{i}\frac{1-(1+W_n)^2}{2h\epsilon} - \mathrm{i}\frac{\pi}{4}\right) \text{ for } n \leq -2\,, \tag{2.309}$$

$$T_{-1/2}^- = \tau_0^- \frac{-\mathrm{e}^{-\mathrm{i}\pi/6}}{\pi^{1/2}(2h)^{1/4}\epsilon^{1/2-\alpha/4}} \exp\left(-\frac{\mathrm{i}}{2h\epsilon}\right), \tag{2.310}$$

$$T_{2n-1/2}^- = \tau_n^- \left(\frac{2\pi h\epsilon}{1+W_n}\right)^{-1/2} \exp\left(-\mathrm{i}\frac{1-(1+W_n)^2}{2h\epsilon} + \mathrm{i}\frac{3\pi}{4}\right) \text{ for } n \geq 1\,. \tag{2.311}$$

Considering the exponential pre-factor on $\Phi_{t-}(z)$, we evaluate this with the change of variables

$$\exp\left(\mathrm{i}\frac{u(x_-)}{\epsilon}z\right) = \exp\left(\mathrm{i}2\delta u_0(x_-)\left(\frac{\chi_-}{\epsilon^{1-\alpha}} + \mathrm{i}\tilde{Y} - \frac{\mathrm{i}}{2}\right)\right) \tag{2.312}$$

which is exactly a term that appears in all the expansions (2.293), (2.301), (2.302), (2.303), and (2.304) of the formal asymptotic solutions in the classically allowed and forbidden regions. Thus, we can factor this out when we match at the left edge of the transition region, i.e. for $\chi_- > 0$ on a compact interval, we have

$$0 = \exp\left(-\mathrm{i}\frac{u(x_-)}{\epsilon}z\right)\left(\Phi_{f-}(z) - \Phi_{t-}(z)\right) \tag{2.313}$$

$$\begin{aligned} &= \frac{f_{-1}^- - \tau_{-1}^-}{(-\chi_-)^{1/4}} \exp\left(-\frac{h^{1/2}}{3\epsilon^{1-3\alpha/2}}(-2\chi_-)^{3/2} - \mathrm{i}\left(\frac{\chi_-}{\epsilon^{1-\alpha}} + \mathrm{i}\tilde{Y}\right)\right)\left[1 + O\left(\epsilon^{1-3\alpha/2}\right)\right] \\ &\quad + \frac{f_0^- - \tau_0^-}{(-\chi_-)^{1/4}} \exp\left(\frac{h^{1/2}}{3\epsilon^{1-3\alpha/2}}(-2\chi_-)^{3/2} - \mathrm{i}\left(\frac{\chi_-}{\epsilon^{1-\alpha}} + \mathrm{i}\tilde{Y}\right)\right)\left[1 + O\left(\epsilon^{1-3\alpha/2}\right)\right] \\ &\quad + \sum_{n\neq -1,0} (f_n^- - \tau_n^-) \exp\left(\mathrm{i}W_n(-\mathrm{e}^{-1})\left(\frac{\chi_-}{\epsilon^{1-\alpha}} + \mathrm{i}\tilde{Y}\right)\right)\left[1 + O\left(\epsilon^{2\alpha-1}\right)\right]. \end{aligned} \tag{2.314}$$

Since $\mathrm{Im}\left[W_n(-\mathrm{e}^{-1})\right]$ are all distinct for $n \neq -1, 0$ and the $n = -1, 0$ terms are differentiated by a positive and negative $(-2\chi)^{3/2}$ exponential scaling, every term in the sum above has a differentiated exponential scale for the magnitude. Thus, the only way they could cancel

identically on an entire interval is if the coefficients are all zero. Neglecting the error, this results in

$$\tau_n^- = f_n^- \text{ for } n \leq -1\,, \tag{2.315}$$

$$\tau_n^- = f_n^- = 0 \text{ for } n \geq 0\,. \tag{2.316}$$

Now we match at the right edge of the transition region with $\chi_- > 0$ on a compact interval. We similarly define new constants $\{a_n^-\}_{n\in\mathbb{Z}}$ to eliminate trivial constants in the expansions of the solutions

$$A_n^- = a_n^- \left(\frac{-2\delta W_n}{1+W_n}\right)^{-1/2} \exp\left(-\frac{2\delta u_0(x_-)+W_n}{2}\right) \text{ for } n \neq -1, 0\,, \tag{2.317}$$

$$A_{-1}^- = a_{-1}^- \frac{\mathrm{i}(2h_-)^{1/4}\epsilon^{\alpha/4}}{(2\delta)^{1/2}} \exp\left(-\frac{2\delta u_0(x_-)+1}{2}\right), \tag{2.318}$$

$$A_0^- = a_0^- \frac{(2h_-)^{1/4}\epsilon^{\alpha/4}}{(2\delta)^{1/2}} \exp\left(-\frac{2\delta u_0(x_-)+1}{2}\right). \tag{2.319}$$

Conducting the actual matching,

$$0 = \exp\left(-\mathrm{i}\frac{u(x_-)}{\epsilon}z\right)\left(\Phi_{a-}(z) - \Phi_{t-}(z)\right) \tag{2.320}$$

$$\begin{aligned}
&= \frac{\mathrm{e}^{-\mathrm{i}\chi/\epsilon^{1-\alpha}+\tilde{Y}}}{(\chi_-)^{1/4}}\Bigg(a_{-1}^- \exp\left(\mathrm{i}\frac{h_-^{1/2}}{3\epsilon^{1-3\alpha/2}}(2\chi_-)^{3/2}\right)\left[1+O\left(\epsilon^{2\alpha-1}\right)\right] \\
&\qquad + a_0^- \exp\left(-\mathrm{i}\frac{h_-^{1/2}}{3\epsilon^{1-3\alpha/2}}(2\chi_-)^{3/2}\right)\left[1+O\left(\epsilon^{2\alpha-1}\right)\right] \\
&\qquad - 2\tau_{-1}^-\left[\cos\left(-\frac{h_-^{1/2}}{3\epsilon^{1-3\alpha/2}}(2\chi_-)^{3/2}-\frac{\pi}{4}\right)+O\left(\epsilon^{1-3\alpha/2}\right)\right] \\
&\qquad - \tau_0^- \exp\left(-\mathrm{i}\frac{h_-^{1/2}}{3\epsilon^{1-3\alpha/2}}(2\chi_-)^{3/2}-\mathrm{i}\frac{\pi}{4}\right)\left[1+O\left(\epsilon^{2\alpha-1}\right)\right]\Bigg) \\
&\quad + \sum_{n\neq -1,0}(a_n^- - \tau_n^-)\exp\left(\mathrm{i}W_n(-\mathrm{e}^{-1})\left(\frac{\chi_-}{\epsilon^{1-\alpha}}+\mathrm{i}\tilde{Y}\right)\right)\left[1+O\left(\epsilon^{2\alpha-1}\right)\right]\,.
\end{aligned} \tag{2.321}$$

Matching here we have the conditions

$$a_n^- = \tau_n^- = f_n^- \text{ for } n \leq -2\,, \tag{2.322}$$

$$a_{-1}^- = \mathrm{e}^{\mathrm{i}\pi/4}\tau_{-1}^- = \mathrm{e}^{\mathrm{i}\pi/4} f_{-1}^-\,, \tag{2.323}$$

$$a_0^- = \mathrm{e}^{-\mathrm{i}\pi/4}\tau_{-1}^- + \mathrm{e}^{-\mathrm{i}\pi/4}\tau_0^- = \mathrm{e}^{-\mathrm{i}\pi/4} f_{-1}^-\,, \tag{2.324}$$

$$a_n^- = \tau_n^- = 0 \text{ for } n \geq 1\,. \tag{2.325}$$

Now we wish to carry out the same matching procedure on the right turning point $x_+(\zeta)$. But first, we notice that the formal asymptotic solutions (2.26) obey the same parity symmetry as the basis solutions of the model turning point equation. Specifically, in the classically forbidden region

$$\Phi_n(-z;\zeta,x_0) = \Phi^*_{-1-n}(-z^*;\zeta,-x_0) \text{ for } n \in \mathbb{Z}\,. \tag{2.326}$$

taking $u(x) = u_0(x)$ in (2.26) for the ones on the left and $u(x) = u_0(-x)$ for the ones on the right. This is due to the Lambert W-function terms coming in conjugate pairs identified by $n \to -1-n$. In order for the solution to be normalizable, we have that $F_n^+ = 0$ for all $n \geq 0$. The matching argument on the right side of the right turning point goes through exactly like the left side of the left turning point but with sub- and superscripts changed from $-$ to $+$ and the replacements $f_n^- \to f_{-1-n}^+$ have to be made.

$$\tau_n^+ = f_{-1-n}^+ \text{ for } n \leq -1\,, \tag{2.327}$$

$$\tau_n^+ = f_{-1-n}^+ = 0 \text{ for } n \geq 0\,. \tag{2.328}$$

where the constants $\{f_n^+\}_{n\in\mathbb{Z}} \subset \mathbb{C}$ are defined by the same relations as (2.305), (2.306) and (2.307) but with the coefficients conjugated and $n \to -1-n$ replaced

$$F_n^+ = f_n^+ \left(\frac{-2\delta W_n}{1+W_n}\right)^{-1/2} \exp\left(-\frac{2\delta u_0(x_-)+W_n}{2}\right) \text{ for } n \neq -1, 0\,, \tag{2.329}$$

$$F_{-1}^+ = f_{-1}^+ \frac{(2h_+)^{1/4}\epsilon^{\alpha/4}\mathrm{e}^{-\mathrm{i}\pi/4}}{(2\delta)^{1/2}} \exp\left(-\frac{2\delta u_0(x_-)+1}{2}\right), \tag{2.330}$$

$$F_0^+ = f_0^+ \frac{(2h_+)^{1/4}\epsilon^{\alpha/4}\mathrm{e}^{\mathrm{i}\pi/4}}{(2\delta)^{1/2}} \exp\left(-\frac{2\delta u_0(x_-)+1}{2}\right), \tag{2.331}$$

while the $\{\tau_n^+\}_{n\in\mathbb{Z}} \subset \mathbb{C}$ are defined by the same relations as (2.308), (2.309), (2.310), and

(2.311) but with the coefficients just conjugated

$$T^+_{-\infty} = \tau^+_{-1} \frac{-1}{\pi^{1/2}(2h)^{1/4}\epsilon^{1/2-\alpha/4}} \exp\left(\frac{\mathrm{i}}{2h\epsilon}\right), \tag{2.332}$$

$$T^+_{2n+3/2} = \tau^+_n \left(\frac{2\pi h\epsilon}{1+W_{-1-n}}\right)^{-1/2} \exp\left(\mathrm{i}\frac{1-(1+W_{-1-n})^2}{2h\epsilon} + \mathrm{i}\frac{\pi}{4}\right) \text{ for } n \leq -2\,, \tag{2.333}$$

$$T^+_{-1/2} = \tau^+_0 \frac{-\mathrm{e}^{\mathrm{i}\pi/6}}{\pi^{1/2}(2h)^{1/4}\epsilon^{1/2-\alpha/4}} \exp\left(\frac{\mathrm{i}}{2h\epsilon}\right), \tag{2.334}$$

$$T^+_{2n-1/2} = \tau^+_n \left(\frac{2\pi h\epsilon}{1+W_{-1-n}}\right)^{-1/2} \exp\left(\mathrm{i}\frac{1-(1+W_{-1-n})^2}{2h\epsilon} - \mathrm{i}\frac{3\pi}{4}\right) \text{ for } n \geq 1\,. \tag{2.335}$$

Now, in the classically allowed region, because the Lambert W expressions for $n = -1, 0$ are real, they do not get swapped under the parity symmetry. That is

$$\Phi_n(-z;\zeta,x_0) = \Phi^*_{-1-n}(-z^*;\zeta,-x_0) \text{ for } n \neq -1, 0\,, \tag{2.336}$$

$$\Phi_n(-z;\zeta,x_0) = \Phi^*_n(-z^*;\zeta,-x_0) \text{ for } n = -1, 0\,, \tag{2.337}$$

again taking $u(x) = u_0(x)$ in for the ones on the left and $u(x) = u_0(-x)$ for the ones on the right. Thus, the left side of the right turning point matching argument gives the same coefficient relations as the right side of the left turning point, but with the replacements $a^-_n \to a^+_{-1-n}$ only for $n \neq -1, 0$ and the coefficients need to be conjugated,

$$a^+_n = \tau^+_{-1-n} = 0 \text{ for } n \leq -2\,, \tag{2.338}$$

$$a^+_{-1} = \mathrm{e}^{-\mathrm{i}\pi/4}\tau^+_{-1} = \mathrm{e}^{-\mathrm{i}\pi/4} f^+_0\,, \tag{2.339}$$

$$a^+_0 = \mathrm{e}^{\mathrm{i}\pi/4}\tau^+_{-1} + \mathrm{e}^{\mathrm{i}\pi/4}\tau^+_0 = \mathrm{e}^{\mathrm{i}\pi/4} f^+_0\,, \tag{2.340}$$

$$a^+_n = \tau^+_{-1-n} = 0 \text{ for } n \geq 1\,, \tag{2.341}$$

where the definitions of the $\{a^+_n\}_{n\in\mathbb{Z}} \subset \mathbb{C}$ again should have their coefficients conjugated and $n \to -1-n$.

$$A^+_n = a^+_n \left(\frac{-2\delta W_n}{1+W_n}\right)^{-1/2} \exp\left(-\frac{1}{2}\left(2\delta u_0(x_+) - W_n\right)\right) \text{ for } n \neq -1, 0\,, \tag{2.342}$$

$$A^+_{-1} = a^+_{-1} \frac{-\mathrm{i}(2h_+)^{1/4}\epsilon^{\alpha/4}}{(2\delta)^{1/2}} \exp\left(-\frac{1}{2}\left(2\delta u_0(x_+) - 1\right)\right), \tag{2.343}$$

$$A^+_0 = a^+_0 \frac{(2h_+)^{1/4}\epsilon^{\alpha/4}}{(2\delta)^{1/2}} \exp\left(-\frac{1}{2}\left(2\delta u_0(x_+) - 1\right)\right). \tag{2.344}$$

As already stated, since the coefficients A_n^- and A_n^+ are related by (2.286). If we combine this with (2.322), (2.325), (2.338), and (2.325), then we arrive at the equalities

$$f_n^- = \tau_n^- = a_n^- = a_n^+ = \tau_n^+ = f_n^+ = 0 \text{ for all } n \neq -1, 0\,. \tag{2.345}$$

As one might have expected, the extraneous formal asymptotic solutions do not contribute to a normalizable solution under the matching arguments. Returning to the actual matching, we see that each extraneous solution matches at each turning point one and only one basis solution to the turning point model equation. These are the basis solutions which only ever contain simple saddle points and so appear to be expanding the regular behavior of the associated formal asymptotic solutions near the turning point. While one could have guessed this the case from the outset, the more important result here is that none of the simple saddle point basis solutions to the turning point model equation contribute in any way to the asymptotics of the scattering solutions' turning point behavior, a fact that was less obvious from the start. Continuing, we apply (2.286) with (2.318), (2.319), (2.343) and (2.344) to (2.323), (2.324), (2.339) and (2.340) to get

$$F_{-1}^- = \left\{ \begin{array}{rcl} -A_{-1}^- & = -\exp\left(-\dfrac{\mathrm{i}}{\epsilon}\displaystyle\int_{x_-}^{x_+} G_{-1}^{-1}(u(x');\zeta)\,\mathrm{d}x'\right) A_{-1}^+ \\ A_0^- & = \exp\left(-\dfrac{\mathrm{i}}{\epsilon}\displaystyle\int_{x_-}^{x_+} G_0^{-1}(u(x');\zeta)\,\mathrm{d}x'\right) A_0^+ \end{array} \right. , \quad \left. \begin{array}{c} -A_{-1}^+ \\ A_0^+ \end{array} \right\} = F_0^+\,. \tag{2.346}$$

Starting at F_{-1}^- and following a circuit around the equalities across the top and then back along the bottom, we see that we end up with F_{-1}^- times an exponential phase. In order for the solution to be nonzero, it must be that this exponential phase is one:

$$1 = \exp\left(\frac{\mathrm{i}}{\epsilon}\int_{x_-(\zeta)}^{x_+(\zeta)} G_0^{-1}(u(x);\zeta) - G_{-1}^{-1}(u(x);\zeta)\,\mathrm{d}x\right)\,. \tag{2.347}$$

We simplify the integrand and define the function $R : [1/2\delta, \zeta_{\max}]_{\mathcal{Q}_\delta} \to \mathbb{R}_+$ by

$$R(\zeta) := \frac{1}{4\delta}\int_{x_-(\zeta)}^{x_+(\zeta)} W_0\left(-2\delta\zeta \mathrm{e}^{-2\delta(\zeta+u_0(x))}\right) - W_{-1}\left(-2\delta\zeta \mathrm{e}^{-2\delta(\zeta+u_0(x))}\right)\,\mathrm{d}x\,. \tag{2.348}$$

Note, this is positive because the integral is take over the classically allowed region, and here W_0 is real and greater than $-1/2\delta$ while W_{-1} is real and less than $1/2\delta$, hence we are integrating a positive function. Then the condition that the solution constructed by matching be normalizable take a form similar to the Weyl law for the Schödinger equation.

We will call this the ILW Weyl law:

$$n\pi\epsilon = R(\zeta_n)\,. \tag{2.349}$$

Proposition 2.3.1. *Some properties of the Weyl Law:*

1. $R(1/2\delta)$ *is finite if*
$$\int_{-\infty}^{+\infty} \sqrt{u_0(x)}\,\mathrm{d}x < \infty\,. \tag{2.350}$$
2. $R(\zeta_{\max}) = 0$.
3. $R(\zeta)$ *is continuous and decreasing on* $[1/2\delta, \zeta_{\max}]_{\mathcal{Q}_\delta}$ *and differentiable on* $(1/2\delta, \zeta_{\max})_{\mathcal{Q}_\delta}$ *with parameterized derivative*
$$\frac{\mathrm{d}}{\mathrm{d}\kappa}R(\zeta(\kappa)) = -\frac{1}{2}\zeta'(\kappa)\,E'(\zeta(\kappa))\int_{x_-(\zeta(\kappa))}^{x_+(\zeta(\kappa))} r(\zeta(\kappa); u_0(x))\,\mathrm{d}x \tag{2.351}$$
where
$$r(\zeta;u) := \frac{W_0\left(-2\delta\zeta \mathrm{e}^{-2\delta(\zeta+u)}\right)}{1+W_0\left(-2\delta\zeta\mathrm{e}^{-2\delta(\zeta+u)}\right)} - \frac{W_{-1}\left(-2\delta\zeta \mathrm{e}^{-2\delta(\zeta+u)}\right)}{1+W_{-1}\left(-2\delta\zeta\mathrm{e}^{-2\delta(\zeta+u)}\right)} \tag{2.352}$$
defined for all $\zeta \in \mathcal{Q}_\delta$ *and* $u \geq 0$.

Proof. The first property follows from noting that as $\zeta \to 1/2\delta$, $x_\pm(\zeta) \to \pm\infty$. Then plugging in $\zeta = 1/2\delta$ into the integrand, we have simply plugging in $\zeta_{\max}$

$$W_0\left(-\mathrm{e}^{-1-2\delta u_0(x)}\right) - W_{-1}\left(-\mathrm{e}^{-1-2\delta u_0(x)}\right)\,. \tag{2.353}$$

Once more using the series (2.229), we see that for large enough $|x|$, this integrand behaves like $\sqrt{u_0(x)}$, so the condition (2.350) guarantees that this integrand is integrable over $\mathbb{R}$, and thus $R(1/2\delta)$ is finite. On the other hand, for $\zeta = \zeta_{\max}$, $x_\pm(\zeta) = x_{\max}$. Thus, the integral returns zero here.

Let $\zeta < \xi \in [1/2\delta, \zeta_{\max}]_{\mathcal{Q}_\delta}$, then $E(\zeta) < E(\xi)$. Thus, we have after adding $u_0(x)$, multiplying by -2δ, exponentiating and then negating,

$$-2\delta\zeta\mathrm{e}^{-2\delta(\zeta+u_0(x))} < -2\delta\xi\mathrm{e}^{-2\delta(\xi+u_0(x))}\,. \tag{2.354}$$

We also have $x_-(\zeta) < x_-(\xi) < x_+(\xi) < x_+(\zeta)$. Using the fact that W_{-1} and W_0 are monotone

on $(-\mathrm{e}^{-1}, 0)$,

$$W_{-1}\left(-2\delta\zeta \mathrm{e}^{-2\delta(\zeta+u_0(x))}\right) > W_{-1}\left(-2\delta\xi \mathrm{e}^{-2\delta(\xi+u_0(x))}\right), \tag{2.355}$$

$$W_{0}\left(-2\delta\zeta \mathrm{e}^{-2\delta(\zeta+u_0(x))}\right) < W_{0}\left(-2\delta\xi \mathrm{e}^{-2\delta(\xi+u_0(x))}\right), \tag{2.356}$$

for $x_-(\xi) < x < x_+(\xi)$. Additionally, the integrand of $R(\zeta)$ is positive outside of this, we have $R(\zeta) > R(\xi)$. Moreover, everything here is continuous, along with the endpoints of the integration, and we've already shown that this is integrable for all $\zeta \in [1/2\delta, \zeta_{\max}]_{\mathcal{Q}_\delta}$, we get continuity of R.

Lastly, differentiability is inherited from the formulas involved. The derivative of R contains a boundary term from differentiating the endpoints and an integral term from differentiating the integrand. The boundary term is easily shown to be zero, due to the fact that both the $n = -1, 0$ branches return the same value at the turning points. What remains is the integrand. After plugging in the parameterization $\zeta(\kappa)$ and taking the derivative with respect to κ, we have the terms present in $r(\zeta(\kappa); u_0(x))$, along with some extra terms from chain rule and a term from the derivative of Lambert W:

$$\frac{-2\delta + (2\delta)^2\zeta(\kappa)}{-2\delta\zeta(\kappa)}\zeta'(\kappa) = \left(\frac{1}{\zeta(\kappa)} - 2\delta\right)\zeta'(\kappa) \tag{2.357}$$

$$= 2\delta E'(\zeta(\kappa))\zeta'(\kappa)\,. \tag{2.358}$$

Since the terms in $r(\zeta(\kappa); u_0(x))$ have no worse than inverse square-roots at the end points, we collect these terms and get the formula (2.351). □

Since the maximal value $R(1/2\delta) < \infty$, for each $\epsilon > 0$, there is a maximal $N \in \mathbb{Z}$ such that the Weyl Law can be satisfied. This means there are always a finite number of asymptotic approximate eigenvalues, but the total number $N = O(1/\epsilon)$ as $\epsilon \to 0^+$.

Miloh and Minzoni [46] first provided this Weyl law for the eigenvalues of the ILW scattering equation by a similar matching argument, the details of which I've filled in above. Now, we will go a step further and use our constructed approximate formal normalizable eigenfunction to compute the asymptotic form of the normalization constant C_n associated to an approximated eigenvalue ζ_n with eigenfunction Φ. Using the definition (1.20), accounting for the transformations (2.2) and (1.21) and the small dispersion scaling (1.75), we have

$$C_n = \left(\int_{-\infty}^{+\infty} |\Phi(x)|^2 \,\mathrm{d}x\right)^{-1}. \tag{2.359}$$

where the normalization of Φ is chosen so that

$$\lim_{x\to+\infty} \Phi(z)\mathrm{e}^{\mathrm{i}\zeta^* z/\epsilon} = 1\,. \tag{2.360}$$

We can use this normalization condition to fix the final undetermined constant in our matched solution. As $x \to +\infty$, we eventually pass into the right classically forbidden region, and forever after, can use the formal asymptotic solution Φ_0, which was the only one determined to contribute in this region.

$$\begin{aligned}
&\lim_{x\to+\infty} \Phi_0(x+\mathrm{i}y;\zeta,x_+)\mathrm{e}^{\mathrm{i}\zeta^*(x+\mathrm{i}y)/\epsilon} \\
&\quad= \lim_{x\to+\infty} \left(\frac{-2\delta W_0\left(-2\delta\zeta \mathrm{e}^{-2\delta(\zeta+u(x))}\right)}{1+W_0\left(-2\delta\zeta \mathrm{e}^{-2\delta(\zeta+u(x))}\right)}\right)^{1/2} \\
&\qquad\qquad \times \exp\left(-\frac{\mathrm{i}}{\epsilon}\int_{x_+}^{x} G_0^{-1}(u(x');\zeta)\,\mathrm{d}x' + \frac{y}{\epsilon} G_0^{-1}(u(x);\zeta) \right. \\
&\qquad\qquad\qquad \left. + \frac{\mathrm{i}}{\epsilon}\zeta^*(x+\mathrm{i}y) + O(\epsilon) \right) \qquad (2.361) \\
&\quad= \left(\frac{(2\delta)^2\zeta^*}{1-2\delta\zeta^*}\right)^{1/2} \lim_{x\to+\infty} \exp\left(\frac{\mathrm{i}}{\epsilon}\left[\zeta^* x_+(\zeta) + \int_{x_+}^{x} \zeta^* - G_0^{-1}(u(x');\zeta)\,\mathrm{d}x'\right] \right. \\
&\qquad\qquad\qquad \left. - \frac{y}{\epsilon}\big(\zeta^* - G_0^{-1}(u(x);\zeta)\big) + O(\epsilon) \right). \qquad (2.362)
\end{aligned}$$

Because $u_0(x) \to 0$ as $x \to +\infty$, $G_0^{-1}(U;\zeta)$ is differentiable at $U = 0$ for $\zeta \in (1/2\delta,\ \zeta_{\max})$, and $G_0^{-1}(0;\zeta) = \zeta^*$, it follows that

$$G_0^{-1}(U;\zeta) - \zeta^* = O(U) \tag{2.363}$$

for U small enough. Thus, this is integrable as $x \to +\infty$ and we know the limit exists:

$$\begin{aligned}
\lim_{x\to+\infty} \Phi_0(x+\mathrm{i}y;\zeta,x_+)\mathrm{e}^{\mathrm{i}\zeta^*(x+\mathrm{i}y)/\epsilon} &= \left(\frac{(2\delta)^2\zeta^*}{1-2\delta\zeta^*}\right)^{1/2} \\
&\quad \exp\left(\frac{\mathrm{i}}{\epsilon}\left[\zeta^* x_+(\zeta) + \int_{x_+(\zeta)}^{+\infty} \zeta^* - G_0^{-1}(u(x');\zeta)\,\mathrm{d}x'\right]\right) \\
&\quad \times (1 + O(\epsilon))\,. \qquad (2.364)
\end{aligned}$$

In order for the normalization (2.360) to be satisfied for our matched solution, it must be

that

$$F_0^+ = \left(\frac{1-2\delta\zeta^*}{(2\delta)^2\zeta^*}\right)^{1/2} \exp\left(-\frac{\mathrm{i}}{\epsilon}\left[\zeta^* x_+(\zeta) + \int_{x_+(\zeta)}^{+\infty} \zeta^* - G_0^{-1}(u(x');\zeta)\,\mathrm{d}x'\right]\right)(1+O(\epsilon))\,. \tag{2.365}$$

Now, to compute the associated norming constant C_n to an eigenvalue ζ_n, we need to integrate the norm-squared of our matched solution. We do this by focusing on in each of the five regions:

1. *The left classically forbidden region.* Clearly as ϵ shrinks, the exponential here goes to zero faster, and the contribution to the norm-squared out here should limit to zero.

$$\int_{-\infty}^{a_-(\epsilon)} |\Phi_{f-}(x;\zeta_n)|^2\,\mathrm{d}x = |F_{-1}^-|^2 \int_{-\infty}^{a_-(\epsilon)} |\Phi_{-1}(x;\zeta_n,x_-)|^2\,\mathrm{d}x \tag{2.366}$$

where $a_-(\epsilon) = x_-(\zeta_n) - \epsilon^\alpha 2\delta M_\chi^-$. Focusing on bounding the integral, we increase the upper bound to the turning point

$$\int_{-\infty}^{a_-(\epsilon)} |\Phi_{-1}(x;\zeta_n,x_-)|^2\,\mathrm{d}x \le \int_{-\infty}^{x_-(\zeta)} |A_{-1}(u(x),\zeta_n)|^2 \exp\left(\frac{I(x)}{\epsilon}\right)\mathrm{d}x\,, \tag{2.367}$$

where $I_- : (-\infty, x_-(\zeta_n)] \to (-\infty, 0]$ is defined as

$$I_-(x) := \int_{x_-(\zeta)}^{x} \mathrm{Im}\left[W_{-1}\left(-2\delta\zeta_n \mathrm{e}^{-2\delta(\zeta_n+u(x))}\right)\right]\mathrm{d}x'\,. \tag{2.368}$$

Because $\mathrm{Im}\left[W_{-1}\left(-2\delta\zeta_n \mathrm{e}^{-2\delta(\zeta_n+u(x))}\right)\right]$ increases monotonically to $\mathrm{Im}\left[\zeta\right]$ as $x \to -\infty$ and behaves like a square-root near $x = x_-(\zeta_n)$, I_- has a differentiable inverse $I_-^{-1} : (-\infty, 0] \to (-\infty, x_-(\zeta_n)]$ with no worse than an inverse two-thirds-root singularity at zero. Moreover, we saw in the normalization procedure, the integral in the exponent is asymptotic to a line, thus the derivative $1/I_-'(I_-^{-1}(s))$ approaches a constant as $s \to -\infty$. Then we can change variables in our integral:

$$\int_{-\infty}^{a_-(\epsilon)} |\Phi_{-1}(x;\zeta_n,x_-)|^2\,\mathrm{d}x \le \int_{-\infty}^{0} I_-'(I_-^{-1}(s))\left|A_{-1}\Big(u\big(I_-^{-1}(s)\big),\zeta_n\Big)\right|^2 \exp\left(\frac{s}{\epsilon}\right)\mathrm{d}s\,. \tag{2.369}$$

Since $A_n(u(x),\zeta_n)$ has an inverse fourth-root singularity at $x = x_-(\zeta_n)$,

$$I_-'(I_-^{-1}(s))\left|A_{-1}\Big(u\big(I_-^{-1}(s)\big),\zeta_n\Big)\right|^2 = O\left(\frac{1}{(-s)^{2/3}}\right)\,. \tag{2.370}$$

Everywhere else, this is regular and approaches a constant as $s \to -\infty$. Thus, we can apply Watson's Lemma and be assured that

$$\int_{-\infty}^{a_-(\epsilon)} |\Phi_{f-}(x;\zeta_n)|^2 \, \mathrm{d}x = |F_{-1}^-|^2 \, O\left(\epsilon^{1/3}\right) . \tag{2.371}$$

2. *The left transition region.* Again we expect this contribution to be small since as ϵ shrinks, so we look for a bounding argument.

$$\int_{a_-(\epsilon)}^{b_-(\epsilon)} |\Phi_{t-}(x;\zeta_n)|^2 \, \mathrm{d}x = |T_{-\infty}^-|^2 \int_{a_-(\epsilon)}^{b_-(\epsilon)} |\psi_{-\infty}(x;\epsilon,h_-)|^2 \, \mathrm{d}x \tag{2.372}$$

where $b_-(\epsilon) = x_-(\zeta_n) + \epsilon^\alpha 2\delta M_\chi^-$. From (2.306), (2.308) and the matching condition, we have

$$|T_{-\infty}^-|^2 = |F_{-1}^-|^2 \frac{\delta \mathrm{e}^{2\delta u_0(x_-)+1}}{\pi h_- \epsilon^{1-\alpha}} . \tag{2.373}$$

Changing variables in the integral and using the asymptotic formula for $\Phi_{-\infty}$, we have

$$\begin{aligned}\int_{a_-(\epsilon)}^{b_-(\epsilon)} |\Phi_{t-}(x;\zeta_n)|^2 \, \mathrm{d}x = (2\pi)^2 \epsilon^{4/3} 2h_- \int_{-c(\epsilon)}^{c(\epsilon)} \mathrm{Ai}^2\left(s + O\left(\epsilon^\alpha\right)\right) \mathrm{d}s \\ + O\left(\epsilon^{5/3-3\alpha/2}\right) .\end{aligned} \tag{2.374}$$

where $c(\epsilon) = 2\delta M_\chi^- (2h_-)^{1/3}/\epsilon^{2/3-\alpha}$ Splitting the integral over the positive and negative portion, we note the integral of Ai^2 over the positive half-line converges to a constant. Then, focusing on the negative part, we can bound it above by its asymptotic amplitude

$$\int_{-c(\epsilon)}^{0} \mathrm{Ai}^2\left(s + O\left(\epsilon^\alpha\right)\right) \mathrm{d}s \le \int_0^{c(\epsilon)} \frac{\mathrm{d}s}{\pi \left(s + O\left(\epsilon^\alpha\right)\right)^{1/2}} = \frac{\sqrt{c(\epsilon)}}{\pi}(1 + O\left(\epsilon^\alpha\right)) . \tag{2.375}$$

Bringing these all together, we have

$$\int_{a_-(\epsilon)}^{b_-(\epsilon)} |\Phi_{t-}(x;\zeta_n)|^2 \, \mathrm{d}x = |F_{-1}^-|^2 \, O\left(\epsilon^{\alpha/2}\right) . \tag{2.376}$$

3. *The classically allowed region.*

$$\int_{b_-(\epsilon)}^{a_+(\epsilon)} |\Phi_a(x;\zeta_n)|^2 \, \mathrm{d}x = \int_{b_-(\epsilon)}^{a_+(\epsilon)} \left|A_{-1}^- \Phi_{-1}(x;\zeta_n,x_-) + A_0^- \Phi_0(x;\zeta_n,x_-)\right|^2 \mathrm{d}x \tag{2.377}$$

$$= |F_{-1}^-|^2 \int_{b_-(\epsilon)}^{a_+(\epsilon)} |\Phi_{-1}(x;\zeta_n,x_-) - \Phi_0(x;\zeta_n,x_-)|^2 \, \mathrm{d}x \tag{2.378}$$

where $a_+(\epsilon) = x_+(\zeta_n) - \epsilon^\alpha 2\delta M_\chi^+$. We expand the norm-squared.

$$\begin{aligned}
&\int_{b_-(\epsilon)}^{a_+(\epsilon)} |\Phi_{-1}(x;\zeta_n,x_-) - \Phi_0(x;\zeta_n,x_-)|^2 \,\mathrm{d}x \\
&\quad = \int_{b_-(\epsilon)}^{a_+(\epsilon)} |\Phi_{-1}(x;\zeta_n,x_-)|^2 + |\Phi_0(x;\zeta_n,x_-)|^2 \\
&\qquad\qquad - 2\mathrm{Re}\left[\Phi_{-1}(x;\zeta_n,x_-)^*\Phi_0(x;\zeta_n,x_-)\right] \,\mathrm{d}x \quad (2.379) \\
&\quad = \int_{b_-(\epsilon)}^{a_+(\epsilon)} \frac{2\delta W_{-1}(-2\delta\zeta_n \mathrm{e}^{-2\delta(\zeta_n+u_0(x))})}{1+W_{-1}(-2\delta\zeta_n \mathrm{e}^{-2\delta(\zeta_n-u_0(x))})} + \frac{2\delta W_0(-2\delta\zeta_n \mathrm{e}^{-2\delta(\zeta_n+u_0(x))})}{1+W_0(-2\delta\zeta_n \mathrm{e}^{-2\delta(\zeta_n+u_0(x))})} \\
&\qquad - 2\sqrt{\frac{2\delta W_{-1}(-2\delta\zeta_n \mathrm{e}^{-2\delta(\zeta_n+u_0(x))})}{1+W_{-1}(-2\delta\zeta_n \mathrm{e}^{-2\delta(\zeta_n+u_0(x))})}\frac{-2\delta W_0(-2\delta\zeta_n \mathrm{e}^{-2\delta(\zeta_n+u_0(x))})}{1+W_0(-2\delta\zeta_n \mathrm{e}^{-2\delta(\zeta_n+u_0(x))})}} \\
&\qquad\qquad \times \sin\left(\frac{1}{\epsilon}\int_{x_-(\zeta)}^{x} G_{-1}^{-1}(u(x');\zeta_n) - G_0^{-1}(u(x');\zeta_n)\,\mathrm{d}x'\right) \mathrm{d}x \quad (2.380)
\end{aligned}$$

where we used the facts that $-1 \leq 2\delta W_0 < 0$ and $2\delta W_{-1} \leq -1$, with these Lambert W's evaluated as above in the classically allowed region, in order to evaluate the principal square-roots, the magnitudes and real part. From replacing the sine term with one, we see that the integrand is bounded by an inverse square-root at the turning points. This means that if we extend the integration domain to the turning points, the function is integrable here and the error is $O\left(\epsilon^{\alpha/2}\right)$. The sine term then can be bounded with the method of stationary phase similar to the exponential term in case 1, $O\left(\epsilon^{1/3}\right)$. What remains is integrable and constant in ϵ, so we have

$$\begin{aligned}
&\int_{b_-(\epsilon)}^{a_+(\epsilon)} |\Phi_a(x;\zeta_n)|^2 \,\mathrm{d}x \\
&\quad = |F_{-1}^-|^2 \int_{x_-(\zeta_n)}^{x_+(\zeta_n)} \frac{2\delta W_{-1}(-2\delta\zeta_n \mathrm{e}^{-2\delta(\zeta_n+u_0(x))})}{1+W_{-1}(-2\delta\zeta_n \mathrm{e}^{-2\delta(\zeta_n+u_0(x))})} - \frac{2\delta W_0(-2\delta\zeta_n \mathrm{e}^{-2\delta(\zeta_n+u_0(x))})}{1+W_0(-2\delta\zeta_n \mathrm{e}^{-2\delta(\zeta_n+u_0(x))})} \,\mathrm{d}x \\
&\qquad + |F_{-1}^-|^2 O\left(\epsilon^{\alpha/2}\right) . \quad (2.381)
\end{aligned}$$

4. *Right transition region.* Here, the bounding argument works the same as in the left transition region but the coefficient $T_{-\infty}^+$ is connected to the coefficient F_0^+,

$$\int_{a_+(\epsilon)}^{b_+(\epsilon)} |\Phi_{t+}(x;\zeta_n)|^2 \,\mathrm{d}x = |F_0^+|^2 \; O\left(\epsilon^{\alpha/2}\right) , \quad (2.382)$$

where $b_+(\epsilon) = x_+(\zeta_n) + \epsilon^\alpha 2\delta M_\chi^+$.

5. *Right classically forbidden region.* Here, again, the bounding argument works the same

as in the left classically forbidden region but we have the coefficient F_0^+,

$$\int_{b_+(\epsilon)}^{+\infty} |\Phi_{f+}(x;\zeta_n,x_+)|^2 \,\mathrm{d}x = |F_0^+|^2 \, O\left(\epsilon^{1/3}\right) . \tag{2.383}$$

These results, with the fact that

$$|F_{-1}^-|^2 = \left|\exp\left(-\frac{\mathrm{i}}{\epsilon}\int_{x_-}^{x_+} G_0^{-1}(u(x');\zeta)\,\mathrm{d}x'\right) F_0^+\right|^2 = |F_0^+|^2 \tag{2.384}$$

from matching, we can compute the asymptotic form of the norming constants from (2.359).

Proposition 2.3.2.

$$\begin{aligned} C_n = \exp\left(\frac{2}{\epsilon}\theta_+(\zeta_n)\right) &\left|\frac{(2\delta)^2\zeta_n}{1-2\delta\zeta_n}\right| \\ &\times \left(\int_{x_-(\zeta_n)}^{x_+(\zeta_n)} \frac{2\delta W_{-1}(-2\delta\zeta_n \mathrm{e}^{-2\delta(\zeta_n+u_0(x))})}{1+W_{-1}(-2\delta\zeta_n \mathrm{e}^{-2\delta(\zeta_n+u_0(x))})} - \frac{2\delta W_0(-2\delta\zeta_n \mathrm{e}^{-2\delta(\zeta_n+u_0(x))})}{1+W_0(-2\delta\zeta_n \mathrm{e}^{-2\delta(\zeta_n+u_0(x))})}\,\mathrm{d}x\right)^{-1} \\ &\times \left(1+O\left(\epsilon^{\alpha/2}\right)\right) \end{aligned} \tag{2.385}$$

where $\theta_+ : [1/2\delta,\ \zeta_{\max}]_{\mathcal{Q}_\delta} \to \mathbb{R}_+$ *is*

$$\theta_+(\zeta) := \mathrm{Im}\,[\zeta]\, x_+(\zeta) + \int_{x_+(\zeta)}^{+\infty} \mathrm{Im}\left[\zeta + \frac{1}{2\delta} W_{-1}\left(-2\delta\zeta \mathrm{e}^{-2\delta(\zeta+u_0(x))}\right)\right] \mathrm{d}x\,, \tag{2.386}$$

and determines the leading order contribution to $\log C_n$.

Here we will also define the function $\theta_- : [1/2\delta,\ \zeta_{\max}]_{\mathcal{Q}_\delta} \to \mathbb{R}_+$ by

$$\theta_-(\zeta) := \mathrm{Im}\,[\zeta]\, x_-(\zeta) - \int_{-\infty}^{x_-(\zeta)} \mathrm{Im}\left[\zeta + \frac{1}{2\delta} W_{-1}\left(-2\delta\zeta \mathrm{e}^{-2\delta(\zeta+u_0(x))}\right)\right] \mathrm{d}x\,. \tag{2.387}$$

2.4 The Modified Scattering Data

The eigenvalues and the norming constants make up most of the scattering data that Kodama, Ablowitz and Satsuma [27] first laid out for the ILW scattering equation, what remains is the reflection coefficient. This is supposed to be a measure of how much the scattering solutions mix for $\zeta > 1/2\delta$. Since this means that $-2\delta\zeta \mathrm{e}^{-2\delta\zeta} < -\mathrm{e}^{-1}$, then the formal asymptotic solution for all $n \in \mathbb{Z}$ have regular amplitudes for all $x \in \mathbb{R}$ because, as $u_0(x) > 0$

$$-2\delta\zeta \mathrm{e}^{-2\delta(\zeta+u_0(x))} < -\mathrm{e}^{-1}\,. \tag{2.388}$$

This means there is no position to even consider placing turning points, and so no possible way that these solutions can mix. The natural conclusion is that this is a sign the reflection coefficient goes to zero as ϵ shrinks, potentially at a rate beyond all orders in ϵ. However, the way in which the reflection coefficient goes to zero cannot be uniform over all ϵ, because as $\epsilon \to 0^+$, more eigenvalues are added to the potential, looking at our Weyl Law, we see that there should be particular values of ϵ where eigenvalues are "born" at the vertex of the quadratrix, $1/2\delta$. This is a shared point with the continuous spectrum, and, as we will see in the subsequent chapter, the inverse scattering transform with zero reflection coefficient is only well-defined if all of the eigenvalues have nonzero imaginary parts. So the expectation is that when eigenvalues are born, there is nontrivial information being passed from the continuous to discrete spectrums, and the N-soliton formula is a poor approximation to the solution at these values of ϵ. To avoid this issue, we will require that the ϵ we consider for our inverse scattering problem has associated eigenvalues that are always well-separated from the vertex. Since the number of eigenvalues changes discretely, we may as well consider a discrete sequence of ϵ enumerated by the number of eigenvalues. This motivates the following definition:

Definition 2.4.1 (The Modified Scattering Data)**.** *Let $u_0 : \mathbb{R} \to \mathbb{R}^+$ satisfy the conditions laid out at the beginning of* (2.3) *as well as* (2.350)*. We define the sequence $\{\epsilon_N\}_{N\in\mathbb{N}}$ by*

$$\epsilon_N = \frac{R\left(1/2\delta\right)}{(N+1/2)\pi}\,. \tag{2.389}$$

Then we define the set of eigenvalues $\{\zeta_n\}_{n\in\mathbb{Z}_N}$ and associated set of norming constants $\{C_n\}_{n\in\mathbb{Z}_N}$ for ϵ_N to be given by

$$R(\zeta_n) = \pi n \epsilon_N\,, \tag{2.390}$$

$$C_n = \exp\left(-\frac{2}{\epsilon}\theta_+(\zeta_n)\right) \tag{2.391}$$

for all $1 \le n \le N$. Lastly, we take the reflection coefficient to be identically zero.

Note that we have dropped everything but the leading order behavior in ϵ in the definition of our modified scattering data. Because the matching argument did not handle errors in a rigorous way, we cannot make any statements about the small dispersion limit for an exact initial condition. Instead, we content ourselves to study the inverse problem for this modified scattering data, which we expect to be close to the true scattering data as we take the small dispersion limit. This technique has been employed in several analyzes of small dispersion limits before: KdV [34, 35], BO [45, 55], focusing NLS [25], and the sine-Gordon

[9] equations. Verification that the inverse scattering problem on the modified scattering data recovers the same initial condition that was used to generate it provides evidence that the asymptotics are accurate at leading order. This will be shown for the ILW modified scattering data in Chapter 3.

CHAPTER 3

Intermediate Long Wave Equation Inverse Problem for Modified Scattering Data

Superposition, real world wisdom
Everything is moving to the beauty of this system
Total question, fearless reason
We; one; I; many, superposition

King Gizzard and the Lizard Wizard, *Superposition* (2017)

We have chosen our modified spectral data such that the reflection coefficient is identically zero. This means the solution to the small dispersion ILW equation associated with the modified scattering data is described exactly by the N-soliton formula:

$$u_N^{\mathrm{ILW}}(x,t;\epsilon_N) = -\mathrm{i}\epsilon_N\partial_x \ln\det\left(\frac{\mathrm{I}_N + \Delta_N\left(\frac{x}{\epsilon_N} + \mathrm{i}\delta, \frac{t}{\epsilon_N}\right)}{\mathrm{I}_N + \Delta_N\left(\frac{x}{\epsilon_N} - \mathrm{i}\delta, \frac{x}{\epsilon_N}\right)}\right). \tag{3.1}$$

We remind the reader that the N-soliton formula is one of only a few aspects of the ILW IST that rests on rigorous foundation since Matsuno proved that it indeed solves the ILW equation [42] for any distinct set of eigenvalues $\{\zeta_n\}_{n=1}^N$ and associated positive norming constants $\{0 < C_n\}_{n=1}^N$. As $N \to \infty$, $\epsilon_N \to 0^+$, so analyzing the small dispersion limit for the solutions associated to the modified scattering data amounts to studying the behaviour of this determinant as the matrix size grows without bound.

3.1 Expanding the Determinant

We begin this by conducting a "Fredholm-type expansion" of the determinants that appear in the N-soliton solution (3.1) To demonstrate this expansion, let $M \in \mathbb{N}$ and $A \in \mathbb{C}_{M\times M}$

and consider

$$\det\left(\mathrm{I}_M + A\right) = \begin{vmatrix} 1 + A_{1\,1} & A_{1\,2} & \cdots & A_{1\,M} \\ A_{2\,1} & 1 + A_{2\,2} & \cdots & A_{2\,M} \\ \vdots & \vdots & \ddots & \vdots \\ A_{M\,1} & A_{M\,2} & \cdots & 1 + A_{M\,M} \end{vmatrix}. \tag{3.2}$$

We use linearity of the determinant in the first column to expand our determinant into a sum of two: one with the contribution from I_M in the first column and another with the contribution from A in the first column.

$$\det\left(\mathrm{I}_M + A\right) = \begin{vmatrix} 1 & A_{1\,2} & \cdots & A_{1\,M} \\ 0 & 1 + A_{2\,2} & \cdots & A_{2\,M} \\ \vdots & \vdots & \ddots & \vdots \\ 0 & A_{M\,2} & \cdots & 1 + A_{M\,M} \end{vmatrix} + \begin{vmatrix} A_{1\,1} & A_{1\,2} & \cdots & A_{1\,M} \\ A_{2\,1} & 1 + A_{2\,2} & \cdots & A_{2\,M} \\ \vdots & \vdots & \ddots & \vdots \\ A_{M\,1} & A_{M\,2} & \cdots & 1 + A_{M\,M} \end{vmatrix}. \tag{3.3}$$

Now we expand on the second column of each of these determinants. The first matrix will yield a sum of two: both of which will have the first row inherited from I_M, but one with its second row from I_M and the other with its second row from A. likewise, the second determinant above splits into two: both of which will have the first column inherited from A, but one with its second row from I_M and the other with its second row from A.

$$\det\left(\mathrm{I}_M + A\right) = \begin{vmatrix} 1 & 0 & \cdots & A_{1\,M} \\ 0 & 1 & \cdots & A_{2\,M} \\ \vdots & \vdots & \ddots & \vdots \\ 0 & 0 & \cdots & 1 + A_{M\,M} \end{vmatrix} + \begin{vmatrix} 1 & A_{1\,2} & \cdots & A_{1\,M} \\ 0 & A_{2\,2} & \cdots & A_{2\,M} \\ \vdots & \vdots & \ddots & \vdots \\ 0 & A_{M\,2} & \cdots & 1 + A_{M\,M} \end{vmatrix} \tag{3.4}$$

$$+ \begin{vmatrix} A_{1\,1} & 0 & \cdots & A_{1\,M} \\ A_{2\,1} & 1 & \cdots & A_{2\,M} \\ \vdots & \vdots & \ddots & \vdots \\ A_{M\,1} & 0 & \cdots & 1 + A_{M\,M} \end{vmatrix} + \begin{vmatrix} A_{1\,1} & A_{1\,2} & \cdots & A_{1\,M} \\ A_{2\,1} & A_{2\,2} & \cdots & A_{2\,M} \\ \vdots & \vdots & \ddots & \vdots \\ A_{M\,1} & A_{M\,2} & \cdots & 1 + A_{M\,M} \end{vmatrix}. \tag{3.5}$$

Continuing this procedure, it is clear that immediately prior to the column k expansion, the sum occurs over all possible matrices formed by selecting each column less than k to be from either I_M or A, and the remaining columns in each matrix are identical to the original one. After the expansion of the column k, the sum now occurs over all possible matrices formed by selecting each column less than or equal to k to be from either I_M or A, and the remaining columns to be from the original matrix. Following this procedure to its end after M expansions, we have a sum over all matrices formed by selecting every column to be from either I_M or A. Each of these matrices can be associated with a unique subset of $\mathbb{Z}_M$ by

forming the set of column numbers which are inherited from the matrix A. The sum is then conducted over the power set of $\mathbb{Z}_M$.

$$\det\left(\mathrm{I}_M + A\right) = \sum_{S \subset \mathbb{Z}_M} \det(A^S) \tag{3.6}$$

where A^S is the matrix that has for each index in S, the associated column of A, and all other columns from I_M. Now, we simplify some of these determinants once more by noting that performing a Laplace expansion of $\det(A^S)$ on a column which comes from I_M, the only minor which contributes is the one where the column that we expanded on and the associated row are removed. This is due to all other elements in the expanding column being zero. Iteratively Laplace expanding on the columns of A^S which come from I_M, the only minor that survives each step is the one where each expanded column and the associated row have been removed. We write the final minor remaining after all I_M columns have been expanded on as $\mathrm{Minor}_S\left(A\right)$, that is, the minor which only contains the index elements of the set S. Note that $\mathrm{Minor}_{\mathbb{Z}_M}\left(A\right) = A$ and that $\mathrm{Minor}_{\varnothing}\left(A\right)$ would be empty, but this minor would result from expanding the matrix determinant $\det(A^{\varnothing}) = \det(\mathrm{I}_M) = 1$, so we set $\mathrm{Minor}_{\varnothing}\left(A\right) = \left[\,1\,\right]$ to write our final formula simply as:

$$\det\left(\mathrm{I}_M + A\right) = \sum_{S \subset \mathbb{Z}_M} \det\left(\mathrm{Minor}_S\left(A\right)\right) . \tag{3.7}$$

We may now apply this formula to $\det(\mathrm{I}_N + \Delta_N(z/\epsilon_N, t/\epsilon_N))$, for now with any $z \in \mathbb{C}$. We begin by noting that the decomposition of (1.29) extends to the principal minors $\mathrm{Minor}_S\left(\Delta_N(z,t;\epsilon_N)\right)$ since the left and right matrices in the decomposition are diagonal. For any $S \subset \mathbb{Z}_N$,

$$\det \mathrm{Minor}_S\left(\Delta_N\left(\frac{z}{\epsilon_N}, \frac{t}{\epsilon_N}\right)\right) = \det \mathrm{Minor}_S\left(D_N\left(\frac{z}{\epsilon_N}, \frac{t}{\epsilon_N}\right)\right)^2 \det \mathrm{Minor}_S\left(C_N\right) \tag{3.8}$$

$$= \left(\prod_{n \in S} C_n \exp\left(-2\mathrm{Im}\left[\zeta_n\right]\frac{z}{\epsilon_N} - 2\mathrm{Im}\left[\left(\zeta_n - \frac{1}{2\delta}\right)^2\right]\frac{t}{\epsilon_N}\right)\right)$$

$$\times \left(\prod_{n \in S} \frac{1}{2\mathrm{Im}\left[\zeta_n\right]} \prod_{n < \ell \in S} \frac{\left|\zeta_\ell - \zeta_n\right|^2}{\left|\zeta_\ell - \zeta_n^*\right|^2}\right) \tag{3.9}$$

where it is understood that a product over $S = \varnothing$ is one, to be consistent with $\det \mathrm{Minor}_{\varnothing}\left(\diamond\right) = 1$. Since this constituted of several products, it will be useful bring everything into one exponential function. Everything that is not yet written as an exponential is positive, and so there is no issue taking the logarithm. We also plug in the definition of

our norming constants from the modified scattering data (2.391) to get

$$\det \mathrm{Minor}_S \left(\Delta_N \left(\frac{z}{\epsilon_N}, \frac{t}{\epsilon_N} \right) \right) = \exp \left(-2 \sum_{n \in S} \mathrm{Im}\left[\zeta_n\right] \frac{z}{\epsilon_N} + \mathrm{Im}\left[\left(\zeta_n - \frac{1}{2\delta} \right)^2 \right] \frac{t}{\epsilon_N} + 2 \sum_{n \in S} \frac{\theta_+(\zeta_n)}{\epsilon_N} + 2 \sum_{n < \ell \in S} \log \frac{|\zeta_\ell - \zeta_n|}{|\zeta_\ell - \zeta_n^*|} + \sum_{n \in S} \log \left(2\mathrm{Im}\left[\zeta_n\right] \right) \right) . \quad (3.10)$$

Again, we note that sums over $S = \varnothing$ should be taken to be zero. The full determinant $\det(\mathrm{I}_N + \Delta_N(z/\epsilon_N, t/\epsilon_N))$ consists of a sum of these terms over all possible $S \subset \mathbb{Z}_N$. We search for a dominant balance in the exponent and find it by collecting a factor of ϵ_N with every sum over S (i.e. ϵ_N^2 with the double sum). As we take $N \to \infty$, we may then expect that these sums behave like Riemann sums, and limit to an integral. Towards this end, we define for $S \in \mathbb{Z}_N$, the associated point measures in one variable, which we think of as the imaginary part of the quadratrix,

$$\mathrm{d}\mu_S(\kappa) = \epsilon_N \pi \sum_{n \in S} \delta(\kappa - \mathrm{Im}\left[\zeta_n\right]) \, \mathrm{d}\kappa \quad (3.11)$$

for $0 \leq \kappa \leq \kappa_{\max} < \pi/2\delta$ where

$$\kappa_{\max} := \mathrm{Im}\left[\zeta_{\max}\right] , \quad (3.12)$$

δ here is the Dirac-delta unit point measure and $\mathrm{d}\kappa$ is the Lebesgue measure on the line. We also define the associated point measures in two variables where the diagonal between the two variables has been removed

$$\mathrm{d}^2\mu_S^2(\kappa, \eta) = \epsilon_N^2 \pi^2 \sum_{n \neq \ell \in S} \delta(\kappa - \mathrm{Im}\left[\zeta_n\right]) \delta(\eta - \mathrm{Im}\left[\zeta_\ell\right]) \, \mathrm{d}\kappa \, \mathrm{d}\eta \, . \quad (3.13)$$

For ease of notation, we will define several quantities, splitting the real from imaginary contributions. For $x, t \in \mathbb{R}$

$$V(\zeta; x, t) := x \operatorname{Im}[\zeta] + t \operatorname{Im}\left[\left(\zeta - \frac{1}{2\delta}\right)^2\right] - \theta_+(\zeta), \tag{3.14}$$

$$E_{N,S}(x,t) := \int V(\zeta(\kappa); x, t)\, \mathrm{d}\mu_S(\kappa) + \frac{1}{2\pi} \int\int \log\left|\frac{\zeta(\kappa) - \zeta(\eta)^*}{\zeta(\kappa) - \zeta(\eta)}\right| \mathrm{d}^2\mu_S^2(\zeta, \eta), \tag{3.15}$$

$$P_S := \int \kappa\, \mathrm{d}\mu_S(\kappa), \tag{3.16}$$

$$Q_S := \int \operatorname{Im}\left[\left(\zeta - \frac{1}{2\delta}\right)^2\right] \mathrm{d}\mu_S(\kappa). \tag{3.17}$$

Thus, using the notation (3.14), (3.15) and (3.16) to simplify the result (3.10) and then plug this into (3.7) to get an expression for the full determinant $\det(\mathrm{I}_N + \Delta_N(z/\epsilon_N, t/\epsilon_N))$

$$\det\left(\mathrm{I}_N + \Delta_N\left(\frac{z}{\epsilon_N}, \frac{t}{\epsilon_N}\right)\right) = \sum_{S \subset \mathbb{Z}_N} \exp\left(-\frac{2}{\epsilon_N^2 \pi}\big(E_S(\operatorname{Re}[z], t) + \mathrm{i}\operatorname{Im}[z]\, P[\mu_S]\big)\right). \tag{3.18}$$

This is a 2^N term sum which will grow large exponentially fast. Since the real part of the exponent is determined by $E_{N,S}(\operatorname{Re}[z]; x, t)$ with a large negative coefficient, we may expect that the sum will be dominated in some way by the minimal value of $E_{N,S}$ as we take $N \to +\infty$. We will identify the minimum value for each $N \in \mathbb{N}$ and $x, t \in \mathbb{R}$ by

$$\mathrm{e}_N^{\min}(x,t) := \min_{S \subset \mathbb{Z}_N} E_S(x,t). \tag{3.19}$$

We will now prove some bounds on the magnitude of $\det(\mathrm{I}_N + \Delta_N(z/\epsilon_N, t/\epsilon_N))$.

Theorem 3.1.1. *For all $z \in \mathcal{S}_\delta$ and $t \in \mathbb{R}$,*

$$\left[d\left(\frac{\operatorname{Im}[\zeta_{\max}] \operatorname{Im}[z]}{\epsilon_N}\right)\right]^N \leq \left|\det\left(\mathrm{I}_N + \Delta_N\left(\frac{z}{\epsilon_N}, \frac{t}{\epsilon_N}\right)\right)\right| \leq 2^N \exp\left(-\frac{2}{\epsilon_N^2 \pi} \mathrm{e}_N^{\min}(\operatorname{Re}[z], t)\right), \tag{3.20}$$

where the function d is defined in (1.35).

Proof. The right side of (3.20) follows from an application of the triangle inequality and the

fact that $\mathrm{e}_N^{\min}(x,t)$ bounds all of the $E_{N,S}(x,t)$ from below, by its definition:

$$\left|\det\left(\mathrm{I}_N+\Delta_N\left(\frac{z}{\epsilon_N},\frac{t}{\epsilon_N}\right)\right)\right| \leq \sum_{S\subset\mathbb{Z}_N}\left|\exp\left(-\frac{2}{\epsilon_N^2\pi}\left[E_{N,S}(\mathrm{Re}\left[z\right],t)+\mathrm{iIm}\left[z\right]P_{N,S}\right]\right)\right| \tag{3.21}$$

$$= \sum_{S\subset\mathbb{Z}_N}\exp\left(-\frac{2}{\epsilon_N^2\pi}E_{N,S}(\mathrm{Re}\left[z\right],t)\right) \tag{3.22}$$

$$\leq \sum_{S\subset\mathbb{Z}_N}\exp\left(-\frac{2}{\epsilon_N^2\pi}\mathrm{e}_N^{\min}(\mathrm{Re}\left[z\right],t)\right) \tag{3.23}$$

$$= 2^N\exp\left(-\frac{2}{\epsilon_N^2\pi}\mathrm{e}_N^{\min}(\mathrm{Re}\left[z\right],t)\right). \tag{3.24}$$

Note that this upper bound is independent of $\mathrm{Im}\left[z\right]$. The left side of (3.20) comes from applying Lemma 1.2.1 which gives us the lower bound in magnitude

$$\left[d\left(\frac{\pi\mathrm{Im}\left[z\right]}{\epsilon_N h_N}\right)\right]^N \leq \left|\det\left(\mathrm{I}_N+\Delta_N\left(\frac{z}{\epsilon_N},\frac{t}{\epsilon_N}\right)\right)\right| \tag{3.25}$$

for all $z/\epsilon_N\in\mathcal{S}_\delta$ where $h_N>0$ is given by

$$h_N := \frac{\pi}{2\max\limits_{1\leq n\leq N}\mathrm{Im}\left[\zeta_n\right]}. \tag{3.26}$$

The modified spectral data has, for all $N\in\mathbb{N}$, a fixed $\zeta_{\max}\in\mathcal{Q}_{\delta+}$ such that

$$\max_{1\leq n\leq N}\mathrm{Im}\left[\zeta_n\right] < \mathrm{Im}\left[\zeta_{\max}\right] < \frac{\pi}{2\delta}. \tag{3.27}$$

Multiplying through by $2/\pi$ gives

$$\frac{2\max\limits_{1\leq n\leq N}\mathrm{Im}\left[\zeta_n\right]}{\pi} < \frac{2\mathrm{Im}\left[\zeta_{\max}\right]}{\pi} < \frac{1}{\delta}. \tag{3.28}$$

And lastly, inverting the above formula, defining the fixed height

$$h = \frac{\pi}{2\mathrm{Im}\left[\zeta_{\max}\right]} \tag{3.29}$$

and using the definition of h_N, we have

$$\delta < h < h_N. \tag{3.30}$$

From the definition of d (1.35), it is clear that

$$d\left(\frac{\pi\left|\mathrm{Im}\left[z\right]\right|}{\epsilon_N h}\right) \leq d\left(\frac{\pi\left|\mathrm{Im}\left[z\right]\right|}{\epsilon_N h_N}\right) \tag{3.31}$$

for all $|\mathrm{Im}\left[z\right]| \leq \epsilon_N h$, which means after applying this to (3.25), we have the lower bound in (3.20) for all $z \in \mathcal{S}_{\epsilon_N \delta}$. □

3.2 From Discrete Minimizing Subset to Continuous Minimizing Distribution

Looking again at the definitions of (3.14), (3.15) and (3.16), we remark on a physical interpretation to these quantities. Noting that $-\log|\zeta - \xi|$ for $\zeta, \xi \in \mathbb{C}$ is the Green's function of the Laplacian in two dimensions, we might identify this physically as the Coulomb potential between two like charges located at ζ and η in the plane. The addition of the term $\log|\zeta - \xi^*|$ is then a Coulomb interaction between different signed charges at ζ and ξ^*, which is reflected across the real axis from ξ. Together, through the method of images, these constitute the Coulomb interaction of two like charges in the presence of a perfect conductor on the real axis. The double integral term involving this logarithmic kernel and the point measures computes the total potential energy between ϵ_N-proportional charges which sit at the sites along the upper half of the quadratrix determined by the set of eigenvalues $\{\zeta_n\}_{n=1}^N$ and the particular subset $S \in \mathbb{Z}_N$. The single integral term in $E_{N,S}(x,t)$ (3.15) can then be viewed as interaction between the charges and an external applied field $V(\zeta; x, t)$ (3.14) which is dependent on parameters $x, t \in \mathbb{R}$. Lastly, for real values of $z \in \mathbb{R}$, we note that the expansion of $\det\left(\mathrm{I}_N + \Delta_N\left(z/\epsilon_N, t/\epsilon_N\right)\right)$ in (3.20) represents a statistical partition function for the system in thermal equilibrium with a heat bath of temperature $k_\mathrm{b}T = \pi\epsilon_N^2/2$ and where the statistical ensemble includes all possible single charge populations of the lattice sites $\{\zeta_n\}_{n=1}^N$.

From a physical perspective, we would then expect that as we take $N \to +\infty$, and the charge sites become more densely packed along the upper quadratrix, the discrete charge distributions involved may start approximating "continuous" charge densities. Continuous in the sense that a continuum of position is now available to be occupied by charge, the actual function representation of the densities that are approximated, obviously, may not be continuous. The description of these continuous densities was laid out for the small dispersion limit of the KdV equation by Lax and Levermore [34, Section 2]. We can use the very same mathematical machinery that they developed, with a few small modifications, for

the ILW equation's small dispersion limit.

Theorem 3.2.1. *The measures $\mu_S(\kappa)$ for all $S \subset \mathbb{Z}_N$ and $N \in \mathbb{N}$ have uniform bounded variation. Moreover $\{\mu_{\mathbb{Z}_N}(\kappa)\}_{N=1}^{\infty}$, i.e. the measures where all sites are populated with charges, have the weak limit, i.e. integration against continuous functions,*

$$\mathrm{w}-\lim_{N\to+\infty} \mu_{\mathbb{Z}_N}(\kappa) = \rho^{\mathrm{Wyl}}(\kappa) := -\frac{\mathrm{d}}{\mathrm{d}\kappa} R(\zeta(\kappa)) \tag{3.32}$$

where R is the Weyl law (2.348).

Proof. First, the measures $\mu_S(\kappa)$ are nonnegative, and we have the clear bound

$$\int \mu_S(\kappa)\mathrm{d}\kappa \leq \int \mu_{\mathbb{Z}_N}(\kappa)\mathrm{d}\kappa = \epsilon_N \pi N \leq R\left(\frac{1}{2\delta}\right) < \infty\,, \tag{3.33}$$

where we used the definition of the modified scattering data (2.390) and the properties of the Weyl law in Proposition 2.3.1. Now let $f : [0, \kappa_{\max}] \to \mathbb{R}$ be a continuous function. We want to show the limit of $\mu_{\mathbb{Z}_N}(\kappa)$ as $N \to +\infty$ integrated against f matches the integral of $\rho^{\mathrm{Wyl}}(\kappa)$ against f. This can be done by using $r = R(\zeta(\kappa))$ to change variables, letting $R^{-1}(r) = \kappa$ denote the inverse. Because the the point masses of $\mu_{\mathbb{Z}_N}(\kappa)$ are chosen by the Weyl law, we have

$$\int f(\kappa)\,\mathrm{d}\mu_{\mathbb{Z}_N}(\kappa) = \epsilon_N \pi \sum_{n=1}^{N} f(\mathrm{Im}\,[\zeta_n]) \tag{3.34}$$

$$= \epsilon_N \pi \sum_{n=1}^{N} f(R^{-1}(\epsilon_N \pi n))\,. \tag{3.35}$$

This is exactly the right endpoint Riemann sum approximate to the integral

$$\int_0^{R(1/2\delta)} f(R^{-1}(r))\mathrm{d}r = -\int_0^{\kappa_{\max}} f(\kappa)\frac{\mathrm{d}}{\mathrm{d}\kappa} R(\zeta(\kappa))\,\mathrm{d}\kappa = \int_0^{\kappa_{\max}} f(\kappa)\rho^{\mathrm{Wyl}}(\kappa)\,\mathrm{d}\kappa\,. \tag{3.36}$$

Because this is integrable and the integrands are continuous, we know that the right endpoint Riemann sum limits to the integral, and thus,

$$\lim_{N\to+\infty} \int f(\kappa)\,\mathrm{d}\mu_{\mathbb{Z}_N}(\kappa) = \int_0^{\kappa_{\max}} f(\kappa)\rho^{\mathrm{Wyl}}(\kappa)\,\mathrm{d}\kappa\,. \tag{3.37}$$

□

Knowing that the discrete measures have lower and upper bounds which have limits as $N \to +\infty$, we can define the admissible set of continuous charge densities as the set of

measurable functions

$$\mathcal{A} := \left\{ \rho \;\middle|\; \rho \text{ where } \rho \text{ is a measurable function and } 0 \leq \rho \leq \rho^{\mathrm{Wyl}} \right\}. \tag{3.38}$$

Since $\rho^{\mathrm{Wyl}}\,\mathrm{d}\kappa$ as a measure has trivially bounded variation

$$\int_0^{\kappa_{\max}} \rho^{\mathrm{Wyl}}(\kappa)\,\mathrm{d}\kappa = R\left(\frac{1}{2\delta}\right) < \infty\,, \tag{3.39}$$

each $\rho \in \mathcal{A}$ has an associated measure $\rho\mathrm{d}\kappa$ with uniformly bounded variation. We can define now the continuous versions of the Coulomb potential for a charge distribution $\rho \in \mathcal{A}$,

$$L\{\rho\}(\zeta(\kappa)) := \frac{1}{\pi}\int_0^{\kappa_{\max}} \log\left|\frac{\zeta(\kappa)-\zeta(\eta)^*}{\zeta(\kappa)-\zeta(\eta)}\right| \rho(\eta)\,\mathrm{d}\eta\,, \tag{3.40}$$

as well as the total energy,

$$E\{\rho\}(x,t) := \int_0^{\kappa_{\max}} \left(V(\zeta(\kappa);x,t)\ \rho(\kappa) + \frac{1}{2}L\{\rho\}(\zeta(\kappa))\right)\ \rho(\kappa)\,\mathrm{d}\kappa\,, \tag{3.41}$$

and finally the dipole as well,

$$P\{\rho\} := 2\delta \int \kappa\ \rho(\kappa)\,\mathrm{d}\kappa\,. \tag{3.42}$$

We note that the logarithmic kernel of L is positive, has no worse than a logarithmic singularity when $\kappa = \eta$ and that

Theorem 3.2.2. *$L\{\rho^{\mathrm{Wyl}}\}$ is continuous on the upper half-plane and takes the value*

$$L\{\rho^{\mathrm{Wyl}}\}(\zeta(\kappa)) = \theta_+(\kappa) - \theta_-(\kappa) \tag{3.43}$$

on the interval along the quadratrix parameterized by $\kappa \in [0, \kappa_{\max}]$. Additionally,

$$0 \leq L\{\rho\}(\zeta) \leq L\{\rho^{\mathrm{Wyl}}\}(\zeta) \tag{3.44}$$

for all $\rho \in \mathcal{A}$ and ζ in the upper half-plane.

The proof of the first statement is presented with the proof of Corollary 3.4.4.1. The second statement follows trivially from noticing that the kernel of L is positive on the upper half-plane as well as the bounds on $\rho \in \mathcal{A}$. From these properties, making the appropriate adjustments to [34, Theorem 2.2], we have

Theorem 3.2.3.

$$\lim_{N\to+\infty} E_N^{\min}(x,t) = \mathrm{e}_\infty^{\min}(x,t) \tag{3.45}$$

uniformly on compact subsets in spacetime where

$$\mathrm{e}_\infty^{\min}(x,t) := \min_{\rho\in\mathcal{A}} E\{\rho\}(x,t)\,. \tag{3.46}$$

That is to say, the limit of the discrete minimal energies is equal to the minimum energy over the continuous charge densities in $\mathcal{A}$. Should the reader want an in depth explanation of these proofs, we direct their attention to Levermore's own dissertation [37, Chapter 2].

3.3 The Distributional Limit of the Solution

We will define some new quantities from statistical mechanics for ease of notation based on the physical interpretation of the ensemble of electric charge densities: the (complex) partition function

$$\begin{aligned} Z_N(z,t) &:= \det\left(\mathrm{I}_N + \Delta_N\left(\frac{z}{\epsilon_N},\frac{t}{\epsilon_N}\right)\right) \\ &= \sum_{S\subset\mathbb{Z}_N} \exp\left(-\frac{2}{\epsilon_N^2\pi}\Big[E_S(\mathrm{Re}\,[z]\,,t;\epsilon_N) + \mathrm{iIm}\,[z]\,P[\mu_S]\Big]\right) \end{aligned} \tag{3.47}$$

and the (complex) Helmholtz free energy

$$F_N(z,t) := 2\delta\epsilon_N^2 \ln Z_N(z,t) = 2\delta\epsilon_N^2 \ln\det\left(\mathrm{I}_N + \Delta_N\left(\frac{z}{\epsilon_N},\frac{t}{\epsilon_N}\right)\right)\,. \tag{3.48}$$

Then the ILW N-soliton solution with the modified spectral data can be written as

$$u_N^{\mathrm{ILW}}(x,t) = \partial_x D_{\mathrm{i}\delta\epsilon_N} F_N(x,t)\,, \tag{3.49}$$

where $D_{\mathrm{i}\delta\epsilon_N}$ is the symmetric, finite-difference operator

$$D_{\mathrm{i}\delta\epsilon_N} F_N(x,t) := \frac{F_N(x+\mathrm{i}\delta\epsilon_N,t) - F_N(x-\mathrm{i}\delta\epsilon_N,t)}{\mathrm{i}2\delta\epsilon_N}\,. \tag{3.50}$$

Theorem 3.3.1. *The distributional limit of the ILW solution with modified scattering data is given by*

$$\mathrm{d}-\lim_{N\to\infty} u_N^{\mathrm{ILW}}(x,t) = -\frac{4\delta}{\pi}\partial_x^2 \mathrm{e}_\infty^{\min}(x,t) \tag{3.51}$$

where $\mathrm{e}_\infty^{\min}(x,t)$ *is defined in* (3.46).

Proof. We will prove the distributional limit from definition, let $\chi \in \mathcal{C}_0^\infty(\mathbb{R}^2)$ and let $K \subset \mathbb{R}^2$ be a compact spacetime support of χ, then there is a closed ball of radius $R > 0$ and center (x_0, t_0), $\mathcal{B}_R(x_0, t_0)$, that contains K. We then let $\chi : \mathcal{B}_R(x_0, t_0) \to \mathbb{C}$ be a C^∞ function such that χ and its x-derivative χ_x vanish on the boundary. Then, for $|t - t_0| \leq R$, we can define the x-endpoints on the boundary as $a_\pm(t) = x_0 \pm \sqrt{R^2 - (t - t_0)^2}$ and consider the solution $u_N^{\mathrm{ILW}}(x,t)$ integrated against χ in x:

$$\int_{a_-(t)}^{a_+(t)} \chi(x,t)\ u_N^{\mathrm{ILW}}(x,t)\,\mathrm{d}x = \int_{a_-(t)}^{a_+(t)} \chi(x,t)\ \partial_x D_{\mathrm{i}\delta\epsilon_N} F_N(x,t)\,\mathrm{d}x\,. \tag{3.52}$$

Moving the derivative onto χ is a standard invoking of integration-by-parts:

$$\begin{aligned}\int_{a_-(t)}^{a_+(t)} \chi(x,t)\ u_N^{\mathrm{ILW}}(x,t)\,\mathrm{d}x &= \Big[\chi(x,t) D_{\mathrm{i}\delta\epsilon_N} F_N(x,t)\Big]_{a_-(t)}^{a_+(t)} \\ &\qquad - \int_{a_-(t)}^{a_+(t)} \chi_x(x,t)\ D_{\mathrm{i}\delta\epsilon_N} F_N(x,t)\,\mathrm{d}x \qquad (3.53)\\ &= -\int_{a_-(t)}^{a_+(t)} \chi_x(x,t)\ D_{\mathrm{i}\delta\epsilon_N} F_N(x,t)\,\mathrm{d}x\,. \qquad (3.54)\end{aligned}$$

The boundary term here is zero by assumption: $\chi(a_\pm(t), t) = 0$. Dealing with the finite difference is much trickier. We will exploit the fact that the difference is shrinking with ϵ_N and using a near analytic extension of χ to get our bounds. First, define $\phi_+ : \mathcal{B}_R(x_0, t_0) \times [0, \delta\epsilon_N] \to \mathbb{C}$ by

$$\phi_+(x,t,y) := \chi_x(x,t) + \mathrm{i}(y - \delta\epsilon_N)\chi_{xx}(x,t)\,. \tag{3.55}$$

Then, note that from a generalization of Cauchy's theorem

$$\int_{C(t)} \phi_+(x,t,y)\ F_N(x + \mathrm{i}y, t)\,\mathrm{d}(x + \mathrm{i}y) = \int_{a_-(t)}^{a_+(t)} \int_0^{\delta\epsilon_N} \overline{\partial}_{x+\mathrm{i}y}\big(\phi_+(x,t,y)\ F_N(x + \mathrm{i}y, t)\big)\,\mathrm{d}x\mathrm{d}y \tag{3.56}$$

with $C(t)$ being the boundary of the rectangle of integration on the left-hand side oriented positively. Since F_N is analytic, which follows from Theorem 3.1.1 where the determinant was shown to be nonzero for all $|y| \leq \delta\epsilon_N$, we have that $\overline{\partial}_{x+\mathrm{i}y}$ on F_N is zero, so product rule

gives

$$\overline{\partial}_{x+\mathrm{i}y}\big(\phi_+(x,t,y)\ F_N(x+\mathrm{i}y,t)\big) = F_N(x+\mathrm{i}y,t)\ \left(\frac{\partial}{\partial x}+\mathrm{i}\frac{\partial}{\partial y}\right)\phi_+(x,t,y) \tag{3.57}$$

$$= F_N(x+\mathrm{i}y,t)\ \left(\chi_{xx}(x,t)+\mathrm{i}(y-\delta\epsilon_N)\chi_{xxx}(x,t)-\chi_{xx}(x,t)\right) \tag{3.58}$$

$$= \mathrm{i}(\delta\epsilon_N - y)\chi_{xxx}(x,t)\ F_N(x+\mathrm{i}y,t)\,. \tag{3.59}$$

Since χ is $\mathcal{C}^\infty$, there is a maximum magnitude of $|\chi_{xxx}|$ on $\mathcal{B}(x_0,t_0)$, call it $M_{\chi,3}\geq 0$. Let us also introduce the sup-norm bound of F_N (equivalent to the maximum since F_N is continuous from its definition) on a y-symmetric region

$$M_{F_N} := \max_{\substack{(x,t)\in\mathcal{B}_R(x_0,t_0)\\ y\in[-\delta\epsilon_N,\delta\epsilon_N]}} |F_N(x+\mathrm{i}y,t)|\,. \tag{3.60}$$

Thus, inserting (3.59) into the integrand of the right side of (3.56), we have the bound of the integral over the rectangular area

$$\left|\int_{a_-(t)}^{a_+(t)}\int_0^{\delta\epsilon_N}\overline{\partial}_{x+\mathrm{i}y}\big(\phi_+(x,t,y)\ F_N(x+\mathrm{i}y,t)\big)\,\mathrm{d}x\mathrm{d}y\right|$$

$$\leq \big(a_+(t)-a_-(t)\big)M_{\chi,3}M_{F_N}\int_0^{\delta\epsilon_N}|\delta\epsilon_N-y|\mathrm{d}y \tag{3.61}$$

$$\leq \frac{\delta^2\epsilon_N^2}{2}RM_{\chi,3}M_{F_N}\,. \tag{3.62}$$

Now let us consider the contour integral on the left side of (3.56) by parameterization:

$$\int_{C(t)}\phi_+(x,t,y)\ F_N(x+\mathrm{i}y,t)\,\mathrm{d}(x+\mathrm{i}y)$$

$$\begin{aligned}
&= \int_{a_-(t)}^{a_+(t)}\phi_+(x,t,0)\ F_N(x,t)\,\mathrm{d}x\\
&\quad+\int_0^{\delta\epsilon_N}\phi_+(a_+(t),t,y)\ F_N(a_+(t)+\mathrm{i}y,t)\ \mathrm{i}\mathrm{d}y\\
&\quad+\int_{a_+(t)}^{a_-(t)}\phi_+(x,t,\delta\epsilon_N)\ F_N(x+\mathrm{i}\delta\epsilon_N,t)\,\mathrm{d}x\\
&\quad+\int_{\delta\epsilon_N}^{0}\phi_+(a_-(t),t,y)\ F_N(a_-(t)+\mathrm{i}y,t)\ \mathrm{i}\mathrm{d}y
\end{aligned} \tag{3.63}$$

where the integrals on the right side of the equal sign represent the bottom horizontal, the

right vertical, the top horizontal and the left vertical, respectively. We plug in the form of ϕ_+ (3.55) and simplify,

$$\begin{aligned}\int_{C(t)} \phi_+(x,y,t)\ F_N(x+\mathrm{i}y,t)\,\mathrm{d}(x+\mathrm{i}y) \\ &= \int_{a_-(t)}^{a_+(t)} \big(\chi_x(x,t) - \mathrm{i}\delta\epsilon_N \chi_{xx}(x,t)\big)\ F_N(x,t)\,\mathrm{d}x \\ &\quad - \int_{\delta\epsilon_N}^{0} (y-\delta\epsilon_N)\chi_{xx}(a_+(t),t)\ F_N(a_+(t)+\mathrm{i}y,t)\,\mathrm{d}y \\ &\quad - \int_{a_-(t)}^{a_+(t)} \chi_x(x,t)\ F_N(x+\mathrm{i}\delta\epsilon_N,t)\,\mathrm{d}x \\ &\quad + \int_{0}^{\delta\epsilon_N} (y-\delta\epsilon_N)\chi_{xx}(a_-(t),t)\ F_N(a_-(t)+\mathrm{i}y,t)\,\mathrm{d}y \end{aligned} \tag{3.64}$$

where the χ_x terms disappeared in the vertical segments due to the boundary conditions $\chi_x(a_\pm(t),t)=0$. Because of this vanishing, the vertical segments can be bounded much like the rectangular integral in (3.62):

$$\left|\int_0^{\delta\epsilon_N} (\delta\epsilon_N - y)\chi_{xx}(a_\pm(t),t)\ F_N(a_\pm(t)+\mathrm{i}y,t)\,\mathrm{d}y\right| \le \frac{\delta^2\epsilon_N^2}{2} M_{\chi,2} M_{F_N} \tag{3.65}$$

where $M_{\chi,2}$ is a uniform bound on $|\chi_{xx}|$ over $\mathcal{B}_R(x_0,t_0)$. Now, we do the exact same exercise but for a rectangle in the lower half-plane and for a function $\phi_- : \mathcal{B}_R(x_0,t_0)\times[-\delta\epsilon_N,0]\to\mathbb{C}$ defined by

$$\phi_-(x,t,y) := \chi_x(x,t) + \mathrm{i}(y+\delta\epsilon_N)\chi_{xx}(x,t)\,. \tag{3.66}$$

This gives identical bounds since the bounds on χ were y-independent and the bound on F_N was chosen to be on the y-symmetric rectangle. The bounds on the rectangular area (3.62) and the vertical components (3.65) along with the equalities (3.56) and (3.64) shows that the remaining unbounded horizontal components of the upper and lower half-plane rectangles must limit to zero as $N\to+\infty$. Subtracting these remaining horizontal integral terms and dividing by $\mathrm{i}2\delta\epsilon_N$ lets us assemble an approximation for the integral with the finite difference

in (3.54):

$$\frac{1}{\mathrm{i}2\delta\epsilon_N}\left(\int_{a_-(t)}^{a_+(t)}\chi_x(x,t)\ F_N(x+\mathrm{i}\delta\epsilon_N,t)\,\mathrm{d}x-\int_{a_-(t)}^{a_+(t)}\Big(\chi_x(x,t)-\mathrm{i}\delta\epsilon_N\chi_{xx}(x,t)\Big)\ F_N(x,t)\,\mathrm{d}x\right.$$
$$\left.-\int_{a_-(t)}^{a_+(t)}\chi_x(x,t)\ F_N(x-\mathrm{i}\delta\epsilon_N,t)\,\mathrm{d}x+\int_{a_-(t)}^{a_+(t)}\Big(\chi_x(x,t)+\mathrm{i}\delta\epsilon_N\chi_{xx}(x,t)\Big)\ F_N(x,t)\,\mathrm{d}x\right)$$
$$=\int_{a_-(t)}^{a_+(t)}\chi_x(x,t)\ D_{\mathrm{i}\delta\epsilon_N}F_N(x,t)\,\mathrm{d}x+\int_{a_-(t)}^{a_+(t)}\chi_{xx}(x,t)\ F_N(x,t)\,\mathrm{d}x\,. \tag{3.67}$$

Nearly there, we combine our first integration-by-parts result (3.54) with (3.67) get our first approximation to the integral of $u_N^{\mathrm{ILW}}(x,t)$ against χ:

$$\left|\int_{a_-(t)}^{a_+(t)}\chi(x,t)\ u_N^{\mathrm{ILW}}(x,t)\,\mathrm{d}x-\int_{a_-(t)}^{a_+(t)}\chi_{xx}(x,t)\ F_N(x,t)\,\mathrm{d}x\right|$$
$$=\left|\int_{a_-(t)}^{a_+(t)}\chi_x(x,t)\ D_{\mathrm{i}\delta\epsilon_N}F_N(x,t)\,\mathrm{d}x+\int_{a_-(t)}^{a_+(t)}\chi_{xx}(x)\ F_N(x,t)\,\mathrm{d}x\right| \tag{3.68}$$
$$\leq\frac{\delta\epsilon_N}{2}\Big(RM_{\chi,3}+M_{\chi,2}\Big)M_{F_N}\,. \tag{3.69}$$

We note that, through a somewhat more arduous bounding process, in which integrals from the upper and lower half-plane rectangles are matched and subtracted from each other, two additional powers of ϵ_N may be gained in (3.68) through the use of Lemma 1.2.1. However, these are not particularly needed in the following analysis, so we leave it as a homework problem for the interested reader.

We split F_N into real and imaginary parts

$$\mathrm{Re}\left[F_N(x+\mathrm{i}y,t)\right]=2\delta\epsilon_N^2\ln\left|Z_N(x+\mathrm{i}y,t)\right|\,, \tag{3.70}$$
$$\mathrm{Im}\left[F_N(x+\mathrm{i}y,t)\right]=2\delta\epsilon_N^2\arg\left(Z_N(x+\mathrm{i}y,t)\right)\,, \tag{3.71}$$

and then applying Theorem 3.1.1, noting that $0<d(2\delta\mathrm{Im}\left[\zeta_{\max}\right])\leq d(2\mathrm{Im}\left[\zeta_{\max}\right]y/\epsilon_N)$ for all $|y|\leq\delta\epsilon_N$, and (1.36) from Lemma 1.2.1 to the right sides of the above equalities, we have the bounds on the real and imaginary parts of F_N

$$2\delta\epsilon_N^2N\ln d(2\delta\mathrm{Im}\left[\zeta_{\max}\right])\leq\mathrm{Re}\left[F_N(x+\mathrm{i}y,t)\right]\leq-\frac{4\delta}{\pi}\mathrm{e}_N^{\min}(x,t)+2\delta\epsilon_N^2N\ln 2\,, \tag{3.72}$$
$$0\leq\left|\mathrm{Im}\left[F_N(x+\mathrm{i}y,t)\right]\right|\leq4\delta^2\epsilon_N^2N\mathrm{Im}\left[\zeta_{\max}\right]\,. \tag{3.73}$$

As $N\to+\infty$, all of terms in these bounds limit to zero independent of x,t except for

the term $-4\delta/\pi\ \mathrm{e}_N^{\min}(x,t)$. Indeed, the terms $\epsilon_N^2 N$ present in all three tend to zero, by the construction of ϵ_N (2.389). $\mathrm{e}_N^{\min}(x,t)$, due to Theorem 3.2.3, has a uniform limit on $\mathcal{B}_R(x_0,t_0)$. Since its real and imaginary parts have uniform bounds, so too does $|F_N|$ and hence M_{F_N}. This shows that the bound in (3.69) tends to zero as $N \to +\infty$.

Lastly, since we now only have F_N evaluated at $x \in \mathbb{R}$ in our first approximation to the integral of $u_N^{\mathrm{ILW}}(x,t)$ against χ, we can establish a tighter lower bound than (3.72), relying directly on the fact that $Z_N(x,t)$ (3.47) is a sum of positive terms:

$$
\begin{aligned}
F_N(x,t) &= 2\delta\epsilon_N^2 \ln\big(Z_N(x,t)\big) && (3.74)\\
&= 2\delta\epsilon_N^2 \ln\left[\sum_{S\subset\mathbb{Z}_N} \exp\left(-\frac{2}{\epsilon_N^2\pi}E_S(x,t)\right)\right] && (3.75)\\
&\geq 2\delta\epsilon_N^2 \ln\left[\exp\left(-\frac{2}{\epsilon_N^2\pi}E_N^{\min}(x,t)\right)\right] && (3.76)\\
&\geq -\frac{4\delta}{\pi}E_N^{\min}(x,t)\,. && (3.77)
\end{aligned}
$$

This with the upper bound from (3.72) yields the double bound

$$
0 \leq F_N(x,t) + \frac{4\delta}{\pi}E_N^{\min}(x,t) \leq 2\delta\epsilon_N^2 N \ln 2\,. \tag{3.78}
$$

By the sandwich theorem, we have that $F_N(x,t) \to -4\delta/\pi\ E_N^{\min}(x,t)$ uniformly in x and t as $N \to +\infty$. Considering

$$
\begin{aligned}
&\left|\int_{a_-(t)}^{a_+(t)} \chi(x,t)\ u_N^{\mathrm{ILW}}(x,t)\,\mathrm{d}x + \int_{a_-(t)}^{a_+(t)} \chi_{xx}(x,t)\ \frac{4\delta}{\pi}\mathrm{e}_\infty^{\min}(x,t)\,\mathrm{d}x\right| \\
&\qquad\leq \left|\int_{a_-(t)}^{a_+(t)} \chi(x,t)\ u_N^{\mathrm{ILW}}(x,t)\,\mathrm{d}x - \int_{a_-(t)}^{a_+(t)} \chi_{xx}(x,t)\ F_N(x,t)\,\mathrm{d}x\right| \\
&\qquad\quad + \left|\int_{a_-(t)}^{a_+(t)} \chi_{xx}(x,t)\ \left(F_N(x,t) + \frac{4\delta}{\pi}\mathrm{e}_N^{\min}(x,t)\right)\,\mathrm{d}x\right| \\
&\qquad\quad + \left|\frac{4\delta}{\pi}\int_{a_-(t)}^{a_+(t)} \chi_{xx}(x,t)\ \big(\mathrm{e}_N^{\min}(x,t) - \mathrm{e}_\infty^{\min}(x,t)\big)\,\mathrm{d}x\right| && (3.79)\\
&\qquad\leq \frac{\delta\epsilon_N}{2}\Big(RM_{\chi,3} + M_{\chi,2}\Big)M_{F_N} \\
&\qquad\quad + M_{\chi,2}\int_{a_-(t)}^{a_+(t)} \left|F_N(x,t) + \frac{4\delta}{\pi}\mathrm{e}_N^{\min}(x,t)\right| + \frac{4\delta}{\pi}\big|\mathrm{e}_N^{\min}(x,t) - \mathrm{e}_\infty^{\min}(x,t)\big|\,\mathrm{d}x\,, && (3.80)
\end{aligned}
$$

where in the first step we added and subtracted terms and split using the triangle identity, then in the second step we bounded the first term on the right in (3.79) using (3.69) and the next two terms by the triangle inequality for integrals. Lastly, we have that the first term in (3.80) tends to zero since M_{F_N} is uniformly bounded by (3.72) and (3.73) while the second term also tends to zero by (3.78) and Theorem 3.2.3. Since $\chi \in \mathcal{C}_0^\infty$ was arbitrary, this proves that the limit of $u_N^{\mathrm{ILW}}(x,t)$ coincides with $-4\delta/\pi\ \partial_x^2 \mathrm{e}_\infty^{\min}(x,t)$ in a distributional sense. □

Theorem 3.3.1 demonstrates two important qualities of the ILW small dispersion solution: first that the finite difference in the N-soliton solution between the two edges of the strip $\mathcal{S}_{\delta\epsilon_N}$ can be approximated in a distributional sense by ϵ_N times a derivative on the center of the strip as $\epsilon_N \to 0^+$, as one might expect. And second, the limit of the Helmholtz free energy of the electrostatic ensemble as $k_{\mathrm{b}}T = \pi\epsilon_N^2/2 \to 0^+$ is dominated by the minimal energy configuration of the admissible continuous charge distributions. The energy minimizing charge density can also be thought of as the one that establishes an equilibrium between the coulomb interaction and the external applied electric field. It is interesting that, according to Theorem 3.3.1, the energy associated to this equilibrium charge density directly determines the ILW small dispersion solution.

3.4 Solving the Energy Minimization Problem

We want to characterize the minimizing admissible distribution $\rho \in \mathcal{A}$. We've previously been guaranteed by Theorem 3.2.3 that there exists a minimizer of $E\{\diamond\}(x,t)$ in $\mathcal{A}$, we will soon show that this minimizer is unique and give a set of necessary and sufficient conditions that the minimizer must satisfy. This will follow from

Lemma 3.4.1. *For any $\rho_1, \rho_2 \in \mathcal{A}$ let $\rho = \rho_1 - \rho_2$, then*

$$\int_0^{\kappa_{\max}} L\{\rho\}(\zeta(\kappa))\ \rho(\kappa)\,\mathrm{d}\kappa \geq 0\,, \tag{3.81}$$

with equality iff $\rho_1 = \rho_2$.

Proof. Let ρ be as in the hypothesis, then $\rho \in L^1[0,\kappa_{\max}]$, so we can define the two dimensional Fourier transform restricted along the quadratrix by

$$\hat{\rho}(k_1,k_2) := \int_{-\kappa_{\max}}^{\kappa_{\max}} \mathrm{e}^{-\mathrm{i}k_1 \mathrm{Re}[\zeta(\kappa)] - \mathrm{i}k_2\kappa}\ \rho(\kappa)\,\mathrm{d}\kappa \tag{3.82}$$

where we just extend ρ to $[-\kappa_{\max}, 0)$ with odd symmetry. We note that because of this odd symmetry, $\hat{\rho}(0,0) = 0$ and $\hat{\rho}$ is differentiable at $(k_1, k_2) = (0,0)$ because ρ is compactly supported. We define the mollified sequence of two-dimensional densities $\rho_n : \mathbb{R}^2 \to \mathbb{R}$ for $n \in \mathbb{N}$,

$$\rho_n(\xi, \kappa) := \int_{-\kappa_{\max}}^{\kappa_{\max}} \chi_n\big(\xi - \operatorname{Re}\left[\zeta(\kappa')\right],\ \kappa - \kappa'\big)\ \rho(\kappa')\,\mathrm{d}\kappa'\,, \tag{3.83}$$

where $\chi_n(\xi, \kappa) := n^2\chi(n\xi, n\kappa)$ and $\chi \in C_0^\infty(\mathbb{R}^2)$ is nonnegative, radially symmetric, decreasing radially outwards, and $||\chi||_{L^1} = 1$. The net result of this mollification is that the charge density ρ, which can be thought of as a distribution supported on the quadratrix, is spread out into the plane in a radially symmetric manner proportional to $1/n$. Note that ρ_n are Schwartz-class functions which inherent odd symmetry in κ from ρ.

Since $\kappa_{\max} < \pi/2\delta$, for large enough n, the support of ρ_n is interior to the bounds $-\pi/2\delta < \kappa < \pi/2\delta$, thus we can define a twice-indexed sequence of Schwartz-class functions $\rho_{nm} : \mathbb{R}^2 \to \mathbb{R}$ for $m \in \mathbb{N}$ by

$$\rho_{nm}(\xi, \kappa) := \begin{cases} m\rho_n\Big(m\big(\xi - \operatorname{Re}\left[\zeta(\kappa)\right]\big) + \operatorname{Re}\left[\zeta(\kappa)\right], \kappa\Big) & \text{if } |\kappa| < \pi/2\delta \\ 0 & \text{if } |\kappa| \geq \pi/2\delta \end{cases}\,. \tag{3.84}$$

This shrinks the density ρ_n, preserving the total mass, in the horizontal direction around the quadratrix with factor $1/m$. Thus, as $m \to \infty$, ρ_{nm} should approach a distribution supported on the quadratrix, not exactly ρ, but a smoothed version.

We exploit the inherited odd symmetry and Schwartz-class properties of ρ_{nm} to compute the double-integral log-convolution which is present in (3.81), but in two dimensions and with the smoothed ρ_{nm}, using Parseval's theorem.

$$\begin{aligned} \int_0^{\kappa_{\max}} \int_0^{\kappa_{\max}} \int_{\mathbb{R}} \int_{\mathbb{R}} \log \left| \frac{\xi - \xi' + \mathrm{i}(\kappa + \kappa')}{\xi - \xi' + \mathrm{i}(\kappa - \kappa')} \right| \rho_{nm}(\xi, \kappa)\rho_{nm}(\xi', \kappa')\,\mathrm{d}\xi\,\mathrm{d}\xi'\,\mathrm{d}\kappa\,\mathrm{d}\kappa' \\ = -\frac{1}{2} \int_{\mathbb{R}^2} \int_{\mathbb{R}^2} \log\left|\xi - \xi' + \mathrm{i}(\kappa - \kappa')\right| \rho_{nm}(\kappa, \xi)\rho_{nm}(\kappa', \xi')\,\mathrm{d}\kappa\,\mathrm{d}\xi\,\mathrm{d}\kappa'\mathrm{d}\xi' \qquad (3.85) \\ = \frac{1}{4\pi} \int_{\mathbb{R}^2} \frac{\left|\hat{\rho}_{nm}(k_1, k_2)\right|^2}{k_1^2 + k_2^2}\,\mathrm{d}k_1\,\mathrm{d}k_2\,, \qquad (3.86) \end{aligned}$$

where $\hat{\rho}_{nm}$ are the standard two dimensional Fourier transforms of each ρ_{nm}. We are interested in taking the limit $m \to \infty$. In the initial expression of (3.86), we can isolate the integrals in ξ and ξ' and, for fixed $0 \leq \kappa, \kappa' < \pi/2\delta$, writing each ρ_{nm} in terms of ρ_n and

invoking a change of variables.

$$\int_{\mathbb{R}}\int_{\mathbb{R}} \log\left|\frac{\xi-\xi'+\mathrm{i}(\kappa+\kappa')}{\xi-\xi'+\mathrm{i}(\kappa-\kappa')}\right| \rho_{nm}(\xi,\kappa)\rho_{nm}(\xi',\kappa')\,\mathrm{d}\xi\,\mathrm{d}\xi'$$
$$= \int_{\mathbb{R}}\int_{\mathbb{R}} \log\left|\frac{\frac{\xi-\xi'}{m}+\frac{(m-1)(\mathrm{Re}[\zeta(\kappa)]-\mathrm{Re}[\zeta(\kappa')])}{m}+\mathrm{i}(\kappa+\kappa')}{\frac{\xi-\xi'}{m}+\frac{(m-1)(\mathrm{Re}[\zeta(\kappa)]-\mathrm{Re}[\zeta(\kappa')])}{m}+\mathrm{i}(\kappa-\kappa')}\right| \rho_n(\xi,\kappa)\rho_n(\xi',\kappa')\,\mathrm{d}\xi\,\mathrm{d}\xi'\,. \quad (3.87)$$

As $m\to\infty$, for any $\kappa\neq\kappa'$, the integrand in (3.87) has a clear point-wise limit. From a geometric argument, the kernel is positive and maximized over $\xi,\xi'\in\mathbb{R}$ when the real parts of the numerator and denominator are both zero. Plugging this maximum in, what remains is absolutely integrable, giving us by the dominated convergence theorem

$$\lim_{m\to\infty}\int_{\mathbb{R}}\int_{\mathbb{R}} \log\left|\frac{\xi-\xi'+\mathrm{i}(\kappa+\kappa')}{\xi-\xi'+\mathrm{i}(\kappa-\kappa')}\right| \rho_{nm}(\xi,\kappa)\rho_{nm}(\xi',\kappa')\,\mathrm{d}\xi\,\mathrm{d}\xi'$$
$$= \int_{\mathbb{R}}\int_{\mathbb{R}} \log\left|\frac{\mathrm{Re}\left[\zeta(\kappa)\right]-\mathrm{Re}\left[\zeta(\kappa')\right]+\mathrm{i}(\kappa+\kappa')}{\mathrm{Re}\left[\zeta(\kappa)\right]-\mathrm{Re}\left[\zeta(\kappa')\right]+\mathrm{i}(\kappa-\kappa')}\right| \rho_n(\xi,\kappa)\rho_n(\xi',\kappa')\,\mathrm{d}\xi\,\mathrm{d}\xi' \quad (3.88)$$
$$= \log\left|\frac{\zeta(\kappa)-\zeta(\kappa')^*}{\zeta(\kappa)-\zeta(\kappa')}\right| \rho_n(\kappa)\rho_n(\kappa')\,, \quad (3.89)$$

where $\rho_n:\mathbb{R}\to\mathbb{R}$ is defined as

$$\rho_n(\kappa) := \int_{\mathbb{R}} \rho_n(\xi,\kappa)\,\mathrm{d}\xi\,. \quad (3.90)$$

This trivially extends to $|\kappa|\geq\pi/2\delta$. Now we look at the Fourier side of (3.86) as $m\to\infty$ by evaluating $\hat{\rho}_{nm}$ and using the same change of variables as before,

$$\lim_{m\to\infty}\hat{\rho}_{nm}(k_1,k_2) = \lim_{m\to\infty}\int_{\mathbb{R}}\int_{\mathbb{R}} \mathrm{e}^{-\mathrm{i}k_1\xi-\mathrm{i}k_2\kappa}\rho_{nm}(\xi,\kappa)\,\mathrm{d}\xi\,\mathrm{d}\kappa \quad (3.91)$$
$$= \lim_{m\to\infty}\int_{-\kappa_{\max}}^{\kappa_{\max}}\int_{\mathbb{R}} \mathrm{e}^{-\mathrm{i}k_1(\xi/m+(m-1)\mathrm{Re}[\zeta(\kappa)]/m)-\mathrm{i}k_2\kappa}\rho_n(\xi,\kappa)\,\mathrm{d}\xi\,\mathrm{d}\kappa \quad (3.92)$$
$$= \int_{-\kappa_{\max}}^{\kappa_{\max}} \mathrm{e}^{-\mathrm{i}k_1\mathrm{Re}[\zeta(\kappa)]-\mathrm{i}k_2\kappa}\rho_n(\kappa)\,\mathrm{d}\kappa\,, \quad (3.93)$$

where the final step is done again by the dominated convergence theorem, just like above. We can now take the $m\to\infty$ limit of both sides of (3.86), this goes through by dominated convergence theorem and we just plug in results (3.89) and (3.93),

$$\int_0^{\kappa_{\max}} L\{\rho_n\}\rho_n(\kappa)\,\mathrm{d}\kappa = \frac{1}{4\pi}\int_{\mathbb{R}^2}\frac{\left|\hat{\rho}_n(k_1,k_2)\right|^2}{k_1^2+k_2^2}\,\mathrm{d}k_1\,\mathrm{d}k_2\,, \quad (3.94)$$

where $\hat{\rho}_n : \mathbb{R}^2 \to \mathbb{R}$ is the two dimensional Fourier transform of ρ_n on the quadratrix

$$\hat{\rho}_n(k_1, k_2) := \int_{-\kappa_{\max}}^{\kappa_{\max}} \mathrm{e}^{-\mathrm{i}k_1 \mathrm{Re}[\zeta(\kappa)] - \mathrm{i}k_2 \kappa} \rho_n(\kappa)\, \mathrm{d}\kappa\,. \tag{3.95}$$

It is worth noting that the Fourier side of (3.94) is integrable because $\rho_n(0,0) = 0$, due to odd symmetry, ρ_n is differentiable at $(0,0)$ and decays at infinity beyond all orders, due to ρ_n being Schwartz-class.

Now we wish to show that $L\{\rho_n\}$ integrated against ρ_n approaches the integral in (3.81) as we take $n \to \infty$. This is done by subtracting the two integrals and completing the square, since the two integrals have the same kernel,

$$\begin{aligned}
&\left| \int_0^{\kappa_{\max}} L\{\rho_n\}(\zeta(\kappa))\ \rho_n(\kappa)\, \mathrm{d}\kappa - \int_0^{\kappa_{\max}} L\{\rho\}(\zeta(\kappa))\ \rho(\kappa)\, \mathrm{d}\kappa \right| \\
&\qquad = \left| \int_0^{\kappa_{\max}} L\{\rho_n + \rho\}(\zeta(\kappa))\ \big(\rho_n(\kappa) - \rho(\kappa)\big)\, \mathrm{d}\kappa \right| \qquad (3.96) \\
&\qquad \leq ||L\{\rho_n + \rho\}||_{L^\infty}\, ||\rho_n - \rho||_{L^1}\ . \qquad (3.97)
\end{aligned}$$

$||\rho_n - \rho||_{L^1} \to 0$ from a slight modification to the proof of this convergence for mollifiers. $||L\{\rho_n + \rho\}||_{L^\infty}$ is bounded from Theorem 3.2.2 since $-\rho^{\mathrm{Wyl}} \leq \rho \leq \rho^{\mathrm{Wyl}}$. Comparing with (3.94), we see the Fourier integral must have the limit

$$\int_0^{\kappa_{\max}} L\{\rho\}(\zeta(\kappa))\ \rho(\kappa)\, \mathrm{d}\kappa = \frac{1}{4\pi} \int_{\mathbb{R}^2} \frac{|\hat{\rho}(k_1, k_2)|^2}{k_1^2 + k_2^2}\, \mathrm{d}k_1\, \mathrm{d}k_2 \geq 0\,, \tag{3.98}$$

with equality only when the Fourier transform (3.82) is zero, i.e. $\rho = 0$. □

Now we are ready to characterize the minimizing charge density.

Theorem 3.4.2. *For each x, t, the minimizing charge distribution $\rho^{\min}(\kappa; x, t)$ is uniquely determined by the variational conditions*

$$\begin{cases} \rho^{\min}(\kappa; x, t) = 0 & \text{if } (\kappa, x, t) \in I_-, \quad \textit{(voids)} \\ 0 \leq \rho^{\min}(\kappa; x, t) \leq \rho^{\mathrm{Wyl}}(\kappa) & \text{if } (\kappa, x, t) \in I_0, \quad \textit{(bands)} \\ \rho^{\min}(\kappa; x, t) = \rho^{\mathrm{Wyl}}(\kappa) & \text{if } (\kappa, x, t) \in I_+, \quad \textit{(saturations)} \end{cases}, \tag{3.99}$$

where the sets I_-, I_0, I_+ partition $[0, \kappa_{\max}] \times \mathbb{R} \times \mathbb{R}$ according to

$$I_- = \left\{ (\kappa, x, t) \in [0, \kappa_{\max}] \times \mathbb{R} \times \mathbb{R} \;\middle|\; \frac{\delta E}{\delta \rho}\{\rho^{\min}\}(\kappa; x, t) < 0 \right\}, \tag{3.100}$$

$$I_0 = \left\{ (\kappa, x, t) \in [0, \kappa_{\max}] \times \mathbb{R} \times \mathbb{R} \;\middle|\; \frac{\delta E}{\delta \rho}\{\rho^{\min}\}(\kappa; x, t) = 0 \right\}, \tag{3.101}$$

$$I_+ = \left\{ (\kappa, x, t) \in [0, \kappa_{\max}] \times \mathbb{R} \times \mathbb{R} \;\middle|\; \frac{\delta E}{\delta \rho}\{\rho^{\min}\}(\kappa; x, t) > 0 \right\}. \tag{3.102}$$

and the Fréchet derivative of E is given by

$$\frac{\delta E}{\delta \rho}\{\rho\}(\zeta; x, t) := V(\zeta; x, t) + L\{\rho\}(\zeta)\,. \tag{3.103}$$

Proof. Uniqueness of the minimizer will follow from the convexity of the admissible set of charge densities $\mathcal{A}$ and the functional $E\{\diamond\}(x,t)$, which in turn follows trivially from the quadratic form of E and the positive-definiteness of the quadratic term in Lemma 3.4.1. The variational conditions can be derived using these properties. Take $\rho \in \mathcal{A}$ and let $\rho^{\min}$ be a minimizer of consider $\rho_\theta = (1-\theta)\rho^{\min} + \theta\rho \in \mathcal{A}$ for $0 \le \theta \le 1$. Then, we have

$$E\{\rho_\theta\}(x,t) - E\{\rho^{\min}\}(x,t) = \theta \int_0^{\kappa_{\max}} \left[V\left(\zeta(\kappa); x, t\right) + L\{\rho^{\min}\}(\zeta(\kappa)) \right] \left(\rho(\kappa) - \rho^{\min}(\kappa)\right) \mathrm{d}\kappa \tag{3.104}$$

$$+ \frac{\theta^2}{2} \int_0^{\kappa_{\max}} L\{\rho - \rho^{\min}\}(\zeta(\kappa)) \left(\rho(\kappa) - \rho^{\min}(\kappa)\right) \mathrm{d}\kappa\,. \tag{3.105}$$

Since $\rho^{\min}$ is the unique minimizer, this difference is always nonnegative, and thus, the coefficient of the linear term in θ must be nonnegative. The integrand of the linear term without the difference $\rho - \rho^{\min}$ we identify as the Fréchet derivative (3.103). We notate the (x,t)-slices of the sets $I_\pm, I_0$ by $I_\pm(x,t)$ and $I_0(x,t)$. We begin by constructing $\rho \in \mathcal{A}$ defined as

$$\rho(\kappa) = \begin{cases} \rho^{\mathrm{Wyl}}(\kappa) & \text{if } s \in I_-(x,t) \\ \rho^{\min}(\kappa; x, t) & \text{if } s \notin I_-(x,t) \end{cases}. \tag{3.106}$$

We then have

$$\int_0^{\kappa_{\max}} \frac{\delta E}{\delta \rho}\{\rho^{\min}\}(\zeta(\kappa)) \left(\rho(\kappa) - \rho^{\min}(\kappa)\right) \mathrm{d}\kappa$$

$$= \int_{I_-(x,t)} \frac{\delta E}{\delta \rho}\{\rho^{\min}\}(\zeta(\kappa)) \left(\rho^{\mathrm{Wyl}}(\kappa) - \rho^{\min}(\kappa)\right) \mathrm{d}\kappa\,. \tag{3.107}$$

If $\rho^{\min}$ differs from the upper bound ρ^{Wyl} on $I_-(x,t)$ then $\rho^{\text{Wyl}} - \rho^{\min}$ is positive while the Fréchet derivative is negative yielding a negative total value if the difference is supported on a nonzero measure set. Thus, we conclude that for $\rho^{\min}$ to truly be the minimizer, it can differ from the upper bound by no more than a set of measure zero on $I_-(x,t)$. Of course, sets of measurable functions are only distinguished up to sets of measure zero, and thus we may set the output on the potentially deviating set to the upper bound and get the top condition in 3.99. By an identical argument with the lower bound on $I_+(x,t)$, we arrive at the bottom condition in 3.99. And by exhaustion of cases, we have the middle condition in 3.99. We have shown that $\rho^{\min}$ satisfies the variational conditions.

Now we assume $\rho \in \mathcal{A}$ satisfies the variational conditions. By assumption, we have

$$\int_0^{\kappa_{\max}} \frac{\delta E}{\delta \rho}\left(\zeta(\kappa); x, t\right)\left(\rho^{\min}(\kappa) - \rho(\kappa)\right)\, \mathrm{d}\kappa \geq 0\,. \tag{3.108}$$

Adding this to the same expression but with $\rho^{\min}$ plugged into the Frćhet derivative, since we now know it satisfies the variational conditions, the V-terms cancel and we can combine the L-terms, accounting for an overall negative sign, to get

$$\int_0^{\kappa_{\max}} L\{\rho - \rho^{\min}\}(\kappa)\left(\rho(\kappa) - \rho^{\min}(\kappa)\right)\, \mathrm{d}\kappa \leq 0. \tag{3.109}$$

By lemma 3.4.1, it must be that this integral is zero and $\rho = \rho^{\min}$. This shows that the variational conditions determine the minimizer. □

3.4.1 Solving the Variational Conditions

Instead of attempting to use the variational conditions to construct the minimizing charge density directly, we will assume first that we may differentiate the charge density with respect to x and t, differentiate the variational conditions:

$$\begin{cases} L\{\rho_x^{\min}\}(\kappa) = -\mathrm{Im}\left[\zeta(\kappa)\right] & \text{if } s \in I_0^{\mathrm{o}}(x,t), \\ \rho_x^{\min}(\kappa) = 0 & \text{if } s \notin I_0^{\mathrm{o}}(x,t). \end{cases}, \tag{3.110}$$

$$\begin{cases} L\{\rho_t^{\min}\}(\kappa) = -\mathrm{Im}\left[\left(\zeta(\kappa) - {}^1\!/_{2\delta}\right)^2\right] & \text{if } s \in I_0^{\mathrm{o}}(x,t), \\ \rho_t^{\min}(\kappa) = 0 & \text{if } s \notin I_0^{\mathrm{o}}(x,t). \end{cases}. \tag{3.111}$$

If we can solve these differential variational conditions, which consist of two separate logarithmic potential problems, show that the solutions can be consistently integrated to a density which depends on the two variables x and t, and verify the integrated charge density satisfies the full variational conditions, then by Theorem 3.4.2, we have constructed the

unique minimizing charge density. From this, the distributional limit of the ILW equation with modified scattering data can be expressed.

To continue, we will make one more assumption, which is that $I_0(x,t)$ consists of a single symmetric interval. This is consistent with the KdV small dispersion limit [34] and, as it will turn out, it will constrain us to the simplest case possible in which we can evaluate the solution $u_N^{\mathrm{ILW}}(x,t)$.

3.4.1.1 Consider a single symmetric interval: the one band case

As it turns out, this problem can be solved by inspection and then verifying that our ansatz has all of the properties required to establish it as the unique solution. The thing we must "inspect" is the solution process of Lax and Levermore [34, 35], to the analogous problem for the KdV equation. Underlying their solution to the differentiated variational conditions for a single symmetric band is an extension of the function which determines the derivative of the fast WKB phases, one that is analytic away from the band in the complex plane. The properties of this analytic function are exactly what leads to the potential satisfying the variational conditions due to the asymptotic scattering data being derived from the same function. Thus, to look for the solution to the ILW differentiated variational conditions, we should try to determine the analytic continuation of the derivative of the fast phase.

Since the Lambert W-function was used to compute the derivative of the fast phase in Section 2.1, we search for an analytic continuation of these formulas away from the quadratrix. It is natural to associate the $n = 0$ solution with the side of the quadratrix corresponding to the $n = 0$ branch region, and the same for the $n = -1$ solution. From here, if we wish to analytically extend this formula to the full plane, there is only one way to do this: The central formula involved will be the map $z \mapsto W(-z\mathrm{e}^{-z-y})$ where we use the branch of Lambert W which corresponds to the input $z \in \mathbb{C}$, i.e. if we define a function $n : \mathbb{C} \to \mathbb{Z}$ where $n(z)$ indicates which branch range region z belongs to, then

$$W(-z\mathrm{e}^{-z-y}) := W_{n(z)}(-z\mathrm{e}^{-z-y}). \tag{3.112}$$

Furthermore, we restrict $y \geq 0$ since it is a stand-in variable for the potential, which we will plug in later. It is easiest to analyze $W(-z\mathrm{e}^{-z-y})$ in three steps, $z_0 \mapsto z_1 := -z_0\mathrm{e}^{-z_0}$, $z_1 \mapsto z_2 := z_1\mathrm{e}^{-y}$, and then $z_2 \mapsto z_3 := W(z_2)$, for each of the branch regions. Follow along the steps in Figure 3.1 to get a visual understanding of how each of these maps acts of the three characteristic branch regions: 0, -1 and -2.

1. In each of these regions the map $z_0 \mapsto z_1 = -z_0\mathrm{e}^{-z_0}$ is onto the whole complex plane. For the 0-region, the boundary points along the inside of the quadratrix are mapped

to the two sides of the negative real axis below the branch point of W for this branch, $-\mathrm{e}^{-1}$. For the ± 1-regions, there are two branch points: 0 and $-\mathrm{e}^{-1}$. The outside boundary points of the quadratrix are also mapped to the negative real axis below the branch point $-\mathrm{e}^{-1}$ while the boundary points along the positive real axis above 1 are mapped between the two branches. The other continuous boundary curves, the ones shared with the ± 2-regions, are mapped around the other side of the negative real axis. Then, for all other n-regions, the boundaries map to complementary sides of the negative real axis, around the single branch point: 0.

2. For $y \geq 0$, $z_1 \mapsto z_2 \mathrm{e}^{-y}$ is just a dilation of the plane, specifically, a shrinking of the plane. In the 0-region, this means the boundary points "slide inwards" on the negative axis, resulting in a symmetric interval along the boundary mapping to negative real numbers greater than the branch point. In the ± 1-regions, an identical thing happens to the boundary values along the interval. Note that the boundary points shared with the ± 2-regions are still mapped to the entirety of the negative real line. Similarly, all other boundary points in the other regions map to complementary sides of the negative real line since all other branch points are 0, invariant under the dilation.

3. Lastly, $z_2 \mapsto z_3 = W(z_2)$, because of the chosen branch evaluations, returns each complex plane mapped to in the first step to the negative of the original region, but the scaling in between can have a dramatic effect on where exactly the original z_0 map to. Since the scaling of step two never moved points across the branch cuts, the full mapping must be analytic on the interiors of each region. For the boundary points in the 0-region, the points which were scaled past the branch point now map to the positive real line interior to the quadratrix. All of the other points which are still below the branch point map along the quadratrix, just a different point from where they started. A similar result is true of the quadratrix boundary points in the ± 1-regions, but they now map to the positive real line exterior to the quadratrix. For all other boundaries, since these points were never scaled past their branch points, they all still map along their same boundaries, again just to different points along these boundaries.

For any boundary points which still map to their original boundary, the full map has to be continuous at these points since taking the same boundary value in two adjacent regions must give the same value under $z_0 \mapsto z_1 = -z_0 \mathrm{e}^{-z_0}$ and $z_1 \mapsto z_2 = -z_1 \mathrm{e}^{-y}$. Then, choosing the correct branch for the region, $z_2 \mapsto z_3 = W(z_2)$ gives the same value as well since the points are still on the shared boundary between the two regions. It is easy to show that this continuity implies analyticity using Morera's theorem. This means the only discontinuity in

$W(-z\mathrm{e}^{-z-y})$ is along this symmetric interval of the quadratrix where on one side the values lie on the positive real line interior to the negated quadratrix, and on the other side the values lie on the positive real line exterior to the quadratrix.

We note that the branch points of $W(-z\mathrm{e}^{-z-y})$ are those on the quadratrix which satisfy $-z\mathrm{e}^{-z-y} = -\mathrm{e}^{-1}$. Since $-z\mathrm{e}^{-z}$ is monotone increasing from $-\mathrm{e}^{-1}$ to $+\infty$ on the upper and lower quadratrix, we can generate any sized symmetric interval along the quadratrix for the branch cut by picking the correct y value.

Lastly, we can compute the asymptotic behavior of $W(-z\mathrm{e}^{-z-y})$ using the asymptotics of Lambert W. From this, we can guarantee that this is analytic at $z = \infty$. From more didactic purposes, we can calculate the Laurent expansion $z = \infty$ by considering matching $x\mathrm{e}^x = -z\mathrm{e}^{-z-y}$ for large x and z. Then $0 = 1 + x\mathrm{e}^{x+z+y}/z$ which implies that $x = -z - y + c_1/z + c_2/z^2 + O\left(1/z^3\right)$. Substitute this in

$$0 = 1 + \frac{1}{z}\left(-z - y + \frac{c_1}{z} + \frac{c_2}{z^2} + O\left(\frac{1}{z^3}\right)\right)\mathrm{e}^{c_1/z + c_2/z^2 + O\left(1/z^3\right)} \tag{3.113}$$

$$= 1 + \left(-1 - \frac{y}{z} + \frac{c_1}{z^2} + O\left(\frac{1}{z^3}\right)\right)\left(1 + \frac{c_1}{z} + \frac{c_2 + c_1^2/2}{z^2} + O\left(\frac{1}{z^3}\right)\right) \tag{3.114}$$

$$= -\frac{y + c_1}{z} + \frac{c_1 - c_2 - c_1^2/2 - yc_1}{z^2} + O\left(\frac{1}{z^3}\right) \tag{3.115}$$

which implies that $c_1 = -y$ and $c_2 = c_1 - c_1^2/2 - yc_1$. This gives,

$$W(-z\mathrm{e}^{-z-y}) = -z - y - \frac{y}{z} + \frac{y^2/2 - y}{z} + O\left(\frac{1}{z^2}\right). \tag{3.116}$$

The properties of this function allow us to solve the differentiated variational conditions as the following theorem demonstrates.

Theorem 3.4.3. *If ρ is Hölder continuous with power $1/2$ and has logarithmic potential $L\{\rho\}$ which satisfies the differentiated variational conditions* (3.110) *or* (3.111)*, then the density and its logarithmic potential are uniquely identified by the properties:*

1. *harmonic away from I and continuous up to the interval,*
2. *the value on I is dictated by the differential variational conditions* (3.110) *or* (3.111)*,*
3. *odd symmetry under reflection across the real axis: $L\{\rho\}(\zeta) = -L\{\rho\}(\zeta^*)$,*
4. *decay at infinity $L\{\rho\}(\zeta) = O\left(1/\zeta\right)$ as $\zeta \to \infty$.*

Proof. First, it is clear from the formula for $L\{\rho^{\min}_{x,t}\}$ that it satisfies these properties. Now, if we subtract some other logarithmic potential with these properties, the result is a function

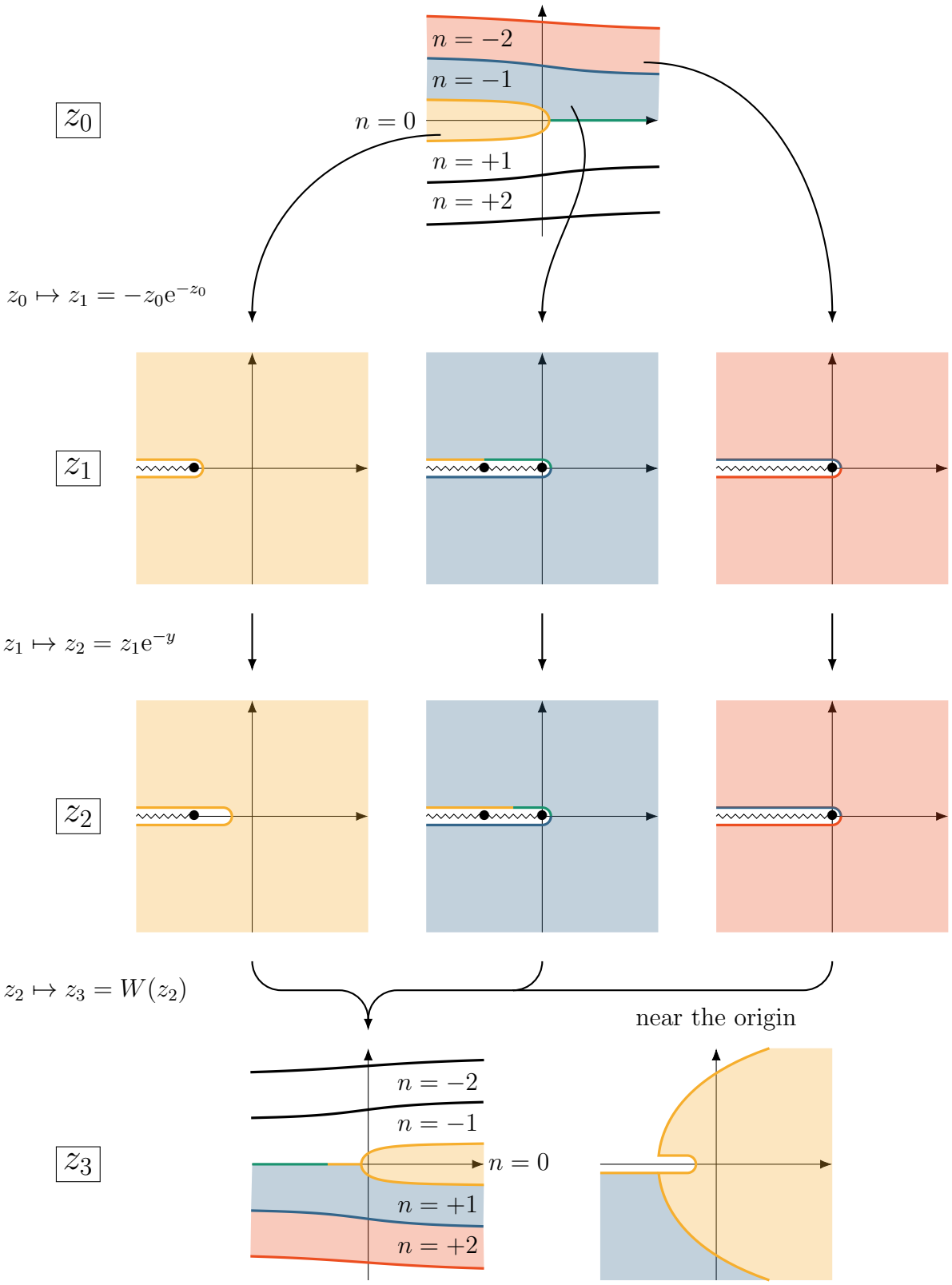


Figure 3.1: $z \mapsto W(-ze^{-z-y})$ demonstrated via three intermediate mappings for three characteristic branch regions. The colored regions and boundaries describe where the points in the top image are mapped to in the complex plane at each step.

on ζ which is harmonic away from the quadratrix interval, zero on it and decays to zero as $\zeta \to \infty$. By the extremum principal of harmonic functions, any maximum or minima of this difference must occur on the interval, or at infinity, or the difference is constant. In all cases, it must be identically zero. Thus, $L\{\rho^{\min}_{x,t}\}$ is uniquely determined by the conditions. Lastly, from [51, Theorem 1.3] the density can be recovered from the log-potential by

$$\rho^{\min}_{x,t}(\kappa) = \operatorname{Im}\left[\zeta'(\kappa)\Big(\partial_\zeta L\{\rho^{\min}_{x,t}\}^-(\zeta(\kappa)) - \partial_\zeta L\{\rho^{\min}_{x,t}\}^+(\zeta(\kappa))\Big)\right] \tag{3.117}$$

where the $+$ and $-$ indicate the left and right boundary values to the quadratrix respectively and $\partial_\zeta = (\partial_{\mathrm{Re}[\zeta]} - \mathrm{i}\partial_{\mathrm{Im}[\zeta]})/2$. □

The properties that we concluded about the Lambert W expression can be used to construct functions which satisfy the properties in Theorem 3.4.3.

Corollary 3.4.3.1. *For any sized interval there is a $y \leq 0$ such that the expressions*

$$L\{\rho^{\min}_x\}(\zeta) = -\operatorname{Im}\left[\zeta + \frac{y}{2\delta} + \frac{1}{2\delta}W\left(-2\delta\zeta \mathrm{e}^{-2\delta\zeta - y}\right)\right], \tag{3.118}$$

$$L\{\rho^{\min}_t\}(\zeta) = -\operatorname{Im}\left[\left(\zeta - \frac{1}{2\delta}\right)^2 + \frac{y}{2\delta^2} - \left(\frac{y+1+W\left(-2\delta\zeta \mathrm{e}^{-2\delta\zeta - y}\right)}{2\delta}\right)^2\right], \tag{3.119}$$

solve the differentiated variational conditions and the associated densities for $\zeta \in \mathcal{Q}_{\delta+}$ are given by

$$\rho^{\min}_x(\kappa) = \frac{\zeta'(\kappa)E'(\zeta)}{2}\mathrm{Re}\left[\frac{W_{-1}\left(-2\delta\zeta \mathrm{e}^{-2\delta\zeta - y}\right)}{1+W_{-1}\left(-2\delta\zeta \mathrm{e}^{-2\delta\zeta - y}\right)} - \frac{W_0\left(-2\delta\zeta \mathrm{e}^{-2\delta\zeta - y}\right)}{1+W_0\left(-2\delta\zeta \mathrm{e}^{-2\delta\zeta - y}\right)}\right]\Bigg|_{\zeta=\zeta(\kappa)}, \tag{3.120}$$

$$\rho^{\min}_t(\kappa) = \frac{\zeta'(\kappa)E'(\zeta)}{2\delta}\mathrm{Re}\left[W_0\left(-2\delta\zeta \mathrm{e}^{-2\delta\zeta - y}\right) - W_{-1}\left(-2\delta\zeta \mathrm{e}^{-2\delta\zeta - y}\right)\right]\Bigg|_{\zeta=\zeta(\kappa)} - \frac{y}{\delta}\rho_x(\kappa)\,. \tag{3.121}$$

Proof. First, we focus on the x-derivative case. As noted before, for a symmetric interval of any size on the quadratrix, we can find a $y \leq 0$ such that the Lambert W term has a branch cut along that interval. Upon fixing this y, we see that the expression of (3.118) inside of the imaginary part,

$$\zeta + \frac{y}{2\delta} + \frac{1}{2\delta}W\left(-2\delta\zeta \mathrm{e}^{-2\delta\zeta - y}\right), \tag{3.122}$$

1. is analytic away from the interval,

2. is continuous up to the interval with the boundary values given by the first two terms plus the real boundary values of the Lambert W expression

3. is Schwartz symmetric,

4. and has decay at infinity since the first two terms explicitly cancel the leading-order asymptotics of the Lambert W term.

The properties above, along with $y \in \mathbb{R}$, directly result in the imaginary part of this function satisfying the list of properties in Theorem 3.4.3 that uniquely determine the solution to the x-derivative variational conditions (3.110). For the t-derivative (3.119), all of the same properties can be shown about the function inside of the imaginary part,

$$\left(\zeta - \frac{1}{2\delta}\right)^2 + \frac{y}{2\delta^2} - \left(\frac{y + 1 + W\left(-2\delta\zeta \mathrm{e}^{-2\delta\zeta - y}\right)}{2\delta}\right)^2 . \tag{3.123}$$

However, in this case, the first term has been chosen so that the value of the imaginary part on the interval is as desired, and then the remaining terms have been chosen so the asymptotics of the Lambert W expression cancel the first couple terms for large ζ and the whole function decays to zero at infinity.

Moreover, from Theorem 3.4.3, we also have that the densities are determined by the difference of the ∂_ζ-derivatives across the interval, which gives the formulas (3.120) and (3.121). To simplify the evaluation of (3.117), note that one can express the ∂_ζ-derivatives of the log-potentials (3.118) and (3.119) in terms of the complex derivatives of (3.122) and (3.123) respectively using the Cauchy-Riemann equations. □

We now have formulas for the logarithmic potentials and the densities in the one band case in terms of this auxiliary parameter $y \geq 0$ which controls the size of the band interval. Since we expect that the band will change size as we change x and t, we regard $y(x,t)$ as a dynamical parameter which evolves with at least one derivative each. We now need to verify that these solutions can be integrated in x and t in a consistent manner and that the result solves the variational conditions. For consistency, we must require that the x and t-derivatives of either the density ρ or logarithmic potential $L\{\rho\}$ are interchangeable. Since the density should be recoverable from the logarithmic potential, we focus on the latter at

any point ζ not on the band,

$$0 = \partial_x L\{\rho_t\}(\zeta) - \partial_t L\{\rho_x\}(\zeta) \tag{3.124}$$

$$= \operatorname{Im}\left[\frac{y_t}{2\delta} - \frac{y_t}{2\delta}\frac{W\left(-2\delta\zeta \mathrm{e}^{-2\delta\zeta - y}\right)}{1+W\left(-2\delta\zeta \mathrm{e}^{-2\delta\zeta-y}\right)}\right] - \tag{3.125}$$

$$\operatorname{Im}\left[\frac{y_x}{2\delta^2} - \left(y_x - \frac{y_x W\left(-2\delta\zeta \mathrm{e}^{-2\delta\zeta-y}\right)}{1+W\left(-2\delta\zeta \mathrm{e}^{-2\delta\zeta-y}\right)}\right)\frac{y+1+W\left(-2\delta\zeta \mathrm{e}^{-2\delta\zeta-y}\right)}{2\delta^2}\right]$$

$$= \operatorname{Im}\left[\frac{y_t}{2\delta}\frac{1}{1+W\left(-2\delta\zeta \mathrm{e}^{-2\delta\zeta-y}\right)} + 2\frac{y_x}{2\delta}\frac{y}{2\delta}\frac{1}{1+W\left(-2\delta\zeta \mathrm{e}^{-2\delta\zeta-y}\right)} - \frac{y_x}{2\delta^2}\right] \tag{3.126}$$

$$= \left(\frac{y_t}{2\delta} + 2\frac{y_x}{2\delta}\frac{y}{2\delta}\right)\operatorname{Im}\left[\frac{1}{1+W\left(-2\delta\zeta \mathrm{e}^{-2\delta\zeta-y}\right)}\right]. \tag{3.127}$$

Since the imaginary part in (3.127) is in general not zero, in order for the logarithmic potentials to be consistently integrated in x and t, we must require the scaled auxiliary parameter $y/2\delta$ solve invicid Burgers' equation (1.80). This is very promising, as according to the numerical simulations in Section 1.4, we expect that the small dispersion limit should indeed be described before the emergence of the dispersive shock wave by invicid Burgers' equation. This leads us to consider how the distributional limit of the N-soliton solution (3.51) is determined by the auxiliary parameter.

$$\mathrm{d} - \lim_{N\to\infty} u_N^{\mathrm{ILW}}(x,t) = -\frac{4\delta}{\pi}\partial_x^2 \int_0^{\kappa_{\max}} \left(V(\zeta(\kappa);x,t) + \frac{1}{2}L\{\rho^{\min}\}(\zeta)\right)\rho^{\min}(\kappa)\,\mathrm{d}\kappa \tag{3.128}$$

$$= -\frac{4\delta}{\pi}\partial_x \int_0^{\kappa_{\max}} \left[\left(\operatorname{Im}\left[\zeta(\kappa)\right] + \frac{1}{2}L\{\rho_x^{\min}\}(\zeta(\kappa))\right)\rho^{\min}(\kappa)\right. \tag{3.129}$$

$$\left. + \left(V(\zeta(\kappa);x,t) + \frac{1}{2}L\{\rho^{\min}\}(\zeta(\kappa))\right)\rho_x^{\min}(\kappa)\right]\mathrm{d}\kappa$$

where we have used that the x-derivatives of these quantities are absolutely integrable, which will be justified *a posteriori*. We rearrange using the symmetry of the L operator and to collect the Fréchet derivative multiplied by $\rho_x^{\min}$. Since the Fréchet derivative is zero on the band and $\rho_x^{\min}$ is zero on the rest of $[0,\kappa_{\max}]$, we can eliminate that contribution:

$$\mathrm{d} - \lim_{N\to\infty} u_N^{\mathrm{ILW}}(x,t) = -\frac{4\delta}{\pi}\partial_x \int_0^{\kappa_{\max}} \left[\operatorname{Im}\left[\zeta(\kappa)\right]\rho^{\min}(\kappa) + \frac{\delta E}{\delta\rho}(\zeta(\kappa);x,t)\rho_x^{\min}(\kappa)\right]\mathrm{d}\kappa \tag{3.130}$$

$$= -\frac{4\delta}{\pi}\operatorname{Im}\left[\int_0^{\kappa_{\max}} \zeta(\kappa)\ \rho_x^{\min}(\kappa)\,\mathrm{d}\kappa\right]. \tag{3.131}$$

On what remains, we can use the formula for $\rho_x^{\min}$ (3.120) for some expected $y \geq 0$. We notice

that, because of its derivation through (3.117), the resulting integrand is a parameterization of the difference of the boundary values of an analytic function across a branch cut on the quadratrix. Indeed, $\rho_x^{\min}$ as in (3.120) has a real part which needs to be taken, however on the cut the boundary values are exactly real. Additionally, we can divide by two and extend the integral to the lower-half of the quadratrix due to the odd symmetry of the logarithmic potential. We may write this as a contour integral for a contour C which traces along outside and inside of the symmetric branch cut along the quadratrix with positive orientation

$$\mathrm{d} - \lim_{N\to\infty} u_N^{\mathrm{ILW}}(x,t) = -\frac{\delta}{\pi}\mathrm{Im}\left[\int_C \zeta E'(\zeta)\frac{W\left(-2\delta\zeta \mathrm{e}^{-2\delta\zeta - y}\right)}{1+W\left(-2\delta\zeta\mathrm{e}^{-2\delta\zeta-y}\right)}\,\mathrm{d}\zeta\right]. \tag{3.132}$$

Because the function has no worse than inverse square-root branch cuts, we may use Cauchy's theorem to pull the contour away from the cut. Noticing everything besides the leading ζ factor is a total derivative, we use integration-by-parts to simplify the integrand,

$$\mathrm{d} - \lim_{N\to\infty} u_N^{\mathrm{ILW}}(x,t) = \frac{\delta}{\pi}\mathrm{Im}\left[\int_C \frac{1}{2\delta} W\left(-2\delta\zeta\mathrm{e}^{-2\delta\zeta-y}\right)\,\mathrm{d}\zeta\right]. \tag{3.133}$$

Lastly, Cauchy's theorem again lets us blow-up the contour, evaluating the integral by residue at infinity, which is easily picked off from the expansion (3.116),

$$\begin{aligned}
\mathrm{d} - \lim_{N\to\infty} u_N^{\mathrm{ILW}}(x,t) &= \frac{1}{2\pi}\mathrm{Im}\left[\int_C \left(2\delta\zeta - y + \frac{y}{2\delta\zeta} + O\left(\frac{1}{\zeta^2}\right)\right)\,\mathrm{d}\zeta\right] && (3.134)\\
&= \frac{1}{2\pi}\mathrm{Im}\left[2\pi\mathrm{i}\frac{y}{2\delta}\right] && (3.135)\\
&= \frac{y}{2\delta}. && (3.136)
\end{aligned}$$

At $t = 0$, we should expect to recover the initial condition. Combining this fact with the observation of x and t integrable consistency from (3.127), we have the ansatz

$$y(x,t) := 2\delta u^{\mathrm{B}}(x,t) \tag{3.137}$$

where u^{B} solves invicid Burgers' equation (1.80) with initial condition $u^{\mathrm{B}}(x,0) = u_0(x)$. Recall that invicid Burgers' equation will only have a global solution up to a critical time t_{c} given by (1.84).

Now, we are ready to show that our ansatz, after integrating, satisfies the variational conditions.

Theorem 3.4.4. *For u_0 with the conditions provided, the variational conditions are satisfied*

for $x \in \mathbb{R}$ and $0 \leq t \leq t_c$ by the logarithmic potential for $\zeta \in \mathbb{C}$

$$L\{\rho^{\min}(\diamond; x, t)\}(\zeta) = \int_x^{+\infty} \operatorname{Im}\left[\zeta + \frac{1}{2\delta} W\left(-2\delta\zeta \mathrm{e}^{-2\delta(\zeta + u^{\mathrm{B}}(x',t))}\right)\right] \mathrm{d}x' \tag{3.138}$$

and energy minimizing density for $\zeta \in \mathcal{Q}_{\delta+}$

$$\rho^{\min}(\kappa; x, t) = \frac{\zeta'(\kappa) E'(\zeta)}{2} \int_x^{+\infty} \operatorname{Re}\left[r(\zeta(\kappa); u^{\mathrm{B}}(x', t))\right] \mathrm{d}x' \,. \tag{3.139}$$

where r is as in (2.352)*.*

Proof. First working at $t = 0$, we replace $u^{\mathrm{B}}(x, 0) = u_0(x)$. The formulas we then see are the integrals of the x-derivatives $\rho_x^{\min}$ and $L\{\rho_x^{\min}\}$. Focusing on $L\{\rho^{\min}\}(\zeta)$, we know the maxima of the absolute value of the integrand is obtained at the upper endpoint of the band, $\beta(x) \in \mathcal{Q}_\delta$ determined by $E(\beta(x)) = u_0(x)$. As $x \to +\infty$, $u_0(x) \to 0$. This corresponds to $\beta(x) \to 1/2\delta$. Around this point on the quadratrix, $E(\zeta) \geq 2\delta \mathrm{Im}\,[\zeta]^2$. Thus, for x large enough

$$\left|\zeta + u_0(x') + \frac{1}{2\delta} W\left(-2\delta\zeta \mathrm{e}^{-2\delta(\zeta + u(x'))}\right)\right| \leq \operatorname{Im}\left[\beta(x')\right] \leq \sqrt{\frac{u_0(x)}{2\delta}} \,. \tag{3.140}$$

Thus, by assumption on the decay of u_0, the integrand is uniformly integrable. Additionally, the integral inherits all of the properties that uniquely determine the log-potential in terms of its density from $L\{\rho_x^{\min}\}$, Theorem 3.4.3. The integrability of the boundary values of $L\{\rho_x^{\min}\}$ assures us that the density for this logarithmic potential can be generated by integrating the derivative density formula (3.120).

Now, we will identify the voids, bands, and saturations by considering the logarithmic potential formula (3.138). As x decreases from $+\infty$, the cut in the analytic function which appears in the integrand opens from the center of the quadratrix and spreads. For a given $\zeta \in (1/2\delta, \zeta_{\max})_{\mathcal{Q}_\delta}$, the edge of the cut $\beta(x)$ will pass this point exactly when $x = x_+(\zeta)$, so long as $x > x_{\max}$, where the cut's size is maximal $\beta(x_{\max}) = \zeta_{\max}$. As x decreases past $x_{\max}$, the size of the cut will begin to decrease and, at $x = x_-(\zeta)$, the endpoint of the cut $\beta(x)$ again passes ζ. The size of the cut continues to shrink to zero as $x \to -\infty$. For this reason, we split up the evaluation of the integral into cases and simplify using the values in these

cases for $\zeta \in (1/2\delta, \zeta_{\max}]_{\mathcal{Q}_\delta}$

$$L\{\rho^{\min}\}(\zeta) = \begin{cases} \displaystyle\int_x^{+\infty} \operatorname{Im}\left[\zeta + \frac{1}{2\delta} W_{-1}\left(-2\delta\zeta \mathrm{e}^{-2\delta(\zeta+u(x'))}\right)\right] \mathrm{d}x' & \text{if } \zeta \in (\beta(x), \zeta_{\max}]_{\mathcal{Q}_\delta} \\ & \text{and } x_{\max} \leq x \\ \displaystyle\int_x^{x_+(\zeta)} \operatorname{Im}[\zeta]\, \mathrm{d}x' & \\ \displaystyle + \int_{x_+(\zeta)}^{+\infty} \operatorname{Im}\left[\zeta + \frac{1}{2\delta} W_{-1}\left(-2\delta\zeta \mathrm{e}^{-2\delta(\zeta+u(x'))}\right)\right] \mathrm{d}x' & \text{if } \zeta \in [0, \beta(x)]_{\mathcal{Q}_\delta} \\ \displaystyle\int_x^{x_-(\zeta)} \operatorname{Im}\left[\zeta + \frac{1}{2\delta} W_{-1}\left(-2\delta\zeta \mathrm{e}^{-2\delta(\zeta+u(x'))}\right)\right] \mathrm{d}x' & \\ \displaystyle + \int_{x_-(\zeta)}^{x_+(\zeta)} \operatorname{Im}[\zeta]\, \mathrm{d}x' & \text{if } \zeta \in (\beta(x), \zeta_{\max}]_{\mathcal{Q}_\delta} \\ & \text{and } x < x_{\max} \\ \displaystyle + \int_{x_+(\zeta)}^{+\infty} \operatorname{Im}\left[\zeta + \frac{1}{2\delta} W_{-1}\left(-2\delta\zeta \mathrm{e}^{-2\delta(\zeta+u(x'))}\right)\right] \mathrm{d}x' & \end{cases} . \tag{3.141}$$

We can then use the definition of θ_+ (2.386) from the modified scattering data, as well as directly evaluating some of the integrals to simplify these expressions:

$$L\{\rho^{\min}\}(\zeta) = \begin{cases} -\operatorname{Im}[\zeta]\, x + \theta_+(\zeta) & \text{if } \zeta \in (\beta(x), \zeta_{\max}]_{\mathcal{Q}_\delta} \\ \displaystyle\quad - \frac{1}{2\delta} \int_{x_+(\zeta)}^{x} \operatorname{Im}\left[W_{-1}\left(-2\delta\zeta \mathrm{e}^{-2\delta(\zeta+u(x'))}\right)\right] \mathrm{d}x' & \text{and } x_{\max} \leq x \\ -\operatorname{Im}[\zeta]\, x + \theta_+(\zeta) & \text{if } \zeta \in [0, \beta(x)]_{\mathcal{Q}_\delta} \\ -\operatorname{Im}[\zeta]\, x + \theta_+(\zeta) & \text{if } \zeta \in (\beta(x), \zeta_{\max}]_{\mathcal{Q}_\delta} \\ \displaystyle\quad + \frac{1}{2\delta} \int_{x}^{x_-(\zeta)} \operatorname{Im}\left[W_{-1}\left(-2\delta\zeta \mathrm{e}^{-2\delta(\zeta+u(x'))}\right)\right] \mathrm{d}x' & \text{and } x < x_{\max} \end{cases} . \tag{3.142}$$

Lastly, we add $V(\zeta; x, 0) = \operatorname{Im}[\zeta]\, x + \theta_+(\zeta)$ to compute the value of the Fréchet derivative,

$$\frac{\delta E}{\delta \rho}\{\rho^{\min}\}(\zeta) = \begin{cases} -\dfrac{1}{2\delta}\displaystyle\int_{x_+(\zeta)}^{x} \operatorname{Im}\left[W_{-1}\left(-2\delta\zeta \mathrm{e}^{-2\delta(\zeta+u(x'))}\right)\right] \mathrm{d}x' & \text{if } \zeta \in (\beta(x), \zeta_{\max}]_{\mathcal{Q}_\delta} \\ & \quad \text{and } x_{\max} \le x \\ 0 & \text{if } \zeta \in [0, \beta(x)]_{\mathcal{Q}_\delta} \\ \dfrac{1}{2\delta}\displaystyle\int_{x}^{x_-(\zeta)} \operatorname{Im}\left[W_{-1}\left(-2\delta\zeta \mathrm{e}^{-2\delta(\zeta+u(x'))}\right)\right] \mathrm{d}x' & \text{if } \zeta \in (\beta(x), \zeta_{\max}]_{\mathcal{Q}_\delta} \\ & \quad \text{and } x < x_{\max} \end{cases} . \tag{3.143}$$

In the first case above the imaginary part in the integrand is positive and for ζ above $\beta(x)$ on the quadratrix, $x > x_+(\zeta)$. This means the term in the first case is always nonpositive, and zero only when $x = x_+(\zeta)$. A similar analysis reveals that the term in the third case is nonnegative. This lets us identify the intervals in the three cases as a void, band and saturation, respectively, according to (3.100), (3.101), and (3.102). Integrating $\rho_x^{\min}$ gives the associated charge density to the potential in the cases listed above.

$$\rho^{\min}(\kappa) = \begin{cases} 0 & \text{if } \zeta \in (\beta(x), \zeta_{\max}]_{\mathcal{Q}_\delta} \\ & \quad \text{and } x_{\max} \le x \\ \dfrac{\zeta'(\kappa)E'(\zeta(\kappa))}{2}\displaystyle\int_{x}^{x_+(\zeta(\kappa))} r\big(\zeta(\kappa); u_0(x')\big)\, \mathrm{d}x' & \text{if } \zeta \in [0, \beta(x)]_{\mathcal{Q}_\delta} \\ \dfrac{\zeta'(\kappa)E'(\zeta(\kappa))}{2}\displaystyle\int_{x_-(\zeta(\kappa))}^{x_+(\zeta(\kappa))} r\big(\zeta(\kappa); u_0(x')\big)\, \mathrm{d}x' & \text{if } \zeta \in (\beta(x), \zeta_{\max}]_{\mathcal{Q}_\delta} \\ & \quad \text{and } x < x_{\max} \end{cases} . \tag{3.144}$$

Once we note that the integrands above are positive, and identifying the third case formula, being integrated between the two turning points, is exactly ρ^{Wyl}, we can note that the second formula is less than this. This exactly satisfies the $\rho^{\min}$ conditions of a void, band and saturation, confirming that these formulas solve the variational conditions 3.99.

Now, considering $0 < t \le t_{\mathrm{c}}$, we could use the t-derivative potential to integrate up the solution. However, the result is not easily parsed for the conditions of satisfying the variational conditions. So instead, we consider how the derived WKB scattering data changes as we let the potential $u^{\mathrm{B}}(x,t)$ evolve under invicid Burgers' equation. First, we know how $x_\pm(\zeta)$ changes from the characteristics (1.81) and (1.82), and the level condition $E(\zeta) = u^{\mathrm{B}}(x_\pm(\zeta;t),t)$ which defines the turning points:

$$x_\pm(\zeta;t) := x_\pm(\zeta) - 2E(\zeta)t\,. \tag{3.145}$$

Next, we see how the Weyl law (2.348) depends on the parameter t,

$$R(\zeta;t) := \int_{x_-(\zeta;t)}^{x_+(\zeta;t)} \left(W_{-1}\left(-2\delta\zeta \mathrm{e}^{-2\delta(\zeta+u^{\mathrm{B}}(x',t))}\right) - W_0\left(-2\delta\zeta \mathrm{e}^{-2\delta(\zeta+u^{\mathrm{B}}(x',t))}\right) \right) \mathrm{d}x' \,. \quad (3.146)$$

We do this by computing the t-derivative and exploiting that $u^{\mathrm{B}}(x,t)$ solves invicid Burgers' equation:

$$\begin{aligned} R_t(\zeta;t) &= 2E(\zeta)\left(W_{-1}\left(-2\delta\zeta \mathrm{e}^{-2\delta(\zeta+u^{\mathrm{B}}(x_+(\zeta;t),t))}\right) - W_0\left(-2\delta\zeta \mathrm{e}^{-2\delta(\zeta+u^{\mathrm{B}}(x_+(\zeta;t),t))}\right) \right) \\ &\quad - 2E(\zeta)\left(W_{-1}\left(-2\delta\zeta \mathrm{e}^{-2\delta(\zeta+u^{\mathrm{B}}(x_-(\zeta;t),t))}\right) - W_0\left(-2\delta\zeta \mathrm{e}^{-2\delta(\zeta+u^{\mathrm{B}}(x_-(\zeta;t),t))}\right) \right) \\ &\quad + \int_{x_-(\zeta;t)}^{x_+(\zeta;t)} \left(\frac{W_{-1}\left(-2\delta\zeta \mathrm{e}^{-2\delta(\zeta+u^{\mathrm{B}}(x',t))}\right)}{1+W_{-1}\left(-2\delta\zeta \mathrm{e}^{-2\delta(\zeta+u^{\mathrm{B}}(x',t))}\right)} - \frac{W_0\left(-2\delta\zeta \mathrm{e}^{-2\delta(\zeta+u^{\mathrm{B}}(x',t))}\right)}{1+W_0\left(-2\delta\zeta \mathrm{e}^{-2\delta(\zeta+u^{\mathrm{B}}(x',t))}\right)} \right) \\ &\qquad\qquad \times u_t^{\mathrm{B}}(x',t)\,\mathrm{d}x' \quad (3.147) \\ &= 2E(\zeta)\left(W_{-1}\left(-\mathrm{e}^{-1}\right) - W_0\left(-\mathrm{e}^{-1}\right) \right) - 2E(\zeta)\left(W_{-1}\left(-\mathrm{e}^{-1}\right) - W_0\left(-\mathrm{e}^{-1}\right) \right) \\ &\quad - 2\int_{x_-(\zeta;t)}^{x_+(\zeta;t)} \left(\frac{W_{-1}\left(-2\delta\zeta \mathrm{e}^{-2\delta(\zeta+u^{\mathrm{B}}(x',t))}\right)}{1+W_{-1}\left(-2\delta\zeta \mathrm{e}^{-2\delta(\zeta+u^{\mathrm{B}}(x',t))}\right)} - \frac{W_0\left(-2\delta\zeta \mathrm{e}^{-2\delta(\zeta+u^{\mathrm{B}}(x',t))}\right)}{1+W_0\left(-2\delta\zeta \mathrm{e}^{-2\delta(\zeta+u^{\mathrm{B}}(x',t))}\right)} \right) \\ &\qquad\qquad \times u^{\mathrm{B}}(x',t) u_x^{\mathrm{B}}(x',t)\,\mathrm{d}x' \,. \quad (3.148) \end{aligned}$$

Since $W_{-1}(-\mathrm{e}^{-1}) = W_0(-\mathrm{e}^{-1}) = -1$ at the branch point, the first terms reduce to zero. For the integral term, we can change variables: $u = u^{\mathrm{B}}(x,t)$, $\mathrm{d}u = u_x^{\mathrm{B}}(x,t)\,\mathrm{d}x$. We have to do this on two separate intervals $[x_-(\zeta;t), x_{\max} + 2u_{\max}t]$ and $[x_{\max} + 2u_{\max}t, x_+(\zeta;t)]$ where $u^{\mathrm{B}}(x,t)$ is respectively increasing and decreasing. The value of $u^{\mathrm{B}}(x,t)$ at each of the turning points is the same $-E(\zeta)$.

$$\begin{aligned} R_t(\zeta;t) &= -2\int_{-E(\zeta)}^{u_{\max}} \left(\frac{W_{-1}\left(-2\delta\zeta \mathrm{e}^{-2\delta(\zeta+u)}\right)}{1+W_{-1}\left(-2\delta\zeta \mathrm{e}^{-2\delta(\zeta+u)}\right)} - \frac{W_0\left(-2\delta\zeta \mathrm{e}^{-2\delta(\zeta+u)}\right)}{1+W_0\left(-2\delta\zeta \mathrm{e}^{-2\delta(\zeta+u)}\right)} \right) u\,\mathrm{d}u \quad (3.149) \\ &\quad - 2\int_{u_{\max}}^{-E(\zeta)} \left(\frac{W_{-1}\left(-2\delta\zeta \mathrm{e}^{-2\delta(\zeta+u)}\right)}{1+W_{-1}\left(-2\delta\zeta \mathrm{e}^{-2\delta(\zeta+u)}\right)} - \frac{W_0\left(-2\delta\zeta \mathrm{e}^{-2\delta(\zeta+u)}\right)}{1+W_0\left(-2\delta\zeta \mathrm{e}^{-2\delta(\zeta+u)}\right)} \right) u\,\mathrm{d}u \\ &= 0\,, \quad (3.150) \end{aligned}$$

because the two integrals are clearly integrable, having no worse singularities than square-

roots at the $u = -E(\zeta)$ endpoints. This means $R(\zeta;t)$ is independent of t, and thus

$$R(\zeta;t) = R(\zeta)\,. \tag{3.151}$$

Next, we consider the t-dependence of the function that determines the norming constants (2.386)

$$\theta_+(\zeta;t) := \mathrm{Im}\,[\zeta]\,x_+(\zeta;t) + \int_{x_+(\zeta;t)}^{+\infty} \mathrm{Im}\left[\zeta + \frac{1}{2\delta} W_{-1}\left(-2\delta\zeta \mathrm{e}^{-2\delta(\zeta+u^{\mathrm{B}}(x,t))}\right)\right] \mathrm{d}x\,. \tag{3.152}$$

Again, we compute the t-derivative of this to determine the dependence,

$$\begin{aligned}\theta_{+,t}(\zeta;t) &= 2\mathrm{Im}\,[\zeta]\,E(\zeta) - 2E(\zeta)\,\mathrm{Im}\left[\zeta + \frac{1}{2\delta} W_{-1}\left(-2\delta\zeta \mathrm{e}^{-2\delta(\zeta+u^{\mathrm{B}}(x_+(\zeta;t),t))}\right)\right] \\ &\qquad - \int_{x_+(\zeta;t)}^{+\infty} \mathrm{Im}\left[\frac{W_{-1}\left(-2\delta\zeta \mathrm{e}^{-2\delta(\zeta+u^{\mathrm{B}}(x,t))}\right)}{1+W_{-1}\left(-2\delta\zeta \mathrm{e}^{-2\delta(\zeta+u^{\mathrm{B}}(x,t))}\right)}\right] u_t^{\mathrm{B}}(x,t)\,\mathrm{d}x \qquad (3.153)\\ &= -\frac{E(\zeta)}{\delta}\mathrm{Im}\left[W_{-1}(-\mathrm{e}^{-1})\right] \\ &\qquad + 2\int_{x_+(\zeta;t)}^{+\infty} \mathrm{Im}\left[\frac{W_{-1}\left(-2\delta\zeta \mathrm{e}^{-2\delta(\zeta+u^{\mathrm{B}}(x,t))}\right)}{1+W_{-1}\left(-2\delta\zeta \mathrm{e}^{-2\delta(\zeta+u^{\mathrm{B}}(x,t))}\right)}\right] u^{\mathrm{B}}(x,t) u_x^{\mathrm{B}}(x,t)\,\mathrm{d}x\,. \qquad (3.154)\end{aligned}$$

$W_{-1}(-\mathrm{e}^{-1}) = -1 \in \mathbb{R}$ so this first term is zero. We again change variables $u = u^{\mathrm{B}}(x,t)$, but this time $u^{\mathrm{B}}(x,t)$ is now only decreasing on $[x_+(\zeta;t), +\infty)$. Then, since what remains inside the integral is a derivative times u, we can integrate by parts:

$$\theta_{+,t}(\zeta;t) = -2\mathrm{Im}\left[\int_0^{-E(\zeta)} \frac{W_{-1}\left(-2\delta\zeta \mathrm{e}^{-2\delta(\zeta+u)}\right)}{1+W_{-1}\left(-2\delta\zeta \mathrm{e}^{-2\delta(\zeta+u)}\right)} u\,\mathrm{d}u\right] \tag{3.155}$$

$$= \left[\frac{1}{\delta}\mathrm{Im}\left[W_{-1}\left(-2\delta\zeta \mathrm{e}^{-2\delta(\zeta+u)}\right)\right] u\right]_0^{-E(\zeta)} - \frac{1}{\delta}\mathrm{Im}\left[\int_0^{-E(\zeta)} W_{-1}\left(-2\delta\zeta \mathrm{e}^{-2\delta(\zeta+u)}\right)\,\mathrm{d}u\right]. \tag{3.156}$$

The endpoint evaluations of the first term both give zero. Now we change variables once more to conduct the final integral to $w = W_{-1}(-2\delta\zeta \mathrm{e}^{-2\delta(\zeta+u)})$ which results in $\mathrm{d}w = -2\delta w/(1+$

$w)\,\mathrm{d}u$. The mapping is decreasing from $w = -2\delta\zeta$ to $w = -1$.

$$\theta_{+,t}(\zeta;t) = \frac{1}{2\delta^2}\mathrm{Im}\left[\int_{-2\delta\zeta}^{-1}(1+w)\,\mathrm{d}w\right] \tag{3.157}$$

$$= \frac{1}{2\delta^2}\mathrm{Im}\left[\left[\frac{(1+w)^2}{2}\right]_{-2\delta\zeta}^{-1}\right] \tag{3.158}$$

$$= -\mathrm{Im}\left[\left(\zeta - \frac{1}{2\delta}\right)^2\right]. \tag{3.159}$$

This with our initial value at $t = 0$, gives the result:

$$\theta_+(\zeta;t) = \theta_+(\zeta) - \mathrm{Im}\left[\left(\zeta - \frac{1}{2\delta}\right)^2\right]t\,. \tag{3.160}$$

From these results, we see that the statement of the variational conditions for u_0 as the initial potential at $0 < t < t_\mathrm{c}$ are equivalent to the variational conditions for $u^\mathrm{B}(\diamond,t)$ as the initial potential with no additional time dependence. Since $u^\mathrm{B}(\diamond,t)$ satisfies all of the same properties we required of the initial condition u_0 up to the critical time, the result above for $t = 0$ can be applied here to prove the chosen forms satisfy the original variational conditions for all $0 < t \leq t_\mathrm{c}$. □

This justifies *a posteriori* that the minimizing potential and density were indeed differentiable. We can also see immediately that

Corollary 3.4.4.1. *For all* $\zeta \in [1/2\delta, \zeta_\mathrm{max}]_{\mathcal{Q}_\delta}$,

$$L\{\rho^\mathrm{Wyl}\}(\zeta) = \int_{-\infty}^{+\infty}\mathrm{Im}\left[\zeta + \frac{1}{2\delta}W_{-1}\left(-2\delta\zeta^{-2\delta(\zeta+u_0(x))}\right)\right]\mathrm{d}x\,. \tag{3.161}$$

This just follows from considering the minimizing potential $L\{\rho^\mathrm{min}\}$ (3.142) and density ρ^min (3.144) at $t = 0$ and taking the limit as $x \to +\infty$. Since $\beta(x) \to 1/2\delta$, the only thing that remains is a saturation over all $[1/2\delta, \zeta_\mathrm{max}]_{\mathcal{Q}_\delta}$, which is by definition ρ^Wyl. By taking the limit in (3.143) and rearranging the x-dependent terms into (2.387), we get the proof of the first statement in Theorem 3.2.2.

Now we wish to upgrade the distributional limit to a strong L^2 limit. For this, we will need the following lemma.

Lemma 3.4.5.

$$\lim_{N\to\infty}\left|\left|u_N^\mathrm{ILW}(\diamond,t)\right|\right|_{L^2} = ||u_0||_{L^2} \tag{3.162}$$

uniformly for all $t \in \mathbb{R}$.

Proof. We work at fixed $t \in \mathbb{R}$ and begin with the fact that the N-soliton equation for any $N \in \mathbb{N}$ solves exactly the small dispersion ILW equation. Then we integrate this formula starting from negative infinity. Due to the exponential fall-off at infinity for the N-soliton formula and its derivatives, it is indeed integrable here. There are two terms in the ILW equation which are total derivatives, evaluating the anti-derivatives at $x = -\infty$ can be shown to be zero:

$$0 = \int_{-\infty}^{x} \partial_t u_N^{\mathrm{ILW}}(x', t; \epsilon_N) \, \mathrm{d}x' + \left(u_N^{\mathrm{ILW}}(x,t)\right)^2 + \epsilon_N \partial_x \mathcal{T}_{\delta\epsilon_N} \left[u_N^{\mathrm{ILW}}(\diamond, t)\right](x) \,. \tag{3.163}$$

If we use (3.49) as the N-soliton formula, we can take the integral in (3.163) and solve for the quadratic term,

$$\left(u_N^{\mathrm{ILW}}(x,t)\right)^2 = \mathrm{i}\epsilon_N \partial_t D_{\mathrm{i}\delta\epsilon_N} F_N(x,t) - \epsilon_N \partial_x \mathcal{T}_{\delta\epsilon_N} \left[u_N^{\mathrm{ILW}}(\diamond, t)\right](x) \,. \tag{3.164}$$

Now we integrate (3.164) over all $x \in \mathbb{R}$. Since the second term is a derivative, we can evaluate based on the difference of the endpoints. Additionally, given the functional form of u_N^{ILW} (3.49), $\mathcal{T}_{\delta\epsilon_N}$ (1.10) operates according to [42, Equation 5.144], where the convolution with the cotangent kernel acts akin to a Hilbert transform but on the strip $\mathcal{S}_{\delta\epsilon_N}$, i.e. turning the difference of boundary values into the sum, and the sgn convolution acts like twice a negative integral on the argument [42, Equation 5.149],

$$\int_{-\infty}^{+\infty} \partial_x \mathcal{T}_{\delta\epsilon_N} \left[u_N^{\mathrm{ILW}}(\diamond, t)\right](x) \, \mathrm{d}x = -\mathrm{i}\epsilon_N \left[\mathcal{T}_{\delta\epsilon_N} \left[\partial_x D_{\mathrm{i}\delta\epsilon_N} F_N(\diamond, t)\right](x)\right]_{-\infty}^{+\infty} \tag{3.165}$$

$$= \epsilon_N \Bigg[\partial_x F_N(x + \mathrm{i}\delta\epsilon_N, t) + \partial_x F_N(x - \mathrm{i}\delta\epsilon_N, t) - \frac{F_N(x + \mathrm{i}\delta\epsilon_N, t) - F_N(x - \mathrm{i}\delta\epsilon_N, t)}{\mathrm{i}\delta\epsilon_N}\Bigg]_{-\infty}^{+\infty} . \tag{3.166}$$

Considering the formula of F_N (3.47), and we recall that $E_S(z,t)$ is linear in z and t. The overall z-coefficients in the exponentials of (3.47) are $-2P_S/\pi\epsilon_N$, while the t-coefficients are $-2Q_S/\pi\epsilon_N$. From the positivity of $\mathrm{Im}\,[\zeta_n]$ and $\mathrm{Im}\,[(\zeta_n - 1/2\delta)^2]$, the minimal z-coefficient corresponds to $S = \mathbb{Z}_N$ and the maximal z-coefficient corresponds to $S = \varnothing$. Thus, if we consider $\mathrm{Re}\,[z] \to +\infty$, the maximum z-coefficient exponential, which is one, dominates, i.e. every other exponential in (3.47) decreases. This means that, regardless of the z-independent

terms in the exponentials,

$$\lim_{\mathrm{Re}[z]\to+\infty} F_N(z,t) = \lim_{\mathrm{Re}[z]\to+\infty} \log\left(1+\sum_{\substack{S\subset\mathbb{Z}_N\\S\neq\varnothing}} \exp\left(-\frac{2}{\epsilon_N^2\pi}E_S(z,t)\right)\right) = 0 \tag{3.167}$$

uniformly for all $-\delta\epsilon_N \leq \mathrm{Im}\,[z] \leq \delta\epsilon_N$. Now as $\mathrm{Re}\,[z] \to -\infty$, the minimal z-coefficient term exponentially dominates, i.e. after factoring out this term, the remaining sum is one plus terms whose magnitudes exponentially decrease. For $\mathrm{Im}\,[z] = 0$, we can split the log since we are working on the principal branch on the real positive axis. Then, to match the original log values, for $\mathrm{Im}\,[z] \neq 0$ we define the logs' branches via continuity. This means as $\mathrm{Re}\,[z] \to -\infty$

$$F_N(z,t) = \log\left(\exp\left(-\frac{2}{\epsilon_N^2\pi}E_{\mathbb{Z}_N}(z,t)\right)\left(1+\sum_{\substack{S\subset\mathbb{Z}_N\\S\neq\mathbb{Z}_N}} \exp\left(-\frac{2}{\epsilon_N^2\pi}\Big[E_S(z,t)-E_{\mathbb{Z}_N}(z,t)\Big]\right)\right)\right) \tag{3.168}$$

$$= -\frac{2}{\epsilon_N^2\pi}E_{\mathbb{Z}_N}(z,t) + o(1) \tag{3.169}$$

uniformly for all $-\delta\epsilon_N \leq y \leq \delta\epsilon_N$. Note that we could not take the limit since $E_{\mathbb{Z}_N}(z,t)$ blows up as $\mathrm{Re}\,[z] \to -\infty$. However, in the difference of boundary values that will be evaluated in (3.166), we use the linear form of $E_{\mathbb{Z}_N}(z,t)$ to separate real and imaginary parts, then the divergent real parts cancel and the result is a finite limit

$$\lim_{x\to-\infty} F_N(x+\mathrm{i}\delta\epsilon_N,t) - F_N(x-\mathrm{i}\delta\epsilon_N,t) = \lim_{x\to-\infty} -\frac{2}{\epsilon_N^2\pi}E_{\mathbb{Z}_N}(x+\mathrm{i}\delta\epsilon_N,t) + o(1) \tag{3.170}$$

$$+\frac{2}{\epsilon_N^2\pi}E_{\mathbb{Z}_N}(x-\mathrm{i}\delta\epsilon_N,t) + o(1) \tag{3.171}$$

$$= \lim_{x\to-\infty} -\frac{2}{\epsilon_N^2\pi}E_{\mathbb{Z}_N}(x,t) - \mathrm{i}\frac{2\delta}{\epsilon_N\pi}P_{\mathbb{Z}_N} \tag{3.172}$$

$$+\frac{2}{\epsilon_N^2\pi}E_{\mathbb{Z}_N}(x,t) - \mathrm{i}\frac{2\delta}{\epsilon_N\pi}P_{\mathbb{Z}_N} \tag{3.173}$$

$$= -\mathrm{i}\frac{4\delta}{\epsilon_N\pi}P_{\mathbb{Z}_N}\,. \tag{3.174}$$

Now, since $F_N(z,t)$ is analytic at the boundaries of the strip, the derivative in the real direction along the boundary is equivalent to the complex derivative. Then these derivative

boundary terms in (3.166) can be computed easily

$$\partial_z F_N(z,t) = \frac{\displaystyle\sum_{S\subset\mathbb{Z}_N} -\frac{2}{\epsilon_N^2\pi} P_S \exp\left(-\frac{2}{\epsilon_N^2\pi} E_S(z,t)\right)}{\displaystyle\sum_{S\subset\mathbb{Z}_N} \exp\left(-\frac{2}{\epsilon_N^2\pi} E_S(x,t)\right)}\,. \tag{3.175}$$

Again, we have that as $\mathrm{Re}\,[z] \to +\infty$, the denominator limits to one. Moreover, in the numerator, the only exponential term which has nonzero limit, $S = \varnothing$, is multiplied by $P_\varnothing = 0$, and so the numerator limits to zero

$$\lim_{\mathrm{Re}[z]\to+\infty} \partial_z F_N(z,t) = 0 \tag{3.176}$$

uniformly for all $-\delta\epsilon_N \le \mathrm{Im}\,[z] \le \delta\epsilon_N$. Similarly for $\mathrm{Re}\,[z] \to -\infty$, we factor out the $S = \mathbb{Z}_N$ exponential terms in both the numerator and denominator. The sums over the remaining exponentials all limit to zero and we have

$$\lim_{\mathrm{Re}[z]\to-\infty} \partial_z F_N(z,t) = \lim_{\mathrm{Re}[z]\to-\infty} -\frac{2}{\epsilon_N^2\pi} \frac{P_{\mathbb{Z}_N} + \displaystyle\sum_{\substack{S\subset\mathbb{Z}_N \\ S\neq\mathbb{Z}_N}} P_S \exp\left(-\frac{2}{\epsilon_N^2\pi}\Big[E_S(z,t) - E_{\mathbb{Z}_N}(z,t)\Big]\right)}{1 + \displaystyle\sum_{\substack{S\subset\mathbb{Z}_N \\ S\neq\mathbb{Z}_N}} \exp\left(-\frac{2}{\epsilon_N^2\pi}\Big[E_S(z,t) - E_{\mathbb{Z}_N}(z,t)\Big]\right)} \tag{3.177}$$

$$= -\frac{2}{\epsilon_N^2\pi} P_{\mathbb{Z}_N} \tag{3.178}$$

uniformly for all $-\delta\epsilon_N \le \mathrm{Im}\,[z] \le \delta\epsilon_N$. Plugging these results back into (3.166), we see that all terms miraculously cancel,

$$\int_{-\infty}^{+\infty} \partial_x \mathcal{T}_{\delta\epsilon_N}\left[u_N^{\mathrm{ILW}}(\diamond,t;\epsilon_N)\right](x)\,\mathrm{d}x = \epsilon_N\left(0 + \frac{2}{\epsilon_N^2\pi}P_{\mathbb{Z}_N} + \frac{2}{\epsilon_N^2\pi}P_{\mathbb{Z}_N} - \frac{1}{\mathrm{i}\delta\epsilon_N}\mathrm{i}\frac{4\delta}{\epsilon_N\pi}P_{\mathbb{Z}_N}\right) = 0\,. \tag{3.179}$$

Taking this into account with (3.164), we get

$$\int_{-\infty}^{+\infty} \left(u_N^{\mathrm{ILW}}(x,t)\right)^2 \mathrm{d}x = \mathrm{i}\epsilon_N \int_{-\infty}^{+\infty} \partial_t D_{\mathrm{i}\delta\epsilon_N} F_N(x,t)\,\mathrm{d}x\,. \tag{3.180}$$

We may exchange the differentiation and finite difference evaluation, thus focusing for a

moment on

$$\partial_t F_N(z,t) = \frac{\displaystyle\sum_{S\subset\mathbb{Z}_N} -\frac{2}{\epsilon_N^2\pi} Q_S \exp\left(-\frac{2}{\epsilon_N^2\pi} E_S(z,t)\right)}{\displaystyle\sum_{S\subset\mathbb{Z}_N} \exp\left(-\frac{2}{\epsilon_N^2\pi} E_S(z,t)\right)}\,. \tag{3.181}$$

Looking at the large $\mathrm{Re}\,[z]$ limits of this function, they are identical to analyzing the z-derivative above.

$$\lim_{\mathrm{Re}[z]\to+\infty} \partial_t F_N(z,t) = 0 \quad \text{and} \quad \lim_{\mathrm{Re}[z]\to-\infty} \partial_t F_N(z,t) = -\frac{2}{\epsilon_N^2\pi} Q_{\mathbb{Z}_N} \tag{3.182}$$

uniformly for all $-\delta\epsilon_N \le \mathrm{Im}\,[z] \le \delta\epsilon_N$. Moreover, we note that the rate of convergence is exponential in $\mathrm{Re}\,[z]$. Now, consider the contour $C(a,b)$, positively oriented, that is the boundary of the rectangular strip segment $R(a,b) = \{\ z \in \mathcal{S}_{\delta\epsilon_N} \mid \mathrm{Re}\,[z] \in [a,b]\ \}$. Since $\partial_t F_N(z,t)$ is analytic in and on the boundary of the strip, we have that

$$\begin{aligned}
0 &= \int_{C(a,b)} \partial_t F_N(z,t)\,\mathrm{d}z && (3.183)\\
&= \int_a^b \partial_t F_N(x - \mathrm{i}\delta\epsilon_N, t)\,\mathrm{d}x + \int_b^a \partial_t F_N(x + \mathrm{i}\delta\epsilon_N, t)\,\mathrm{d}x && (3.184)\\
&\quad + \int_{-\delta\epsilon_N}^{\delta\epsilon_N} \partial_t F_N(b + \mathrm{i}y, t)\ \mathrm{i}\mathrm{d}y + \int_{\delta\epsilon_N}^{-\delta\epsilon_N} \partial_t F_N(a + \mathrm{i}y, t)\ \mathrm{i}\mathrm{d}y && (3.185)\\
&= -\int_a^b D_{\mathrm{i}\delta\epsilon_N} \partial_t F_N(x,t)\,\mathrm{d}x + \mathrm{i}\int_{-\delta\epsilon_N}^{\delta\epsilon_N} \Big(\partial_t F_N(b + \mathrm{i}y, t) - \partial_t F_N(a + \mathrm{i}y, t)\Big)\,\mathrm{d}y\,. && (3.186)
\end{aligned}$$

Solving for the x-integral and taking the limits as $a \to -\infty$ and $b \to +\infty$, the integral converges due to the uniform exponential convergence of $\partial_t F_N$ to a constant in either directions. The y-integral on the other side then also converges to the integral of the constant asymptotic values,

$$\int_{-\infty}^{+\infty} D_{\mathrm{i}\delta\epsilon_N} \partial_t F_N(x,t)\,\mathrm{d}x = \mathrm{i}\int_{-\delta\epsilon_N}^{\delta\epsilon_N} \Big(0 + \frac{2}{\epsilon_N^2\pi} Q_{\mathbb{Z}_N}\Big)\,\mathrm{d}y = \mathrm{i}\frac{4\delta}{\epsilon_N\pi} Q_{\mathbb{Z}_N}\,. \tag{3.187}$$

Combining with (3.180) gives

$$\int_{-\infty}^{+\infty} \big(u_N^{\mathrm{ILW}}(x,t)\big)^2\,\mathrm{d}x = -\frac{4\delta}{\pi} Q_{\mathbb{Z}_N}\,. \tag{3.188}$$

Note up until now, all of the steps have been exact and this equality is independent of the

choice $t \in \mathbb{R}$. Thus, we now evoke Theorem 3.2.1 which implies that

$$\lim_{N\to\infty} Q_{\mathbb{Z}_N} = \lim_{N\to\infty} \int \operatorname{Im}\left[\left(\zeta - \frac{1}{2\delta}\right)^2\right] \mathrm{d}\mu_{\mathbb{Z}_N}(\kappa) \tag{3.189}$$

$$= \int_0^{\kappa_{\max}} \operatorname{Im}\left[\left(\zeta - \frac{1}{2\delta}\right)^2\right] \rho^{\mathrm{Wyl}}(\kappa)\,\mathrm{d}\kappa\,. \tag{3.190}$$

We can conduct this final integral by pulling the imaginary part outside of the integral, and then use the formula for ρ^{Wyl} (3.32). This formula involves the x-integral of the difference across the quadratrix of the boundary values of a function analytic away from an x-dependent cut along the quadratrix $[\beta(x)^*, \beta(x)]_{\mathcal{Q}_\delta}$. Since the difference is zero off of the cut, we have on all $[\zeta^*_{\max}, \zeta_{\max}]_{\mathcal{Q}_\delta}$

$$\rho^{\mathrm{Wyl}}(\kappa) = \frac{\zeta'(\kappa)E'(\zeta)}{2} \int_{-\infty}^{+\infty} \left[\frac{W\left(-2\delta\zeta \mathrm{e}^{-2\delta(\zeta+u_0(x))}\right)}{1+W\left(-2\delta\zeta \mathrm{e}^{-2\delta(\zeta+u_0(x))}\right)}\right]_{\zeta(\kappa)^-}^{\zeta(\kappa)^+} \mathrm{d}x\,, \tag{3.191}$$

where the square brackets are to indicate that the difference is take between the two evaluations and the $\pm$ in the evaluations indicate the boundary, $+$ inside and $-$ outside the quadratrix. We may interchange the order of the difference with the integration and we may remove a derivative in ζ since this is a total derivative

$$\rho^{\mathrm{Wyl}}(\kappa) = -\frac{\zeta'(\kappa)}{4\delta} \left[\partial_\zeta \int_{-\infty}^{+\infty} \zeta + W\left(-2\delta\zeta \mathrm{e}^{-2\delta(\zeta+u_0(x))}\right)\,\mathrm{d}x\right]_{\zeta(\kappa)^-}^{\zeta(\kappa)^+}. \tag{3.192}$$

The formula being a difference of boundary values of an analytic function with a factor of $\zeta'(\kappa)$ out front, along with the odd symmetry, lets us write (3.190) using a contour oriented positively along the two sides of the cut,

$$\int_0^{\kappa_{\max}} \operatorname{Im}\left[\left(\zeta - \frac{1}{2\delta}\right)^2\right] \rho^{\mathrm{Wyl}}(\kappa)\,\mathrm{d}\kappa$$

$$= \frac{1}{8\delta}\operatorname{Im}\left[\int_C \left(\zeta - \frac{1}{2\delta}\right)^2 \partial_\zeta \int_{-\infty}^{+\infty} \zeta + W\left(-2\delta\zeta \mathrm{e}^{-2\delta(\zeta+u_0(x))}\right)\,\mathrm{d}x\,\mathrm{d}\zeta\right] \tag{3.193}$$

$$= -\frac{1}{4\delta}\operatorname{Im}\left[\int_C \left(\zeta - \frac{1}{2\delta}\right) \int_{-\infty}^{+\infty} \zeta + W\left(-2\delta\zeta \mathrm{e}^{-2\delta(\zeta+u_0(x))}\right)\,\mathrm{d}x\,\mathrm{d}\zeta\right], \tag{3.194}$$

where we used integration by parts. The Laurent series (3.116) is integrable near $\zeta = \infty$

because of the ζ that is added in the integrand. With $y = 2\delta u_0(x)$ set, we get

$$\int_{-\infty}^{+\infty} W\left(-2\delta\zeta \mathrm{e}^{-2\delta(\zeta+u_0(x))}\right) \mathrm{d}x$$

$$= \int_{-\infty}^{+\infty} -u_0(x) - \frac{u_0(x)}{\zeta} + \frac{1}{\zeta^2}\left(\frac{\big(u_0(x)\big)^2}{2} - \frac{u_0(x)}{2\delta}\right) + O\left(\frac{1}{\zeta^3}\right) \mathrm{d}x \tag{3.195}$$

$$= -\left(1 + \frac{1}{\zeta} + \frac{1}{2\delta\zeta^2}\right)\int_{-\infty}^{+\infty} u_0(x)\,\mathrm{d}x + \frac{1}{2\zeta^2}\int_{-\infty}^{+\infty} \big(u_0(x)\big)^2\,\mathrm{d}x + O\left(\frac{1}{\zeta^3}\right). \tag{3.196}$$

Using Cauchy's theorem, we can push the contour in (3.194) off to infinity and evaluate using the Laurent series (3.196) by residue,

$$\int_0^{\kappa_{\max}} \mathrm{Im}\left[\left(\zeta - \frac{1}{2\delta}\right)^2\right] \rho^{\mathrm{Wyl}}(\kappa)\,\mathrm{d}\kappa = -\frac{\pi}{4\delta}\int_{-\infty}^{+\infty} \big(u_0(x)\big)^2\,\mathrm{d}x\,. \tag{3.197}$$

Combining (3.197) with (3.190), (3.188), and taking a square-root, we have (3.162). □

With Lemma 3.4.5 and 3.3.1, following the logic of [34, 35, Theorems 2.12, 4.2, 4.3, and 4.5], it is straightforward to show

Theorem 3.4.6. *$u_N^{\mathrm{ILW}}(\diamond, t)$ converges strongly in $L^2(\mathbb{R})$ to the solution of invicid Burgers' equation $u(x,t)$ as $N \to +\infty$ and uniformly for all of $0 \le t < t_{\mathrm{c}}$.*

CHAPTER 4

Universality in the Benjamin-Ono Small Dispersion Limit for Rational Initial Data

As discussed in Section 1.3, the BO equation has eluded any strong or uniform approximations of the small dispersion limit up until now. Gérard's formula [23] constitutes a large step forward by providing an explicit solution (1.74) to the BO equation. In our analysis, we restrict ourselves to considering real rational initial conditions: let $N \in \mathbb{N}$, $c_1, \ldots, c_N \in \mathbb{C}$ be some nonzero coefficients and $p_1, \ldots, p_N \in \mathbb{C}$ be some poles in the upper half-plane, i.e. $\mathrm{Im}\,[p_k] > 0$ for all $1 \leq k \leq N$, and define the initial condition

$$u_0(x) = \sum_{k=1}^{N} \frac{c_k}{x - p_k} + \frac{c_k^*}{x - p_k^*}\,. \tag{4.1}$$

As Blackstone, Gassot, Gérard and Miller have recently found [6], the solution of the small dispersion BO equation (1.78) for

$$u(x, 0; \epsilon) = u_0(x) \tag{4.2}$$

and for all $\epsilon > 0$, is expressed as a ratio of $N + 1 \times N + 1$ matrix determinants:

$$u(x, t; \epsilon) = 2\mathrm{Re}\left[\frac{D_0(x, t; \epsilon)}{D(x, t; \epsilon)}\right] \tag{4.3}$$

with the definitions

$$D_0(x,t;\epsilon) = \begin{vmatrix} \int_{C_0} u_0(z)\mathrm{e}^{-\mathrm{i}h(z;x,t)/\epsilon}\,\mathrm{d}z & \int_{C_0} \dfrac{\mathrm{e}^{-\mathrm{i}h(z;x,t)/\epsilon}}{z-p_1}\mathrm{d}z & \cdots & \int_{C_0} \dfrac{\mathrm{e}^{-\mathrm{i}h(z;x,t)/\epsilon}}{z-p_N}\mathrm{d}z \\ \int_{C_1} u_0(z)\mathrm{e}^{-\mathrm{i}h(z;x,t)/\epsilon}\,\mathrm{d}z & \int_{C_1} \dfrac{\mathrm{e}^{-\mathrm{i}h(z;x,t)/\epsilon}}{z-p_1}\mathrm{d}z & \cdots & \int_{C_1} \dfrac{\mathrm{e}^{-\mathrm{i}h(z;x,t)/\epsilon}}{z-p_N}\mathrm{d}z \\ \vdots & \vdots & \ddots & \vdots \\ \int_{C_N} u_0(z)\mathrm{e}^{-\mathrm{i}h(z;t,x)/\epsilon}\,\mathrm{d}z & \int_{C_N} \dfrac{\mathrm{e}^{-\mathrm{i}h(z;t,x)/\epsilon}}{z-p_1}\mathrm{d}z & \cdots & \int_{C_N} \dfrac{\mathrm{e}^{-\mathrm{i}h(z;t,x)/\epsilon}}{z-p_N}\mathrm{d}z \end{vmatrix}, \quad (4.4)$$

$$D(x,t;\epsilon) = \begin{vmatrix} \int_{C_0} \mathrm{e}^{-\mathrm{i}h(z;x,t)/\epsilon}\,\mathrm{d}z & \int_{C_0} \dfrac{\mathrm{e}^{-\mathrm{i}h(z;x,t)/\epsilon}}{z-p_1}\mathrm{d}z & \cdots & \int_{C_0} \dfrac{\mathrm{e}^{-\mathrm{i}h(z;x,t)/\epsilon}}{z-p_N}\mathrm{d}z \\ \int_{C_1} \mathrm{e}^{-\mathrm{i}h(z;x,t)/\epsilon}\,\mathrm{d}z & \int_{C_1} \dfrac{\mathrm{e}^{-\mathrm{i}h(z;x,t)/\epsilon}}{z-p_1}\mathrm{d}z & \cdots & \int_{C_1} \dfrac{\mathrm{e}^{-\mathrm{i}h(z;x,t)/\epsilon}}{z-p_N}\mathrm{d}z \\ \vdots & \vdots & \ddots & \vdots \\ \int_{C_N} \mathrm{e}^{-\mathrm{i}h(z;t,x)/\epsilon}\,\mathrm{d}z & \int_{C_N} \dfrac{\mathrm{e}^{-\mathrm{i}h(z;t,x)/\epsilon}}{z-p_1}\mathrm{d}z & \cdots & \int_{C_N} \dfrac{\mathrm{e}^{-\mathrm{i}h(z;t,x)/\epsilon}}{z-p_N}\mathrm{d}z \end{vmatrix}, \quad (4.5)$$

and where $C_0, \ldots, C_N$ are some particular contours of integration which lie in the domain of analyticity of the exponent function

$$h(z;x,t) := \frac{(z-x)^2}{4t} + \sum_{j=1}^{N} \left[c_j \left(\log\left(\mathrm{e}^{\mathrm{i}\pi/4}(z-p_j)\right) + \mathrm{i}\frac{\pi}{4} \right) + c_j^* \left(\log\left(\mathrm{e}^{-\mathrm{i}3\pi/4}(z-p_j^*)\right) + \mathrm{i}\frac{\pi}{4} \right) \right]. \quad (4.6)$$

Before defining the integration contours, we first note that the large z behavior of h is dominated by the quadratic term. Looking at the modulus of the exponential terms in the integrand, we realize that the integrand decays rapidly when z heads off to infinity with asymptotic argument $-\pi/4$ or $3\pi/4$. It is now meaningful why the particular anti-derivative of u_0 in (4.6) was chosen, i.e. so the branch cuts of the logarithms aligned with these directions. Integrals over contours that extend between these branch cuts and out to infinity will therefore be absolutely convergent. We let the contours $C_1, \ldots, C_N$ be any basis of the homotopy class of contours which completely connect all of the $N-1$ "troughs" between the N branch cuts and the two sectors to either side of all of the branch cuts in the upper half-plane. The contour C_0 is reserved for a contour that connects any of the troughs or sectors in the upper half-plane, to the sector to the right of all of the branch cuts in the lower half-plane. See Figure 4.1 for an example set of such contours.

It does not matter to the solution (4.3) which basis of the homotopy class we choose; this is because the determinant allows us to, after expressing any basis of contours in terms of another, expand rows along contour contributions and eliminate determinants that have

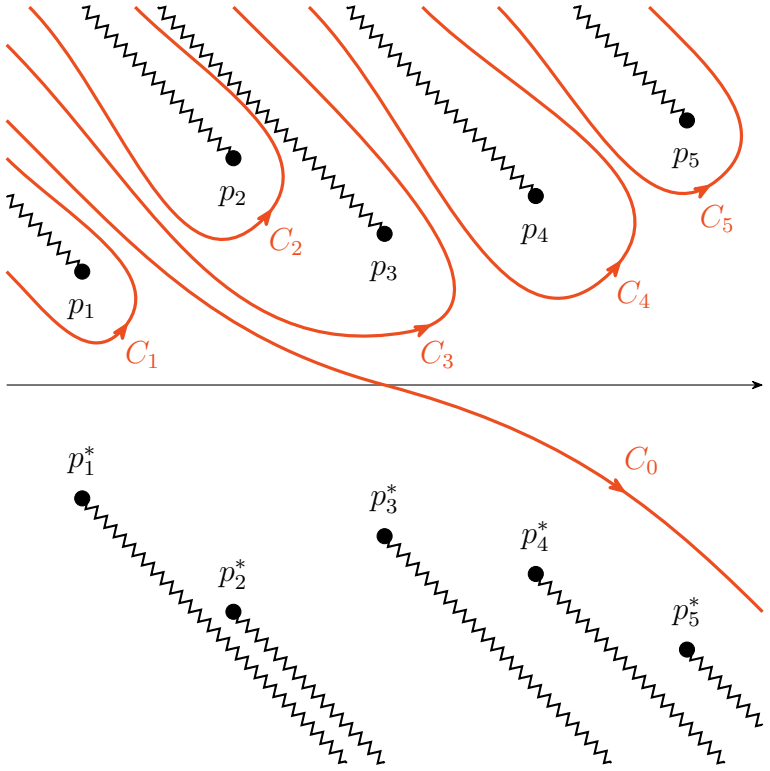


Figure 4.1: Example for $N = 5$ of some admissible contours $C_1, \ldots, C_5$ for the Benjamin-Ono solution with initial rational data.

the same contours contributing to different rows until only the new basis contours are represented, one in each row. The final determinant may pick up an overall nonzero (due to linear independence of a basis) coefficient, but the ratio eliminates this coefficient as the same manipulations have to be carried out in the numerator as in the denominator.

We neglected to mention that for some pole positions $p_1, \ldots, p_N$, it may happen that two or more lie along the same branch cut, and there is no actual trough between those branch cuts. However, as we will make explicit use of latter, we may modify the branch cut definitions so as to have some cuts extend vertically first and then travel their 45° paths out to infinity which ensures there are indeed always $N-1$ troughs. The resulting exponential function h is still valid in the solution (4.3). For completeness, we note that by [7], if it were the case that $\mathrm{e}^{-\mathrm{i}h(z;t,x)/\epsilon}$ were analytic at any of the poles, which would be whenever $\mathrm{i}c_j/\epsilon \in \mathbb{N}$ for some $1 \leq j \leq N$, then the contour that should go around it has to instead terminate at the point p_j. However, we will make an assumption later that excludes this scenario.

4.1 Steepest Descent Analysis of the Exponential Integrals

Since all elements of the matrix determinants (4.4) and (4.5) are exponential integrals with analytic integrands (so long as the contours stay away from the branch cuts) and have exponents proportional to the large parameter $1/\epsilon$, we are immediately implored to attempt a steepest descent analysis. The saddle points of h are characterized by the condition

$$0 = h_z(z;x,t) = \frac{z-x}{2t} + u_0(z)\,. \tag{4.7}$$

Since u_0 is rational, we can clear fractions to write the equivalent form of h_z,

$$h_z(z;x,t) = \frac{Q(z;x,t)}{2t\ P(z)} \tag{4.8}$$

where $P(z)$ and $Q(z;x,t)$ are the polynomials in z

$$P(z) := \prod_{j=1}^{N} (z-p_j)(z-p_j^*)\,, \tag{4.9}$$

$$Q(z;x,t) := (z-x)P(z) + 4t\sum_{j=1}^{N} \left(\mathrm{Re}\,[c_j]\,z - \mathrm{Re}\left[c_j p_j^*\right]\right) \prod_{k\neq j} (z-p_k)(z-p_k^*)\,. \tag{4.10}$$

Thus, from a straightforward computation, P is degree $2N$ and Q is degree $2N+1$ in z. This means there are $2N+1$ saddle points with multiplicity, specifically the roots of $Q(\diamond; x, t)$. One may suspect that the number of true solutions could be reduced if a root of $Q(\diamond; x, t)$ happens to coincide with one of P. However, all of the roots of P are present as poles in u_0 and thus h_z, so this can never be.

Since P and Q are Schwarz symmetric in z, there is always an odd number of real saddle points since the complex ones always come in conjugate pairs. We can define the integer spacetime function $J : \mathbb{R}^2 \to \mathbb{N}_0$ such that $2J(x,t)+1$ counts the number of real saddle points, with multiplicity. Note $0 \leq J(x,t) \leq N$, and this leaves a total of $2N - 2J(x,t)$ complex saddle points with multiplicity, $N - J(x,t)$ in the upper or lower half-planes. When working in a subset of spacetime where $J(x,t) = J$ is constant, we label the real saddle points $y_0(x,t) \geq \cdots \geq y_{2J}(x,t)$ and the complex saddle points in the upper half-plane $z_{J+1}(x,t), \ldots, z_N(x,t)$, noting that the labels of the saddle points in the upper half-plane are not important as long as they are chosen so that the resulting functions of x and t are continuous. This can always be done because the coefficients of the powers of z in Q depend on x and t in a continuous manner. Moreover, the definition of the labeling of the real saddle points also guarantees they are continuous in x and t.

Looking back at (4.7), we notice that the real saddle points satisfy

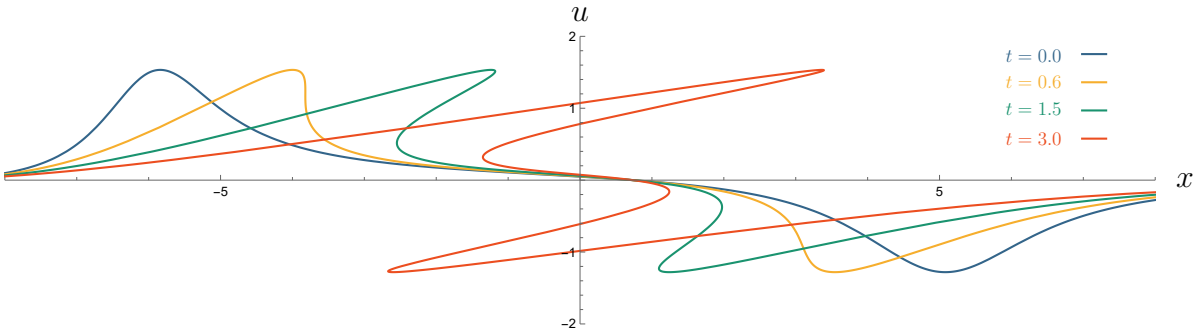
$$0 = y_j(x,t) - x + 2u_0\big(y_j(x,t)\big)t\,. \tag{4.11}$$

Comparing with (1.83), we see the saddle points $y_j(x,t)$ are exactly the origin points at $t=0$ of the inviscid Burgers' characteristics, with initial condition u_0, which have traveled to the point (x,t). This means that the potentially multivalued invicid Burgers' solution branches can be written in terms of the real saddle points

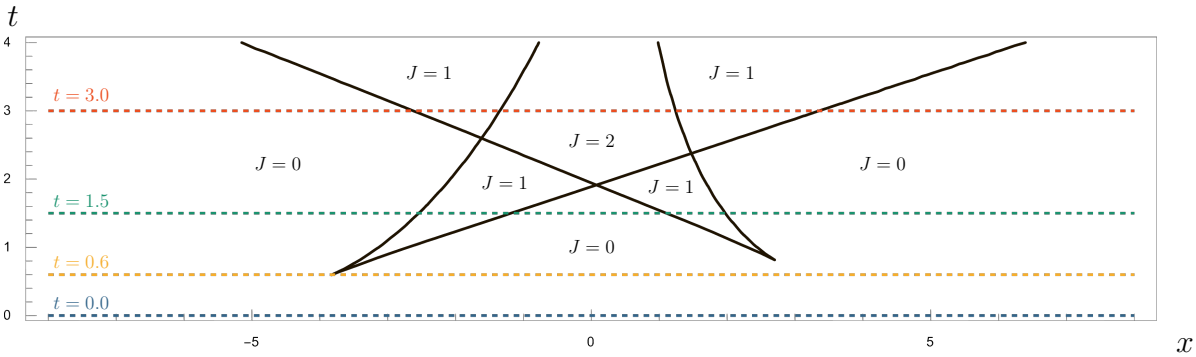
$$u_j^{\mathrm{B}}(x,t) = u_0\big(y_j(x,t)\big) \text{ for } 0 \leq j \leq 2J. \tag{4.12}$$

For characteristics that meet at a point (x,t) with $t > 0$, those that begin further to the left must have a greater velocity that those that begin further to the right. Since the velocities are determined as in (1.81) and the value along the characteristics are (1.82), this means that the chosen ordering of the saddle points admits the ordering of the branches $u_0^{\mathrm{B}}(x,t) \leq \cdots \leq u_{2J}^{\mathrm{B}}(x,t)$.

For $t > 0$, we know that inviscid Burgers' equation forms a shock for every local minimum $x_{\min}$ of u_0' at time $t_{\mathrm{shock}} = -1/u_0''(x_{\min})$. If $u_0'''(x_{\min}) \neq 0$, then three local branches of the solution are produced after the shock point. The spatial interval where these branches overlap grows as time moves forward, owed to the right edge where the upper two branches meet



(a) The multivalued solution of invicid Burgers' equation for $x \in [-7, 7]$ and at select times. Note that the positive levels on the left travel to the right with greater velocity corresponding to a higher level and vice versa for the negative levels on the left.



(b) The spacetime region $x \in [-7, 7]$ and $t \in [0, 4]$ with several time slices indicated and the corresponding solution as a function of x shown in Figure 4.2a. The caustic curves are shown in black and the regions that the separate have their J values labeled.

Figure 4.2: A multivalued solution to Burgers' equation with initial condition corresponding to $N = 2$, $c_1 = 1/4 - \mathrm{i}3/4$, $c_2 = -1/10 - \mathrm{i}1/2$, $p_1 = -6 + \mathrm{i}$ and $p_2 = 5 + \mathrm{i}3/2$.

being higher than the left edge where the lower two branches meet, and thus the difference in speeds is positive. In spacetime regions like these $J = 1$ and for every point (x, t) in the interior, there are three distinct characteristics which originate from three distinct points, $y_0(x,t), y_1(x,t)$ and $y_2(x,t)$, that travel through the point (x,t). If we assume the branches from any other shocks remain outside of this area of spacetime, then as we move towards either the left or right edges of the $J = 1$ region, two of the branches must approach each other. Correspondingly, the origin points of the associated characteristics must also approach each other, until at the edge they fuse into one. These edges are called *caustic curves* and mark a distinct change in the behavior of the characteristics. On the other side of these caustics are regions where $J = 0$. This means, watching the saddle points as we hold t fixed and move x from inside the $J = 1$ region, through the caustic curve boundary into the $J = 0$ region, we would see two saddle points collide at the x value along the edge and then move off of the real axis becoming a complex-conjugate pair. Along the caustic curve, since two simple saddle points have fused together, we must have a real, double saddle point characterized by

$$0 = h_{zz}(z) = \frac{1}{2t} + u_0'(z) \tag{4.13}$$

in addition to (4.7). As has been anticipated by previous works [55] and was recently shown rigorously [6], $J = 1$ regions exactly correspond to the simplest form of a dispersive shock wave in the small dispersion limit with wavelength $O(\epsilon)$. If we view this dispersive shock wave as being comprised of rank ordered, nonlinearly interacting solitons with widths $O(\epsilon)$ that travel to the right, then at the right edge is where the tallest and fastest solitons will be emerging from the dispersive shock wave. For this reason we will denote the right caustic $x_{\mathrm{s}}(t)$ for $t \in K_{\mathrm{s}}$ a compact interval such that the caustic does not contact any shock points or any other caustic boundaries which cross into or out of the $J = 1$ region. We refer to this as the *soliton edge*. Since this is where the two upper Burgers' branches meet, this edge can be characterized in terms of the saddle points of h_z as when there is exactly one simple $y_0(t)$ and one double $y_{\mathrm{s}}(t)$ real saddle point with $y_{\mathrm{s}}(t) < y_0(t)$.

Conversely, the left edge is referred to as the *dispersive edge* and denoted $x_{\mathrm{d}}(t)$ for $t \in K_{\mathrm{d}}$ a compact interval, again requiring that the caustic curve does not contact any shock points or other caustics. Since this is where the two lower branches meet, the dispersive edge can be identified by the saddle points of h_z as where there is exactly one simple $y_2(t)$ and one double $y_{\mathrm{d}}(t)$ real saddle points such that $y_2(t) < y_{\mathrm{d}}(t)$. At these edges, we can parameterize all of the complex simple saddle points by t as well with notation $z_j(t) = z_j(x_{\mathrm{s,d}}(t), t)$. At the soliton edge, we also have $y_0(t) = y_0(x_{\mathrm{s}}(t), t)$ and $y_{\mathrm{s}}(t) = y_1(x_{\mathrm{s}}(t), t) = y_2(x_{\mathrm{s}}(t), t)$ while at the dispersive edge $y_{\mathrm{d}}(t) = y_0(x_{\mathrm{s}}(t), t) = y_1(x_{\mathrm{s}}(t), t)$ and $y_2(t) = y_2(x_{\mathrm{s}}(t), t)$. We acknowledge

that only the notation on the double saddle points makes explicit which edge the evaluation is occurring at, but in the subsequent analysis, this will be clear from context.

Since the saddle point condition (4.7) is always satisfied for $x_{\mathrm{s,d}}(t)$ at the double saddle point, we can solve for $x_{\mathrm{s,d}}(t)$, differentiate, and then make use of (4.13) to determine the instantaneous speed of the caustic

$$v_{\mathrm{s,d}}(t) = x'_{\mathrm{s,d}}(t) = \big(1 + 2u_0\big(y_{\mathrm{s,d}}(t)\big)t\big)\, y'_{\mathrm{s,d}}(t) + 2u_0\big(y_{\mathrm{s,d}}(t)\big) = 2u^{\mathrm{B}}_{\mathrm{s,d}}(t)\,. \tag{4.14}$$

4.1.1 Choice of Contours for steepest descent analysis

In [6] the authors describe an extensive constructive procedure for a basis of contours that are amenable to steepest descent analysis in the case where all of the saddle points of h are simple. Since we are interested in an explicit situation where two saddle points are colliding, becoming a double saddle point, we cannot use this construction without first some modification.

We now describe briefly the results of the indicated construction of the steepest descent analysis contours. For the full, detailed construction, which involves moving the branch cuts of the logarithms in h, forming contours as the unions of arcs of steepest descent contours and level contours of $\mathrm{Im}\,[h]$, as well as as the application of some graph theory to the connected network of contours, we direct the reader to [6, Section 4]. We note that this construction requires the condition that $\mathrm{Re}\,[c_j] \neq 0$ and $\mathrm{Im}\,[c_j] \neq 0$ for all $1 \leq j \leq N$. For each simple saddle point in the upper-half plane $z_j(x,t)$, i.e. for each $J+1 \leq j \leq N$, a contour $W_{z_j}(x,t)$ is constructed which:

1. traverses the saddle point along a finite arc of its steepest descent contour $S_{z_j}(x,t)$,
2. has $\mathrm{Im}\,[h(z;x,t)]$ stay below the levels at the endpoints of S_{z_j} along the remainder of the contour,
3. winds once around around a single pole p_k which is uniquely identified with the saddle point $z_j(x,t)$,
4. and has asymptotic argument $3\pi/4$ as both ends of the contour travel off to infinity.

For the simple real saddle points, since h is Schwarz symmetric, the steepest descent contours always traverse the real axis at $\pm 45°$. For $y_0(x,t)$, we can construct the contour $W_{y_0}(x,t)$ which:

1. traverses the saddle point along a finite arc of its steepest descent contour $S_{y_0}(x,t)$,

2. has $\mathrm{Im}\,[h(z;x,t)]$ stay below the levels at the endpoints of $S_0(x,t)$ along the remainder of the contour,

3. has an asymptotic argument of $3\pi/4$ at the beginning of the contour,

4. and an asymptotic argument of $-\pi/4$ at the end of the contour.

When $J=1$, we have constructed N total contours, $N-1$ for the complex saddle points and one for the real saddle point $y_0(x,t)$. The final contour $W_{y_{1,2}}(x,t)$ is constructed with the properties:

1. it traverses the saddle point $y_2(x,t)$ along a finite arc of its steepest descent contour $S_{y_2}(x,t)$ from the upper half plane to the lower-half plane,

2. takes a straight line segment a fixed distance below the real axis from the end point of $S_{y_2}(x,t)$ to the end point of $S_{y_1}(x,t)$, a finite arc of the steepest descent contour over the saddle point $y_1(x,t)$ traveling from the lower half-plane to the upper half-plane,

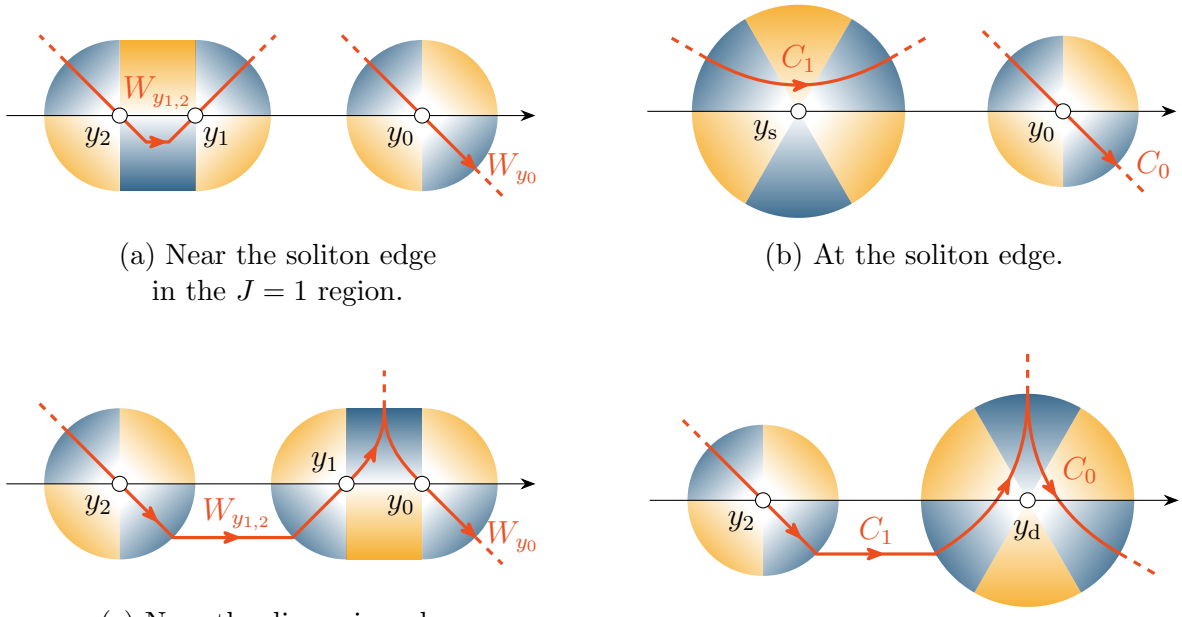
3. has $\mathrm{Im}\,[h(z;x,t)]$ stay below the levels at the endpoints of $S_{y_2}(x,t)$ and $S_{y_1}(x,t)$ along the remainder of the contour,

4. it winds once around around the remaining pole which is not represented in the contours $W_{z_2}(x,t),\ldots,W_{z_N}(x,t)$,

5. and has asymptotic argument $3\pi/4$ as both ends of the contour as it travels off to infinity.

This contour finishes the basis for $J=1$ with simple saddle points: $W_{y_0}(x,t), W_{y_{1,2}}(x,t), W_{z_2}(x,t),\ldots,W_{z_N}(x,t)$.

We are interested in a basis of contours that are amenable to steepest descent analysis when two real saddle points collide, right at the transition between a $J=0$ and $J=1$ spacetime region. First, we require that no other saddle points are colliding at the soliton or dispersive edges, $(x_{\mathrm{s,d}}(t),t)$ for $t\in K_{\mathrm{s,d}}$. If that is the case, by continuity of the saddle points, there is some $\delta>0$ such that for all $|x-x_{\mathrm{s,d}}(t)|<\delta$, all complex saddle points and the noncolliding real saddle point remain simple for all $t\in K_{\mathrm{s,d}}$. Additionally, we can take δ small enough that the two colliding saddle points are always interior to a fixed radius disk centered on $x_{\mathrm{s,d}}(t)$ in the complex plane; we will denote this disk $D_{\mathrm{s,d}}(t)$. Outside of this disk, the constructions of the contours can be done according to the procedure above, and we take the contours $C_j=W_{z_j}(x,t)$ for $2\le j\le N$. Inside the disk, the landscape looks much like a cubic, with two real saddle points for some (x,t) and two conjugate saddle



(a) Near the soliton edge in the $J = 1$ region.

(b) At the soliton edge.

(c) Near the dispersive edge in the $J = 1$ region.

(d) At the dispersive edge.

Figure 4.3: Schematics of the local landscapes around the real saddle points near to (left column) and at (right column) the soliton (top row) and dispersive (bottom row) edges. The color and saturation indicate the value of $\mathrm{Im}\,[h(\diamond; x, t)]$ relative to that at the associated saddle point(s), blue is below and yellow is above. Schematics of the contours constructed by the procedure [6, Section 4] W_{y_0} and $W_{y_{1,2}}$ as well as the modified contours that we define C_0 and C_1 are also depicted in maroon and labeled.

points for other (x, t). For C_0 and C_1, we can take the portions of $W_{y_0}(x, t)$ and $W_{y_{1,2}}(x, t)$ respectively exterior to $D_{\mathrm{s,d}}(t)$, and then interior to $D_{\mathrm{s,d}}(t)$, we just take a smooth arc that connects the two ends of the original contour. Because of the local cubic landscape, we can be assured that there is a possibly smaller $\delta > 0$ such that the end points remain a fixed distance below the level of $\mathrm{Im}\,[h(y_{\mathrm{s,d}}(t), x, t)]$. The resulting behaviors of the contours C_0 and C_1 are captured in Figure 4.3.

4.1.2 Steepest Descent Approximation for Colliding Saddle Points

The model equation here is given by

$$h(z; x, t) - h_{\mathrm{s,d}}(x, t) = \frac{\Omega_{\mathrm{s,d}}^3(z; x, t)}{3} - a(x, t)\,\Omega_{\mathrm{s,d}}(z; x, t) + b(x, t) \tag{4.15}$$

where $h_{\mathrm{s,d}}(x, t) = h\big(y_{\mathrm{s,d}}(t); x, t\big)$. Just like in Section 2.2.4.2, case 2, we are guaranteed the existence of the map $\Omega_{\mathrm{s,d}}(\diamond; x, t)$ and its inverse by equating the values of the saddle points

on either side of (4.15)

$$\frac{2}{3}\big(a(x,t)\big)^{3/2} = \frac{h(z_{\mathrm{s,d}-}(x,t);x,t) - h(z_{\mathrm{s,d}+}(x,t);x,t)}{2}, \tag{4.16}$$

$$b(x,t) = \frac{h(z_{\mathrm{s,d}-}(x,t);x,t) + h(z_{\mathrm{s,d}+}(x,t);x,t)}{2} - h_{\mathrm{s,d}}(x,t)\,, \tag{4.17}$$

where $z_{\mathrm{s,d}\pm}(x,t)$ are the colliding saddle points, ordered by real or imaginary part. When $x = x_{\mathrm{s,d}}(t)$, the left-hand side of (4.15) is cubic at leading order in $z - y_{\mathrm{s,d}}(t)$, so we know $a(x_{\mathrm{s,d}}(t),t) = b(x_{\mathrm{s,d}}(t),t) = 0$ and we can find the first couple of coefficients of the analytic map.

$$\frac{h^{(3)}_{\mathrm{s,d}}(t)}{6}\big(z - y_{\mathrm{s,d}}(t)\big)^3 + \frac{h^{(4)}_{\mathrm{s,d}}(t)}{24}\big(z - y_{\mathrm{s,d}}(t)\big)^4 + O\left(\big(z - y_{\mathrm{s,d}}(t)\big)^5\right) = \frac{\Omega^3_{\mathrm{s,d}}(z;x_{\mathrm{s,d}}(t),t)}{3} \tag{4.18}$$

where $h^{(3)}_{\mathrm{s,d}}(t) = h_{zzz}(y_{\mathrm{s,d}}(t);x_{\mathrm{s,d}}(t),t)$, etc. Before solving for $\Omega_{\mathrm{s,d}}(z;x_{\mathrm{s,d}}(t),t)$, we should see what the argument of the leading coefficient is so we can wisely take our cube root. From (4.8), we have

$$h_z(z;x_{\mathrm{s,d}}(t),t) = \frac{\big(z - y_0(x_{\mathrm{s,d}}(t),t)\big)\big(z - y_{\mathrm{s,d}}(t)\big)^2}{2t}\frac{\prod_{j=3}^N \big(z - z_j(x_{\mathrm{s,d}}(t),t)\big)\big(z - z_j(x_{\mathrm{s,d}}(t),t)^*\big)}{\prod_{j=1}^N (z-p_j)(z-p_j^*)}. \tag{4.19}$$

Taking two derivatives and plugging in $z = y_{\mathrm{s,d}}(t)$, its clear the only term that survives is

$$h_{zzz}(y_{\mathrm{s,d}}(t);x_{\mathrm{s,d}}(t),t) = \frac{y_{\mathrm{s,d}}(t) - y_0(x_{\mathrm{s,d}}(t),t)}{t}\frac{\prod_{j=3}^N \big|y_{\mathrm{s,d}}(t) - z_j(x_{\mathrm{s,d}}(t),t)\big|^2}{\prod_{j=1}^N |y_{\mathrm{s,d}}(t) - p_j|^2}\,. \tag{4.20}$$

So, as expected, the third derivative of h is always real, while the sign is determined by the ordering of the double and single real saddle points. As stated above, the soliton edge is characterized by $y_{\mathrm{s}}(t) < y_0(x_{\mathrm{s}}(t),t)$ while a dispersive edge is characterized by $y_{\mathrm{d}}(t) > y_0(x_{\mathrm{d}}(t),t)$. To make the sign explicit, we define $\sigma_{\mathrm{s}} = -1$ and $\sigma_{\mathrm{d}} = +1$. Then, labeling the expansion coefficients

$$\Omega_{\mathrm{s,d}}(z;x_{\mathrm{s,d}}(t),t) = \sigma_{\mathrm{s,d}}\,\nu_{\mathrm{s,d}}(t)\,\big(z - y_{\mathrm{s,d}}(t)\big) + c_{\mathrm{s,d}}(t)\,\big(z - y_{\mathrm{s,d}}(t)\big)^2 + O\left(\big(z - y_{\mathrm{s,d}}(t)\big)^3\right)\,, \tag{4.21}$$

and then cubing the series, we get

$$\frac{\Omega^3_{\mathrm{s,d}}(z;x_{\mathrm{s,d}}(t),t)}{3} = \sigma_{\mathrm{s,d}}\frac{\nu^3_{\mathrm{s,d}}(t)}{3}\big(z - y_{\mathrm{s,d}}(t)\big)^3 + \nu^2_{\mathrm{s,d}}(t)c_{\mathrm{s,d}}(t)\big(z - y_{\mathrm{s,d}}(t)\big)^4 + O\left(\big(z - y_{\mathrm{s,d}}(t)\big)^5\right)\,. \tag{4.22}$$

Comparing the coefficients in (4.22) to those in (4.18), we can compute the universal coefficient $\nu_{\mathrm{s,d}}(t)$ and the next-to-leading-order coefficient $c_{\mathrm{s,d}}(t)$,

$$\nu_{\mathrm{s,d}}(t) = \left(\frac{|h_{zzz}(y_{\mathrm{s,d}}(t); x_{\mathrm{s,d}}(t), t)|}{2}\right)^{1/3} = \left(\frac{\left|u_0''\big(y_{\mathrm{s,d}}(t)\big)\right|}{2}\right)^{1/3}, \tag{4.23}$$

$$c_{\mathrm{s,d}}(t) = \left(\frac{2}{|u_0''(y_{\mathrm{s,d}}(t)|}\right)^{2/3} \frac{h_{zzzz}(y_{\mathrm{s,d}}(t); x_{\mathrm{s,d}}(t), t)}{24} = \frac{2^{2/3} u_0'''\big(y_{\mathrm{s,d}}(t)\big)}{24\left|u_0''\big(y_{\mathrm{s,d}}(t)\big)\right|^{2/3}}. \tag{4.24}$$

In order to expand these in ϵ, we differentiate them in x. We will start with a,

$$a_x(x,t)\big(a(x,t)\big)^{1/2} = \frac{h_x(z_{\mathrm{s,d}-}(x,t); x, t) - h_x(z_{\mathrm{s,d}+}(x,t); x, t)}{2} \tag{4.25}$$

$$= \frac{z_{\mathrm{s,d}+}(x,t) - z_{\mathrm{s,d}-}(x,t)}{4t}, \tag{4.26}$$

where we used the fact that $z_{\mathrm{s,d}\pm}(x,t)$ are saddle points to eliminate the h_z terms in the beginning, and then just took the x-derivative of (4.6). If we divide over the $\big(a(x,t)\big)^{1/2}$ term when it is not zero, then we can actually rewrite the result using the Residue theorem as a contour integral around the boundary of the disk, oriented positively, which encloses the two saddle points.

$$a_x(x,t) = \frac{1}{2t}\left(\frac{z_{\mathrm{s,d}-}(x,t) - y_{\mathrm{s,d}}(t)}{-2\big(a(x,t)\big)^{1/2}} + \frac{z_{\mathrm{s,d}+}(x,t) - y_{\mathrm{s,d}}(t)}{2\big(a(x,t)\big)^{1/2}}\right) \tag{4.27}$$

$$= \frac{1}{4t\pi\mathrm{i}} \int_{\partial D_{\mathrm{s,d}}(t)} \frac{\big(z - y_{\mathrm{s,d}}(t)\big)\partial_z \Omega_{\mathrm{s,d}}(z; x, t)\ \mathrm{d}z}{\big(\Omega_{\mathrm{s,d}}(z; x, t)\big)^2 - a(x,t)}. \tag{4.28}$$

This formula correctly captures the limit as $x \to x_{\mathrm{s,d}}(t)$ and $a(x,t) \to 0$:

$$a_x(x_{\mathrm{s,d}}(t), t) = \frac{1}{4t\pi\mathrm{i}} \int_{\partial D_{\mathrm{s,d}}(t)} \frac{\big(z - y_{\mathrm{s,d}}(t)\big)\ \partial_z \Omega_{\mathrm{s,d}}(z; x_{\mathrm{s,d}}(t), t)\ \mathrm{d}z}{\big(\Omega_{\mathrm{s,d}}(z; x_{\mathrm{s,d}}(t), t)\big)^2} \tag{4.29}$$

$$= \frac{1}{4t\pi\mathrm{i}} \int_{\partial D_{\mathrm{s,d}}(t)} \frac{\sigma_{\mathrm{s,d}}\nu_{\mathrm{s,d}}(t)\big(z - y_{\mathrm{s,d}}(t)\big) + O\left(\big(z - y_{\mathrm{s,d}}(t)\big)^2\right)}{\nu_{\mathrm{s,d}}^2(t)\big(z - y_{\mathrm{s,d}}(t)\big)^2 + O\left(\big(z - y_{\mathrm{s,d}}(t)\big)^3\right)}\ \mathrm{d}z \tag{4.30}$$

$$= \frac{\sigma_{\mathrm{s,d}}}{2t\nu_{\mathrm{s,d}}(t)}. \tag{4.31}$$

Since $a(x,t)$ is analytic in x, it must have a second derivative, which must be bounded on a

compact spacetime set, and thus we conclude

$$a(x,t) = \frac{\sigma_{\mathrm{s,d}}}{2t\nu_{\mathrm{s,d}}(t)}\big(x - x_{\mathrm{s,d}}(t)\big) + O\left(\big(x - x_{\mathrm{s,d}}(t)\big)^2\right). \tag{4.32}$$

If we want to bring a dominant balance to the exponent after changing variables, we should pick the new x-coordinate X in a compact interval with the ϵ scaling

$$x = \epsilon^{2/3} k_{\mathrm{s,d}}(t) X + x_{\mathrm{s,d}}(t) \tag{4.33}$$

where $k_{\mathrm{s,d}}(t) = 2t\nu_{\mathrm{s,d}}(t)$ is a universal function. For ϵ small enough, X on any compact interval will result in the valid use of (4.32), then a admits a series expansion in powers of ϵ:

$$a(x,t) = \sigma_{\mathrm{s,d}} \epsilon^{2/3} X + O\left(\epsilon^{4/3}\right). \tag{4.34}$$

Now for b,

$$b_x(x,t) = \frac{h_x(z_{\mathrm{s,d}-}(x,t);x,t) + h_x(z_{\mathrm{s,d}+}(x,t);x,t)}{2} - h_x(y_{\mathrm{s,d}}(x,t);x,t) \tag{4.35}$$

$$= \frac{2x - z_{\mathrm{s,d}-}(x,t) - z_{\mathrm{s,d}+}(x,t)}{4t} - \frac{x - y_{\mathrm{s,d}}(t)}{2t}, \tag{4.36}$$

again, using that $z_{\mathrm{s,d}\pm}(x,t)$ are saddle points to eliminate the h_z terms at the start and differentiating (4.6) with respect to x. Now, plugging in $x = x_{\mathrm{s,d}}(t)$, by construction, $z_{\mathrm{s,d}\pm}(x_{\mathrm{s,d}}(t),t) = y_{\mathrm{s,d}}(t)$, (4.36) yields $b_x(x_{\mathrm{s,d}}(t),t) = 0$. Lastly, since b is again analytic in x, we have a bounded second derivative on a compact spacetime set and, using (4.33), the ϵ expansion

$$b(x,t) = O\left(\epsilon^{4/3}\right). \tag{4.37}$$

With everything in place, we begin our analysis of the integral over a contour C that passes near the colliding saddle points. Let $R := \cup_{t\in K_{\mathrm{s,d}}} D_{\mathrm{s,d}}(t)$ be the region swept by the disk $D_{\mathrm{s,d}}(t)$ and $f : R \to \mathbb{C}$ be an analytic function in the disk. Conducting the change of variables $\omega = \Omega_{\mathrm{s,d}}(z;x,t)$, we have

$$\int_{C\cap D_{\mathrm{s,d}}(t)} \mathrm{e}^{-\mathrm{i}h(z;x,t)/\epsilon} f(z)\,\mathrm{d}z = \mathrm{e}^{-\mathrm{i}\left[h(y_{\mathrm{s,d}}(t);x,t)+b(x,t)\right]/\epsilon} \int_{C^{\omega}_{\mathrm{s,d}}(x,t)} \mathrm{e}^{-\mathrm{i}(\omega^3/3 - a(x,t)\omega)/\epsilon} \tilde{f}_{\mathrm{s,d}}(\omega;x,t)\,\mathrm{d}\omega \tag{4.38}$$

where $\tilde{f}_{\mathrm{s,d}}(\omega;x,t) = f(\Omega^{-1}_{\mathrm{s,d}}(\omega;x,t))\ \partial_\omega \Omega^{-1}_{\mathrm{s,d}}(\omega;x,t)$ and $C^{\omega}_{\mathrm{s,d}}(x,t)$ is the image of $C \cap D_{\mathrm{s,d}}(t)$ under $\Omega(\diamond;x,t)$. For ϵ small, the map is close to (4.21), especially away from the center of the disk. Thus, we see that this essentially leaves the contour alone or negates it depending on the sign of $\sigma_{\mathrm{s,d}}$. Then, to bring the contour into line with the definition of the Airy

contour, i.e. beginning with argument $-\pi/3$ and ending with argument $\pi/3$, we conduct another change of variables $\omega = -\mathrm{i}\mathrm{e}^{\mathrm{i}2\pi n/3}\epsilon^{1/3}\zeta$,

$$\begin{aligned}\int_{C^{\omega}_{\mathrm{s,d}}(x,t)} & \mathrm{e}^{-\mathrm{i}\left[\omega^3/3 - a(x,t)\omega\right]/\epsilon}\tilde{f}_{\mathrm{s,d}}(\omega;x,t)\ \mathrm{d}\omega \\ &= -\mathrm{i}\mathrm{e}^{\mathrm{i}2\pi n/3}\epsilon^{1/3}\int_{C^{\zeta}_{\mathrm{s,d}}(x,t)} \mathrm{e}^{\zeta^3/3 + \mathrm{e}^{\mathrm{i}2\pi n/3}\epsilon^{-2/3}a(x,t)\zeta}\tilde{f}_{\mathrm{s,d}}(-\mathrm{i}\mathrm{e}^{\mathrm{i}2\pi n/3}\epsilon^{1/3}\zeta;x,t)\ \mathrm{d}\zeta \end{aligned} \tag{4.39}$$

where $C^{\zeta}_{\mathrm{s,d}}(x,t) = -\mathrm{i}\mathrm{e}^{-\mathrm{i}2\pi n/3}\epsilon^{-1/3}C^{\omega}_{\mathrm{s,d}}(x,t)$ and $n = \pm 1$, or 0, which ever brings the contour into line with the Airy contour. For the soliton edge, looking at how C_0 approaches $y_{\mathrm{s}}(t)$ in Figure 4.3, we should take $n = 0$ and note that the contour traces the Airy contour in the opposite direction, so we pick up an overall sign. For the dispersive edge, looking at how C_0 and C_1 approach $y_{\mathrm{d}}(t)$ in Figure 4.3, we should take $n = +1$ for C_0 and we should take $n = -1$ for C_1, both of which again traces opposite the Airy contour. Now we use the standard expansion technique [11] to get

$$\begin{aligned}\frac{1}{2\pi\mathrm{i}}\int_{C^{\zeta}_{\mathrm{s,d}}(x,t)} & \mathrm{e}^{\zeta^3/3 + \mathrm{e}^{\mathrm{i}2\pi n/3}\epsilon^{-2/3}a(x,t)\zeta}\tilde{f}_{\mathrm{s,d}}(-\mathrm{i}\mathrm{e}^{\mathrm{i}2\pi n/3}\epsilon^{1/3}\zeta;x,t)\ \mathrm{d}\zeta \\ &= \mathrm{Ai}\left(-\mathrm{e}^{\mathrm{i}2\pi n/3}\frac{a(x,t)}{\epsilon^{2/3}}\right)\left[\tilde{f}_{\mathrm{s,d}}(0;x,t) + O\left(\epsilon^{2/3}\right)\right] \\ &\quad + \mathrm{Ai}'\left(-\mathrm{e}^{\mathrm{i}2\pi n/3}\frac{a(x,t)}{\epsilon^{2/3}}\right)\left[-\mathrm{i}\mathrm{e}^{\mathrm{i}2\pi n/3}\epsilon^{1/3}\partial_{\omega}\tilde{f}_{\mathrm{s,d}}(0;x,t) + O\left(\epsilon\right)\right]. \end{aligned} \tag{4.40}$$

Since $a(x,t)/\epsilon^{2/3} = -\sigma_{\mathrm{s,d}}X + O\left(\epsilon^{2/3}\right)$ and X is on compact interval, the Airy function and its derivative are always uniformly bounded, thus we can expand on the arguments and collect all error terms into one. We can use the differentiability of the map Ω once again

$$\tilde{f}_{\mathrm{s,d}}(0;x,t) = \tilde{f}_{\mathrm{s,d}}(0;x_{\mathrm{s,d}}(t),t) + O\left(\epsilon^{2/3}\right), \tag{4.41}$$

$$\partial_z\tilde{f}_{\mathrm{s,d}}(0;x,t) = \partial_z\tilde{f}_{\mathrm{s,d}}(0;x_{\mathrm{s,d}}(t),t) + O\left(\epsilon^{2/3}\right). \tag{4.42}$$

We can use the Lagrange-Bürmann formula to write these evaluations as contour integrals

$$\partial^n_{\omega}\tilde{f}_{\mathrm{s,d}}(0;x_{\mathrm{s,d}}(t),t) = \frac{1}{2\pi\mathrm{i}}\int_{\partial D_{\mathrm{s,d}}(t)}\frac{f(z)\ \mathrm{d}z}{\left(\Omega_{\mathrm{s,d}}(z;x_{\mathrm{s,d}}(t),t)\right)^{n+1}}. \tag{4.43}$$

Now we can evaluate these remaining terms directly from using the series (4.18)

$$\tilde{f}_{\mathrm{s,d}}(0;x_{\mathrm{s,d}}(t),t)=\frac{1}{2\pi\mathrm{i}}\int_{\partial D_{\mathrm{s,d}}(t)}\frac{f(z)\ \mathrm{d}z}{\Omega_{\mathrm{s,d}}(z;x_{\mathrm{s,d}}(t),t)}=\frac{\sigma_{\mathrm{s,d}}}{\nu_{\mathrm{s,d}}(t)}f\big(y_{\mathrm{s,d}}(t)\big) \tag{4.44}$$

$$\partial_\omega\tilde{f}_{\mathrm{s,d}}(0;x_{\mathrm{s,d}}(t),t)=\frac{1}{2\pi\mathrm{i}}\int_{\partial D_{\mathrm{s,d}}(t)}\frac{f(z)\ \mathrm{d}z}{\big(\Omega_{\mathrm{s,d}}(z;x_{\mathrm{s,d}}(t),t)\big)^2}=\frac{f'\big(y_{\mathrm{s,d}}(t)\big)}{\nu^2_{\mathrm{s,d}}(t)}-2\frac{\sigma_{\mathrm{s,d}}c_{\mathrm{s,d}}(t)}{\nu^3_{\mathrm{s,d}}(t)}f\big(y_{\mathrm{s,d}}(t)\big)\,. \tag{4.45}$$

Now we combine (4.44) and (4.45) with (4.41) and (4.42) and insert them into (4.40),

$$\begin{aligned}\frac{1}{2\pi\mathrm{i}}\int_{C^\zeta_{\mathrm{s,d}}(x,t)}&\mathrm{e}^{\zeta^3/3+\mathrm{e}^{\mathrm{i}2\pi n/3}\epsilon^{-2/3}a(x,t)\zeta}\,\tilde{f}_{\mathrm{s,d}}(-\mathrm{i}\mathrm{e}^{\mathrm{i}2\pi n/3}\epsilon^{1/3}\zeta;x,t)\ \mathrm{d}\zeta\\ &=\mathrm{Ai}\left(-\mathrm{e}^{\mathrm{i}2\pi n/3}\sigma_{\mathrm{s,d}}X\right)\frac{\sigma_{\mathrm{s,d}}}{\nu_{\mathrm{s,d}}(t)}f\big(y_{\mathrm{s,d}}(t)\big)\\ &\quad-\mathrm{i}\mathrm{e}^{\mathrm{i}2\pi n/3}\epsilon^{1/3}\mathrm{Ai}'\left(-\mathrm{e}^{\mathrm{i}2\pi n/3}\sigma_{\mathrm{s,d}}X\right)\left(\frac{f'\big(y_{\mathrm{s,d}}(t)\big)}{\nu^2_{\mathrm{s,d}}(t)}-2\frac{\sigma_{\mathrm{s,d}}c_{\mathrm{s,d}}(t)}{\nu^3_{\mathrm{s,d}}(t)}f\big(y_{\mathrm{s,d}}(t)\big)\right)\\ &\quad+O\left(\epsilon^{2/3}\right)\,.\end{aligned} \tag{4.46}$$

Finally, we roll this result back through (4.39) and (4.38), we get the full form of the expansion

$$\begin{aligned}\int_{C\cap D}&\mathrm{e}^{-\mathrm{i}h(z;x,t)/\epsilon}f(z)\ \mathrm{d}z\\ &=\sigma_{\mathrm{s,d}}\frac{2\pi\epsilon^{1/3}}{\nu_{\mathrm{s,d}}(t)}\mathrm{e}^{-\mathrm{i}h(y_{\mathrm{s,d}}(t);x,t)/\epsilon+\mathrm{i}2\pi n/3}\Bigg[\mathrm{Ai}\left(-\mathrm{e}^{\mathrm{i}2\pi n/3}\sigma_{\mathrm{s,d}}X\right)f\big(y_{\mathrm{s,d}}(t)\big)\\ &\quad-\mathrm{i}\frac{\mathrm{e}^{\mathrm{i}2\pi n/3}\epsilon^{1/3}}{\nu_{\mathrm{s,d}}(t)}\mathrm{Ai}'\left(-\mathrm{e}^{\mathrm{i}2\pi n/3}\sigma_{\mathrm{s,d}}X\right)\left(\sigma_{\mathrm{s,d}}f'\big(y_{\mathrm{s,d}}(t)\big)-2\frac{c_{\mathrm{s,d}}(t)}{\nu_{\mathrm{s,d}}(t)}f\big(y_{\mathrm{s,d}}(t)\big)\right)\\ &\quad+O\left(\epsilon^{2/3}\right)\Bigg]\,.\end{aligned} \tag{4.47}$$

4.1.3 Steepest descent Approximation for Simple Saddle Points

For contours $C_2,\ldots,C_N$, which involve steepest descent contour arcs $S_{z_2}(x,t),\ldots,S_{z_N}(x,t)$ that pass through one complex saddle point $z_2(x,t),\ldots,z_N(x,t)$, and then on the rest of the contour, $\mathrm{Im}\,[h]$ remains below the level, we are guaranteed that the contributions from the contours $C_2\setminus S_{z_2}(x,t),\ldots,C_N\setminus S_{z_N}(x,t)$ are (relatively) beyond all orders in ϵ. Thus, we need only worry about the contributions from $S_{z_2}(x,t),\ldots,S_{z_N}(x,t)$. Just like in Section

2.2.4.2, we can construct changes of variables around these steepest descent arcs

$$\mathrm{i}\big(h(z;x,t) - h_j(x,t)\big) = \frac{\big(\Omega_j(z;x,t)\big)^2}{2} \tag{4.48}$$

where $h_j(x,t) = h(z_j(x,t);x,t)$ for $2 \leq j \leq N$ and we take the principal square-root of the left side in the definition of Ω. The expansion of the integral can then be computed as normal

$$\int_{S_{z_j}(x,t)} \mathrm{e}^{-\mathrm{i}h(z;x,t)/\epsilon} f(z)\,\mathrm{d}z = \mathrm{e}^{-\mathrm{i}h_j(x,t)/\epsilon} \int_{\Omega(S_{z_j})} \mathrm{e}^{-\omega^2/2\epsilon} \tilde{f}(\omega;x,t)\,\mathrm{d}z \tag{4.49}$$

where

$$\tilde{f}(\omega;x,t) := f(\Omega^{-1}(\omega;x,t))\ \Omega_\omega^{-1}(\omega;x,t)\,. \tag{4.50}$$

Taylor expanding and bounding the quadratic remainder term, we have that the integral of this remainder term contributes $O\left(\epsilon^{3/2}\right)$. The contour $\Omega(S_{z_j})$ is then just a line segment on the real axis with endpoints bounded away from zero. The orientation is currently unknown, but it is either to the right or left, and we can include this in the computation via a sign $\sigma_j = \pm 1$. Adding on the contributions out to infinity at the cost of another beyond all orders error, we have

$$\int_{C_j} \mathrm{e}^{-\mathrm{i}h(z;x,t)/\epsilon} f(z)\,\mathrm{d}z = \mathrm{e}^{-\mathrm{i}h_j(x,t)/\epsilon} \left(\sigma_j \sqrt{2\pi\epsilon}\,\tilde{f}(0;x,t) + O\left(\epsilon^{3/2}\right)\right). \tag{4.51}$$

We can compute from the change of variables directly

$$\tilde{f}(0;x,t) = \frac{f(z_j(x,t))}{\big(\mathrm{i}h_j''(x,t)\big)^{1/2}} \tag{4.52}$$

with $h_j''(x,t) := h_{zz}(z_j(x,t);x,t)$ and the principal square-root is taken. Lastly, we can expand the saddle point and f to leading order using Taylor series and (4.33) to get $f(z_j(x,t)) = f(z_j(t)) + O\left(\epsilon^{2/3}\right)$ where $z_j(t) = z_j(x_{\mathrm{s,d}}(t),t)$. This yields the final expansion

$$\int_{C_j} \mathrm{e}^{-\mathrm{i}h(z;x,t)/\epsilon} f(z)\,\mathrm{d}z = \sigma_j \left(\frac{2\pi\epsilon}{\mathrm{i}h_j''(x,t)}\right)^{1/2} \mathrm{e}^{-\mathrm{i}h_j(x,t)/\epsilon} \Big[f(z_j(t)) + O\left(\epsilon^{2/3}\right) \Big] \tag{4.53}$$

where, again, the principal square-root is taken. Note that all of the above analysis, though explicitly only written for the complex saddle points, is also valid for the contribution of the steepest descent arc which passes through the simple real saddle point. However, for the

contour on which this arc lies, we must also be aware that there may be another contribution, depending on the exact configuration depicted in Figure 4.3.

4.2 Universal Behavior at the Soliton Edge

We will focus first on an expansion of $D_0(x,t;\epsilon)$ (4.4). Applying the colliding saddle point approximation (4.47) with $n=0$ and an extra overall sign—see discussion following (4.39)—to the first row and the simple saddle point expansion (4.53) to the subsequent N rows, we can factor out the exponential pre-factors from each row, defining

$$E_{\mathrm{s}}(x,t;\epsilon) := \frac{2\pi\epsilon^{1/3}}{\nu_{\mathrm{s}}(t)} \mathrm{e}^{-\mathrm{i}h(y_{\mathrm{s}}(t);x,t)/\epsilon} \prod_{j\neq 1} \sigma_j \left(\frac{2\pi\epsilon}{\mathrm{i}h_j''(x,t)}\right)^{1/2} \mathrm{e}^{-\mathrm{i}h_j(x,t)/\epsilon}, \tag{4.54}$$

we use the linearity of the determinant in the rows to split the leading order contributions from the error terms iteratively in the last N rows as well as the leading order, next-to-leading order and error terms in the first row to get the expansion

$$\frac{D_0(x,t;\epsilon)}{E_{\mathrm{s}}(x,t;\epsilon)} = \mathrm{Ai}(X)U_{\mathrm{s}}(t) + \mathrm{i}\frac{\epsilon^{1/3}}{\nu_{\mathrm{s}}(t)}\mathrm{Ai}'(X)\left(U_{\mathrm{s}}^{(1)}(t) + 2\frac{c_{\mathrm{s}}(t)}{\nu_{\mathrm{s}}(t)}U_{\mathrm{s}}(t)\right) + O\left(\epsilon^{2/3}\right) \tag{4.55}$$

where $U_{\mathrm{s}}(t)$ is the new matrix determinant

$$U_{\mathrm{s}}(t) := \begin{vmatrix} u_0\big(y_{\mathrm{s}}(t)\big) & \frac{1}{y_{\mathrm{s}}(t)-p_1} & \cdots & \frac{1}{y_{\mathrm{s}}(t)-p_N} \\ u_0\big(y_0(t)\big) & \frac{1}{y_0(t)-p_1} & \cdots & \frac{1}{y_0(t)-p_N} \\ u_0\big(z_2(t)\big) & \frac{1}{z_2(t)-p_1} & \cdots & \frac{1}{z_2(t)-p_N} \\ \vdots & \vdots & \ddots & \vdots \\ u_0\big(z_N(t)\big) & \frac{1}{z_N(t)-p_1} & \cdots & \frac{1}{z_N(t)-p_N} \end{vmatrix} \tag{4.56}$$

while $U_{\mathrm{s}}^{(1)}(t)$ is the same matrix with a derivative taken on the functions in the first row

$$U_{\mathrm{s}}^{(1)}(t) := \begin{vmatrix} u_0'\big(y_{\mathrm{s}}(t)\big) & \frac{-1}{(y_{\mathrm{s}}(t)-p_1)^2} & \cdots & \frac{-1}{(y_{\mathrm{s}}(t)-p_N)^2} \\ u_0\big(y_0(t)\big) & \frac{1}{y_0(t)-p_1} & \cdots & \frac{1}{y_0(t)-p_N} \\ u_0\big(z_2(t)\big) & \frac{1}{z_2(t)-p_1} & \cdots & \frac{1}{z_2(t)-p_N} \\ \vdots & \vdots & \ddots & \vdots \\ u_0\big(z_N(t)\big) & \frac{1}{z_N(t)-p_1} & \cdots & \frac{1}{z_N(t)-p_N} \end{vmatrix}. \tag{4.57}$$

Since $y_{\mathrm{s}}(t), y_0(t), z_3(t), \ldots, z_N(t)$ are all saddle points of h, they satisfy (4.7), which means we can replace the u_0 evaluations with $(x_{\mathrm{s}}(t)-\diamond)/2t$. Moreover, since $y_{\mathrm{s}}(t)$ is a double saddle

point, we have the derivative of (4.7) can also be set to zero, and thus $u_0'(y_{\rm s}(t)) = -1/2t$ in $U_{\rm s}^{(1)}(t)$. These together let us replace all of the u_0 terms in the matrix determinants which we expand via linearity on the first column

$$U_{\rm s}(t) = \frac{x_{\rm s}(t)}{2t} C_0(t) - \frac{1}{2t} C_1(t), \tag{4.58}$$

$$U_{\rm s}^{(1)}(t) = \frac{x_{\rm s}(t)}{2t} C_0^{(1)}(t) - \frac{1}{2t} C_1^{(1)}(t)\,, \tag{4.59}$$

where

$$C_0(t) := \begin{vmatrix} 1 & \frac{1}{y_{\rm s}(t)-p_1} & \cdots & \frac{1}{y_{\rm s}(t)-p_N} \\ 1 & \frac{1}{y_0(t)-p_1} & \cdots & \frac{1}{y_0(t)-p_N} \\ 1 & \frac{1}{z_2(t)-p_1} & \cdots & \frac{1}{z_2(t)-p_N} \\ \vdots & \vdots & \ddots & \vdots \\ 1 & \frac{1}{z_N(t)-p_1} & \cdots & \frac{1}{z_N(t)-p_N} \end{vmatrix}, \qquad C_1(t) := \begin{vmatrix} y_{\rm s}(t) & \frac{1}{y_{\rm s}(t)-p_1} & \cdots & \frac{1}{y_{\rm s}(t)-p_N} \\ y_0(t) & \frac{1}{y_0(t)-p_1} & \cdots & \frac{1}{y_0(t)-p_N} \\ z_2(t) & \frac{1}{z_2(t)-p_1} & \cdots & \frac{1}{z_2(t)-p_N} \\ \vdots & \vdots & \ddots & \vdots \\ z_N(t) & \frac{1}{z_N(t)-p_1} & \cdots & \frac{1}{z_N(t)-p_N} \end{vmatrix}, \tag{4.60}$$

while $C_0^{(1)}(t)$ and $C_1^{(1)}(t)$ are the same as the expressions above but with a derivative taken on the functions in the first row

$$C_0^{(1)}(t) := \begin{vmatrix} 0 & \frac{-1}{(y_{\rm s}(t)-p_1)^2} & \cdots & \frac{-1}{(y_{\rm s}(t)-p_N)^2} \\ 1 & \frac{1}{y_0(t)-p_1} & \cdots & \frac{1}{y_0(t)-p_N} \\ 1 & \frac{1}{z_2(t)-p_1} & \cdots & \frac{1}{z_2(t)-p_N} \\ \vdots & \vdots & \ddots & \vdots \\ 1 & \frac{1}{z_N(t)-p_1} & \cdots & \frac{1}{z_N(t)-p_N} \end{vmatrix}, \quad C_1^{(1)}(t) := \begin{vmatrix} 1 & \frac{-1}{(y_{\rm s}(t)-p_1)^2} & \cdots & \frac{-1}{(y_{\rm s}(t)-p_N)^2} \\ y_0(t) & \frac{1}{y_0(t)-p_1} & \cdots & \frac{1}{y_0(t)-p_N} \\ z_2(t) & \frac{1}{z_2(t)-p_1} & \cdots & \frac{1}{z_2(t)-p_N} \\ \vdots & \vdots & \ddots & \vdots \\ z_N(t) & \frac{1}{z_N(t)-p_1} & \cdots & \frac{1}{z_N(t)-p_N} \end{vmatrix}. \tag{4.61}$$

We note an intimate connection between $C_0(t)$ and $C_1(t)$ and the $N \times N$ Cauchy matrix determinant on the additional variables $w_0, \ldots, w_N, p_0 \in \mathbb{C}$,

$$C(w_0, \ldots, w_N, p_0) := \begin{vmatrix} \frac{1}{w_0-p_0} & \frac{1}{w_0-p_1} & \cdots & \frac{1}{w_0-p_N} \\ \frac{1}{w_1-p_0} & \frac{1}{w_1-p_1} & \cdots & \frac{1}{w_1-p_N} \\ \vdots & \vdots & \ddots & \vdots \\ \frac{1}{w_N-p_0} & \frac{1}{w_N-p_1} & \cdots & \frac{1}{w_N-p_N} \end{vmatrix}. \tag{4.62}$$

Namely, we can expand the Cauchy determinant as a Laurent series for large p_0 by expanding the elements in the first column and using linearity of the determinant over columns

$$C(w_0,\dots,w_N,p_0) = -\frac{1}{p_0}\begin{vmatrix} \frac{1}{1-w_0/p_0} & \frac{1}{w_0-p_1} & \cdots & \frac{1}{w_0-p_N} \\ \frac{1}{1-w_1/p_0} & \frac{1}{w_1-p_1} & \cdots & \frac{1}{w_1-p_N} \\ \vdots & \vdots & \ddots & \vdots \\ \frac{1}{1-w_N/p_0} & \frac{1}{w_N-p_1} & \cdots & \frac{1}{w_N-p_N} \end{vmatrix} \tag{4.63}$$

$$= -\frac{1}{p_0}\begin{vmatrix} 1+\frac{w_0}{p_0}+O\left(\frac{1}{p_0^2}\right) & \frac{1}{w_0-p_1} & \cdots & \frac{1}{w_0-p_N} \\ 1+\frac{w_1}{p_0}+O\left(\frac{1}{p_0^2}\right) & \frac{1}{w_1-p_1} & \cdots & \frac{1}{w_1-p_N} \\ \vdots & \vdots & \ddots & \vdots \\ 1+\frac{w_N}{p_0}+O\left(\frac{1}{p_0^2}\right) & \frac{1}{w_N-p_1} & \cdots & \frac{1}{w_N-p_N} \end{vmatrix} \tag{4.64}$$

$$= -\frac{1}{p_0}\begin{vmatrix} 1 & \frac{1}{w_0-p_1} & \cdots & \frac{1}{w_0-p_N} \\ 1 & \frac{1}{w_1-p_1} & \cdots & \frac{1}{w_1-p_N} \\ \vdots & \vdots & \ddots & \vdots \\ 1 & \frac{1}{w_N-p_1} & \cdots & \frac{1}{w_N-p_N} \end{vmatrix} - \frac{1}{p_0^2}\begin{vmatrix} w_0 & \frac{1}{w_0-p_1} & \cdots & \frac{1}{w_0-p_N} \\ w_1 & \frac{1}{w_1-p_1} & \cdots & \frac{1}{w_1-p_N} \\ \vdots & \vdots & \ddots & \vdots \\ w_N & \frac{1}{w_N-p_1} & \cdots & \frac{1}{w_N-p_N} \end{vmatrix}$$
$$+ O\left(\frac{1}{p_0^3}\right). \tag{4.65}$$

However, the value of the Cauchy determinant is well known, so we may expand this formula as well

$$C(w_0,\dots,w_N,p_0) = \frac{\prod_{i=1}^{N}\prod_{j=0}^{i-1}(w_i-w_j)(p_j-p_i)}{\prod_{i=0}^{N}\prod_{j=0}^{N}(w_i-p_j)} \tag{4.66}$$

$$= \frac{\prod_{i=2}^{N}\prod_{j=1}^{i-1}(w_i-w_j)(p_j-p_i)}{\prod_{i=0}^{N}\prod_{j=1}^{N}(w_i-p_j)}\frac{\prod_{i=1}^{N}(w_i-w_0)(p_0-p_i)}{\prod_{i=0}^{N}(w_i-p_0)} \tag{4.67}$$

$$= \frac{\prod_{i=2}^{N}\prod_{j=1}^{i-1}(w_i-w_j)(p_j-p_i)}{\prod_{i=0}^{N}\prod_{j=1}^{N}(w_i-p_j)}\frac{(-1)^{N+1}}{p_0}\frac{\prod_{i=1}^{N}(w_i-w_0)(1-p_i/p_0)}{\prod_{i=0}^{N}(1-w_i/p_0)} \tag{4.68}$$

$$= -\Delta(w_0,\dots,w_N)\left(\frac{1}{p_0}+\left(\sum_{i=0}^{N}w_i-\sum_{j=1}^{N}p_j\right)\frac{1}{p_0^2}+O\left(\frac{1}{p_0^3}\right)\right) \tag{4.69}$$

where we defined the p_0-independent factor

$$\Delta(w_0,\dots,w_N) := (-1)^N\frac{\prod_{i=2}^{N}\prod_{j=1}^{i-1}(w_i-w_j)(p_j-p_i)}{\prod_{i=0}^{N}\prod_{j=1}^{N}(w_i-p_j)}\prod_{i=1}^{N}(w_i-w_0)\,. \tag{4.70}$$

Comparing the coefficients of the two expansions, we get the equalities

$$\begin{vmatrix} 1 & \frac{1}{w_0-p_1} & \cdots & \frac{1}{w_0-p_N} \\ 1 & \frac{1}{w_1-p_1} & \cdots & \frac{1}{w_1-p_N} \\ \vdots & \vdots & \ddots & \vdots \\ 1 & \frac{1}{w_N-p_1} & \cdots & \frac{1}{w_N-p_N} \end{vmatrix} = \Delta(w_0,\dots,w_N), \tag{4.71}$$

$$\begin{vmatrix} w_0 & \frac{1}{w_0-p_1} & \cdots & \frac{1}{w_0-p_N} \\ w_1 & \frac{1}{w_1-p_1} & \cdots & \frac{1}{w_1-p_N} \\ \vdots & \vdots & \ddots & \vdots \\ w_N & \frac{1}{w_N-p_1} & \cdots & \frac{1}{w_N-p_N} \end{vmatrix} = \Delta(w_0,\dots,w_N)\left(\sum_{i=0}^{N} w_i - \sum_{j=1}^{N} p_j\right). \tag{4.72}$$

Now we can use these to compute the values $C_0(t)$ and $C_1(t)$ in terms of Δ using (4.60), (4.71) and (4.72),

$$C_0(t) = \Delta\big(y_{\mathrm{s}}(t), y_0(t), z_2(t), \dots, z_N(t)\big), \tag{4.73}$$

$$C_1(t) = \Delta\big(y_{\mathrm{s}}(t), y_0(t), z_2(t), \dots, z_N(t)\big)\left(y_{\mathrm{s}}(t) + y_0(t) + \sum_{i=2}^{N} z_j(t) - \sum_{j=1}^{N} p_j\right). \tag{4.74}$$

Furthermore, since the determinants $C_0^{(1)}(t)$ and $C_1^{(1)}(t)$ have derivatives taken on the functions in the first row, due to the linearity of the determinant on rows, we can actually compute these determinants by taking a w_0-derivative of the formulas (4.71) and (4.72),

$$C_0^{(1)}(t) = \Delta_{w_0}\big(y_{\mathrm{s}}(t), y_0(t), z_2(t), \dots, z_N(t)\big), \tag{4.75}$$

$$\begin{aligned} C_1^{(1)}(t) = {} & \Delta_{w_0}\big(y_{\mathrm{s}}(t), y_0(t), z_2(t), \dots, z_N(t)\big)\left(y_{\mathrm{s}}(t) + y_0(t) + \sum_{i=2}^{N} z_j(t) - \sum_{j=1}^{N} p_j\right) \\ & + \Delta\big(y_{\mathrm{s}}(t), y_0(t), z_2(t), \dots, z_N(t)\big). \end{aligned} \tag{4.76}$$

After rolling these back through (4.58) and (4.59) and then (4.55), we get

$$\begin{aligned} \frac{D_0(x,t;\epsilon)}{E_{\mathrm{s}}(x,t;\epsilon)} = \frac{1}{2t}\Bigg(& x_{\mathrm{s}}(t) - y_{\mathrm{s}}(t) - y_0(t) - \sum_{i=2}^{N} z_j(t) + \sum_{j=1}^{N} p_j \Bigg) \\ & \times \left[\mathrm{Ai}(X)\Delta + \mathrm{i}\frac{\epsilon^{1/3}}{\nu_{\mathrm{s}}(t)}\mathrm{Ai}'(X)\left(\Delta_{w_0} + 2\frac{c_{\mathrm{s}}(t)}{\nu_{\mathrm{s}}(t)}\Delta\right)\right] \\ & - \mathrm{i}\frac{\epsilon^{1/3}}{2t\nu_{\mathrm{s}}(t)}\mathrm{Ai}'(X)\Delta + O\left(\epsilon^{2/3}\right) \end{aligned} \tag{4.77}$$

where all of the Δ functions and derivatives are evaluated at $\big(y_{\rm s}(t), y_0(t), z_2(t), \ldots, z_N(t)\big)$. This is as far as we can go with the numerator, so now we work on the denominator matrix determinant (4.5). We expand this the exact same way, but there are no u_0 evaluations, just ones in the first column

$$\frac{D(x,t;\epsilon)}{E_{\rm s}(x,t;\epsilon)} = {\rm Ai}(X)C_0(t) + {\rm i}\frac{\epsilon^{1/3}}{\nu_{\rm s}(t)}{\rm Ai}'(X)\left(C_0^{(1)}(t) + 2\frac{c_{\rm s}(t)}{\nu_{\rm s}(t)}C_0(t)\right) + O\left(\epsilon^{2/3}\right) . \tag{4.78}$$

Evaluating $C_0(t)$ and $C_0^{(1)}(t)$ as above, we get

$$\frac{D(x,t;\epsilon)}{E_{\rm s}(x,t;\epsilon)} = {\rm Ai}(X)\Delta + {\rm i}\frac{\epsilon^{1/3}}{\nu_{\rm s}(t)}{\rm Ai}'(X)\left(\Delta_{w_0} + 2\frac{c_{\rm s}(t)}{\nu_{\rm s}(t)}\Delta\right) + O\left(\epsilon^{2/3}\right) \tag{4.79}$$

where again all of the Δ functions and derivatives are evaluated at $\big(y_{\rm s}(t), y_0(t), z_2(t), \ldots, z_N(t)\big)$. At this point, we look back at (4.77) and notice that the leading order terms in (4.77) appear in there but with a multiplicative factor. Since the leading order terms and the whole of the denominator differ by an $O\left(\epsilon^{2/3}\right)$ error term, and the factor in question is bounded for $t \in K$, we have after dividing

$$\begin{aligned}\frac{D_0(x,t;\epsilon)}{D(x,t;\epsilon)} = \frac{1}{2t}&\left(x_{\rm s}(t) - y_{\rm s}(t) - y_0(t) - \sum_{i=2}^{N} z_j(t) + \sum_{j=1}^{N} p_j\right) \\ &- \frac{\rm i}{2t\nu_{\rm s}(t)}\frac{{\rm Ai}'(X) + O\left(\epsilon^{1/3}\right)}{\frac{1}{\epsilon^{1/3}}{\rm Ai}(X) + \frac{\rm i}{\nu_{\rm s}(t)}{\rm Ai}'(X)\left(\frac{\Delta_{w_0}}{\Delta} + 2\frac{c_{\rm s}(t)}{\nu_{\rm s}(t)}\right) + O\left(\epsilon^{1/3}\right)}\end{aligned} \tag{4.80}$$

where we divided Δ through the numerator and the denominator since it is nonzero, as well as $\epsilon^{1/3}$. This may have seemed ill-advised if we want to expand the inverse function in powers of ϵ, but in fact the leading order ${\rm Ai}(X)$ term can be zero, and so around these points the next-to-leading order term regulates the denominator, as it is purely imaginary. Thus, uniformly expanding the denominator yields

$$\begin{aligned}\frac{D_0(x,t;\epsilon)}{D(x,t;\epsilon)} = \frac{1}{2t}&\left(x_{\rm s}(t) - y_{\rm s}(t) - y_0(t) - \sum_{i=2}^{N} z_j(t) + \sum_{j=1}^{N} p_j\right) \\ &- \frac{\rm i}{2t\nu_{\rm s}(t)}\frac{{\rm Ai}'(X)}{\frac{1}{\epsilon^{1/3}}{\rm Ai}(X) + \frac{\rm i}{\nu_{\rm s}(t)}{\rm Ai}'(X)\left(\frac{\Delta_{w_0}}{\Delta} + 2\frac{c_{\rm s}(t)}{\nu_{\rm s}(t)}\right)} + O\left(\epsilon^{1/3}\right)\end{aligned} \tag{4.81}$$

so long as the next-to-leading order term does not vanish when the leading order does. We confirm this by computing the logarithmic-derivative of Δ

$$\frac{\Delta_{w_0}\big(y_{\rm s}(t), y_0(t), z_2(t), \ldots, z_N(t)\big)}{\Delta\big(y_{\rm s}(t), y_0(t), z_2(t), \ldots, z_N(t)\big)} = \frac{1}{y_{\rm s}(t) - y_0(t)} + \sum_{j=2}^{N} \frac{1}{y_{\rm s}(t) - z_j(t)} - \sum_{j=1}^{N} \frac{1}{y_{\rm s}(t) - p_j}\,. \tag{4.82}$$

As it happens, $2c_{\rm s}(t)/\nu_{\rm s}(t)$ is also related to a logarithmic derivative of u_0'' using (4.24), or equivalently h_{zzz}:

$$2\frac{c_{\rm s}(t)}{\nu_{\rm s}(t)} = \frac{u_0'''\big(y_{\rm s}(t)\big)}{6\,\big|u_0''\big(y_{\rm s}(t)\big)\big|} = \frac{h_{zzzz}\big(y_{\rm s}(t); x_{\rm s}(t), t\big)}{6\,\big|h_{zzz}\big(y_{\rm s}(t); x_{\rm s}(t), t\big)\big|}\,. \tag{4.83}$$

We've already once computed $h_{zzz}(z; x_{\rm s}(t), t)$ in (4.20). Using the fact that the roots of $Q(\diamond; x_{\rm s}(t), t)$ (4.10) are the saddle points, in $h_z(z; x_{\rm s}(t), t)$ (4.8) and splitting $(z - y_{\rm s}(t))^2$ off from the rest of the product, we can use binomial product rule to expand the three derivatives needed to compute $h_{zzzz}(z; x_{\rm s}(t), t)$ and recognize that, after evaluating $z = y_{\rm s}(t)$, only the terms that apply exactly two derivatives to the $(z - y_{\rm s}(t))^2$ term survive, giving

$$h_{zzzz}\big(y_{\rm s}(t); x_{\rm s}(t), t\big) = 6\;\partial_z \left(\frac{\big(z - y_0(t)\big)}{2t} \frac{\prod_{j=3}^{N} \big(z - z_j(t)\big)\big(z - z_j(t)^*\big)}{\prod_{j=1}^{N} (z - p_j)(z - p_j^*)} \right) \Bigg|_{z = y_{\rm s}(t)} \tag{4.84}$$

$$= 3\; h_{zzz}\big(y_{\rm s}(t); x_{\rm s}(t), t\big) \left(\frac{1}{y_{\rm s}(t) - y_0(t)} + \sum_{j=2}^{N} \frac{1}{y_{\rm s}(t) - z_j(t)} + \frac{1}{y_{\rm s}(t) - z_j(t)^*} - \sum_{j=1}^{N} \frac{1}{y_{\rm s}(t) - p_j} + \frac{1}{y_{\rm s}(t) - p_j^*} \right). \tag{4.85}$$

These let us simplify $2c_{\rm s}(t)/\nu_{\rm s}(t)$ further

$$2\frac{c_{\rm s}(t)}{\nu_{\rm s}(t)} = -\frac{1}{2}\left(\frac{1}{y_{\rm s}(t) - y_0(t)} + 2{\rm Re}\left[\sum_{j=2}^{N} \frac{1}{y_{\rm s}(t) - z_j(t)} - \sum_{j=1}^{N} \frac{1}{y_{\rm s}(t) - p_j} \right] \right). \tag{4.86}$$

Thus, putting (4.86) and (4.82) together, the term that appears in the denominator is

$$\frac{\Delta_{w_0}\big(y_{\rm s}(t), y_0(t), z_2(t), \ldots, z_N(t)\big)}{\Delta\big(y_{\rm s}(t), y_0(t), z_2(t), \ldots, z_N(t)\big)} + 2\frac{c_{\rm s}(t)}{\nu_{\rm s}(t)} = \frac{1}{2}\frac{1}{y_{\rm s}(t) - y_0(t)} + {\rm i}\gamma(t)\,, \tag{4.87}$$

where we have defined

$$\gamma(t) := \mathrm{Im}\left[\sum_{j=2}^{N} \frac{1}{y_{\mathrm{s}}(t) - z_j(t)} - \sum_{j=1}^{N} \frac{1}{y_{\mathrm{s}}(t) - p_j}\right] \tag{4.88}$$

to split the real and imaginary parts. Comparing to [6, Proposition 5.3], note that we can write also

$$\gamma(t) = -\frac{\mathrm{d}}{\mathrm{d}y}\left(\sum_{k=1}^{N} \arg(y - p_k) - \sum_{j=2}^{N} \arg(y - z_j(t))\right)\Bigg|_{y=y_{\mathrm{s}}(t)} . \tag{4.89}$$

Therefore, we see that

$$\gamma(t) = \frac{1}{2\pi}\int_0^{+\infty} \left[\frac{g_y(y_{\mathrm{s}}(t)+s,t)}{g(y_{\mathrm{s}}(t)+s,t)} - \frac{g_y(y_{\mathrm{s}}(t)-s,t)}{g(y_{\mathrm{s}}(t)-s,t)}\right]\frac{\mathrm{d}s}{s}\,, \tag{4.90}$$

where $g(y,t)$ is the positive rational function defined for $y \in \mathbb{R}$ and $t \in K$ by

$$g(y,t) := \frac{y + 2tu_0(y) - x_{\mathrm{s}}(t)}{\big(y + 2tu_0\big(y_0(t)\big) - x_{\mathrm{s}}(t)\big)\big(y + 2tu_0\big(y_{\mathrm{s}}(t)\big) - x_{\mathrm{s}}(t)\big)^2}\,. \tag{4.91}$$

This expresses this term in a universal manner, only in terms of information of the initial condition on the real axis and the relevant Burgers' branch solutions. Now we return to the ratio of determinants and multiply through the numerator and denominator by $-\mathrm{i}2\nu_{\mathrm{s}}(t)\big(y_{\mathrm{s}}(t) - y_0(t)\big)/\mathrm{Ai}'(X)$, with the recognition that when the denominator blows up, we take the fraction to be zero.

$$\begin{aligned}\frac{D_0(x,t;\epsilon)}{D(x,t;\epsilon)} = \frac{1}{2t}\Bigg(x_{\mathrm{s}}(t) - y_{\mathrm{s}}(t) - y_0(t) - \sum_{i=2}^{N} z_j(t) + \sum_{j=1}^{N} p_j\Bigg) \\ + \frac{2\left(u_0\big(y_0(t)\big) - u_0\big(y_{\mathrm{s}}(t)\big)\right)}{\mathrm{i}2\big(u_0\big(y_0(t)\big) - u_0\big(y_{\mathrm{s}}(t)\big)\left(\frac{k_{\mathrm{s}}(t)}{\epsilon^{1/3}}\frac{\mathrm{Ai}(X)}{\mathrm{Ai}'(X)} - 2t\gamma(t)\right) + 1} + O\left(\epsilon^{1/3}\right)\end{aligned} \tag{4.92}$$

where we made use of the saddle point condition (4.7) to simplify $\big(y_{\mathrm{s}}(t) - y_0(t)\big)/2t = u_0\big(y_0(t)\big) - u_0\big(y_{\mathrm{s}}(t)\big)$. Lastly, we need to take twice the real part to get the solution as per (4.3). On the fraction term, this is straightforward and is already universal, but the first

term needs to be put into a universal form,

$$2\mathrm{Re}\left[\frac{1}{2t}\left(x_{\mathrm{s}}(t)-y_{\mathrm{s}}(t)-y_0(t)-\sum_{i=2}^{N}z_j(t)+\sum_{j=1}^{N}p_j\right)\right]$$
$$=\frac{1}{2t}\left(2x_{\mathrm{s}}(t)-2y_{\mathrm{s}}(t)-2y_0(t)-\sum_{i=2}^{N}z_j(t)+z_j(t)^*+\sum_{j=1}^{N}p_j+p_j^*\right). \tag{4.93}$$

To make sense of this, we return to (4.10), noting that the sum is at most a polynomial of order $2N-1$ in z, we expand the first term to learn

$$Q(z;x_{\mathrm{s}}(t),t)=z^{2N+1}-\left(x_{\mathrm{s}}(t)+\sum_{j=1}^{N}p_j+p_j^*\right)z^{2N}+O\left(z^{2N-1}\right). \tag{4.94}$$

Then from fact that $Q(\diamond;x,t)$ (4.10) has the saddle points as its roots, we expand and learn

$$Q(z;x_{\mathrm{s}}(t),t)=z^{2N+1}-\left(2y_{\mathrm{s}}(t)+y_0(t)+\sum_{j=2}^{N}z_j(t)+z_j(t)^*\right)z^{2N}+O\left(z^{2N-1}\right). \tag{4.95}$$

Since the two coefficients of the z^{2N} term must be the same, we get the pole-saddle point relationship

$$x_{\mathrm{s}}(t)+\sum_{j=1}^{N}p_j+p_j^*=2y_{\mathrm{s}}(t)+y_0(t)+\sum_{j=2}^{N}z_j(t)+z_j(t)^* \tag{4.96}$$

With this, we reduce the constant term

$$2\mathrm{Re}\left[\frac{1}{2t}\left(x_{\mathrm{s}}(t)-y_{\mathrm{s}}(t)-y_0(t)-\sum_{i=2}^{N}z_j(t)+\sum_{j=1}^{N}p_j\right)\right]=\frac{x_{\mathrm{s}}(t)-y_0(t)}{2t}=u_0(y_0(t))\,. \tag{4.97}$$

Putting all of this together, we get

$$u(x,t;\epsilon)=u_0^{\mathrm{B}}(t)+\frac{4\left(u_{\mathrm{s}}^{\mathrm{B}}(t)-u_0^{\mathrm{B}}(t)\right)}{\left[2\left(u_{\mathrm{s}}^{\mathrm{B}}(t)-u_0^{\mathrm{B}}(t)\right)\left(\frac{k_{\mathrm{s}}(t)}{\epsilon^{1/3}}\frac{\mathrm{Ai}(X)}{\mathrm{Ai}'(X)}-2t\gamma(t)\right)\right]^2+1}+O\left(\epsilon^{1/3}\right). \tag{4.98}$$

4.2.1 Interpretation of the Small Dispersion Formula

For a plot of an example solution approximation at the soliton edge, see Figure 4.4. The solitons of the small dispersion Benjamin-Ono equation [4] are a particular family of Lorentzian

profiles parameterized by $\lambda > 0$

$$L(\xi;\lambda,\epsilon) := \frac{2\lambda}{\left(\frac{\lambda\xi}{\epsilon}\right)^2 + 1}\,. \tag{4.99}$$

The time dynamics of single solitons are linear motion with a speed that is also determined by the parameter $\lambda > 0$, $\xi = x - \lambda t + x_0$, where $x_0 \in \mathbb{R}$ is the initial position of the peak of the soliton. Our derived uniform approximation to $u(x,t;\epsilon)$ (4.98) takes the form of a constant background $u_0^{\mathrm{B}}(t)$ plus the Lorentzian soliton profile (4.99) with

$$\xi = \epsilon^{2/3} k_{\mathrm{s}}(t) \frac{\mathrm{Ai}(X)}{\mathrm{Ai}'(X)} - \epsilon 2t\gamma(t) \tag{4.100}$$

$$\lambda = 2\left(u_0^{\mathrm{B}}(t) - u_{\mathrm{s}}^{\mathrm{B}}(t)\right) \tag{4.101}$$

where recall the $\epsilon^{2/3}$-order change of variables from x to X (4.33). There are three ϵ-scales present in this formula, the slow scale which matches the original x variable scale (i.e. $\epsilon^0 = 1$), a fast scale which matches the width scale of the small dispersion solitons (i.e. ϵ), and a meso-scale that operates between these two which is a phenomenon inherent to the edge due to the collision of saddle points (i.e $\epsilon^{2/3}$). An important behavior on the meso-scale is dictated through the behavior of the Airy-ratio $\mathrm{Ai}(X)/\mathrm{Ai}'(X)$. Note that when this is near zero, the Lorentzian has its peak. Since this ratio always goes through zero with unit derivative, letting $\epsilon^{-r}(X-\alpha)$ be in a compact interval where α is a zero of the Airy function and we require $0 < r < 1/3$, we have

$$\xi = \epsilon^{2/3} k_{\mathrm{s}}(t)(X-\alpha) - \epsilon 2t\gamma(t) + O\left(\epsilon^{2r}\right) \tag{4.102}$$

$$= x - x_{\mathrm{s}}(t) - \epsilon^{2/3} k_{\mathrm{s}}(t)\alpha - \epsilon 2t\gamma(t) + O\left(\epsilon^{2r}\right) \tag{4.103}$$

which is uniformly valid for x in a shrinking compact interval around $x_{\mathrm{s}}(t) - \epsilon^{2/3}k_{\mathrm{s}}(t)\alpha$ and with width proportional to $\epsilon^{2/3+r}$. Since $2/3 + r < 1$, this width goes to zero slower that the width of the Lorentzian soliton profile which is $O(\epsilon)$, demonstrating that the full Lorentzian is resolved in the limit $\epsilon \to 0^+$. This means we can truly identify these Lorentzian peaks as individual solitons just inside the soliton edge, spaced according to the zeros of the Airy function with a $\epsilon^{2/3}k_{\mathrm{s}}(t)$ scaling and a next-to-leading order shift $\epsilon 2t\gamma(t)$.

Note that the solitons do not travel in straight lines like they would if they were isolated. Of course, this is due to the nonlinear interaction of the solitons with each other and the slowly varying background. Specifically, the leading order velocity of the solitons in light of (4.14) is $2u_{\mathrm{s}}^{\mathrm{B}}(t)$, instead of the expected velocity for an isolated soliton $\lambda = 2\left(u_{\mathrm{s}}^{\mathrm{B}}(t) - u_0^{\mathrm{B}}(t)\right)$. This difference can be explained by the Galilean boost symmetry of the Benjamin-Ono

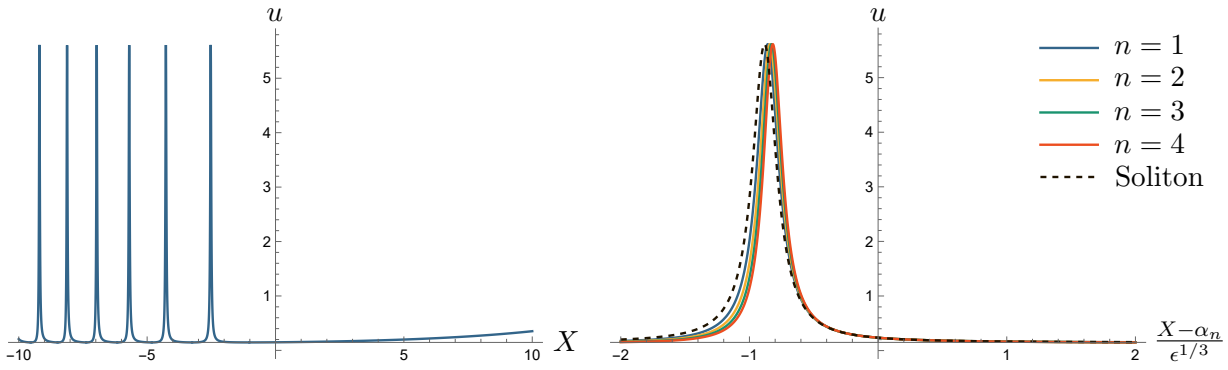


Figure 4.4: An example soliton edge approximation formula for the same initial condition provided in Figure 4.2. On the left is the full formula plotted for $X \in [-10, 10]$, $\epsilon = 0.1$, $t = 1.5$, and $x_{\mathrm{s}}(t) \approx -1.180$. On the right is the same solution, but shifted by the Airy zeros and horizontally scaled by $\epsilon^{1/3}$ to focus on the first four soliton peaks. Also plotted for comparison (dashed) is a true BO soliton Lorenzian profile (4.99) with a constant background, amplitude, horizontal scaling, and horizontal shift that match those predicted by the approximation formula.

equation (1.78). Because these solitons sit on top of the slowly varying background $u_0^{\mathrm{B}}(t)$, their velocities are boosted by exactly twice this amount. The next-to-leading order shift in position $\epsilon^{2/3} k_{\mathrm{s}}(t)\alpha$ can be attributed to the nearby interaction between these solitons close to the edge, since it is derived from information local to the edge and the ranked ordering of the solitons in question through their associated Airy zeros. Lastly, the next-next-to-leading order shift in position $\epsilon 2t\gamma(t)$ can be attributed to the sum of all nonlocal soliton-soliton and soliton-dispersive wave interactions since it is derived from global information.

4.3 Universal Behavior at the Dispersive Edge

Like in section 4.2, we will focus first on the expansion of $D_0(x, t; \epsilon)$. After expanding all of the elements of the matrix (4.4), we pull out of the determinant from each row the common leading multiplicative factors in the expansions of all but the second row. In the second row, the integral has a contribution from both the simple $y_2(x, t)$ and double $y_{\mathrm{d}}(t)$ saddle points on the real line. Thus, the best we can do is pull out one of their pre-factors from the row.

We choose the simple saddle point's factor, and get the overall factor

$$E_{\rm d}(x,t;\epsilon) := -\frac{2\pi\epsilon^{1/3}}{\nu_{\rm d}(t)}{\rm e}^{-{\rm i}h(y_{\rm d}(t);x,t)/\epsilon+{\rm i}2\pi/3}\left(\frac{2\pi\epsilon}{{\rm i}h_{zz}(y_2(t);x,t)}\right)^{1/2}{\rm e}^{-{\rm i}h(y_2(t);x,t)/\epsilon} \\ \times\prod_{j=2}^{N}\sigma_j\left(\frac{2\pi\epsilon}{{\rm i}h_j''(x,t)}\right)^{1/2}{\rm e}^{-{\rm i}h_j(t)/\epsilon} \tag{4.104}$$

multiplying the remaining determinant. This means that there is still a relative multiplicative factor on all of the contributions from the double saddle point in the second row. This takes the form

$$\mathcal{E}_{\rm d}(x,t) := \frac{\big({\rm i}2\pi h_{zz}(y_2(t);x,t)\big)^{1/2}}{\nu_{\rm d}(t)}{\rm e}^{{\rm i}[h_{zz}(y_2(t);x,t)-h(y_{\rm d}(t);x,t)]/\epsilon-{\rm i}2\pi/3}\,. \tag{4.105}$$

Here, we've used the fact that $\sigma_2=+1$, since the saddle points are the roots of $Q(\diamond;x,t)$ in (4.10), we may write

$$h_{zz}\big(y_2(t),x_{\rm d}(t),t\big)=\frac{\big(y_2(t)-y_{\rm d}(t)\big)^2}{2t}\frac{\prod_{j=2}^{N}|y_2(t)-z_j(t)|^2}{\prod_{j=1}^{N}|y_2(t)-p_j|^2}>0\,. \tag{4.106}$$

Thus, the map (4.48) takes the direction of the integration contour depicted in Figure 4.3 to the positive direction on the real axis. After using the linearity of the determinant to expand each row on the ϵ-ordered contributions, we have

$$\frac{D_0(x,t;\epsilon)}{E_{\rm d}(x,t;\epsilon)}=-\frac{\mathcal{E}_{\rm d}(x,t)}{\epsilon^{1/6}}{\rm Ai}({\rm e}^{-{\rm i}\pi/3}X){\rm Ai}({\rm e}^{{\rm i}\pi/3}X)U_{\rm d,d}(t)+{\rm Ai}({\rm e}^{-{\rm i}\pi/3}X)U_{\rm d,1}(t) \\ -{\rm i}\frac{\epsilon^{1/6}\mathcal{E}_{\rm d}(x,t)}{\nu_{\rm d}(t)}\Big[{\rm e}^{-{\rm i}\pi/3}{\rm Ai}'({\rm e}^{-{\rm i}\pi/3}X){\rm Ai}({\rm e}^{{\rm i}\pi/3}X)\left(U_{\rm d,d}^{(1,0)}(t)-2\frac{c_{\rm d}(t)}{\nu_{\rm d}(t)}U_{\rm d,d}(t)\right) \\ +{\rm e}^{{\rm i}\pi/3}{\rm Ai}({\rm e}^{-{\rm i}\pi/3}X){\rm Ai}'({\rm e}^{{\rm i}\pi/3}X)\left(U_{\rm d,d}^{(0,1)}(t)-2\frac{c_{\rm d}(t)}{\nu_{\rm d}(t)}U_{\rm d,d}(t)\right)\Big] \\ +O\left(\epsilon^{1/3}\right) \tag{4.107}$$

where $U_{\mathrm{d,d}}(t)$ and $U_{\mathrm{d,1}}(t)$ are the new matrix determinants

$$U_{\mathrm{d,d}}(t) := \begin{vmatrix} u_0\big(y_{\mathrm{d}}(t)\big) & \frac{1}{y_{\mathrm{d}}(t)-p_1} & \cdots & \frac{1}{y_{\mathrm{d}}(t)-p_N} \\ u_0\big(y_{\mathrm{d}}(t)\big) & \frac{1}{y_{\mathrm{d}}(t)-p_1} & \cdots & \frac{1}{y_{\mathrm{d}}(t)-p_N} \\ u_0\big(z_2(t)\big) & \frac{1}{z_2(t)-p_1} & \cdots & \frac{1}{z_2(t)-p_N} \\ \vdots & \vdots & \ddots & \vdots \\ u_0\big(z_N(t)\big) & \frac{1}{z_N(t)-p_1} & \cdots & \frac{1}{z_N(t)-p_N} \end{vmatrix}, \tag{4.108}$$

$$U_{\mathrm{d,1}}(t) := \begin{vmatrix} u_0\big(y_{\mathrm{d}}(t)\big) & \frac{1}{y_{\mathrm{d}}(t)-p_1} & \cdots & \frac{1}{y_{\mathrm{d}}(t)-p_N} \\ u_0\big(y_2(t)\big) & \frac{1}{y_2(t)-p_1} & \cdots & \frac{1}{y_2(t)-p_N} \\ u_0\big(z_2(t)\big) & \frac{1}{z_2(t)-p_1} & \cdots & \frac{1}{z_2(t)-p_N} \\ \vdots & \vdots & \ddots & \vdots \\ u_0\big(z_N(t)\big) & \frac{1}{z_N(t)-p_1} & \cdots & \frac{1}{z_N(t)-p_N} \end{vmatrix}, \tag{4.109}$$

while $U^{(1,0)}_{\mathrm{d,d}}(t)$ and $U^{(0,1)}_{\mathrm{d,d}}(t)$ have the same matrix as in $U_{\mathrm{d,d}}(t)$ but with a derivative taken on the functions in the first and second rows respectively

$$U^{(1,0)}_{\mathrm{d,d}}(t) := \begin{vmatrix} u_0'\big(y_{\mathrm{d}}(t)\big) & \frac{-1}{(y_{\mathrm{d}}(t)-p_1)^2} & \cdots & \frac{-1}{(y_{\mathrm{d}}(t)-p_N)^2} \\ u_0\big(y_{\mathrm{d}}(t)\big) & \frac{1}{y_{\mathrm{d}}(t)-p_1} & \cdots & \frac{1}{y_{\mathrm{d}}(t)-p_N} \\ u_0\big(z_2(t)\big) & \frac{1}{z_2(t)-p_1} & \cdots & \frac{1}{z_2(t)-p_N} \\ \vdots & \vdots & \ddots & \vdots \\ u_0\big(z_N(t)\big) & \frac{1}{z_N(t)-p_1} & \cdots & \frac{1}{z_N(t)-p_N} \end{vmatrix}, \tag{4.110}$$

$$U^{(0,1)}_{\mathrm{d,d}}(t) := \begin{vmatrix} u_0\big(y_{\mathrm{d}}(t)\big) & \frac{1}{y_{\mathrm{d}}(t)-p_1} & \cdots & \frac{1}{y_{\mathrm{d}}(t)-p_N} \\ u_0'\big(y_{\mathrm{d}}(t)\big) & \frac{-1}{(y_{\mathrm{d}}(t)-p_1)^2} & \cdots & \frac{-1}{(y_{\mathrm{d}}(t)-p_N)^2} \\ u_0\big(z_2(t)\big) & \frac{1}{z_2(t)-p_1} & \cdots & \frac{1}{z_2(t)-p_N} \\ \vdots & \vdots & \ddots & \vdots \\ u_0\big(z_N(t)\big) & \frac{1}{z_N(t)-p_1} & \cdots & \frac{1}{z_N(t)-p_N} \end{vmatrix}. \tag{4.111}$$

Immediately, we can state that $U_{\mathrm{d,d}}(t) = 0$ on account of the first two rows being identical, as well as $U^{(0,1)}_{\mathrm{d,d}}(t) = -U^{(1,0)}_{\mathrm{d,d}}(t)$ on account of the first two rows swapped between the two. This means the leading order term vanishes, which was why we pulled the multiplicative factor off the next-to-leading order term at the start. Furthermore, we can identify the terms on

the second and third lines with a Wronskian of the Airy functions

$$
\begin{aligned}
&W\left[\mathrm{Ai}(\mathrm{e}^{\mathrm{i}\pi/3}\diamond),\ \mathrm{Ai}(\mathrm{e}^{-\mathrm{i}\pi/3}\diamond)\right](X) \\
&\qquad = \mathrm{Ai}(\mathrm{e}^{\mathrm{i}\pi/3}X)\mathrm{e}^{-\mathrm{i}\pi/3}\mathrm{Ai}'(\mathrm{e}^{-\mathrm{i}\pi/3}X) - \mathrm{e}^{\mathrm{i}\pi/3}\mathrm{Ai}'(\mathrm{e}^{\mathrm{i}\pi/3}X)\mathrm{Ai}(\mathrm{e}^{-\mathrm{i}\pi/3}X) \qquad (4.112)\\
&\qquad = \frac{1}{2\pi\mathrm{i}} \qquad (4.113)
\end{aligned}
$$

by [48, Equation 9.2.9]. Plugging these results into (4.107), we get the much simpler formula

$$
\frac{D_0(x,t;\epsilon)}{E_{\mathrm{d}}(x,t;\epsilon)} = \mathrm{Ai}(\mathrm{e}^{-\mathrm{i}\pi/3}X)U_{\mathrm{d},1}(t) - \frac{\epsilon^{1/6}\mathcal{E}_{\mathrm{d}}(x,t)}{2\pi\nu_{\mathrm{d}}(t)}U^{(1,0)}_{\mathrm{d,d}}(t) + O\left(\epsilon^{1/3}\right) . \qquad (4.114)
$$

With the definitions of the saddle points (4.7), we replace u_0 evaluations and with the derivative condition satisfied by the double saddle point (4.13) we replace $u_0'\big(y_{\mathrm{d}}(t)\big)$:

$$
\begin{aligned}
U_{\mathrm{d},1}(t) &= \frac{x_{\mathrm{d}}(t)}{2t}C_{\mathrm{d},0}(t) - \frac{1}{2t}C_{\mathrm{d},1}(t), \qquad (4.115)\\
U^{(1,0)}_{\mathrm{d,d}}(t) &= \frac{x_{\mathrm{d}}(t)}{2t}C^{(1,0)}_{\mathrm{d},0}(t) - \frac{1}{2t}C^{(1,0)}_{\mathrm{d},1}(t)\,, \qquad (4.116)
\end{aligned}
$$

where

$$
C_{\mathrm{d},0}(t) := \begin{vmatrix}
1 & \frac{1}{y_{\mathrm{d}}(t)-p_1} & \cdots & \frac{1}{y_{\mathrm{d}}(t)-p_N}\\
1 & \frac{1}{y_2(t)-p_1} & \cdots & \frac{1}{y_2(t)-p_N}\\
1 & \frac{1}{z_2(t)-p_1} & \cdots & \frac{1}{z_2(t)-p_N}\\
\vdots & \vdots & \ddots & \vdots\\
1 & \frac{1}{z_N(t)-p_1} & \cdots & \frac{1}{z_N(t)-p_N}
\end{vmatrix}, \qquad
C_{\mathrm{d},1}(t) := \begin{vmatrix}
y_{\mathrm{d}}(t) & \frac{1}{y_{\mathrm{d}}(t)-p_1} & \cdots & \frac{1}{y_{\mathrm{d}}(t)-p_N}\\
y_2(t) & \frac{1}{y_2(t)-p_1} & \cdots & \frac{1}{y_2(t)-p_N}\\
z_2(t) & \frac{1}{z_2(t)-p_1} & \cdots & \frac{1}{z_2(t)-p_N}\\
\vdots & \vdots & \ddots & \vdots\\
z_N(t) & \frac{1}{z_N(t)-p_1} & \cdots & \frac{1}{z_N(t)-p_N}
\end{vmatrix}, \qquad (4.117)
$$

while $C^{(1,0)}_{\mathrm{d},0}(t)$ and $C^{(1,0)}_{\mathrm{d},1}(t)$ are the same as the expressions above but with a derivative taken on the functions in the first row

$$
C^{(1,0)}_{\mathrm{d},0}(t) := \begin{vmatrix}
0 & \frac{-1}{(y_{\mathrm{d}}(t)-p_1)^2} & \cdots & \frac{-1}{(y_{\mathrm{d}}(t)-p_N)^2}\\
1 & \frac{1}{y_{\mathrm{d}}(t)-p_1} & \cdots & \frac{1}{y_{\mathrm{d}}(t)-p_N}\\
1 & \frac{1}{z_2(t)-p_1} & \cdots & \frac{1}{z_2(t)-p_N}\\
\vdots & \vdots & \ddots & \vdots\\
1 & \frac{1}{z_N(t)-p_1} & \cdots & \frac{1}{z_N(t)-p_N}
\end{vmatrix}, \quad
C^{(1,0)}_{\mathrm{d},1}(t) := \begin{vmatrix}
1 & \frac{-1}{(y_{\mathrm{d}}(t)-p_1)^2} & \cdots & \frac{-1}{(y_{\mathrm{d}}(t)-p_N)^2}\\
y_{\mathrm{d}}(t) & \frac{1}{y_{\mathrm{d}}(t)-p_1} & \cdots & \frac{1}{y_{\mathrm{d}}(t)-p_N}\\
z_2(t) & \frac{1}{z_2(t)-p_1} & \cdots & \frac{1}{z_2(t)-p_N}\\
\vdots & \vdots & \ddots & \vdots\\
z_N(t) & \frac{1}{z_N(t)-p_1} & \cdots & \frac{1}{z_N(t)-p_N}
\end{vmatrix}. \qquad (4.118)
$$

Just as before, the value of these determinants can be computed explicitly using (4.71) and (4.72),

$$C_{\mathrm{d},0}(t) = \Delta\big(y_{\mathrm{d}}(t), y_2(t), z_2(t), \dots, z_N(t)\big), \tag{4.119}$$

$$C_{\mathrm{d},1}(t) = \Delta\big(y_{\mathrm{d}}(t), y_2(t), z_2(t), \dots, z_N(t)\big) \left(y_{\mathrm{d}}(t) + y_2(t) + \sum_{i=2}^{N} z_j(t) - \sum_{j=1}^{N} p_j \right), \tag{4.120}$$

and

$$C_{\mathrm{d},0}^{(1,0)}(t) = \Delta_{w_0}\big(y_{\mathrm{d}}(t), y_{\mathrm{d}}(t), z_2(t), \dots, z_N(t)\big), \tag{4.121}$$

$$C_{\mathrm{d},1}^{(1,0)}(t) = \Delta_{w_0}\big(y_{\mathrm{d}}(t), y_{\mathrm{d}}(t), z_2(t), \dots, z_N(t)\big) \left(2y_{\mathrm{d}}(t) + \sum_{i=2}^{N} z_j(t) - \sum_{j=1}^{N} p_j \right). \tag{4.122}$$

Note, in general, there should be an additional term in $C_{\mathrm{d},1}^{(1,0)}(t)$ that comes from taking the w_0-derivative of the sum in (4.72). This would be $\Delta\big(y_{\mathrm{d}}(t), y_{\mathrm{d}}(t), z_2(t), \dots, z_N(t)\big)$, but this is zero by direct evaluation because the first two arguments are the same. We insert (4.119), (4.120), (4.121), and (4.122) into (4.115) and (4.116), and then altogether into (4.114) for the slightly more complicated expansion

$$\begin{aligned} \frac{D_0(x,t;\epsilon)}{E_{\mathrm{d}}(x,t;\epsilon)} = \frac{1}{2t} \Bigg(& x_{\mathrm{d}}(t) - y_{\mathrm{d}}(t) - y_2(t) - \sum_{i=2}^{N} z_j(t) + \sum_{j=1}^{N} p_j \Bigg) \\ & \times \left[\mathrm{Ai}(\mathrm{e}^{-\mathrm{i}\pi/3} X) \Delta_{\mathrm{d},1} + \frac{\epsilon^{1/6} \mathcal{E}_{\mathrm{d}}(x,t)}{2\pi \nu_{\mathrm{d}}(t)} \Delta_{w_0;\mathrm{d},\mathrm{d}} \right] \\ & + \frac{y_{\mathrm{d}}(t) - y_2(t)}{2t} \frac{\epsilon^{1/6} \mathcal{E}_{\mathrm{d}}(x,t)}{2\pi \nu_{\mathrm{d}}(t)} \Delta_{w_0;\mathrm{d},\mathrm{d}} + O\left(\epsilon^{1/3}\right) \end{aligned} \tag{4.123}$$

where

$$\Delta_{\mathrm{d},2} = \Delta\big(y_{\mathrm{d}}(t), y_2(t), z_2(t), \dots, z_N(t)\big), \tag{4.124}$$

$$\Delta_{w_0;\mathrm{d},\mathrm{d}} = \Delta_{w_0}\big(y_{\mathrm{d}}(t), y_{\mathrm{d}}(t), z_2(t), \dots, z_N(t)\big). \tag{4.125}$$

The term on the third line above comes from the fact that the original sum factors on the two terms in the second line are slightly different, owed to the evaluation $w_1 = y_2(t)$ on the first term and the evaluation $w_1 = y_{\mathrm{d}}(t)$ on the second term. This term on the third line is what remains after adding and subtracting $y_2(t)$ in the second term's sum to be able to factor the displayed sum out of both.

Now we move on to $D(x,t;\epsilon)$. We conduct the same asymptotic approximations on the

elements of the matrix in (4.5), factor out the same terms, and expand the determinant linearly in the rows. However, the first column is all ones, so we can write the resulting determinants in terms of $C_{\mathrm{d},0}(t)$ and $C^{(1,0)}_{\mathrm{d},0}(t)$. As above, we use (4.119) and (4.121) to simplify,

$$\frac{D(x,t;\epsilon)}{E_{\mathrm{d}}(x,t;\epsilon)} = \mathrm{Ai}(\mathrm{e}^{-\mathrm{i}\pi/3}X)C_{\mathrm{d},0}(t) - \frac{\epsilon^{1/6}\mathcal{E}_{\mathrm{d}}(x,t)}{2\pi\nu_{\mathrm{d}}(t)}C^{(1,0)}_{\mathrm{d},0}(t) + O\left(\epsilon^{1/3}\right) \tag{4.126}$$

$$= \mathrm{Ai}(\mathrm{e}^{-\mathrm{i}\pi/3}X)\Delta_{\mathrm{d},1} - \frac{\epsilon^{1/6}\mathcal{E}_{\mathrm{d}}(x,t)}{2\pi\nu_{\mathrm{d}}(t)}\Delta_{w_0;\mathrm{d},\mathrm{d}} + O\left(\epsilon^{1/3}\right) . \tag{4.127}$$

Since the first two terms in the second line above are the same as those in (4.123) that are multiplied by the sum, we can add and subtract the error term from (4.127) in (4.123) to simplify the ratio

$$\frac{D_0(x,t;\epsilon)}{D(x,t;\epsilon)} = \frac{1}{2t}\left(x_{\mathrm{d}}(t) - y_{\mathrm{d}}(t) - y_2(t) - \sum_{i=2}^{N} z_j(t) + \sum_{j=1}^{N} p_j\right) + \frac{y_{\mathrm{d}}(t) - y_2(t)}{2t}\frac{\epsilon^{1/6}\mathcal{E}_{\mathrm{d}}(x,t)}{2\pi\nu_{\mathrm{d}}(t)}\frac{\Delta_{w_0;\mathrm{d},\mathrm{d}} + O\left(\epsilon^{1/6}\right)}{\mathrm{Ai}(\mathrm{e}^{-\mathrm{i}\pi/3}X)\Delta_{\mathrm{d},1} + O\left(\epsilon^{1/6}\right)} . \tag{4.128}$$

Lastly, since the leading order terms in the numerator and denominator of the fraction term in (4.128) above are uniformly bounded away from infinity and zero respectively for X and t in compact intervals, we can expand the ratio in powers of ϵ to get

$$\frac{D_0(x,t;\epsilon)}{D(x,t;\epsilon)} = \frac{1}{2t}\left(x_{\mathrm{d}}(t) - y_{\mathrm{d}}(t) - y_2(t) - \sum_{i=2}^{N} z_j(t) + \sum_{j=1}^{N} p_j\right) + \frac{y_{\mathrm{d}}(t) - y_2(t)}{2t}\frac{\epsilon^{1/6}\mathcal{E}_{\mathrm{d}}(x,t)}{2\pi\nu_{\mathrm{d}}(t)}\frac{\Delta_{w_0;\mathrm{d},\mathrm{d}}}{\mathrm{Ai}(\mathrm{e}^{-\mathrm{i}\pi/3}X)\Delta_{\mathrm{d},1}} + O\left(\epsilon^{1/3}\right) . \tag{4.129}$$

In order to go any further, we must evaluate the ratio $\Delta_{w_0;\mathrm{d},\mathrm{d}}/\Delta_{\mathrm{d},1}$. Beginning with $\Delta_{w_0;\mathrm{d},\mathrm{d}}$, we notice that the formula for Δ (4.70) has only one factor $(w_0 - w_1)$. Therefore, differentiating on w_0, only the complement product to $(w_0 - w_1)$ survives the evaluation $w_0 = w_1$:

$$\Delta_{w_0}(w_1, w_1, \ldots, w_N) = (-1)^N \frac{\prod_{i=2}^{N}\prod_{j=1}^{i-1}(w_i - w_j)(p_j - p_i)}{\prod_{i=1}^{N}\prod_{j=1}^{N}(w_i - p_j)}\frac{\prod_{i=2}^{N}(w_i - w_1)}{\prod_{j=1}^{N}(w_1 - p_j)} . \tag{4.130}$$

Evaluating this formula with $w_1 = y_{\mathrm{d}}(t), w_2 = z_2(t), \ldots, w_N = z_N(t)$ and comparing to the product terms in $\Delta\big(y_{\mathrm{d}}(t), y_2(t), z_2(t), \ldots, z_N(t)\big)$, many of the terms cancel in the ratio,

leaving only

$$\frac{\Delta_{w_0;\mathrm{d},\mathrm{d}}}{\Delta_{\mathrm{d},1}} = \frac{1}{y_2(t) - y_\mathrm{d}(t)} \prod_{i=2}^{N} \frac{z_i(t) - y_\mathrm{d}(t)}{z_i(t) - y_2(t)} \prod_{j=1}^{N} \frac{y_2(t) - p_j}{y_\mathrm{d}(t) - p_j} \,. \tag{4.131}$$

Again, we are looking for a universal expression that depends only on the initial condition u_0 on the real axis, not its pole data. Staring intently at the product above, we might recall that we've seen the norm-squared of these terms before, specifically in the evaluations of the first nonzero derivatives of h at the real saddle points. So, eagerly we write these using the formula for h_z in terms of saddle points and poles at the dispersive edge,

$$h_z(z; x_\mathrm{d}(t), t) = \frac{(z - y_2(t))(y - y_\mathrm{d}(t))^2}{2t} \frac{\prod_{k=2}^{N} (z - z_k(t)(z - z_k(t)^*)}{\prod_{j=1}^{N} (z - p_j)(z - p_j^*)} \,. \tag{4.132}$$

Using this, we compute

$$h_2''(t) = h_{zz}(y_2(t); x_\mathrm{d}(t), t) = \frac{(y_2(t) - y_\mathrm{d}(t))^2}{2t} \frac{\prod_{k=2}^{N} |y_2(t) - z_k(t)|^2}{\prod_{j=1}^{N} |y_2(t) - p_j|^2} \tag{4.133}$$

and

$$\nu_\mathrm{d}^3(t) = \frac{|h_{zzz}(y_\mathrm{d}(t); x_\mathrm{d}(t), t)|}{2} = \frac{y_\mathrm{d}(t) - y_2(t)}{2t} \frac{\prod_{k=2}^{N} |y_\mathrm{d}(t) - z_k(t)|^2}{\prod_{j=1}^{N} |y_\mathrm{d}(t) - p_j|^2} \,. \tag{4.134}$$

From the fact that at the dispersive edge $y_\mathrm{d}(t) > y_2(t)$, we see these are both positive quantities and therefore can take the positive square-root. Dividing the results and comparing with (4.131), we see that

$$\left| \frac{\Delta_{w_0;\mathrm{d},\mathrm{d}}}{\Delta_{\mathrm{d},1}} \right| = \frac{1}{\sqrt{y_\mathrm{d}(t) - y_2(t)}} \frac{\nu_\mathrm{d}^{3/2}(t)}{\left(h_2''(t)\right)^{1/2}} \,. \tag{4.135}$$

If we account for the phases that have been eliminated in the magnitude, we get

$$\frac{\Delta_{w_0;\mathrm{d},\mathrm{d}}}{\Delta_{\mathrm{d},1}} = -\frac{1}{\sqrt{y_\mathrm{d}(t) - y_2(t)}} \frac{\nu_\mathrm{d}^{3/2}(t)}{\left(h_2''(t)\right)^{1/2}} \mathrm{e}^{\mathrm{i}(\gamma_\mathrm{d}(t) - \gamma_1(t))} \tag{4.136}$$

where the phases $\gamma_\mathrm{d}(t)$ and $\gamma_1(t)$ are defined by

$$\gamma_{\mathrm{d},2} := \sum_{k=2}^{N} \arg\left(y_{\mathrm{d},2}(t) - z_k(t)\right) - \sum_{j=1}^{N} \arg\left(y_{\mathrm{d},2}(t) - p_j\right) . \tag{4.137}$$

As we found before, [6, Proposition 5.3] lets us rewrite these phases in a universal way

$$\gamma_{\mathrm{d},2}(t) = \frac{1}{2\pi}\int_0^{+\infty} \log\left(\frac{g(y_{\mathrm{d},2}(t)+s,t)}{g(y_{\mathrm{d},2}(t)-s,t)}\right)\frac{\mathrm{d}s}{s}\,, \tag{4.138}$$

where $g(y,t)$ in this cases is the positive rational function defined for $y \in \mathbb{R}$ and $t \in K$ by

$$g(y,t) := \frac{y + 2tu_0(y) - x_{\mathrm{d}}(t)}{\big(y + 2tu_2^{\mathrm{B}}(t) - x_{\mathrm{d}}(t)\big)\big(y + 2tu_{\mathrm{d}}^{\mathrm{B}}(t) - x_{\mathrm{d}}(t)\big)^2}\,. \tag{4.139}$$

Now the only remaining terms in our approximation (4.129) to simplify are lumped into $\mathcal{E}_{\mathrm{d}}(x,t)$ (4.105). We start with the exponent $h_2(x,t) - h(y_{\mathrm{d}}(t);x,t)$. Taylor expanding in x, the zero-order term is the evaluation at the edge. Since h is a quadratic plus an anti-derivative of u_0 that is valid everywhere on the real axis, we have

$$\begin{aligned}
\Theta(t) &= h_2\big(x_{\mathrm{d}}(t),t\big) - h\big(y_{\mathrm{d}}(t);x_{\mathrm{d}}(t),t\big) && (4.140)\\
&= \frac{\big(y_2(t)-x_{\mathrm{d}}(t)\big)^2}{4t} - \frac{\big(y_{\mathrm{d}}(t)-x_{\mathrm{d}}(t)\big)^2}{4t} + \int_{y_{\mathrm{d}}(t)}^{y_2(t)} u_0(y)\,\mathrm{d}y && (4.141)\\
&= \Big(\big(u_2^{\mathrm{B}}(t)\big)^2 - \big(u_{\mathrm{d}}^{\mathrm{B}}(t)\big)^2\Big)\,t + \int_{y_{\mathrm{d}}(t)}^{y_2(t)} u_0(y)\,\mathrm{d}y\,, && (4.142)
\end{aligned}$$

where we used the saddle point condition (4.7) to replace the quadratic terms with the square of the Burgers' branches. For the first-order term, we take the x-derivatives explicitly. First, note that

$$\begin{aligned}
\partial_x h_2(x,t)\Big|_{x=x_{\mathrm{d}}(t)} &= \partial_x h\big(y_2(x,t);x_{\mathrm{d}}(t),t\big)\Big|_{x=x_{\mathrm{d}}(t)} && (4.143)\\
&= h_z\big(y_2(t);x_{\mathrm{d}}(t),t\big)\partial_x y_2(x_{\mathrm{d}}(t),t) + h_x\big(y_2(t);x_{\mathrm{d}}(t),t\big) && (4.144)\\
&= -\frac{y_2(t)-x_{\mathrm{d}}(t)}{2t} && (4.145)\\
&= u_2^{\mathrm{B}}(t) && (4.146)
\end{aligned}$$

where we again used the saddle point condition (4.7) to remove the h_z-term and in the last step. The other h is even easier

$$\begin{aligned}
\partial_x h\big(y_{\mathrm{d}}(t);x,t\big)\Big|_{x=x_{\mathrm{d}}(t)} &= h_x\big(y_{\mathrm{d}}(t);x_{\mathrm{d}}(t),t\big) && (4.147)\\
&= -\frac{y_{\mathrm{d}}(t)-x_{\mathrm{d}}(t)}{2t} && (4.148)\\
&= u_{\mathrm{d}}^{\mathrm{B}}(t)\,. && (4.149)
\end{aligned}$$

Finally, the second-order remainder is uniformly bounded for X and t in compact intervals, giving the series and remainder in ϵ

$$h_2(x,t) - h\big(y_{\mathrm{d}}(t);x,t\big) = \Theta(t) + \big(u_{\mathrm{d}}^{\mathrm{B}}(t) - u_2^{\mathrm{B}}(t)\big)\,\epsilon^{2/3} k_{\mathrm{d}}(t) X + O\left(\epsilon^{4/3}\right). \tag{4.150}$$

With the exponent expanded (4.150), the last term in $\mathcal{E}_{\mathrm{d}}(x,t)$ (4.105) is $(\mathrm{i}2\pi h_2''(x,t))^{1/2}$, which we also expand in x at the edge to get

$$\mathcal{E}_{\mathrm{d}}(x,t) = \frac{\sqrt{2\pi h_2''(t)}}{\nu_{\mathrm{d}}(t)} \exp\left(\mathrm{i}\left[\frac{\Theta(t)}{\epsilon} + \frac{u_2^{\mathrm{B}}(t) - u_{\mathrm{d}}^{\mathrm{B}}(t)}{\epsilon^{1/3}} k_{\mathrm{d}}(t) X - \frac{5\pi}{12}\right]\right) + O\left(\epsilon^{1/3}\right) \tag{4.151}$$

where $h_2''(t)$ is defined in (4.133) and we used the fact that this is positive to take the principal square-root on the imaginary unit.

Now we include (4.136) and (4.151) into the approximation (4.129),

$$\begin{aligned}\frac{D_0(x,t;\epsilon)}{D(x,t;\epsilon)} = \frac{1}{2t}&\left(x_{\mathrm{d}}(t) - y_{\mathrm{d}}(t) - y_2(t) - \sum_{i=2}^{N} z_j(t) + \sum_{j=1}^{N} p_j\right) \\ &+ \epsilon^{1/6} \frac{\sqrt{y_{\mathrm{d}}(t) - y_2(t)}}{2t\sqrt{2\pi\nu_{\mathrm{d}}(t)}} \frac{\exp\left(\mathrm{i}\left[\frac{\Theta(t)}{\epsilon} + \frac{u_2^{\mathrm{B}}(t) - u_{\mathrm{d}}^{\mathrm{B}}(t)}{\epsilon^{1/3}} k_{\mathrm{d}}(t) X + \gamma_{\mathrm{d}}(t) - \gamma_2(t) - \frac{5\pi}{12}\right]\right)}{\mathrm{Ai}(\mathrm{e}^{-\mathrm{i}\pi/3} X)} \\ &+ O\left(\epsilon^{1/3}\right).\end{aligned} \tag{4.152}$$

With identical reasoning to what led us to (4.96), we get the same pole-saddle point relationship *mutatis mutandis*. This lets us compute the real part of the constant term in (4.152) to

$$\begin{aligned}&2\mathrm{Re}\left[\frac{1}{2t}\left(x_{\mathrm{d}}(t) - y_{\mathrm{d}}(t) - y_2(t) - \sum_{i=2}^{N} z_j(t) + \sum_{j=1}^{N} p_j\right)\right] \\ &\quad= \frac{1}{2t}\left(2x_{\mathrm{d}}(t) - 2y_{\mathrm{d}}(t) - 2y_2(t) - \sum_{i=2}^{N} z_j(t) + z_j(t)^* + \sum_{j=1}^{N} p_j + p_j^*\right) \qquad (4.153) \\ &\quad= \frac{x_{\mathrm{d}}(t) - y_2(t)}{2t} = u_0\big(y_2(t)\big). \qquad (4.154)\end{aligned}$$

This readily leads to the solution uniform approximation on compact intervals using (4.3),

$$\begin{aligned}u(x,t;\epsilon) = u_2^{\mathrm{B}}(t) + \epsilon^{1/6}&\sqrt{\frac{2\big(u_2^{\mathrm{B}}(t) - u_{\mathrm{d}}^{\mathrm{B}}(t)\big)}{\pi k_{\mathrm{d}}(t)}} \frac{\cos\left(\frac{\Theta(t)}{\epsilon} + \frac{u_2^{\mathrm{B}}(t) - u_{\mathrm{d}}^{\mathrm{B}}(t)}{\epsilon^{1/3}} k_{\mathrm{d}}(t) X + \alpha(X) + \theta(t)\right)}{|\mathrm{Ai}(\mathrm{e}^{\mathrm{i}\pi/3} X)|} \\ &+ O\left(\epsilon^{1/3}\right)\end{aligned} \tag{4.155}$$

where we define the meso-scale offset function α and the slow-scale offset function θ,

$$\alpha(X) := \arg\left(\mathrm{Ai}(\mathrm{e}^{\mathrm{i}\pi/3}X)\right) - \frac{5\pi}{12}, \tag{4.156}$$

$$\theta(t) := \gamma_{\mathrm{d}}(t) - \gamma_2(t)\,, \tag{4.157}$$

where $\alpha(X)$ is taken to be continuous.

4.3.1 Interpretation of the Formula at the Dispersive Edge

For a plot of an example solution approximation at the soliton edge, see Figure 4.4. The approximation (4.155) is made up of a slowly varying background $u_2^{\mathrm{B}}(t)$ with leading order superimposed modulated sinusoidal. The amplitude is proportional to $\epsilon^{1/6}$ and varies in space on the meso-scale proportional to $\epsilon^{2/3}$. From the asymptotics of the Airy function [48, Section 9.7], the amplitude smoothly transitions between the asymptotic behavior

$$\frac{1}{|\mathrm{Ai}(\mathrm{e}^{\mathrm{i}\pi/3}X)|} = \begin{cases} 2\sqrt{\pi}|X|^{1/4}\exp\left(-\frac{2}{3}|X|^{3/2}\right)\left(1+O\left(\frac{1}{|X|^{3/2}}\right)\right) & \text{for large } X<0 \\ 2\sqrt{\pi}|X|^{1/4}\left(1+O\left(\frac{1}{|X|^{3/2}}\right)\right) & \text{for large } X>0 \end{cases}. \tag{4.158}$$

On the left is the $J=0$ region, where the only Burgers' solution is $u_2^{\mathrm{B}}(t)$. Here, the amplitude of the superimposed wave has an exponential decaying envelope, showing the solution does indeed approach the constant background $u_2^{\mathrm{B}}(t)$. On the right is the $J=1$ region. Here, the amplitude is increasing like a fourth root, showing the envelope opening to become the dispersive shock wave. The periodic traveling wave solution of the small dispersion Benjamin-Ono equation takes the form of

$$U(\theta;U_0,U_1,U_2) = U_0 + (U_2-U_1)\frac{1-\dfrac{U_1-U_0}{U_2-U_0}}{1+\dfrac{U_1-U_0}{U_2-U_0}+2\sqrt{\dfrac{U_1-U_0}{U_2-U_0}}\cos\left(\dfrac{\theta}{\epsilon}\right)} \tag{4.159}$$

where $U_0<U_1<U_2$ are any ordered, real values and the spatial and temporal dependence of the solution comes in only in the θ variable

$$\theta(x,t) = (U_1-U_2)\big(x-(U_1+U_2)t\big)+\theta_0\,. \tag{4.160}$$

These U-parameters have been suggestively labeled: when we take $U_j = u_j^{\mathrm{B}}(x,t)$ for $j=0,1$ and 2 in the $J=1$, this formula becomes a slowly varying periodic solution profile.

Expanding near the edge, $U_1 - U_0 = u_1^{\mathrm{B}}(x,t) - u_0^{\mathrm{B}}(x,t)$ vanishes like a square-root in $X > 0$ as they both approach $u_{\mathrm{d}}^{\mathrm{B}}(t)$ and (4.159) becomes

$$U(\theta; U_0, U_1, U_2) = u_2^{\mathrm{B}}(t) + 2\epsilon^{1/6} X^{1/4} \sqrt{\frac{2\left(u_2^{\mathrm{B}}(t) - u_{\mathrm{d}}^{\mathrm{B}}(t)\right)}{k_{\mathrm{d}}(t)}} \cos\left(\frac{\theta}{\epsilon}\right) + O\left(\epsilon^{1/3}\right) \tag{4.161}$$

which then matches exactly the large $X > 0$ asymptotics in (4.158) plugged in for the amplitude in (4.155).

The wave has fast oscillations with wavelength $O(\epsilon)$ from the terms in the cosine that were divided by ϵ,

$$\begin{aligned}\Theta(t) + \left(u_2^{\mathrm{B}}(t) - u_{\mathrm{d}}^{\mathrm{B}}(t)\right)\epsilon^{2/3} k_{\mathrm{d}}(t) X = \left(u_2^{\mathrm{B}}(t) - u_{\mathrm{d}}^{\mathrm{B}}(t)\right)\left(x - \left(u_2^{\mathrm{B}}(t) + u_{\mathrm{d}}^{\mathrm{B}}(t)\right)t - x_{\mathrm{d}}(t)\right) \\ + \int_{y_{\mathrm{d}}(t)}^{y_2(t)} u_0(y)\, \mathrm{d}y\,,\end{aligned} \tag{4.162}$$

where we've used (4.142). We can identify the spatial and temporal time dynamics of the periodic solution with slowly varying constants immediately where the slowly varying initial position is always along the dispersive edge. What remains is a slowly varying change in the overall phase given by the integral term, which appears to be computing a sum effect of local interactions from waves that previously passed the dispersive edge.

In addition to the fast-phase behavior, there is a meso-scale $O\left(\epsilon^{2/3}\right)$ phase shift which is given by $\alpha(X)$. This exhibits a smooth change in behavior between the $J = 0$ and $J = 1$ regions to the left and right of the dispersive edge respectively. We show this by computing the asymptotics for $\alpha(X)$ using again the Airy asymptotics [48, Section 9.7],

$$\alpha(X) = \begin{cases} -\dfrac{\pi}{4} + O\left(\dfrac{1}{|X|^{3/2}}\right) & \text{for large } X > 0 \\ -\dfrac{2}{3}|X|^{3/2} - \dfrac{\pi}{2} + O\left(\dfrac{1}{|X|^{3/2}}\right) & \text{for large } X > 0 \end{cases}, \tag{4.163}$$

where we've verified numerically that there are no additional factors of 2π which enter into the equation from requiring $\alpha(X)$ to be continuous. This appears to be due to a nonlinear amplitude effect of the waves, where once the waves emerge from the background, they begin interacting.

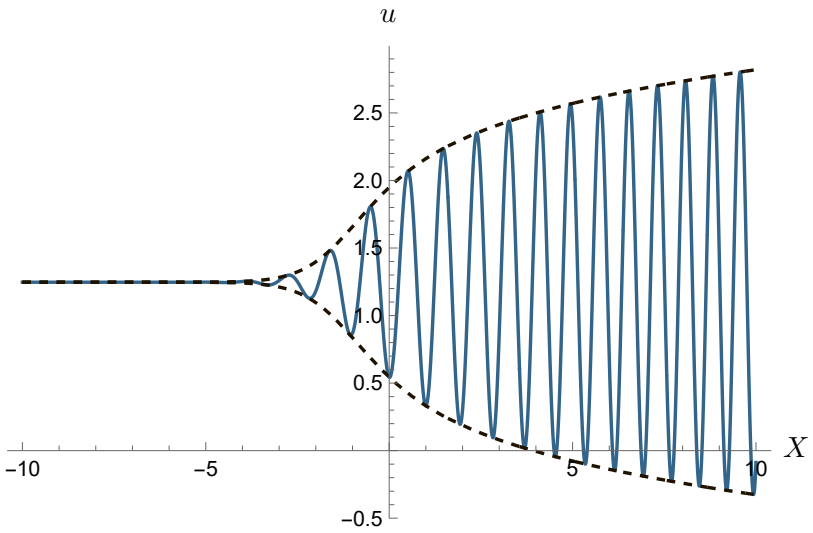


Figure 4.5: An example dispersive edge approximation formula for the same initial condition provided in Figure 4.2. Plotted for $X \in [-10, 10]$, $\epsilon = 0.001$, $t = 1.5$, and $x_{\mathrm{d}}(t) \approx -2.547$. Also plotted is the Airy modulus amplitude profile (dashed).

CHAPTER 5

Conclusion

A dream is all I know
Is all I have to show for my being here
It's all so clear
As much as I have to fear
There's nothing really mine
Just borrowed time
And I haven't had the chance to get things right

The Lemon Twigs, *A Dream Is All I Know*, (2024)

As we come to a close, let us review our results and discuss some further areas of work and questions which remain open.

In Chapter 2, we presented some new formal results regarding the semi-classical limit of the ILW scattering equation. In particular, we studied the asymptotics of the infinite solutions to the model turning point equation and derived heuristically a new asymptotic formula for the norming constants (2.10). Originally, the goal when setting out to study the ILW scattering equation was to derive asymptotic formulæ for the scattering data using a rigorous method than that of Miloh and Minzoni [46]. In 1937, Langer devised a rigorous method from studying the semi-classical Schrödinger operator's spectrum [32]. This *Langer transformation* uses a change of variables, valid for an interval around a turning point, to convert the eigenvalue problem exactly into the model turning point equation, in this case Airy's equation, with the addition of a ϵ-sized forcing term. Then, using variation of parameters, the exact solutions can be analyzed.

In the case of ILW, if one wants to conduct something of a Langer transform on the scattering equation (2.3), one is immediately presented with a choice: use a transformation in z that breaks the analyticity of the wavefunction over the strip domain, or require the transformation is analytic and dramatically alter the domain of definition of the wavefunction. Since the goal is to have the problem after the transformation look like the model turning

point equation, we might opt for the former over the later. For this, we emphasize that the wave function solves a homogeneous $\overline{\partial}$-problem interior to the strip:

$$0 = \mathrm{i}\epsilon\Phi_x^+(x) + u(x)\psi^+(x) - \zeta \mathrm{e}^{-2\delta\zeta}\psi^-(x) \text{ for } x \in \mathbb{R}\,, \tag{5.1}$$

$$0 = \overline{\partial}_z \Phi(z) \text{ for } z \in \mathcal{S}_{\epsilon\delta}\,, \tag{5.2}$$

where $\overline{\partial}_z := (\partial_x + \mathrm{i}\partial_y)/2$. Let $x_0 \in \mathbb{R}$ satisfy the turning point condition (2.29). We introduce $\Phi(z) = \mathrm{e}^{u(x_0)z/\epsilon} w(z)$. This yields:

$$0 = \epsilon w_y^+(x) + \big(u(x) - u(x_0)\big)w^+(x) - \frac{\mathrm{e}^{-1}}{2\delta} w^-(x) \text{ for } x \in \mathbb{R}\,, \tag{5.3}$$

$$0 = \partial_{\bar{z}} w(z) \text{ for } z \in \mathcal{S}_{\epsilon\delta}\,, \tag{5.4}$$

where we assumed that w is analytic at the boundaries to exchange $\mathrm{i}w_x^+(x) = w_y^+(x)$. We introduce the coordinate transform g and set $X = g(x)$, $Y = g'(x)y$ and $Z = X + \mathrm{i}Y$. If we define $W(Z) := w(z)$, then by implicit differentiation

$$0 = \epsilon W_Y^+(X) + \frac{u(x) - u(x_0)}{g'(x)} W^+(X) - \frac{\mathrm{e}^{-1}}{2\delta g'(x)} W^-(X) \text{ for } X \in \mathbb{R}\,, \tag{5.5}$$

$$-\frac{g''(x)}{g'(x)} W_X = \overline{\partial}_Z W(Z) \text{ for } X \in \mathbb{R} \text{ and } |Y| \le \delta\epsilon g(x)\,. \tag{5.6}$$

The idea behind the Langer transform is to require

$$\frac{u(x) - u(x_0)}{g'(x)} = g(x) = X\,, \tag{5.7}$$

so that the scattering equation takes the form of the model turning point equation (2.41). This condition is integrated easily

$$(g(x))^2 = 2\int_{x_0}^{x} u(x') - u(x_0)\ \mathrm{d}x'\,, \tag{5.8}$$

where, since $u(x) - u(x_0)$ looks linear around $x = x_0$, the square-root can be taken to yield a differentiable g. Note, g will only be real when $u(x)$ is increasing through $x = x_0$. If the derivative has the other sign, we need to set (5.7) instead equal to $-X$ and use the conjugation symmetry, as explained in Section 2.2, to recover the model turning point equation.

Interestingly, after exchanging the x derivative for a y derivative and conducting the z-substitution, there is no external forcing term on the left of the boundary equation (5.5). However, the width of the strip is now spatially dependent, $2\delta\epsilon g'(x)$, as seen in the final

term of (5.5) as well as the domain of Y in the bulk equation (5.6). Even more interestingly, the variable X now only appears as a parameter in the boundary equation, and thus for each fixed X, the solutions of the model turning point equation, $\psi_\nu(Z;\epsilon,2\delta g'(x))$ for $\nu \in \{-\infty\} \cup (2\mathbb{Z}-1/2)$ as in (2.58), solve this equation exactly. We might attempt to link together the solutions at each individual X by expressing the solution with X-dependent pre-factors

$$W(Z) = \sum_{\nu\in\{-\infty\}\cup(2\mathbb{Z}-1/2)} c_\nu(X)\ \psi_\nu\big(Z;\epsilon,2\delta g'(x)\big)\,. \tag{5.9}$$

We could then plug this into the bulk equation (5.6), which now has a forcing term, and attempt to find functions c_ν that solve the bulk equation. To continue the analysis, more must be understood about the basis of solutions to the model turning point equation. We expect that:

1. $\psi_\nu(Z;\epsilon,h)$ forms some sort of basis of the interval $|Y| \le h/2$ for each fixed X. If this is true, this might be useful in solving for the functions c_ν explicitly.

2. Since the x-varying width of the wavefunction's strip domain is proportional to ϵ, the forcing from the bulk in (5.6) should only contribute at next-to-leading order in ϵ to the solution.

Lastly, we recall that the $\psi_\nu(Z;\epsilon,h)$ for $\nu \neq -\infty, -1/2$ were matched with extraneous solutions in Section 2.3 and did not contribute to the formation of normalizable wavefunctions. So if a Langer transform, like that illustrated above, can be used to rigorously solve the ILW scattering equation, do these solutions really not contribute to normalizable wavefunctions at all, or do they perhaps contribute beyond all orders in ϵ?

In Chapter 3, we presented an analysis of the ILW inverse scattering problem in the small dispersion limit. After expressing the solution in terms a on equilibrium problem for a particular electronic system, we showed that the limit in an L^2-sense approaches the solution to invicid Burgers' equation up until break time. After invicid Burgers' break time, we currently have no information about the ILW small dispersion solution.

Lax and Levermore, in their analysis of the analogous problem for the KdV equation, were able to calculate the small dispersion limit in a weak-L^2 sense beyond break time by constructing multi-band solutions to their energy minimization problem. They showed that their result in dispersive shock regions coincides with Flaschka, Forest and McLaughlin's algebro-geometric description of modulated wave trains of the KdV equation in terms of differentials on a slowly varying hyperelliptic surface [21]. The connection between the two descriptions can be seen in the fact that Lax and Levermore's constructed equilibrium potential is the restriction to one sheet of the integral of a differential on a hyperelliptic

surface, where the bands in the minimizing charge density represent the cuts between the two sheets. The modulated wave trains are multi-periodic solutions of the KdV equation with fast oscillations and slowly varying parameters which control wavelengths, speeds and amplitudes of the superimposed waves. These multi-periodic solutions are expressed in terms of a theta function associated to the hyperelliptic surface on which the Schrödinger operator's spectrum is defined.

If we imagine the analogy between the KdV and ILW small dispersion limits extends beyond break time, then we should attempt to construct multi-band solutions to the energy minimization problem (3.46). Krichever has an algebro-geometric description of the modulated wave trains of the ILW equation [30] in terms of differentials on a "δ-deformed hyperelliptic surface," identified as genus-n with a function λ analytic everywhere except one point P_∞, identified as infinity in a local coordinate ζ, where the $\lambda(\zeta) = \zeta \mathrm{e}^{2\delta\zeta}(1 + O(1/\zeta))$. More work needs to be done on understanding the Riemann surfaces Krichever has defined. Due to the appearance of the exponential in λ, these surfaces may not be algebraic, and the usual theory of differentials on algebraic varieties may need to be modified. Additionally, while the one band case for ILW as well as cases for KdV could be constructed explicitly in terms of classical functions, it is currently not known if this is true for the ILW multi-band case.

In Chapter 4, we described the universal behavior at the edges of the simplest form of dispersive shock wave which develops in the small dispersion limit of the BO equation for rational initial conditions. The rigorous formulas provided reveal new details regarding the small dispersion dynamics of the BO equation, namely the asymptotic spacing of solitons which emerge from the dispersive shock wave at one edge and the amplitude and phase profiles of the linear wave which generates the dispersive shock wave at the other edge. While the results presented in this dissertation only apply to specifc types of real and rational initial data, Gérards formula for the explicit solution to the BO equation (1.74) can be applied to other types of initial conditions, and maybe some similar results for initial conditions with more general singularities in the complex plane can be worked out. Additionally, there is also the possibility of using rational approximations to broaden the class of initial conditions for which we can prove these universal results.

BIBLIOGRAPHY

[1] M. J. Ablowitz, D. J. Kaup, A. C. Newell, and H. Segur. Nonlinear-evolution equations of physical significance. *Phys. Rev. Lett.*, 31:125–127, Jul 1973.

[2] J. Baik, T. Kriecherbauer, K. D. T. McLaughlin, and P. D. Miller. *Discrete orthogonal polynomials. (AM-164)*. Annals of Mathematics Studies. Princeton University Press, Princeton, NJ, January 2007.

[3] H. Bateman. Some recent researches on the motion of fluids. *Monthly Weather Review*, 43(4):163–170, April 1915.

[4] T. Brooke Benjamin. Internal waves of permanent form in fluids of great depth. *Journal of fluid mechanics*, 29(3):559–592, 1967.

[5] W. H. Beyer. *CRC Standard Mathematical Tables*. CRC Press, Boca Raton, FL, 28th edition, 1987.

[6] E. Blackstone, L. Gassot, P. Gérard, and P. D. Miller. The Benjamin-Ono equation in the zero-dispersion limit for rational initial data generation of dispersive shock waves. *In Preparation*, 2024.

[7] E. Blackstone, L. Gassot, P. Gérard, and P. D. Miller. The Benjamin-Ono initial-value problem for rational data. *In Preparation*, 2024.

[8] J. Boussinesq. Essai sur la théorie des eux courrantes. *Mémoires présentés par divers savants à l'Académie des sciences de l'Institut de France. Extrait des T. 23 et 24*, 1:XXII–680–61, 1877.

[9] R. J. Buckingham and P. D. Miller. The sine-Gordon equation in the semiclassical limit: dynamics of fluxon condensates. *Mem. Amer. Math. Soc.*, 225(1059), 2013.

[10] J. M. Burgers. *A Mathematical Model Illustrating the Theory of Turbulence*, page 171–199. Elsevier, 1948.

[11] C. Chester, B. Friedman, and F. Ursell. An extension of the method of steepest descents. *Mathematical Proceedings of the Cambridge Philosophical Society*, 53(3):599–611, 1957.

[12] W. Choi and R. Camassa. Fully nonlinear internal waves in a two-fluid system. *Journal of Fluid Mechanics*, 396:1–36, 1999.

[13] T. Claeys and T. Grava. Painlevé II asymptotics near the leading edge of the oscillatory zone for the Korteweg-de Vries equation in the small-dispersion limit. *Communications on Pure and Applied Mathematics*, 63(2):203–232, 2010.

[14] T. Claeys and T. Grava. Solitonic asymptotics for the Korteweg-de Vries equation in the small dispersion limit. *SIAM Journal on Mathematical Analysis*, 42(5):2132–2154, 2010.

[15] T. Claeys and T. Grava. Critical asymptotic behavior for the Korteweg-de Vries equation and in random matrix theory, 2012.

[16] P. Deift, S. Venakides, and X. Zhou. New results in small dispersion KdV by an extension of the steepest descent method for Riemann-Hilbert problems. *IMRN: International Mathematics Research Notices*, 1997(6):285–299, 1997.

[17] P. Deift and X. Zhou. A steepest descent method for oscillatory riemann-hilbert problems. asymptotics for the mkdv equation. *The Annals of Mathematics*, 137(2):295, March 1993.

[18] P. G. Drazin and R. S. Johnson. *Solitons: An Introduction*. Cambridge Texts in Applied Mathematics. Cambridge University Press, 2nd edition, 1989.

[19] B. Dubrovin. On Hamiltonian perturbations of hyperbolic systems of conservation laws. II. Universality of critical behaviour. *Comm. Math. Phys.*, 267(1):117–139, 2006.

[20] Henriette Elvang and Matthew Dominique Mitchell. On extended supersymmetry of 4d galileons and 3-brane effective actions. *Journal of High Energy Physics*, 2023(2), February 2023.

[21] H. Flaschka, M. G. Forest, and D. W. McLaughlin. Multiphase averaging and the inverse spectral solution of the Korteweg-de Vries equation. *Communications on Pure and Applied Mathematics*, 33(6):739–784, 1980.

[22] C. S. Gardner, J. M. Greene, M. D. Kruskal, and R. M. Miura. Method for solving the Korteweg-de Vries equation. *Phys. Rev. Lett.*, 19:1095–1097, Nov 1967.

[23] P. Gérard. An explicit formula for the Benjamin–Ono equation. *Tunisian Journal of Mathematics*, 5(3):593–603, November 2023.

[24] R. I. Joseph. Solitary waves in a finite depth fluid. *Journal of physics. A, Mathematical and general*, 10(12):L225–L227, 1977.

[25] S. Kamvissis, K. D. T.-R. McLaughlin, and P. D. Miller. *Semiclassical soliton ensembles for the focusing nonlinear Schrödinger equation*. Annals of Mathematics Studies. Princeton University Press, Princeton, NJ, August 2003.

[26] J. Klipfel. *The Direct Scattering Map for the Intermediate Long Wave Equation*. PhD thesis, University of Kentucky Libraries, 2020.

[27] Y. Kodama, M. J. Ablowitz, and J. Satsuma. Direct and inverse scattering problems of the nonlinear intermediate long wave equation. *Journal of Mathematical Physics*, 23(4):564–576, 1982.

[28] D. J. Korteweg and G. de Vries. Xli. on the change of form of long waves advancing in a rectangular canal, and on a new type of long stationary waves. *The London, Edinburgh, and Dublin Philosophical Magazine and Journal of Science*, 39(240):422–443, 1895.

[29] A. Krajenbrink and P. Le Doussal. Inverse scattering of the Zakharov-Shabat system solves the weak noise theory of the Kardar-Parisi-Zhang equation. *Phys. Rev. Lett.*, 127:064101, August 2021.

[30] Igor M. Krichever. The averaging procedure for the soliton-like solutions of integrable systems. In Mauro Francaviglia, editor, *Mechanics, Analysis and Geometry: 200 Years After Lagrange*, North-Holland Delta Series, pages 99–125. Elsevier, Amsterdam, 1991.

[31] T. Kubota, D. R. S. Ko, and L. D. Dobbs. Weakly-nonlinear, long internal gravity waves in stratified fluids of finite depth. *Journal of Hydronautics*, 12(4):157–165, 1978.

[32] R. E. Langer. On the connection formulas and the solutions of the wave equation. *Phys. Rev.*, 51:669–676, Apr 1937.

[33] P. D. Lax. Integrals of nonlinear equations of evolution and solitary waves. *Communications on Pure and Applied Mathematics*, 21(5):467–490, 1968.

[34] P. D. Lax and C. D. Levermore. The small dispersion limit of the Korteweg-de Vries equation. I. *Communications on pure and applied mathematics*, 36(3):253–290, 1983.

[35] P. D. Lax and C. D. Levermore. The small dispersion limit of the Korteweg-de Vries equation. II. *Communications on pure and applied mathematics*, 36(5):571–593, 1983.

[36] P. D. Lax and C. D. Levermore. The small dispersion limit of the Korteweg-de Vries equation. III. *Communications on pure and applied mathematics*, 36(6):809–829, 1983.

[37] C. D. Levermore. *The Small Dispersion Limit of the Korteweg deVries equation*. PhD thesis, New York University, June 1982.

[38] K. Mallick, H. Moriya, and T. Sasamoto. Exact solution of the macroscopic fluctuation theory for the symmetric exclusion process. *Phys. Rev. Lett.*, 129:040601, Jul 2022.

[39] Solomon Manukure and Timesha Booker. A short overview of solitons and applications. *Partial Differential Equations in Applied Mathematics*, 4:100140, December 2021.

[40] D. Masoero, A. Raimondo, and P. R. S. Antunes. Critical behavior for scalar nonlinear waves. *Physica D: Nonlinear Phenomena*, 292-293:1–7, February 2015.

[41] Y. Matsuno. Number density function of Benjamin-Ono solitons. *Physics letters. A*, 87(1):15–17, 1981.

[42] Y. Matsuno. *Bilinear Transformation Method*. Mathematics in Science and Engineering. Achademic Press, Inc, 1984.

[43] P. D. Miller and A. N. Wetzel. Direct scattering for the Benjamin-Ono equation with rational initial data. *Studies in Applied Mathematics*, 137(1):53–69, 2016.

[44] P. D. Miller and A. N. Wetzel. The scattering transform for the Benjamin-Ono equation in the small-dispersion limit. *Physica D: Nonlinear Phenomena*, 333:185–199, 2016. Dispersive Hydrodynamics.

[45] P. D. Miller and Z. Xu. On the zero-dispersion limit of the Benjamin-Ono cauchy problem for positive initial data. *Communications on Pure and Applied Mathematics*, 64(2):205–270, 2010.

[46] A. A. Minzoni and T. Miloh. On the number of solitons for the intermediate long wave equation. *Wave Motion*, 20(2):131–142, 1994.

[47] A. C. Newell. *Solitons in Mathematics and Physics*. Society for Industrial and Applied Mathematics, January 1985.

[48] F. W. J. Olver, A. B. Olde Daalhuis, D. W. Lozier, B. I. Schneider, R. F. Boisvert, C. W. Clark, B. V. Saunders B. R. Mille and, H. S. Cohl, and eds. M. A. McClain. Nist Digital Library of Mathematical Functions. http://dlmf.nist.gov/, Release 1.0.26 of 2020-03-15, 2020.

[49] H. Ono. Algebraic solitary waves in stratified fluids. *Journal of the Physical Society of Japan*, 39(4):1082–1091, 1975.

[50] J. S. Russell. Report on waves. *Report of the fourteenth meeting of the British Association for the Advancement of Science*, pages 311–390, Plates XLVII–LVII, York, September 1844 (London 1845).

[51] E. B. Saff and V. Totik. *Logarithmic Potentials with External Fields*. Springer Berlin Heidelberg, 1997.

[52] J. Saut. *Benjamin-Ono and Intermediate Long Wave Equations: Modeling, IST and PDE*, pages 95–160. Springer New York, New York, NY, 2019.

[53] S. Venakides. The Korteweg-de Vries equation with small dispersion: higher order Lax-Levermore theory. *Communications on Pure and Applied Mathematics*, 43(3):335–361, 1990.

[54] G. B. Whitham. Non-linear dispersive waves. *Proceedings of the Royal Society of London. Series A, Mathematical and physical sciences*, 283(1393):238–261, 1965.

[55] Z. Xu. *Asymptotic Analysis and Numerical Analysis of the Benjamin-Ono Equation*. PhD thesis, University of Michigan, 2010.

[56] N. J. Zabusky and M. D. Kruskal. Interaction of "solitons" in a collisionless plasma and the recurrence of initial states. *Phys. Rev. Lett.*, 15:240–243, Aug 1965.